

This electronic thesis or dissertation has been downloaded from the King's Research Portal at <https://kclpure.kcl.ac.uk/portal/>



THE ROLE OF PLANT CELL WALLS IN INFLUENCING STARCH BIOACCESSIBILITY

Edwards, Cathrina

Awarding institution:
King's College London

The copyright of this thesis rests with the author and no quotation from it or information derived from it may be published without proper acknowledgement.

END USER LICENCE AGREEMENT



Unless another licence is stated on the immediately following page this work is licensed

under a Creative Commons Attribution-NonCommercial-NoDerivatives 4.0 International

licence. <https://creativecommons.org/licenses/by-nc-nd/4.0/>

You are free to copy, distribute and transmit the work

Under the following conditions:

- Attribution: You must attribute the work in the manner specified by the author (but not in any way that suggests that they endorse you or your use of the work).
- Non Commercial: You may not use this work for commercial purposes.
- No Derivative Works - You may not alter, transform, or build upon this work.

Any of these conditions can be waived if you receive permission from the author. Your fair dealings and other rights are in no way affected by the above.

Take down policy

If you believe that this document breaches copyright please contact librarypure@kcl.ac.uk providing details, and we will remove access to the work immediately and investigate your claim.

THE ROLE OF PLANT CELL WALLS IN INFLUENCING STARCH BIOACCESSIBILITY

Cathrina Hansen Edwards

**A thesis submitted to King's College London for the degree of
Doctor of Philosophy in the Faculty of Science**

Division of Diabetes and Nutritional Sciences

School of Medicine

King's College London

April 2014

*This thesis is dedicated in loving memory of my sister, Camilla Hansen Edwards,
whose exceptional passion for science and education was a true inspiration.*

She is deeply missed.

PREFACE

This thesis was submitted to King's College London for the degree of Doctor of Philosophy. The work presented herein was undertaken in the Division of Diabetes and Nutritional Sciences (previously the Nutritional Sciences Research Division), King's College London, from February 2010 to April 2014.

ABSTRACT

This project was designed to provide new insights into the mechanisms by which plant cell walls ('dietary fibre'), influence starch bioaccessibility ('release') and postprandial glycaemia. Cell walls were hypothesised to limit bioaccessibility by acting as physical barriers to digestive enzymes, and/or by limiting the gelatinisation of starch during hydrothermal processing, with major implications for starch digestion kinetics and consequently, postprandial metabolism.

Chickpeas and durum wheat were milled to create test materials with varying degrees of structural integrity (i.e., amounts of encapsulated starch). The starch digestibility and behaviour of these milled materials were studied *in vitro*, and the data obtained were used to develop a mathematical model of starch digestion. Finally, a postprandial ileostomy study (n=9) was carried out to determine the effects of encapsulation on *in vivo* starch bioaccessibility, and blood glucose, insulin, lipid, and gut hormone responses.

Cell wall permeability and starch gelatinisation studies provided new evidence for the role of cell walls as barriers to digestive enzymes and as restrictors of starch gelatinisation. *In vitro* digestibility studies of hydrothermally processed materials, and subsequent Logarithm of Slope analysis, indicated that the rate and extent of digestion was strongly affected by cellular integrity. *In vivo*, the ingestion of coarsely milled wheat endosperm (~62% encapsulated starch) decreased the glycaemic response by ~30% compared with the ingestion of finely milled endosperm (i.e., containing the same amount of starch but not encapsulated).

Overall, intact cell walls significantly limit starch bioaccessibility, and reduce the postprandial rise in glycaemia and insulinaemia. The differences in digestibility and glycaemia between chickpeas and durum wheat were explained by their contrasting cell wall properties (e.g., permeability and fracturing). This work provides clues as to how plant materials may be manipulated in order to generate new functional food ingredients or products, for instance with slow-release or prebiotic effects.

ACKNOWLEDGEMENTS

First and foremost I would like thank my excellent supervisors, Prof. Peter Ellis, Dr. Peter Butterworth, and Dr. Sarah Berry, who have given me the confidence and granted me the freedom to develop as an independent researcher. Special thanks are also extended to members of the Biopolymers group: Dr. Fred Warren, Mrs. Myriam Grundy, Mr. Hamung Patel and Dr. Terri Grassby for support and insightful conversations, and also to the BBSRC and Premier Foods who funded this project.

I am deeply grateful to the Biogut team, especially Myriam Grundy, who took on the main responsibility of obtaining ethical approval and helped me set-up and run the study in *Chapter 7*, Nurse Dana Naïve, Dr. Shuvra Ray and the CRF for providing clinical cover, Miss Dafni Vasilopoulou for assisting with sample analysis, Terri Grassby for covering the evening shifts, Dr. Jeremy Sanderson (KCL), for specialist clinical advice, Dr. Tracy Nelson and GSTS pathology for blood analyses, Dr. Peter Milligan (KCL) for statistical advice, and of course, the amazing study participants – I couldn't have done this without them. The work in *Chapter 6* would not have been possible without Dr. Giusy Mandalari, Dr. Zara Merali, and others at IFR, who kindly programmed and ran the DGM and SIM, and I am very grateful for their efforts. Special thanks are also extended to Dr. Mary Parker (IFR), and Dr. Gema-Vizcay Barrena (CUI), for microscopy advice and assistance. There are many others who have also contributed to this work, notably Dr. Grant Campbell *et al.*(UoM) and Satake, who provided guidance and facilities for preparation of milled plant materials, Dr. Paul Royall (KCL) and Dr. Simon Gaisford (UCL) who allowed me to use DSC equipment, and RHM analytical services who carried out the proximate analysis.

Finally, I am forever grateful to my boyfriend Alan who has patiently put up with many early starts, sleepless nights, monologues and mood swings, and to my friends and family, especially Mamma, Pappa, Christina, Camilla and Bestemor who have all inspired and encouraged me through difficult times.

ORAL PRESENTATIONS

“A novel method for classifying starch digestion using first-order enzyme kinetics”

NABIM, R&D Seminar, 3rd December 2013, London, UK

“The structural role of fibre- considerations for healthier processed products”

Biosciences KTN Early Careers Researchers Event, 23rd May 2013, London, UK

Awarded prize for oral presentation (from Heinz)

“The role of plant cell walls in influencing starch bioaccessibility and digestion:

An in vitro, in vivo and in silico approach”

Diabetes and Nutritional Sciences Symposium, 22nd May 2013, London, UK

Awarded prize for best oral presentation (Yakult)

“Insight into the structural role of dietary fibre and its implications for nutrient

bioaccessibility: An in vitro, in vivo and in silico approach”

2nd International Conference on Food digestion, 6th - 8th March 2013, Madrid, Spain

“The role of plant cell walls in nutrient bioaccessibility of starch-rich foods”

NABIM, R&D Seminar, 12th November 2012, London, UK

“Role of plant cell walls in nutrient bioaccessibility of starch-rich foods”

Premier Strategic Innovation team, 18th October 2012, St Albans, UK

“The structural role of dietary fibre: Implications for processing of healthier products”

Plant and Seaweed Polysaccharides symposium, 17th-20th July 2012, Nantes, France

“Manipulating the bioaccessibility of starch-rich foods”

DRINC 8th Dissemination event, 15th-16th May 2012, Leeds, UK

POSTER PRESENTATIONS

"Ileostomy study of wheat starch bioaccessibility and glycaemia"

DRINC 10th Dissemination event, 27th- 28th November 2013, Nottingham, UK

Highly commended

"Chickpea cells as potential low Glycaemic Index ingredients"

NutraFormulate, 20th-21st March 2013, Birmingham, UK

"Modelling starch digestion in complex plant foods"

DRINC 9th Dissemination event, 5th- 6th February 2013, Bristol, UK

"Why do chickpeas have a low GI? -The role of plant cell walls"

DRINC 7th Dissemination event, 12th- 13th October 2011, Manchester, UK

Runner-up prize awarded for best poster

"Amylase interactions with encapsulated starch"

DRINC 6th Dissemination event, 13th-14th April 2011, Bristol, UK

"Mechanisms of amylase digestion of plant tissue: The role of cell walls"

Natural Food Biopolymers Meeting, 8th-9th June 2011, Norwich, UK

"Mechanisms of amylase digestion of plant tissue"

School of Medicine Graduate Showcase, 17th June 2011, London, UK

"Amylase diffusion in an alginate model system"

DRINC 5th Dissemination event, 20-21st October 2010, Birmingham, UK

PUBLICATIONS

Edwards CH, Warren FJ, Milligan PJ, Butterworth PJ, Ellis PR (2014) A novel method for classifying starch digestion by modelling the amyololysis of plant foods using first-order enzyme kinetic principles. *Food & Function*. DOI: 10.1039/C4FO00115J

Lovegrove A, **Edwards CH**, *et al.* (2014) Role of Polysaccharides in Food, Digestion and Health. *Critical Reviews in Food Science and Nutrition* (*accepted manuscript*).

Butterworth PJ, Warren FJ, **Edwards CH**, Grassby T, Patel H, Ellis PR (2012) How analysis of data from alpha-amylase catalysed starch digestibility performed in vitro contributes to an understanding of rates and extent of digestion starchy foods in vivo. *The FASEB Journal* **26**(1_MeetingAbstracts), 638.9.

Grassby T, **Edwards CH**, Grundy M, Ellis PR (2013) Functional components and mechanisms of action of 'dietary fibre' in the upper gastrointestinal tract: Implications for health. In 'Stability of Complex Carbohydrate Structures: Biofuels, Foods, Vaccines and Shipwrecks.' Ed. SE Harding. (RSC).

TABLE OF CONTENTS

Preface	iii
Abstract	iv
Acknowledgements	v
Oral Presentations	vi
Poster Presentations	vii
Publications	viii
Table of Contents	9
List of Figures	14
List of Tables	17
List of Equations	18
Abbreviations	19
Symbols	22
Chapter 1: Introduction & Literature Review	24
1.1 INTRODUCTION AND PROJECT OVERVIEW.....	25
1.1.1 Outline of the thesis	26
1.2 LITERATURE REVIEW.....	27
1.2.1 Nutritional significance of starch and plant cell walls	27
1.2.2 Introduction to bioavailability and bioaccessibility	29
1.2.3 Factors that influence starch digestibility and bioaccessibility	31
1.2.4 Botanical classification of starch-rich crops	33
1.2.5 Edible-plants: structural hierarchy.....	35
1.2.6 Starch	39
1.2.6.1 Composition and structure	40
1.2.6.2 Enzymic degradation of starch.....	42
1.2.6.3 Starch swelling, gelatinisation and retrogradation.....	46
1.2.7 Plant cell walls	48
1.2.7.1 Composition and structure	48
1.2.7.2 Enzymic degradation of cell walls	53
1.2.7.3 Cellular integrity and permeability	54
1.2.8 Digestion, metabolism and health	56
1.2.8.1 Digestion in Humans and Physiological aspects	56
1.2.8.2 Glucose homeostasis and Implications for health	62
1.2.8.3 Experimental Digestion Models.....	64
1.2.9 Proposed role of cell walls in starch bioaccessibility.....	66
1.2.10 Relevance of this study	68
1.2.10.1 Aim & Objectives.....	69

Chapter 2: Materials & Methods	70
2.1 PLANT MATERIALS	71
2.1.1 Starches	71
2.1.2 Milled fractions	72
2.1.3 Separated cells.....	76
2.1.4 Protoplasts	78
2.2 CHEMICAL REAGENTS.....	79
2.3 CHEMICAL ANALYSIS	80
2.3.1 Proximate analysis	80
2.3.2 Moisture determination.....	81
2.3.3 Total starch determination.....	82
2.3.4 Sugar determination.....	86
2.3.4.1 DNS assay	86
2.3.4.2 Glucose oxidase.....	87
2.3.4.3 Prussian blue assay.....	87
2.4 MICROSTRUCTURAL ANALYSIS	88
2.4.1 Light microscopy	88
2.4.2 Scanning electron microscopy	91
2.4.3 Thermal cross-polarised microscopy	91
2.5 DETERMINATION OF CELL WALL POROSITY.....	92
2.6 DIFFERENTIAL SCANNING CALORIMETRY	94
2.7 <i>IN VITRO</i> DIGESTIBILITY ASSAY	96
2.8 MULTI-COMPARTMENT DIGESTION MODEL	98
2.9 LOGARITHM OF SLOPE ANALYSIS	98
2.10 ILEOSTOMY STUDY	99
2.11 STATISTICAL AND GRAPHICAL SOFTWARE	99
Chapter 3: Characterisation of Test Materials	100
3.1 INTRODUCTION.....	101
3.1.1 Objectives.....	101
3.2 MATERIALS AND METHODS	102
3.2.1 Plant materials.....	102
3.2.2 Geometric model of cell rupture	102
3.2.3 Proximate analysis	103
3.2.4 Starch damage and amylose-amylopectin ratio.....	103
3.2.5 Cell wall analysis	104
3.2.6 Microscopy	104
3.2.7 Estimation of cell wall porosity	104
3.2.8 Gelatinisation behaviour.....	105
3.2.9 Digestibility assays of native and processed starch and flours.....	105

3.3	RESULTS.....	106
3.3.1	Proximate analysis	106
3.3.2	Starch characteristics	107
3.3.3	Structural characteristics of isolated cells	108
3.3.4	Structural characteristics of milled materials.....	109
3.3.5	Geometric model: Particle size and cellular integrity	112
3.3.6	Cell wall analysis	114
3.3.7	Cell wall pore size	114
3.3.8	Starch gelatinisation behaviour	117
3.3.9	Effect of endogenous compounds <i>on in vitro</i> digestibility	118
3.4	DISCUSSION.....	120
3.5	CONCLUSIONS.....	125
Chapter 4: <i>In Vitro</i> Structure-Function Studies		126
4.1	INTRODUCTION.....	127
4.1.1	Objectives.....	129
4.2	MATERIALS AND METHODS	129
4.2.1	Plant materials.....	129
4.2.2	Digestibility assays	130
4.2.2.1	Experiment I: Effect of cell wall encapsulation on starch digestion kinetics	130
4.2.2.2	Experiment II: Rupturing cells after hydrothermal processing	131
4.2.3	Microscopy	132
4.2.4	FITC-amylase diffusion	132
4.2.5	Differential scanning calorimetry and observations of birefringence	133
4.3	RESULTS.....	134
4.3.1	Effect of altering the proportion of encapsulated starch on digestibility	134
4.3.2	Cell wall permeability to FITC-amylase.....	137
4.3.3	Starch digestibility in homogenised materials	137
4.3.4	Extent of starch gelatinisation	142
4.4	DISCUSSION.....	144
4.5	CONCLUSIONS.....	149
Chapter 5: A Predictive Model of Starch Digestion		150
5.1	INTRODUCTION.....	151
5.1.1	Objectives.....	153
5.2	METHODS	154
5.2.1	Plant materials.....	154
5.2.2	Digestibility assays	154
5.2.3	Theory of LOS analysis.....	155
5.2.4	Mathematical model	157
5.2.5	Hydrolysis Index.....	158

5.2.6	Statistical and Graphical analysis	159
5.3	RESULTS.....	160
5.3.1	Experimental digestibility curves	160
5.3.2	LOS plots.....	161
5.3.3	Residual analysis of model performance	166
5.3.4	Analysis of starch digestion mechanisms from computed curves	169
5.4	DISCUSSION.....	172
5.5	CONCLUSIONS.....	175
Chapter 6: Digestibility Studies in a Multi-Compartmental Gut Model		176
6.1	INTRODUCTION.....	177
6.1.1	Objective	178
6.2	MATERIALS AND METHODS	179
6.2.1	Test meals.....	179
6.2.2	Digestion protocol.....	180
6.2.3	Sample collection and analysis	183
6.2.4	Data analysis.....	183
6.3	RESULTS.....	184
6.4	DISCUSSION.....	191
6.5	CONCLUSIONS.....	195
Chapter 7: <i>In Vivo</i> Effects on Postprandial Metabolism		196
7.1	INTRODUCTION.....	197
7.1.1	Nutrient absorption and post-prandial metabolism	197
7.1.2	Digestion of starch-rich foods in the gastro-intestinal tract	200
7.1.3	The ileostomy model	201
7.1.4	Hypothesis.....	204
7.1.5	Objectives.....	204
7.2	METHODS	205
7.2.1	Ethical considerations	205
7.2.2	Study design.....	205
7.2.2.1	Power calculation	206
7.2.3	Subjects.....	206
7.2.4	Test meals.....	207
7.2.4.1	Randomization and blinding.....	209
7.2.5	Study protocol, sample collection and analysis	209
7.2.6	Meals provided during study visits	211
7.2.7	Data processing and statistical analysis	212
7.3	RESULTS.....	213
7.3.1	Subject details	213

7.3.2	Postprandial responses measured in peripheral blood.....	216
7.3.2.1	Effects on glucose, insulin and C-peptide.....	216
7.3.2.2	Effects on TAG and NEFA	219
7.3.2.3	Effects on gut hormones	221
7.3.3	Ileal output & meal transit.....	223
7.3.4	Starch and sugar recovery	225
7.3.5	Micro-structural observations	227
7.4	DISCUSSION.....	231
7.5	CONCLUSIONS.....	237
Chapter 8: General Conclusions.....		238
8.1	EFFECT ON STARCH DIGESTION KINETICS	239
8.1.1	Cell walls as barriers	242
8.1.2	Cell walls restrict starch gelatinisation	244
8.2	EFFECTS ON POST-PRANDIAL METABOLISM.....	246
8.3	NUTRITIONAL SIGNIFICANCE.....	249
8.4	APPLICATIONS	250
8.5	RECOMMENDATIONS.....	251
8.6	CONCLUSIONS.....	252
References.....		253
Appendices.....		273
	Appendix A: Participant information sheet	274
	Appendix B: Subject screening process	279
	Appendix C: Preparation of test meals	281
	Appendix D: Blood sample collection, processing and analysis	283
	Appendix E: Ileal effluent sample collection, processing and analysis	287
	Appendix F: Meals options for study visit menu.....	289

LIST OF FIGURES

Figure 1.1: Taxonomy classification of common legume crops.....	34
Figure 1.2: Taxonomy classification of common cereal crops.....	35
Figure 1.3: Structural hierarchy of starch-rich crops.....	36
Figure 1.4: Monocot and dicot seed anatomy.....	37
Figure 1.5: Tissue structure of chickpea and durum wheat after hydrothermal processing.	38
Figure 1.6: Starch granular architecture.	42
Figure 1.7: Enzymic degradation of amylose and amylopectin in starch.....	44
Figure 1.8: Stereo drawing of human pancreatic α -amylase molecule.....	46
Figure 1.9: Schematic showing layers of the plant cell wall.....	49
Figure 1.10: Cell wall composition of fruit and vegetables (Type 1), and cereals (Type 2).....	52
Figure 1.11: Structural architecture of Type 1 and 2 cell walls.	53
Figure 1.12: Schematic showing tissue tendency to fracture and separate.	54
Figure 1.13: Digestion of carbohydrate foods in the human gastrointestinal tract.....	58
Figure 1.14: Digestion and absorption of starch hydrolysis products.	60
Figure 1.15: Role of insulin and glucagon in glucose homeostasis.	62
Figure 2.1: Wheat grain layers and de-branning effects.....	72
Figure 2.2: Satake test-roller mill and disposition.	74
Figure 2.3: Particle size and cellular integrity	75
Figure 2.4: Preparation of separated cells from chickpeas.....	76
Figure 2.5: Fresh and dried separated cells.	78
Figure 2.6: High-throughput total starch determination.	83
Figure 2.7: Iodine-stained high amylose and high amylopectin starch.....	90
Figure 2.8: Starch granules under cross-polarised light before after hydrothermal treatment. .	91
Figure 2.9: Fluorescein isothiocyanate (FITC) conjugation to protein.	92
Figure 2.10: Schematic of a DSC heat-flux instrument.....	95
Figure 2.11: Example thermogram for starch gelatinisation in milled plant tissue.....	96
Figure 3.1: Separated cells obtained from durum wheat and chickpea.....	108
Figure 3.2: Light micrographs of native flour and starch from chickpea and durum wheat	109
Figure 3.3: SEM of native milled endosperm and cotyledon	110

Figure 3.4: Hydrothermally processed milled chickpea and durum wheat tissue.....	111
Figure 3.5: Fluorescence micrographs showing permeability of chickpea to FITC-dextrans. .	115
Figure 3.6: Fluorescence micrographs showing permeability of wheat to FITC-dextrans.....	116
Figure 3.7: Birefringence of raw and processed starches from durum wheat and chickpea...	117
Figure 3.8: Birefringence of starch in raw and processed milled chickpea and durum wheat.	118
Figure 3.9: Digestibility curves obtained for native starch and flour of chickpea and wheat. .	119
Figure 3.10: Digestibility of processed starch and flours of chickpea and durum wheat.	120
Figure 4.1: Effect of milling on starch digestibility in processed durum wheat and chickpea. .	135
Figure 4.2: Digestibility curve showing limited starch digestion in processed chickpea cells..	135
Figure 4.3: Digestibility curves and light micrographs of intact cells and protoplasts.....	136
Figure 4.4: Hydrothermally processed chickpea cells and milled wheat with FITC-amylase. .	137
Figure 4.5: Light micrographs of homogenised macroparticles of hydrothermally processed durum wheat before and after <i>in vitro</i> digestion.	138
Figure 4.6: Effect of homogenisation after boiling on starch digestion in durum wheat.	139
Figure 4.7: Effect of homogenisation after boiling on starch digestion in chickpea.	140
Figure 4.8: Light micrographs of homogenised macroparticles of hydrothermally processed chickpea before and after 6 h <i>in vitro</i> digestion.....	141
Figure 4.9: Gelatinisation endotherms of milled size fractions of chickpea and durum wheat	142
Figure 4.10: Effect of cell wall encapsulation on the extent of starch gelatinisation as observed by DSC for milled chickpea and durum wheat.	144
Figure 5.1: Schematic showing how LOS plots are obtained from digestibility plots.....	156
Figure 5.2: Digestibility curves obtained for milled size fractions and starches of hydrothermally processed chickpea and durum wheat.	160
Figure 5.3: LOS plots obtained for hydrothermally processed starches and flours.	161
Figure 5.4: LOS plots obtained for various hydrothermally processed milled fraction.....	163
Figure 5.5: Contribution of each reaction phase to total starch breakdown for various size- fractions of chickpea and durum wheat	165
Figure 5.6: Time and size resolved residual plots for chickpea and durum wheat.	166
Figure 5.7: Bland-Altman plots of chickpea and durum wheat.	167
Figure 5.8: Example of model computed digestibility curve shown alongside a best-fit to experimental data and box-plot of pooled residuals.....	168

Figure 5.9: Effect of cellular integrity on starch hydrolysis index.	170
Figure 5.10: Correlation between extent of starch digestion and gelatinisation in chickpeas.	171
Figure 6.1: DGM mechanics	178
Figure 6.2: Overview of multi-compartment digestion system.	181
Figure 6.3: Light micrographs of <i>Porridge-O</i> and <i>Porridge-F</i> after cooking.....	184
Figure 6.4: Starch breakdown from chickpea digested in oral and gastric phases.	185
Figure 6.5: Effect of gastric retention time on chickpea cells from <i>Porridge-O</i>	186
Figure 6.6: Material recovered at end of duodenal digestion of <i>Porridge-O</i> and <i>Porridge-F</i>	187
Figure 6.7: Total extent of starch digestion after various gastric retention times for <i>Porridge-O</i> and <i>Porridge-F</i>	188
Figure 6.8: Duodenal starch digestibility curves obtained for <i>Porridge-O</i> and <i>Porridge-F</i>	188
Figure 6.9: LOS plots of duodenal starch digestibility curves for <i>Porridge-O</i> and <i>Porridge-F</i>	189
Figure 6.10: Experimentally obtained and model-computed duodenal starch digestibility curves for <i>Porridge-O</i> and <i>Porridge-F</i>	190
Figure 7.1: Gut hormones and their main functions.	199
Figure 7.2: Physiological aspects of an ileostomy.	202
Figure 7.3: Blood and effluent collection time points and meal times.....	210
Figure 7.4: Consort diagram.	214
Figure 7.5: Incremental glucose, insulin and C-peptide response after smooth and coarse porridge test meals.	217
Figure 7.6: Incremental TAG and NEFA response to smooth and coarse porridge meals.	219
Figure 7.7: Changes in plasma gut hormones after smooth and coarse porridge meals.	221
Figure 7.8: Day-time ileal excretion of fresh weight and moisture content of over 24 h.	224
Figure 7.9: Day-time excretion of dry matter and cumulative dry matter output over 24 h.	225
Figure 7.10: Day-time excretion of starch and cumulative starch excretion over 24 h.	226
Figure 7.11: Starch and sugar recovered at terminal ileum during day-time collection.	227
Figure 7.12: Colour change of ileal effluent over time.	227
Figure 7.13: Specimens of coarse and smooth porridge, before and after digestive transit. ...	228
Figure 7.14: Wheat particles from coarse porridge recovered from ileal effluent	229
Figure 7.15: Digested edge of wheat endosperm macro-particle recovered in ileal effluent... ..	230
Figure 7.16: Edible plant materials recovered in ileal effluent.	231

LIST OF TABLES

Table 1.1: Starch characteristics of durum wheat and chickpea	40
Table 1.2: List of common cell wall polysaccharides and their classification	50
Table 1.3: Overview of results from cell wall porosity studies	55
Table 1.4: Overview of major gastro-intestinal hormones	61
Table 2.1: Overview of resins and their properties	90
Table 3.1: Overview of fitc-dextran used in cell wall pore-size determinations	105
Table 3.2: Proximate analysis data obtained for raw chickpea materials	106
Table 3.3: Proximate analysis data obtained for raw durum wheat materials	107
Table 3.4: Starch characteristics	108
Table 3.5: Estimated number of cells in size fractions of milled durum wheat and chickpea ..	113
Table 3.6: Pectic and hemicellulosic polysaccharides in chickpea and wheat cell walls	114
Table 4.1: Overview of milled size fractions	129
Table 4.2: Gelatinisation parameters of size fractions of chickpea and durum wheat	143
Table 5.1: Values of variables estimated from LOS analysis	164
Table 5.2: Regression analysis of model-fit and best-fit to experimental data	168
Table 5.3: Hydrolysis index calculated in two different ways	169
Table 6.1: Nutrient composition of chickpea porridge	179
Table 6.2: Overview of sample collection from the gastric and duodenal models	182
Table 6.3: Parameters of duodenal starch digestibility estimated from LOS plots	190
Table 7.1: Test meal nutritional characteristics	208
Table 7.2: Characteristics of durum wheat particles used in test meals	209
Table 7.3: Nutrient intake during study visit	212
Table 7.4: Characteristics of the nine subjects included in the study	215
Table 7.5: Key parameters of the glycaemic and insulinaemic response to test meals	218
Table 7.6: Key parameters of the lipaemic response to test meals	220
Table 7.7: Key parameters of the gut hormone response to test meals	222
Table 7.8: Outcome measures in ileal effluent after smooth and coarse porridge	223

LIST OF EQUATIONS

Equation 2.1: Calculation of moisture content	82
Equation 2.2: Calculation of starch content.	85
Equation 2.3: Bi-phasic first-order equation	98
Equation 3.1: Surface area of cell and a macroparticle.....	102
Equation 3.2: Volume of a cell and a macroparticle.	102
Equation 3.3: Number of cells in particle volume.	103
Equation 3.4: Number of cells on particle surfaces.	103
Equation 3.5: Proportion of ruptured cells:	103
Equation 4.1: Terminal extent of gelatinisation.....	134
Equation 5.1: First-order equation	155
Equation 5.2: Derived first-order equation	156
Equation 5.3: Logarithmic form of the differentiated first-order equation	156
Equation 5.4: Two-phase equation.	157
Equation 7.1: Calculation of mean transit time.	213

ABBREVIATIONS

Abs	Absorbance
AMG	Amyloglucosidase
ANOVA	Analysis of variance
AOAC	Association of Analytical Communities
AUC	Area under the curve
BCA	Bicinchoninic acid
bioA	Bioaccessibility
BMI	Body mass index
CASE	Collaborative Awards in Science and Engineering
CCK	Cholecystokinin
CRF	Clinical Research Facilities
CUI	Centre for Ultrastructural Imaging (at King's College London)
Cv	Cultivar
Da	Dalton
DGM	Dynamic Gastric Model
DNS	Dinitrosalicylic acid
DPP-IV	Dipeptidyl peptidase-4 inhibitor
DRINC	Diet and Health Research Industry Club
DSC	Differential scanning calorimetry
DW	Dry weight
EC	Enzyme classification
EFSA	European Food Safety Authority
ELISA	Enzyme-Linked Immunosorbent Assay
FITC	Fluorescein isothiocyanate

FRAP	Fluorescence recovery after photobleaching
GI	Glycaemic Index
GIP	Glucose-dependent Insulinotropic peptide
GLP-1	Glucagon-Like peptide-1
GOPOD	Glucose-oxidase-peroxidase
GSTS	Guy's and St Thomas'
HI	Hydrolysis Index
HPLC	High performance liquid chromatography
HRP	Horseradish peroxidase
HSA	Human Salivary Amylase
iAUC	Incremental area under the curve
IFR	Institute of Food Research
KCL	King's College London
LOS	Logarithm of slope
MGAM	Maltase-Glucoamylase
MLE	Maximum likelihood estimation
MTT	Mean transit time
NEFA	Non-esterified fatty acids
NSP	Non-starch polysaccharide
PBS	Phosphate buffer saline
PEG	Polyethylene glycol
Porridge- F	Chickpea porridge prepared from freeze-milled cells
Porridge- O	Chickpea porridge prepared from intact cells
PPA	Porcine pancreatic α -amylase
PYY	Polypeptide YY
RDS	Rapidly digested starch (Englyst classification system)

RHM	Rank Hovis
RS	Resistant starch
SCFA	Short chain fatty acids
SD	Standard deviation
SDS	Slowly digested starch (Englyst classification system)
SDS PAGE	Sodium dodecyl sulphate polyacrylamide gel electrophoresis
SEE	Standard error of the estimate
SEM	Scanning electron microscopy
SEM	Standard error of the mean
SGLT-1	Sodium-glucose cotransporter
SIM	Static Intestinal Model
SSF	Simulated Salivary Fluid
TAG	Triacylglycerol
TEG	Terminal extent of gelatinisation
Total C_{∞}	Sum of $C_{\infty 1}$, $C_{\infty 2}$... etc.
UCL	University of London
UoM	University of Manchester

SYMBOLS

#D	Number of cells in particle depth
#H	Number of cells in particle height
#L	Number of cells in particle length
#S	Number of cells on particle surfaces
#V	Number of cells in particle volume
C_{∞}	Product concentration or amount of starch digested at end of digestion
$C_{1\infty}, C_{2\infty}, \dots$	Product concentration or amount of starch digested at end of phase 1, 2...
C_{int}	Product concentration or amount of starch digested at intersection
C_t	Product concentration or amount of starch digested at time, t .
cSA	Surface area of a cell assumed to be the shape of a rectangular prism
cV	Volume of a cell assumed to be the shape of a rectangular prism
dH_2O	Deionised water
d	Depth
D	Dimensions
h	Height
k, k_1, k_2, \dots	First-order rate constants (subscript numbers indicate reaction phase)
l	Length
n	Number
pSA	Particle surface area
pV	Particle volume
R^2	Co-efficient of determination
r^2	Pearsons' correlation co-efficient, squared
R_G	Radius of gyration
R_{HYD}	Hydrodynamic radius

s	Side length (median of sieve aperture range)
t	Time
T_c	Conclusion temperature
t_{int}	Time of intersection between to digestion phases
T_o	Onset temperature (of starch gelatinisation)
T_p	Peak temperature
$\Delta_{gel}H$	Enthalpy changes associated with gelatinisation
$\Delta_{gel}H_{sp}$	Specific enthalpy change association with gelatinisation of 1 g of starch
λ	Wavelength
♀	Female
♂	Male

CHAPTER 1

INTRODUCTION & LITERATURE REVIEW

1.1 INTRODUCTION AND PROJECT OVERVIEW

It has become increasingly clear that the structure and properties of foods play an important role in influencing their behaviour in the gastrointestinal tract and consequently, their effects on post-prandial metabolism. For example, the physico-chemical properties of foods are known to affect the rate and extent of digestion, absorption and bacterial fermentation of nutrients, such as starch and lipid. Moreover, with the increase in diet-related health problems, there is commercial interest in manipulating food structure and properties to facilitate the design of foods with enhanced nutritional properties. In order to do so, however, further understanding of what constitutes 'healthy food' is required.

The estimation of the nutritional value of food from nutrient-composition data alone is clearly limited, as foods with identical nutrient composition can elicit vastly different metabolic responses, with different consequences for health. It is well known for instance that similar foods containing isoglucidic amounts of starch can produce large variations in postprandial glycaemia; a metabolic response strongly linked to the time course of starch digestion.

Attenuating the fluctuations in postprandial glycaemia and insulinaemia has been shown to be important in the prevention of diet-related conditions such as Type 2 diabetes and cardiovascular disease (Jenkins *et al.* 2002). One important factor, which is the main topic of the current project, is the rate at which sugars become available (*'bioaccessible'*) for digestion and absorption. Accumulating evidence suggests that this process is influenced by the structural integrity of plant cell walls, which are a major source of dietary fibre; however, the underlying mechanisms are not yet fully understood. Therefore, this project was designed to provide new mechanistic insights into the role of plant cell walls in influencing the bioaccessibility of starch in edible plant tissues, and their potential to attenuate post-prandial glycaemia.

In this PhD project, a novel combination of *in vitro*, *in silico* and *in vivo* methods were used. This included studies of the structure, properties and digestibility of cell wall encapsulated starch in edible plant tissues and isolated cells, the development of a predictive model of starch digestion, and finally, a post-prandial study in ileostomy subjects. A comparison between chickpeas (legume) and durum wheat (cereal) is provided throughout this work to gain insight into the behaviour of cell walls and starches from different botanical sources. The proposed mechanisms by which plant cell walls may influence starch digestion kinetics and post-prandial glycaemia are discussed.

This PhD project was funded by the Biotechnology and Biological Sciences Research Council (BBSRC) and Premier Foods (industrial CASE partner) and also contributed significantly to a broader, collaborative project (BB/H004866/1) funded by the Diet and Health Research Industry Club (DRINC) of the BBSRC.

1.1.1 OUTLINE OF THE THESIS

Chapter 1 introduces the research background. The limitations of previous studies are highlighted through a critical review of the relevant literature. These are reflected in the project aims and objectives, which are clearly stated at the end of this Chapter.

Chapter 2 provides an overview of the origin and preparation of the experimental plant-materials, chickpeas and wheat durum, and contains details of the methodologies used throughout this work.

Chapter 3 describes relevant physico-chemical characteristics of the experimental plant materials, which facilitates interpretation of results reported in subsequent chapters.

Chapter 4 presents results from a range of *in vitro* structure-function studies. These studies were designed to determine the role of cell walls in influencing starch digestion

kinetics, and also to explore a number of potential mechanisms by which cell walls may influence starch bioaccessibility.

Chapter 5 describes the development and application of a mathematical model, based on first-order enzyme kinetic principles. This model was used to facilitate the analysis of *in vitro* starch digestibility data obtained for chickpea and durum wheat tissues with varying degrees of structural integrity (i.e. cell wall encapsulation).

Chapter 6 presents the results from starch digestibility studies carried out in a multi-compartment digestibility model, in which the effect of oral, gastric and duodenal digestion on starch bioaccessibility in chickpeas was evaluated.

Chapter 7 describes the results from an *in vivo* ileostomy study carried out to investigate the role of starch bioaccessibility in influencing the post-prandial blood glucose, insulin, lipid and gut hormone responses, and provides insight into the structural breakdown of wheat following digestion in the upper-gastrointestinal tract.

Chapter 8 brings together the general conclusions from the various studies conducted as part of this PhD project and suggests recommendations for further work.

1.2 LITERATURE REVIEW

1.2.1 NUTRITIONAL SIGNIFICANCE OF STARCH AND PLANT CELL WALLS

Starch is an important 'glycaemic' dietary carbohydrate that provides about 45-60% of total dietary energy (EFSA NDA Panel 2010a). During digestion, glucose ('sugar') is released from starch via the action of salivary and pancreatic α -amylase and brush-border enzymes, and then absorbed and metabolised under endocrine (e.g., insulin) regulation to provide energy, or stored as glycogen in liver and muscle (*Section 1.2.8.2.*). The rate and extent of starch digestion is, however, highly variable, and as a result, foods that contain the same amount of starch can elicit vastly different postprandial blood glucose responses (Foster-Powell *et al.* 2002, Jenkins *et al.* 1984).

The postprandial blood glucose response is currently of great interest with regard to public health. For instance, the consumption of starch-rich foods that elicit a large glycaemic response (including many cereal products such as wheat bread) is generally associated with an increased risk of developing type 2 diabetes and cardiovascular disease (*Section 1.2.8.2*), whereas low glycaemic foods (including chickpeas and other pulses) may be recommended for the management and prevention of these conditions (Foster-Powell *et al.* 2002, Jenkins *et al.* 2002). Thus, some sources of starch may be of potential benefit to health, whereas other dietary sources are viewed more negatively. However, it remains difficult to predict the metabolic response to starch from compositional data alone, because of the many factors which influence its digestion and absorption (*Section 1.2.3*).

Plant cell walls are the major components of 'dietary fibre', (i.e., "carbohydrate polymers that are neither digested nor absorbed in the small intestine), and although not nutrients *per se*, plant cell walls are important for gut motility and bowel health (Mann and Cummings 2009, Kendall *et al.* 2010). Plant cell walls, like starch, are also comprised predominantly of carbohydrates, referred to as non-starch polysaccharides (NSPs), but provide relatively small amounts of metabolisable energy (Cummings 1983). The Guideline Daily Amount (GDA) for fibre (stipulated by the European Food Safety Authority, 'EFSA') is currently 24 g/d, which is adequate to maintain normal laxation in most adults, although consumption of more than 25 g/d may have additional benefits with regard to prevention and management of diet and lifestyle related diseases (EFSA NDA panel 2010a). The consumption of fibre has, for instance, been associated with beneficial effects on satiety, blood cholesterol and glucose regulation, and gastro-intestinal microbiota (Brownlee 2011, Anderson *et al.* 2009, Kendall *et al.* 2010); however there is currently insufficient evidence to support most of the health claims of dietary fibre (EFSA NDA panel 2010b).

Thus, starch and plant cell walls are both major dietary constituents of recognised nutritional importance, particularly with regard to glycaemic regulation and bowel function. The mechanisms by which starch and plant cell walls exert these beneficial effects, however, are not fully understood. This thesis is focussed on the specific role of fibre in the form of intact plant cell walls in limiting the availability of starch for digestion and absorption.

1.2.2 INTRODUCTION TO BIOAVAILABILITY AND BIOACCESSIBILITY

It is well-established that a variable proportion of nutrients contained within a food are not absorbed during digestive transit. This has important implications for the nutritional value of food, but is not reflected in current nutrition labelling systems.

The term '*bioavailability*' is used to describe the proportion of nutrients contained in food that are actually absorbed and utilised. In order for nutrients to be absorbed, they must first be exposed to digestive enzymes that break-down macronutrients into smaller units that can be transported across the brush-border of the small intestine. Nutrients that have been released from the food matrix and have the potential to be absorbed are said to be '*bioaccessible*'. Thus, bioaccessibility is an important prerequisite for bioavailability, i.e., nutrients must be available for digestion in order to be subsequently absorbed.

The term '*bioaccessibility*' has previously been defined as "*the release of nutrients (e.g., starch, lipid, micro-nutrients) from a food matrix during digestion*" (Ellis *et al.* 2004, Parada and Aguilera 2011). However, this original definition is somewhat misleading, especially in the context of this thesis, where it is demonstrated that starch granules do not necessarily have to be *released* from the food matrix in order to be digested, for instance, because some food matrices allow ingress of digestive enzymes. Therefore, to reflect the nature of events involved in the digestion of the starch-rich plant materials used in this work, bioaccessibility will be re-defined to describe *the exposure of nutrients to digestive fluids*. This can occur by ingress of

digestive fluids into the food matrix, or by the release of entrapped nutrients from the food matrix.

Bioaccessibility and bioavailability are both important concepts in nutrition, because it is only the absorbed nutrients that elicit a post-prandial response. Currently, however, consumers, dieticians and nutritionists still rely largely on nutrient composition data to estimate the nutritional and energy value of food. Although some efforts have been made to account for differences in bioavailability of carbohydrates when estimating their energy contributions, the factors used (e.g., based on the Atwater system), are too generic and do not provide an accurate indication of nutritional value (Livesey *et al.* 2000). While the limitations of these composition-based systems are recognised, they remain in use because a suitable alternative is not yet available.

In order to develop new systems that better predict the nutritional value of food there is a need to improve understanding of the factors and mechanisms involved in the digestion and absorption of nutrients. This presents a major challenge, because there are so many factors that can influence nutrient bioaccessibility and bioavailability, including physico-chemical properties of food and the site in the gastro-intestinal tract at which nutrients become available for absorption (*Section 1.2.3*).

This thesis is focussed on starch *bioaccessibility* (rather than *bioavailability*), because, in the context of this work, the exposure of starch to digestive enzyme (α -amylase) is thought to be a key rate-limiting step that strongly influences post-prandial glycaemia, whereas the subsequent absorption of sugars (products of starch digestion) is likely to be relatively unhindered. Throughout this work, the mechanisms by which cell walls influence starch bioaccessibility in chickpeas and durum wheat will be investigated. These are both widely-consumed dietary sources of starch, but have some contrasting properties, especially with regard to their glycaemic potential and plant cell wall properties, which makes them particularly interesting plant species for comparison.

1.2.3 FACTORS THAT INFLUENCE STARCH DIGESTIBILITY AND BIOACCESSIBILITY

The release of sugar products from starch hydrolysis during digestion is largely influenced by the physico-chemical properties of starch, which vary between starches of different botanical origin (Gallant *et al.* 1992, Güzel and Sayar 2010, Wang *et al.* 1998). The raw 'native' starches have a highly-ordered structure that is not very susceptible to digestion (e.g., by α -amylase) (*Section 1.2.6.1*). Although some starches that are eaten retain their native structure (e.g., bananas, bread crust), many starch-rich foods contain starch granules that have undergone major physico-chemical changes as a result of food processing. For instance, food products that are hydrothermally processed may contain 'gelatinised' starch, which has a highly amorphous structure (*Section 1.2.6*) and is far more susceptible to amylolysis than the native form (Slaughter *et al.* 2001, Tahir *et al.* 2010). Hence, once gelatinised, the physico-chemical characteristics of native starches become less relevant, and the differences in digestibility of starches from different botanical sources become less pronounced (Slaughter *et al.* 2001).

When starch is consumed as part of a food, other components that are present may influence its bioaccessibility (Parada and Aguilera 2011). Compounds that interfere with the digestion and/or absorption of nutrients are collectively referred to as 'anti-nutritional factors'. In wheat grains and legume seeds, proteinaceous enzyme inhibitors (e.g., albumin and gliadin inhibitors) and a range of polyphenolic compounds have been shown to limit starch digestion (Rehman and Shah 2005, Würsch *et al.* 1986, Singh *et al.* 1982). However, the potential of inhibitory proteins to severely restrict starch digestion *in vivo* is likely to be somewhat limited, because they are generally thermally unstable and susceptible to gastric proteases (e.g. pepsin) (Buonocore *et al.* 1977, Würsch *et al.* 1986, Frias *et al.* 2000).

With regard to the hydrothermally processed plant tissues that are used as experimental materials in this thesis; a more significant factor that is likely to influence

starch bioaccessibility is the 'dietary fibre' component of food. Different definitions of dietary fibre are used in the literature, but EFSA currently define fibre as "*carbohydrate polymers with three or more monomeric units which are neither digested nor absorbed in the human small intestine*" (EFSA NDA panel 2010a). Notably, this definition includes cell wall polysaccharides (e.g., cellulose, hemi-celluloses, pectins, and lignin), but also includes *resistant starch* (i.e., starch that escapes digestion and absorption in the small intestine) and other resistant oligosaccharides (e.g., fructo- and galacto-oligosaccharides, and inulin). Hence, 'dietary fibre' is a generic term that encompasses a broad range of substances that may influence starch bioaccessibility by different mechanisms (Grassby *et al.* 2013).

The effects of 'dietary fibre' in decreasing the bioaccessibility of starch may be related, in part, to the role of fibre in regulating gastro-intestinal function and motility (Parada and Aguilera 2011, Brownlee 2011); however, there are now a number of studies that have demonstrated more specific effects of individual fibre components. These previous studies have focussed largely on the role of specific cell wall polysaccharides (the so-called 'soluble-fibres') such as guar galactomannan and mixed linkage β -glucan, that can generate high levels of viscosity in the gastro-intestinal tract (Cui and Wang 2009). Soluble fibres have been shown to influence digestion, leading to an attenuation of post-prandial blood glucose and insulin responses, and have also been used for therapeutic purposes (Ellis 1999, Würsch and Pi-Sunyer 1997, Judd and Ellis 2005). There have been relatively few studies, however, on the effects of structurally intact cell walls that encapsulate nutrients in edible-plant tissues. The cell wall matrices of many edible plant tissues are largely 'insoluble' and, as far as it is known, resistant to digestion in the upper gastro-intestinal tract. Hence, the encapsulation of nutrients within plant cell walls is likely to limit the bioaccessibility of nutrients *in vivo* (Ellis 1999, Tydeman *et al.* 2010, Berry *et al.* 2008).

Indeed, the structural integrity of the food matrix has been identified as a major factor that influences nutrient bioaccessibility (Bjorck *et al.* 1994). For instance, foods containing intact macro-particles (e.g. pumpernickel-style bread or spaghetti) have been shown to elicit a significantly lower glycaemic response than a de-structured equivalent (e.g. whole meal bread or chopped spaghetti) (Liljeberg H 1992, Granfeldt and Björck 1991). This could be attributed to differences in particle size, which is known to influence starch digestion kinetics and post-prandial glycaemia, presumably because of the effective surface area available for enzyme ingress (Mahasukhonthachat *et al.* 2010, Al-Rabadi *et al.* 2012, Al-Rabadi *et al.* 2009, Ranawana *et al.* 2011). Alternatively, these results may be explained by the greater proportion of intact cells (with encapsulated starch) that are likely to be present in larger particle sizes (Berry *et al.* 2008).

Current understanding of food structural characteristics and the behaviour of various food matrices during processing and digestion is limited, and the diversity of starch-rich foods presents a major challenge. This thesis will focus mainly on the role of cell walls that physically encapsulate starch in limiting starch bioaccessibility. The comparison of starch bioaccessibility in chickpeas and durum wheat, which have contrasting cell wall and glycaemic properties, is therefore of great interest.

1.2.4 BOTANICAL CLASSIFICATION OF STARCH-RICH CROPS

Pulses (e.g., chickpeas) and cereals (e.g., wheat), along with tubers (e.g., potato), are the main dietary sources of starch (Wang *et al.* 1998). In order to understand how work on chickpeas and durum wheat may apply to other starch-rich plant tissues, it is useful to first consider the botanical classification of these species. Chickpeas, *Cicer arietinum* L., belong to the *Leguminosae*, also known as *Fabaceae*, family (see **Figure 1.1**). There are two main groups of chickpeas: *Kabuli*, which have a cream colour and originate from the Middle-East and Mediterranean region, and *Desi*, which have a wrinkled appearance and are of Indian origin (Singh and Diwakar 1995). Other

members of this family ('legumes') include plants whose starch-rich seeds are harvested dry (e.g., beans, lentils and other pulses), plants with oil-rich seeds (e.g., soybean, rapeseed, and peanuts), vegetables which are harvested fresh (peas and green beans), and leguminous seeds used for sowing purposes (e.g. alfa-alfa and red clover).

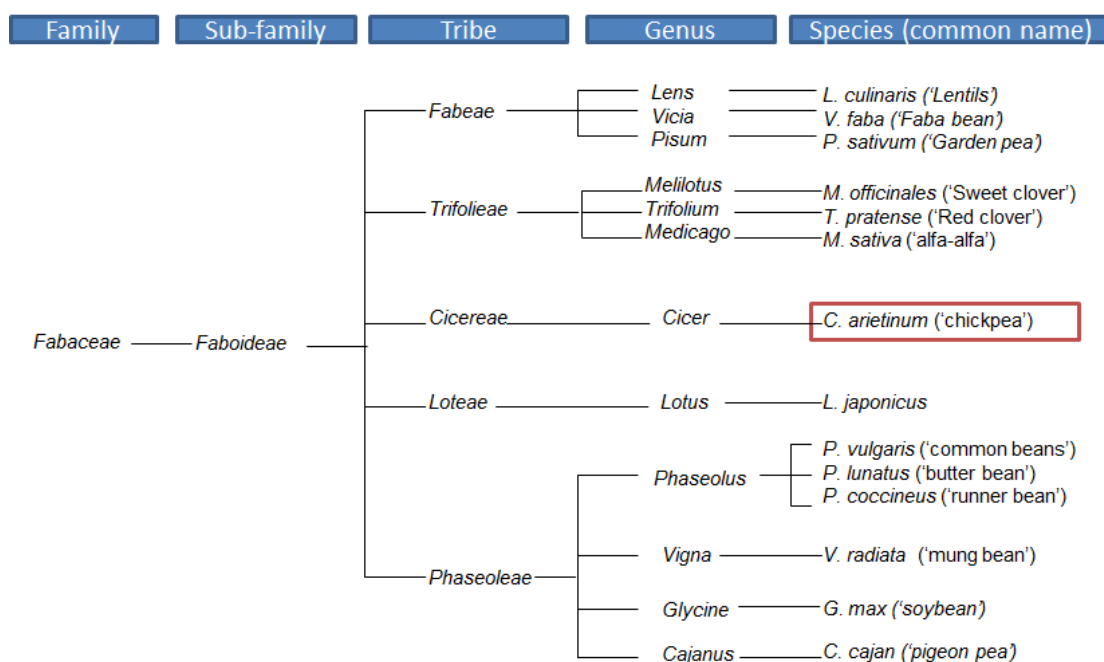


FIGURE 1.1: OVERVIEW OF THE TAXONOMY CLASSIFICATION OF SOME COMMON CROPS OF THE LEGUME (FABACEAE) FAMILY. This family contains 730 genera and over 19,400 species. Only some example species are shown (Choi *et al.* 2004) .

Durum wheat, *Triticum durum* L. (traditional classification) or *Triticum turgidum* var. *durum* (genetic classification) belongs to the *Gramineae* (also known as *Poaceae*) family (**Figure 1.2**). This family includes other common cereal crops, such as rice, maize, oats, rye, barley, and common wheat. In addition, tubers (e.g., potatoes, cassava, yam) are also rich in starch, but these species belong to various other families, and will not be discussed further.

Within the *Gramineae* and *Fabaceae* families, similarities exist in terms of nutrient composition, starch and cell wall structure, and physico-chemical properties. The specific characteristics of chickpeas and durum wheat will be described and compared

throughout this work, although many of their physico-chemical properties are likely to apply to related species within the same family.

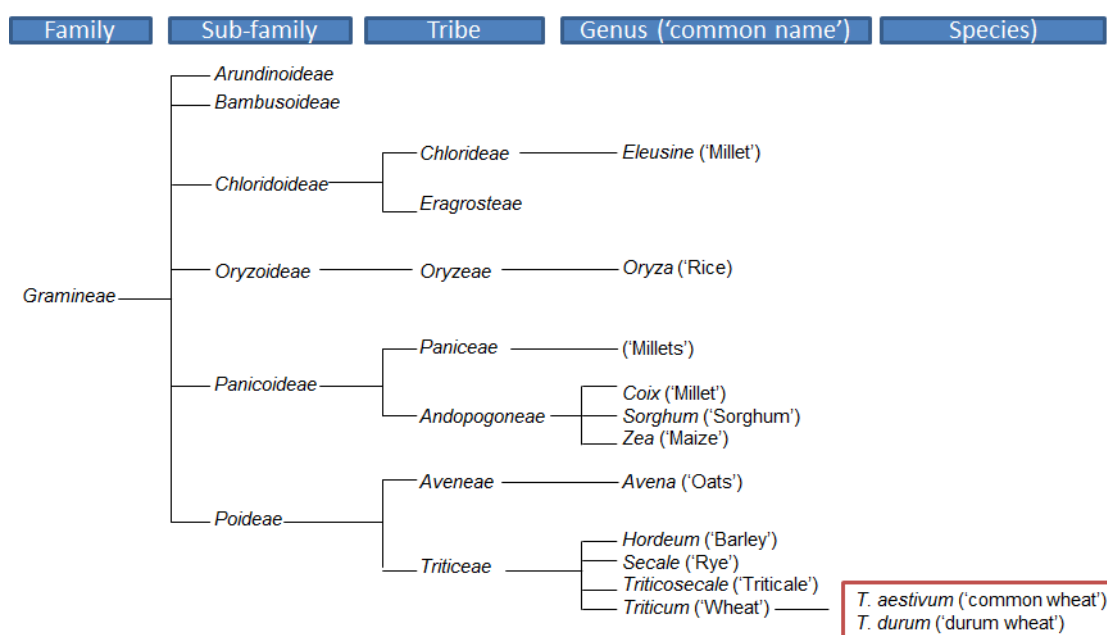


FIGURE 1.2: OVERVIEW OF THE TAXONOMY CLASSIFICATION OF SOME COMMON CEREALS. Only selected species of relevance to this thesis are shown (Kent and Evers 1994).

1.2.5 EDIBLE-PLANTS: STRUCTURAL HIERARCHY

In order to understand the role of plant structure in nutrient bioaccessibility, nutrients (e.g., starch) may be considered as part of a structural hierarchy (**Figure 1.3**), in which the molecular components are the building blocks which provide mechanical strength and physico-chemical properties. Comparison of not only the nutrient composition, but also the way in which these nutrients are assembled into cells, tissues and organs provides insight into how different plant materials might be broken-down during digestion and food processing.

For this purpose, the plant organ represents the highest level of structure described, because it is normally the starch-rich seeds (plant storage organs) of cereal and legume crops that are harvested for human consumption, and incorporated into foods (e.g., granary breads, baked beans).

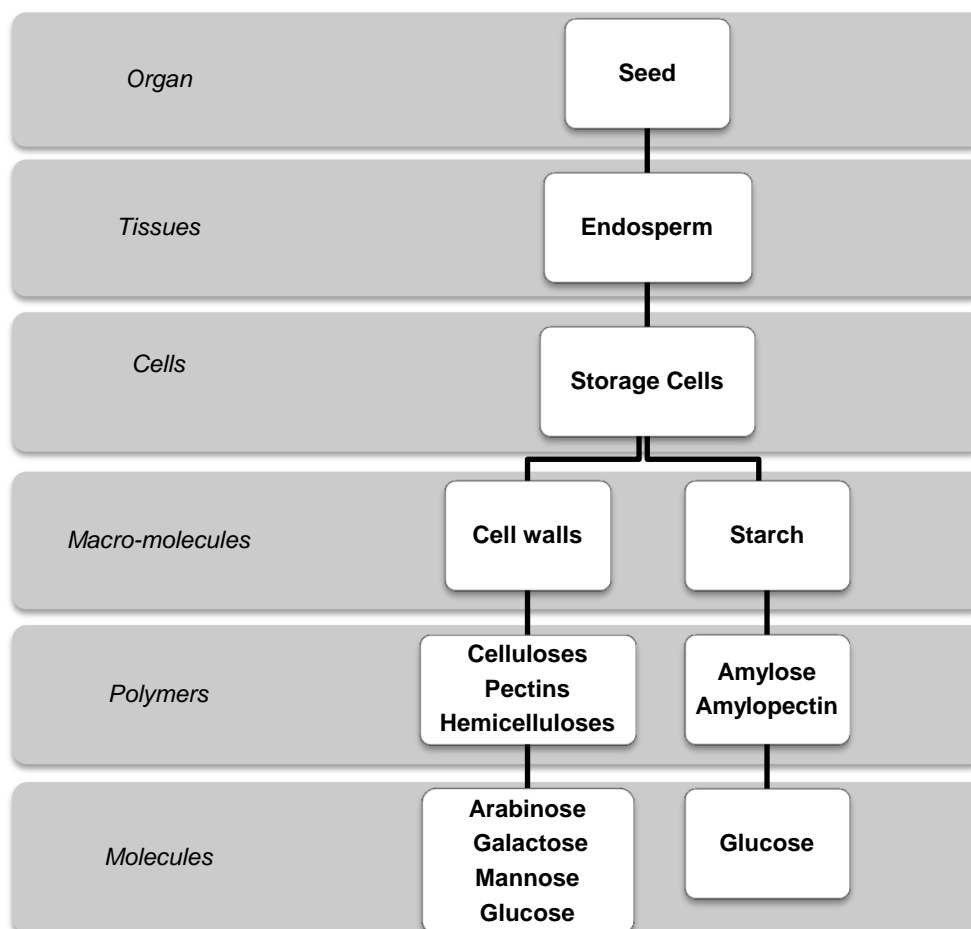
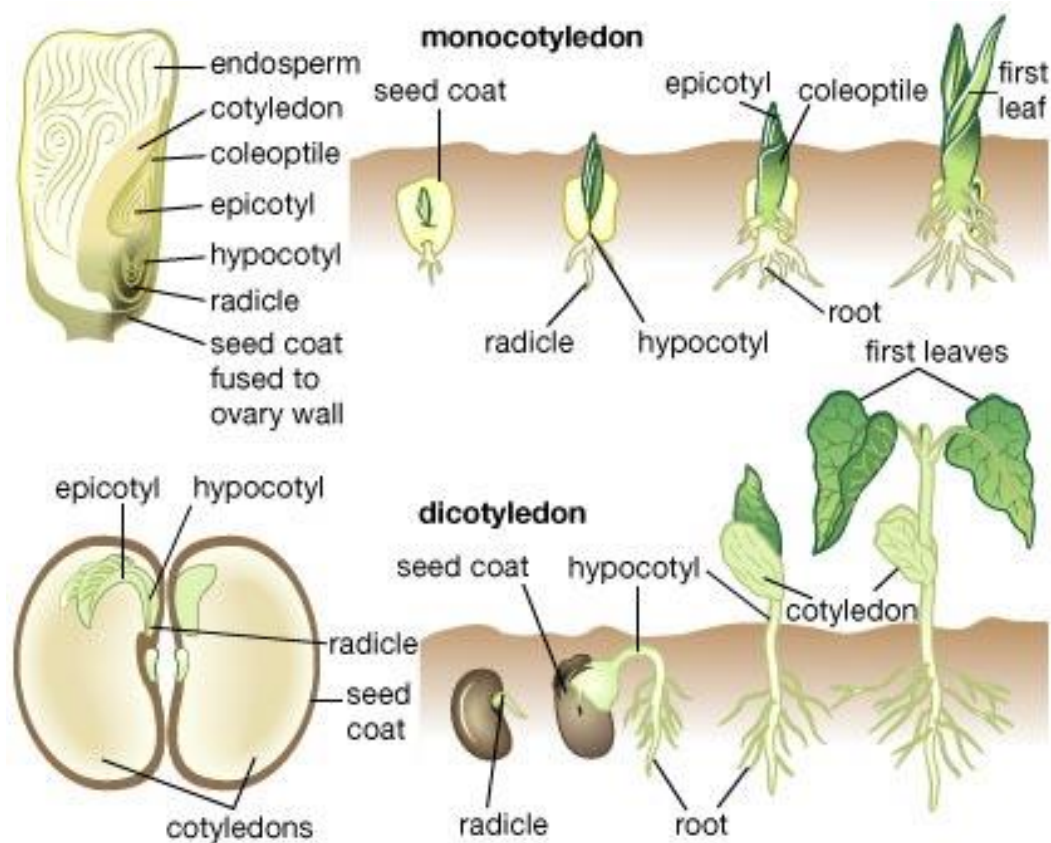


FIGURE 1.3: STRUCTURAL HIERARCHY OF STARCH-RICH CROPS. Shown from the level of the organ (cm), as this represents the highest level of structure that would normally be incorporated into food, down to molecules and individual sugar units (nm).

Seeds consist of three main parts; the embryo, starch-containing endosperm and the fibre-rich seed coat. There are well-known structural differences between the seeds of cereals and legumes (**Figure 1.4**). Cereals are commelinid monocots, and by definition, the seeds (i.e. grains) have only one cotyledon, in which the starch is stored in the endosperm tissue, which forms outside the embryo, but within the seed coat (testa). Most species of the legume family, on the other hand, are rosid eudicots ('dicot') and have two cotyledons, which contain the storage tissue.



© 2006 Merriam-Webster, Inc.

FIGURE 1.4: MONOCOT AND DICOT SEED ANATOMY. 'Monocotyledon' [online], 2006.

At the next level of this hierarchy are plant tissues: Within the harvested seeds, the starch-storage tissue (endosperm) occupies the largest area. In terms of nutrient composition, starch represents around 50 - 70% of the dry tissue weight. The storage tissue also contains protein and dietary fibre (plant cell walls) which provide mechanical strength and maintain the structural integrity of the tissue. The resilience of these tissues to processing and digestion may vary, but the storage tissues of durum wheat and chickpeas that were used in this PhD project remained largely intact after boiling, as shown in **Figure 1.5**.

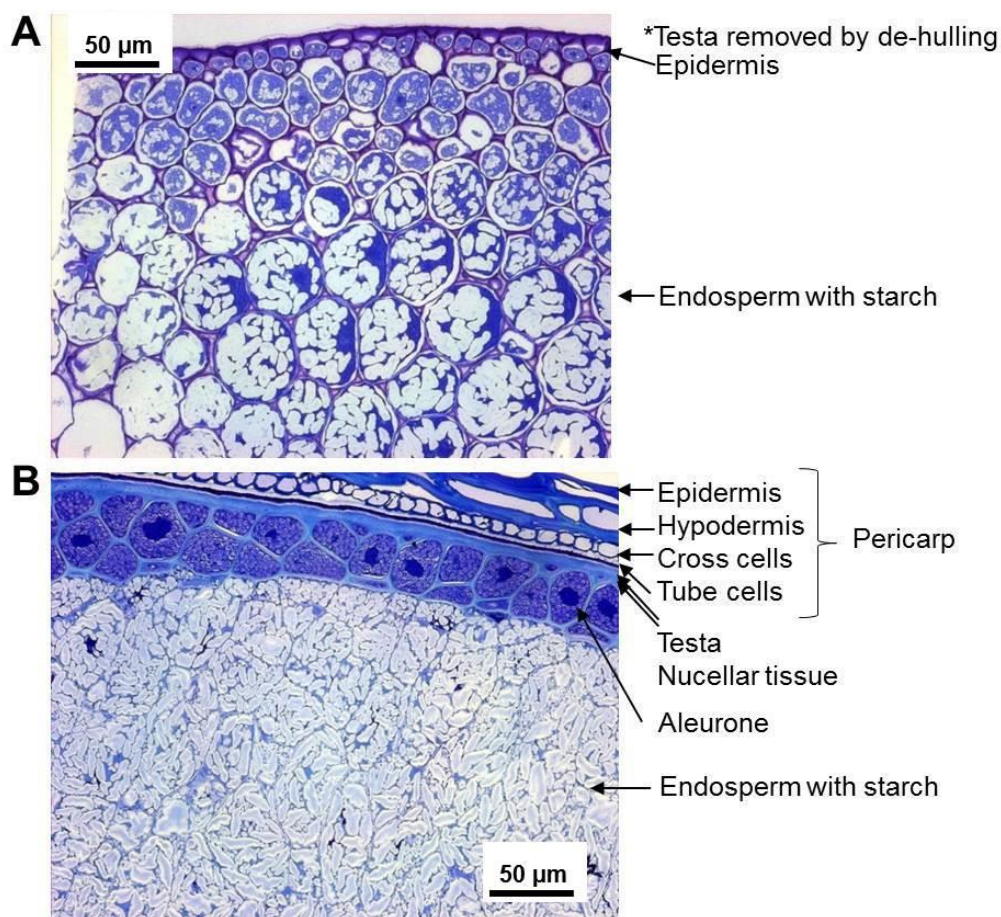


FIGURE 1.5: TISSUES OF (A) DE-HULLED CHICKPEA SEED AND (B) DURUM WHEAT GRAIN FOLLOWING HYDROTHERMAL PROCESSING. Light micrographs of sections 0.5 µm stained with 1% Toluidine blue. Endosperm cells are largely intact and contain swollen starch granules. Scale bars are 50 µm.

Interestingly, when hydrated, the endosperm tissue of wheat has a tendency to fracture, whereas the storage tissues of most leguminous seeds tend to cell separate (Brett and Waldron 1996). This influences the way in which these tissues are disassembled when subjected to external forces, for instance during mastication. When chickpeas are boiled, the pectic material that holds adjacent cells together (the middle lamella), analogous to a type of “glue”, begins to solubilise and pectic polysaccharides de-polymerise by a β -elimination reaction (Jarvis *et al.* 2003), causing the cells that comprise the tissue to separate, but still remain structurally intact. Therefore, a high proportion of intact cells may be consumed in foods such as soup, hummus (made with chickpeas) and baked beans, where the whole pulse seeds are subjected to hydrothermal processing prior to consumption.

The tendency of chickpeas to cell separate applies to the hydrothermally tissue; if the tissue is mechanically processed when *dry* (wheat grains and leguminous seeds have low moisture contents of usually between ~4-14%), the cells will rupture. As a result, the surfaces of dry-milled particles will contain fractured cells, in which the starch granules are no longer physically protected (encapsulated) by the plant cell walls. This means that during dry-milling, the reduction in particle size is associated with a reduction in the number of intact cells present in the milled material. This is an important concept that was used to develop experimental materials that contained varying proportions of cell wall encapsulated starch (*Sections 2.1.2 and 2.1.3*).

At the cellular level, the starch-storage tissue is comprised of relatively large, cells (dimensions between 50 - 270 μm), which are densely packed with starch-granules. These granules are the plants way of storing carbohydrates produced by photosynthesis and are the main source of energy during germination of the seed (Smith 2001, Wang *et al.* 1998). Starch granules can vary in shape (i.e. spherical, polygonal, ellipsoid, platelet and tubular) and size (0.1 – 100 μm), depending on botanical origin (Pérez and Bertoft 2010), and normally swell during hydrothermal processing. The intracellular starch granules represent the substrates that can be digested to release glucose for absorption into the blood, but are ‘encapsulated’ by the plant cell walls, which may provide some protection from digestive conditions. The finer structural architecture of starch and cell walls is important with regard to predicting their behaviour during processing and digestion, and is described further in the following sections.

1.2.6 STARCH

Starch is comprised of mainly amylose and amylopectin, which are polymers of glucose. During digestion, enzymes in the gut lumen and at the mucosal surface liberate these glucose molecules from the macro-molecular structure, making them

available for absorption. The rate and extent to which sugars are released from starch is influenced by the structure and physico-chemical properties of starch.

1.2.6.1 COMPOSITION AND STRUCTURE

The physico-chemical properties of starch vary between botanical sources, and can change when subjected to hydrothermal processing. The following descriptions apply to native (raw) starch, whereas the changes that occur to starch during processing are described in *Section 1.2.6.3*.

For experimental or industrial purposes, starch can be isolated from plant tissues and purified. An overview of the characteristics of purified durum wheat and chickpea starches (typical of cereals and pulses) is presented in **Table 1.1**.

TABLE 1.1 STARCH CHARACTERISTICS OF DURUM WHEAT AND CHICKPEA

	Durum Wheat ^a	Chickpeas ^{b,c}
Amylose	27% amylose	23 - 40%
Granule morphology	Lenticular (A) and spherical (B)	Oval, spherical
Granule size and distribution	Bimodal 15-35 μm (A) and 2-10 μm (B)	Unimodal 9-30 μm
Polymorph	A-type	C-Type
Crystallinity	26% ^d	23 – 28%

Compiled from various sources: ^a (Vansteelandt and Delcour 1999), ^b (Hughes *et al.*), ^c (Hoover *et al.* 2010). ^d (Chanvrier *et al.* 2007) for wheat, rather than durum

Purified starches consist almost exclusively (~98% on a dry weight basis), of amylose and amylopectin molecules, which constitute the 'dietary carbohydrate' component of starch. Amylose is an essentially linear molecule of α -(1,4) linked anhydroglucose, with a molecular weight in the range of 5×10^5 to 10^6 (Buléon *et al.* 1998). Amylopectin also consists predominantly of α -(1,4) linked anhydroglucose, but contains 2-4% α -(1,6) linked glucans, and is highly branched (Wang *et al.* 1998). The amylose content of most starches (see **Table 1.1** for chickpea and durum wheat starch) is 15 - 35% (Pérez and Bertoft 2010); however, waxy genotypes may contain <1% amylose (i.e. nearly all amylopectin), and some mutant starches may contain up to 70% amylose (Buléon *et al.* 1998).

Starch also contains some minor components, namely, proteins (~0.25%), lipids (~1.0%), minerals and moisture (10 -15%) (Anguita *et al.* 2006, Baldwin 2001). The starch associated proteins may be residual material from the intracellular matrix (e.g., glutens and gliadins), which adhere to the surface of the granules, or proteins which form an integral part of the starch granules (Baldwin 2001). Similarly, lipids may also be present on the surface, and/or within the isolated starch (Tester *et al.* 2004). Although these proteins and lipids are minor components of starch, there is some evidence to suggest that they may interact with amylose and thereby influence starch properties (Baldwin 2001, Debet and Gidley 2006).

Together, amylose and amylopectin are assembled into starch granules. In most species (including chickpeas), the size distribution of starch granules is relatively unimodal, although some cereal starches (including wheat, rye and barley, but not sorghum, oats or rice) have a bimodal size distribution, as they contain both large ('A-size') and small ('B-size') granules (Tester *et al.* 2004).

One current model of starch granular architecture is shown in **Figure 1.6**, however, readers are encouraged to refer to a recent review series for details of how these models have evolved over past decades (Seetharaman and Bertoft 2012). Essentially, starch granules consist of alternating amorphous and semi-crystalline shells, which can be observed under the microscope as concentric rings. Within the semi-crystalline shells are alternating layers of amorphous and crystalline regions, comprised of repeating units or 'lamellae' of ~9 nm (Blazek *et al.* 2009). The very centre of the granule, the 'hilum', is surrounded by an amorphous region of predominantly amylose and the disordered reducing ends of amylopectin chains.

The chain distribution model (**Figure 1.6**) depicts how the arrangement of amylose and amylopectin polymers within starch granules gives rise to these different amorphous (amylose-rich) and crystalline (amylopectin-rich) regions.

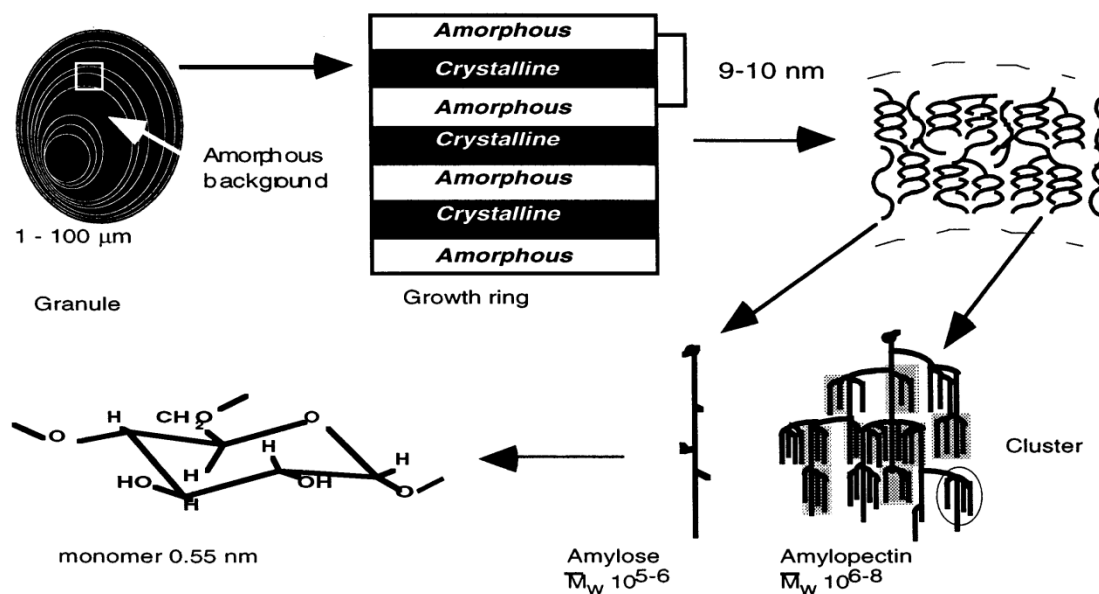


FIGURE 1.6: STARCH GRANULAR ARCHITECTURE. Starch granules consist of alternating amorphous and crystalline regions made up of amylose and amylopectin molecules. Taken from Buléon *et al.*, 1998.

Within the starch granule, the packing of double-helices of amylopectin chains in lamellae give rise to different polymorph structures. Cereal starches are A-type polymorphs, which are denser and bind less water than B-type starches. Starch from pulses tend to have a combination of both polymorphs and are called C-type. Generally, A-type native starches tend to be more readily digested than B-type starches, although this is not necessarily a consequence of the different polymorphic structure, and may instead reflect other differences between starches of different botanical origin (Tester *et al.* 2004, Wang *et al.* 1998, Gallant *et al.* 1992). When viewed under a light microscope fitted with cross-polarisers, the crystalline regions of starch are birefringent, whereas the amorphous regions are not. This gives rise to a 'Maltese-cross' pattern, which is characteristic of native starches (Wang *et al.* 1998).

1.2.6.2 ENZYMIC DEGRADATION OF STARCH

In humans, starch is digested by α -amylases (salivary and pancreatic), which initiate starch breakdown, and oligosaccharidases/disaccharidases, that are required to liberate individual monosaccharides from the products of amylolysis.

The enzymic degradation of starch is illustrated in **Figure 1.7**. First, α -amylase (EC.3.2.1.1) hydrolyses α -(1,4) linkages from linear portions of amylose and amylopectin in starch. The resulting products are predominantly maltose, maltotriose, isomaltose, limit dextrins and a number of linear α -(1,4) linked polyglycan chains. A very limited amount of glucose is also released at this stage (Robyt and French 1970). Because α -amylase cannot cleave α -(1,6) linkages, brush border disaccharidases, such as sucrose-isomaltase, which can hydrolyses α -(1,6) linkages, are required to liberate constituent glucose residues so that they can be absorbed in the small intestine.

At a granular level, the amorphous regions (see **Figure 1.6**) are more susceptible to amylase hydrolysis, and as starch is hydrothermally processed, the starch becomes more amorphous (see next section) and therefore more digestible. Some starch may be resistant to digestion by α -amylase. This can occur, for instance because the starch is encapsulated within cell walls, or because it is structurally resistant, as can occur with raw or retrograded starches (Englyst *et al.* 1992, Perera *et al.* 2010). Although resistant starch escapes digestion in the small intestine, it is eventually fermented by micro-organisms in the colon (Asp *et al.* 1996).

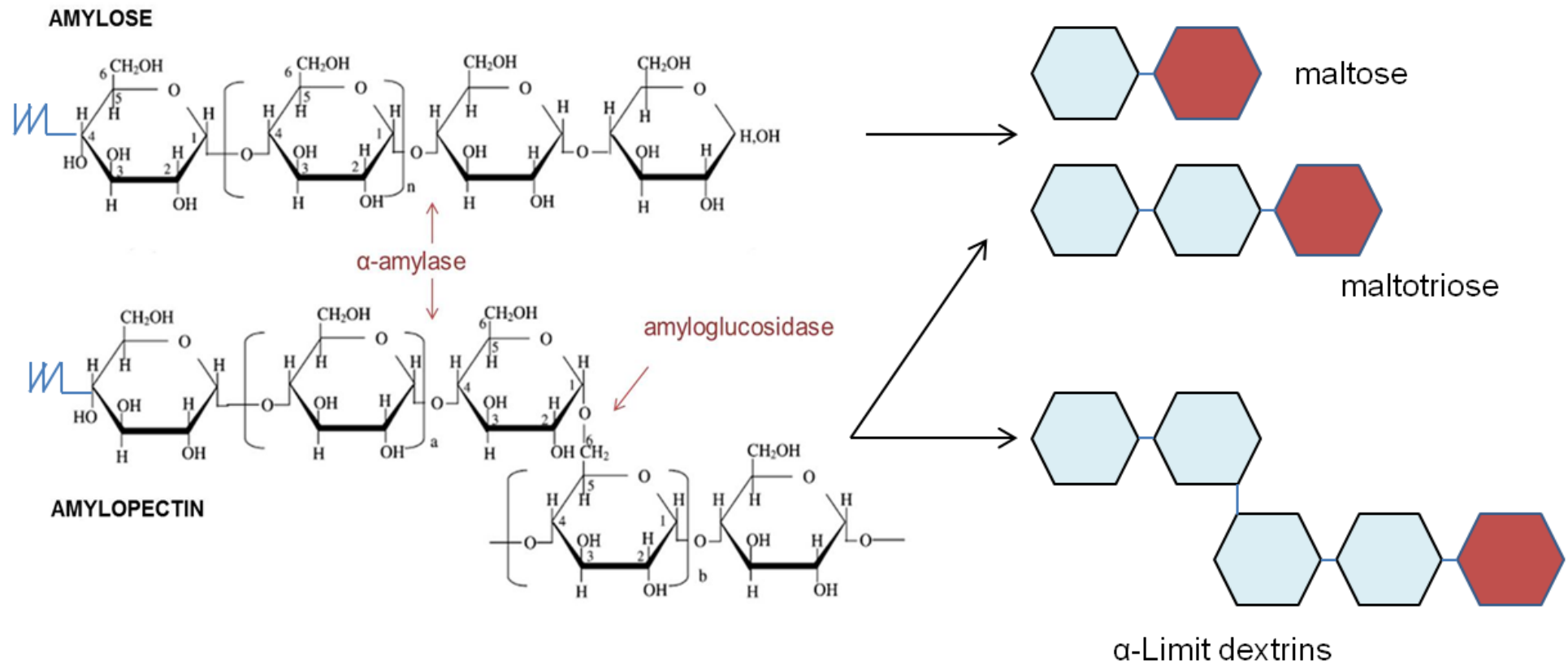


FIGURE 1.7: ENZYMIC DEGRADATION OF AMYLOSE AND AMYLOPECTIN IN STARCH. α -amylase hydrolyses α -(1,4) linkages from linear portions of amylose and amylopectin in starch to yield mainly maltose, maltotriose and limit dextrins with reducing ends shown in red. These products can be cleaved further by amyloglucosidase, which acts on α -(1,6) linkages, and by other disaccharidases to release individual glucose units. Adapted from Tester *et al.* 2004.

A number of studies have demonstrated a correlation between the rate of starch amylolysis measured *in vitro* and the increase in venous glucose concentration observed *in vivo* (Jenkins *et al.* 1982, Goñi *et al.* 1997). Therefore, studying the rate and extent of starch *in vitro* provides a popular means of predicting the glycaemic response (Englyst *et al.* 1992, Woolnough *et al.* 2008). Englyst introduced an *in vitro* system for classifying starch into rapidly and slowly digested starch fractions ('RDS' and 'SDS', respectively). However, this system appears to be based on a misunderstanding of the amylolysis process and does not identify real differences in digestion rate (Englyst and Hudson 1996). It is well known that the enzymic degradation of starch by amylase occurs by a pseudo first-order reaction, in which the rate of degradation slows with time because the concentration of starch continues to fall as it becomes converted to products, i.e. substrate exhaustion (Goñi *et al.* 1997, Butterworth *et al.* 2012). The first-order rate constant is a function of the amylase concentration, which normally remains constant over the time course of an *in vitro* experiment. Thus, the classification of starch into RDS and SDS, which is arbitrarily based on the amount of substrate digested after 20 and 120 min, is therefore questionable from a scientific point of view (Butterworth *et al.* 2012)

For experimental purposes, porcine pancreatic α -amylase is often used as a model of human pancreatic α -amylase, because it can be obtained in pure form, is relatively inexpensive, compared with human α -amylases, and has a near identical structure, sequence homology and function to the human enzymes (MacGregor *et al.* 2001). Alpha-amylases (**Figure 1.8**) are proteins, ~57 kDa with three domains (Simon *et al.* 1974, Brayer *et al.* 1995). The enzyme contains at least one calcium ion, which is thought to hold together domains A and B. Domain C is more loosely attached. The active site lies in a cleft between domains A and B, and contains 5 sub-sites to which glucose residues can bind. The site also contains a chloride ion, which is important for enzyme activation. The size of this digestive enzyme, (radius of gyration = 2.69 nm) is particularly relevant with regard to its ability to access substrate (starch) entrapped

within a structurally complex food matrix (see *Section 1.2.7.3*) and within the granule itself, which is considerably larger than the enzyme.

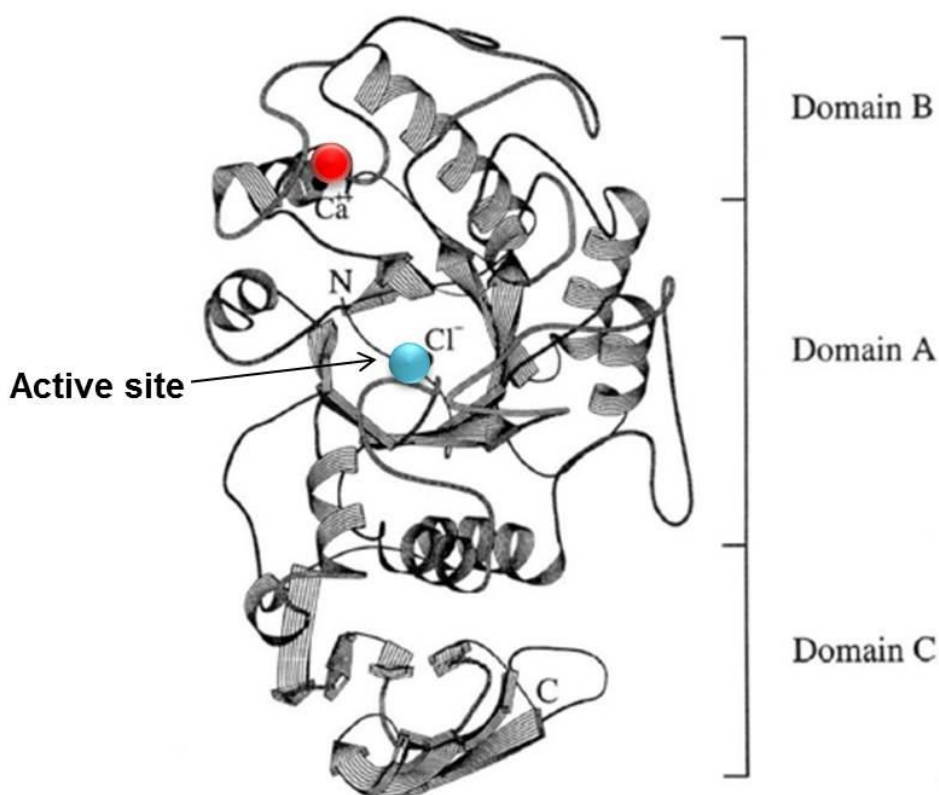


FIGURE 1.8 STEREO DRAWING SHOWING POLYPEPTIDE CHAIN FOLDING AND STRUCTURAL DOMAINS IN HUMAN PANCREATIC α -AMYLASE MOLECULE. A calcium ion (red) and the active site, which contains a chloride ion (blue) is indicated. Adapted from Brayer *et al.*, 1995.

1.2.6.3 STARCH SWELLING, GELATINISATION AND RETROGRADATION

Starch structural architecture and susceptibility to amylase hydrolysis may be altered considerably during food processing. The following descriptions relate to effects of processing on isolated starch; however, it is important to note that when starch is entrapped within a food matrix, other components may interfere with this process (see *Section 1.2.9*).

When heated in excess water, starch granules undergo an irreversible phase transition termed 'gelatinisation', in which the granules become more disordered. During hydrothermal processing, initial water ingress destabilises hydrogen bonds in the amorphous regions of the granule, causing these regions to expand. This contributes to

a loss of stability in the adjacent crystalline regions (Wang and Copeland 2013), which, in turn, enables further water ingress and granular swelling. As the granule hydrates, amylose, which has a lower affinity for water than amylopectin, leaches out (phase-separation) (Tester and Morrison 1990). At a sufficiently high temperature the crystallites, which have become de-stabilised by hypermobility and swelling, undergo a melting transition in which the double helices of amylose unwind, causing the granule to become more amorphous (Donovan 1979, Wang and Copeland 2013). With regard to starch digestibility, the more amorphous structure signifies a greater availability of amylase binding sites, which makes it more susceptible to enzyme hydrolysis (Slaughter *et al.* 2001). If starch has been physically damaged, for instance during milling, the damaged granules will take-up water more quickly and have a greater susceptibility to enzymes. Starch in hard wheats, such as durum, appear to be particularly susceptible to physical damage (Morgan and Williams 1995).

Experimentally, the gelatinisation of starch can be observed as an endothermic transition when it is heated in sufficient water in a differential scanning calorimeter. The loss of crystallinity is also associated with a loss of birefringent properties, and can be visualised using cross-polarised light microscopy (Bogracheva *et al.* 1998, Wang *et al.* 1998). Once gelatinised, only a collapsed granular envelope, often termed a 'granule ghost' can be observed under the light microscope (Debet and Gidley 2007).

Starch gelatinisation is an irreversible process in that the structure of gelatinised starch cannot resume its original native assembly. However, when gelatinised and/or hydrated starch begins to cool, the amylose and amylopectin components of starch begin to re-associate forming a new structure. This process is termed 'retrogradation', and begins within minutes of cooling. Regions of adjacent amylose chains, some of which leach out during hydration, align and may re-associate into double-helices, creating new crystalline regions (Haralampu 2000, Perera *et al.* 2010). Unlike the gelatinised form, retrograded amylose is highly resistant to digestion, and forms a very strong gel that

resists intensive food processing conditions (Perera *et al.* 2010, Haralampu 2000). Retrogradation of the branched side chains of amylopectin, which remain present within the starch granule, is a much slower process, occurring over several days, and is involved in the staling of bread and cakes (Wang and Copeland 2013).

1.2.7 PLANT CELL WALLS

Plant cell walls provide the strength that enables large plants to grow, as well as giving the resilience needed to withstand external forces of nature and internal osmotic pressures. From a nutritional perspective, the plant cell walls resist digestion in the small intestine, but provide an important substrate for fermentation by micro-organisms in the colon. Although there are still many gaps in our understanding of cell walls, their interesting properties are largely attributed to the complex assembly of polymers that constitute the cell wall matrix.

1.2.7.1 COMPOSITION AND STRUCTURE

Plant cell walls consist of two or three layers, which are deposited during growth and development (**Figure 1.9**): i) the middle lamellae, a pectin and protein-rich layer which forms between two adjacent cells, ii) the primary wall, and iii) the secondary wall, which is deposited only in some plant tissues or cells which require additional mechanical strength, (Burton *et al.* 2010, Jarvis 2011, Brett and Waldron 1996). The following descriptions will be limited to primary cell walls and the middle lamellae, as secondary cell walls are not likely to be present in the chickpea and durum wheat tissues used in this project.

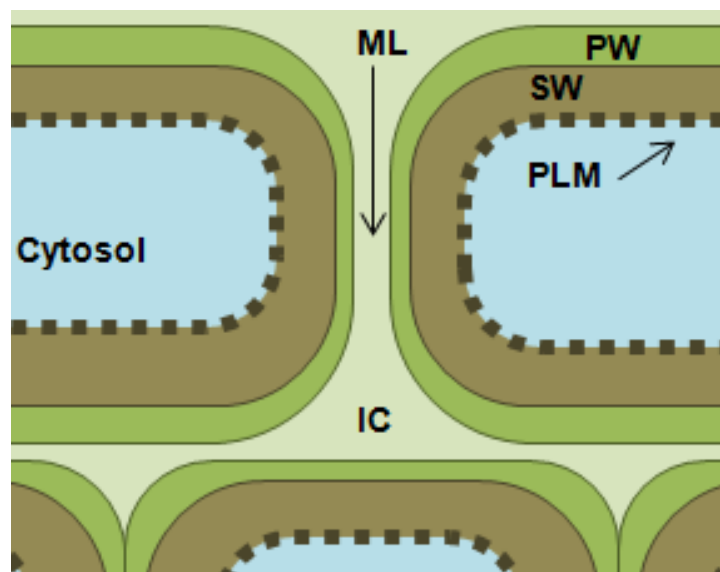


FIGURE 1.9: SCHEMATIC SHOWING LAYERS OF THE PLANT CELL WALL. Abbreviations: PW, primary wall; SW, secondary wall; PLM, plasma membrane; ML, middle lamellae; IC, interstitial space. Not all cell types have secondary walls.

The polysaccharide components of the cell walls (often referred to as non-starch polysaccharides or 'NSPs') are normally classified as cellulose, hemicelluloses or pectins. *Cellulose* is a linear polymer of un-branched β -(1,4)-linked D-glucan, which aggregates to form crystalline microfibrils (~3 nm) through extensive hydrogen bonding and hydrophobic interactions (Cosgrove 2005). *Hemicelluloses* have a backbone resembling cellulose, but have branch-points and other structural modifications that prevent them from forming microfibrils (Cosgrove 2005). *Pectins* generally have a partially methyl-esterified α -(1,4) linked galacturonan backbone with associated side chains, e.g., rhamnogalacturonan I (Brett and Waldron 1996). These NSP's are often defined on the basis of their extraction properties; pectins can be extracted with chelating agents, hemicelluloses with strong alkali, and the residue that remains after pectin and hemicellulose extraction is taken to be cellulose (Brett and Waldron 1996, Grassby *et al.* 2013).

The structural differences between celluloses, hemicelluloses and pectins give rise to different properties. Cellulose is mechanically strong and more resistant to chemical extractions and microbial degradation than the pectic and hemicellulosic

polysaccharides (Brett and Waldron 1996). A well-known example is the different properties of the highly resistant and insoluble β -(1,4) linked cellulose polymer compared with the hemicellulosic mixed-linkage β -(1,3), β -(1,4) glucans, which are known to generate high levels of viscosity in the gastro-intestinal lumen and lower blood glucose and cholesterol concentrations (Cui and Wang 2009). The terms 'soluble' (e.g., pectin) and 'insoluble' (e.g., cellulose) fibre have been used throughout the literature to describe cell wall polysaccharides according to their properties. While it is true that some soluble-fibres can generate viscosity with potential implications for nutrient bioaccessibility, the behaviour of cell walls and individual cell wall polysaccharides during digestive transit *in vivo* is still not well understood.

The specific polysaccharides that constitute the hemicellulosic and pectic fractions of the cell walls vary considerably between botanical species and tissue types (Grassby *et al.* 2013). An overview of the most common polysaccharides, which are named after their sugar constituents and glycosidic linkages (substituent first, backbone second) is provided in **Table 1.2**

TABLE 1.2: LIST OF COMMON CELL WALL POLYSACCHARIDES AND THEIR CLASSIFICATION

CELL WALL POLYSACCHARIDES
Cellulose
Hemicelluloses:
Xylan
Xyloglucan
Arabinoxylan
Mannan
Glucomannan
Galactomannan
Mixed Linkage β (1,3), β (1,4) -glucan
Callose
Pectins:
Homogalacturonan
Rhamnogalacturonan I
Rhamnogalacturonan II
Arabinogalactan I
Arabinogalactan II
Arabinan (polysaccharide side chains to main pectins)
Galactan (polysaccharide side chains to main pectins)

Adapted from Grassby *et al.*, 2013.

There is limited reliable literature on the relative proportions of the specific cell wall polysaccharides present in chickpea parenchyma and durum wheat endosperm, but it can be assumed that chickpeas are similar to other dicots, and that durum wheat cell walls are similar to other *Gramineae*. The dicots (e.g., chickpeas) and most monocots tend to have *Type 1* primary walls that are rich in pectins (e.g. mannans, galactomannans, and galactoglucomannans) and xyloglucan, whereas *Gramineae* (e.g. durum wheat) have *Type 2* primary walls that are lower in pectins, but rich in hemi-celluloses, especially arabinoxylan and mixed linkage β -glucans (Burton *et al.* 2010, Jarvis 2011, Brett and Waldron 1996, Waldron *et al.* 1997). The cell walls of wheat tend to be rich in arabinoxylan, but contain very little of the mixed linkage β -glucans that are found in oats and barely (Cui and Wang 2009).

For comparative purposes, the relative proportions of the major cell wall components found in typical *Type 1* and *Type 2* cell walls is represented graphically in **Figure 1.10**. Essentially, the cell wall assembly consists of cellulose microfibrils, embedded in a flexible and more porous gel matrix of hemicelluloses, pectins and water, as well as other minor components such as proteins (extensins) and phenolics (e.g. lignin) that may be present. (Burton *et al.* 2010, Cosgrove 2005, Somerville *et al.* 2004). Although there are still some uncertainties regarding the structural architecture of plant cell walls, particularly with regard to the interactions between the different classes of polysaccharide (Burton *et al.* 2010), the large differences in the relative proportions of hemi-celluloses, pectins and cellulose in *Type 1* and *Type 2* walls (**Figure 1.10**) give rise to differences in structural architecture, as shown in **Figure 1.11**. Chickpea (*Type 1*) and durum wheat (*Type 2*) cell walls are therefore likely to have different physico-chemical properties that may influence their potential to limit starch bioaccessibility.

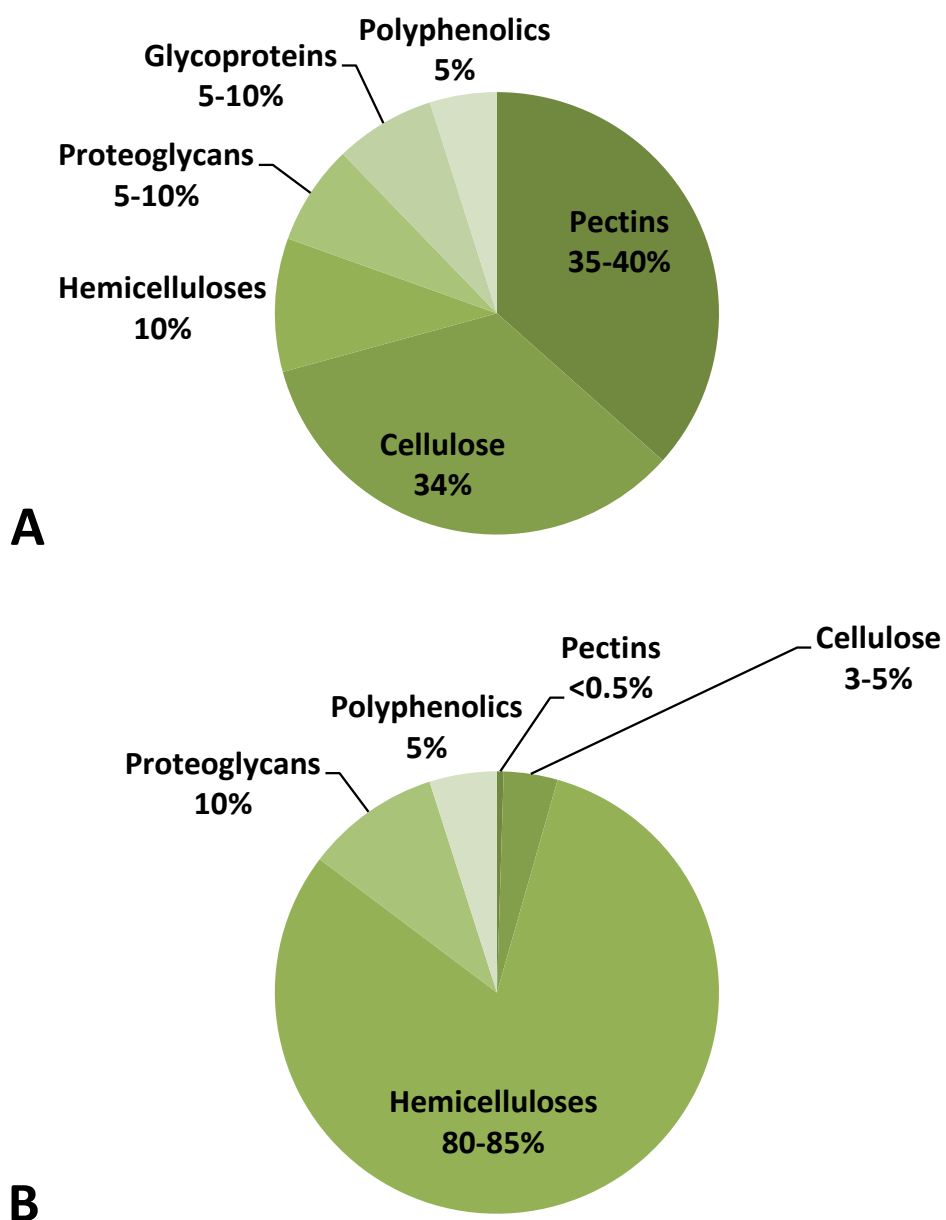


FIGURE 1.10: CELL WALL POLYMER COMPOSITION OF PARENCHYMATOUS TISSUES OF (A) FRUIT AND VEGETABLES (TYPE 1) AND (B) CEREALS (TYPE 2). Re-drawn from data presented by Selvendran, 1987. Values are % dry matter and are approximated from various studies, as indicated in the publication.

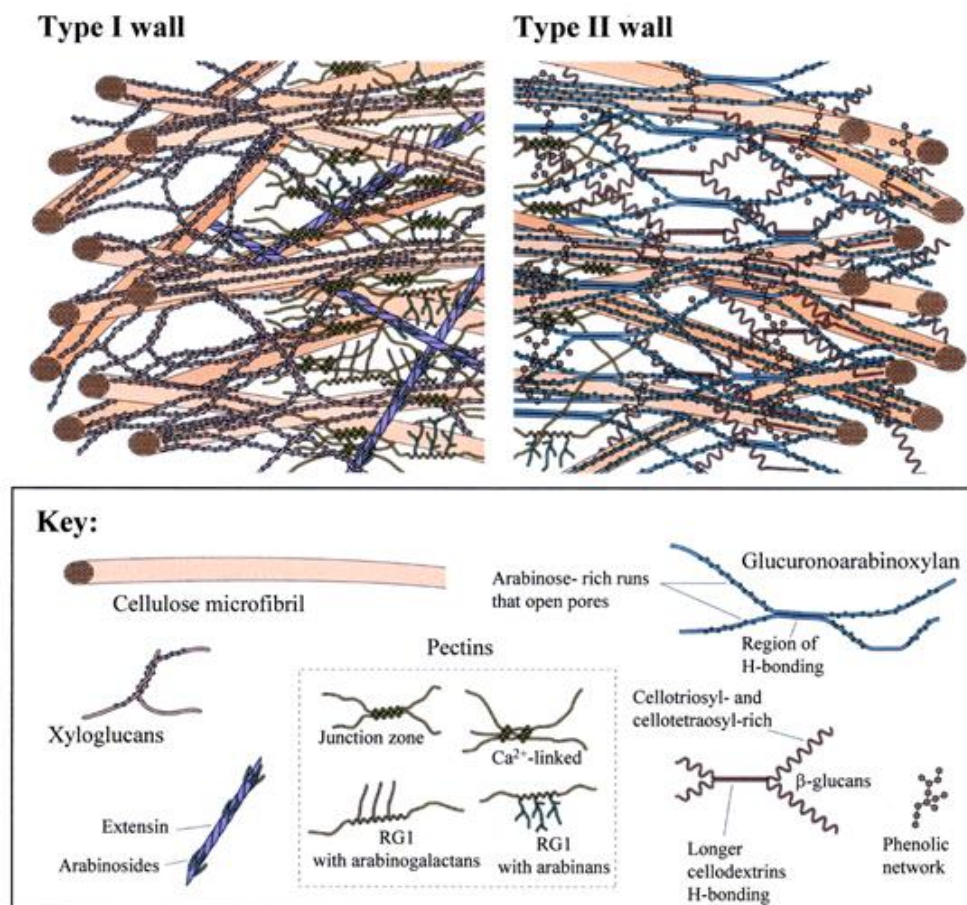


FIGURE 1.11: STRUCTURAL ARCHITECTURE OF TYPE 1 AND 2 CELL WALLS. Taken from Buchanon *et al*, 2000.

1.2.7.2 ENZYMIC DEGRADATION OF CELL WALLS

Although some cell wall polysaccharides, e.g., cellulose, can resemble starch in that they are composed of glucopyranose units, α -amylase is not able to hydrolyse the β -linkages adjoining these polymers. As a result, these cell wall polysaccharides are not likely to be digested in the small intestine of humans. Rather, they are passed on to the colon, which hosts bacteria that possess enzymes (β -galactosidase, β -glucuronidase) that can break-down cell walls (Cummings and Macfarlane 1991). Some cell wall polysaccharides are soluble in an aqueous environment (e.g., when extracted and purified) and may therefore leach out from the cell walls during processing or digestive transit. At present, it is not known to what extent this occurs during digestive transit, and if this has effects on cell wall integrity. It is unlikely, however, that these polysaccharides are digested or absorbed in the small intestine because of the physical entanglement and chemical interactions of the polysaccharide chains.

1.2.7.3 CELLULAR INTEGRITY AND PERMEABILITY

Because cell walls are largely resistant to digestion in the small intestine, they may play an important role in preventing digestion or release of intracellular starch. Consequently, cellular integrity during digestive transit is likely to have implications for nutrient bioaccessibility and consequently digestion kinetics. The tendency of hydrated cells to separate (chickpeas) or fracture (durum wheat), mentioned in *Section 1.2.5*, is an important consideration, because if the cells separate, but stay intact when pressure is applied, the starch is more likely to remain encapsulated by the cell walls during digestive transit. Depending on the permeability of the cell walls to digestive enzymes, this encapsulation of starch could potentially protect the intracellular starch from the digestive fluids in the gut environment (**Figure 1.12**).

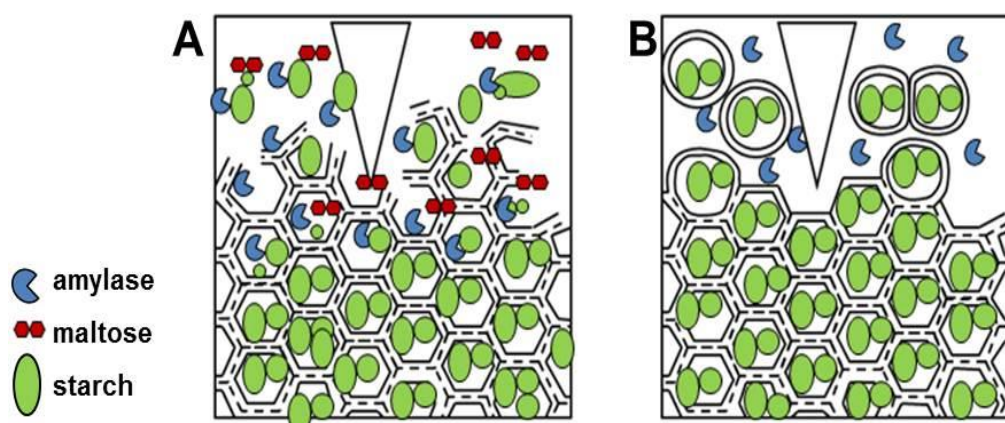


FIGURE 1.12: SCHEMATIC SHOWING TISSUE TENDENCY TO (A) FRACTURE AND (B) SEPARATE. When cells rupture (A), the starch is released as a result of cell rupture, and amylase can immediately hydrolyse it to release maltose. If the cell walls are permeable (A), the enzyme can eventually digest the intracellular starch as well. If cells separate (B) when pressure is applied, but the cells remain intact, all the starch is encapsulated. The cell walls may protect the starch from digestive enzymes by delaying or hindering their access. It should be noted that the permeability of Type 1 and Type 2 cell walls to digestive enzymes is currently not known. Adapted from Brett and Waldron, 1996.

Intact, starch-filled leguminous cells have been recovered *in vivo* from the terminal ileum, i.e, the end of the small intestine, demonstrating that some cells can remain intact during digestive transit (Noah *et al.* 1998). As such, a review of cell wall permeability is of great interest, but unfortunately, the literature on this subject is very limited.

As described in the *Section 1.2.7.1*, cell walls consist mainly of a polysaccharide network, but the permeability of this network to enzymes and other compounds is largely unknown. Metabolites (<800 Da) may be transported between adjacent cells through plasmodesmata (Lucas and Lee 2004). Enzymes, however, are considerably larger (~30,000 – 60,000 Da), and would be more likely to enter cells through the porous polymer network gel of the cell wall matrix, although this has not yet been established. A small number of studies have attempted to determine cell wall pore size using various qualitative or quantitative techniques (Carpita *et al.* 1979, Tepfer and Taylor 1981, Baron-Epel *et al.* 1988, Chesson *et al.* 1997). These studies were performed on plant materials very different to chickpea and durum wheat endosperm, but are summarised in **Table 1.3** because overall, there are few examples of cell wall permeability studies.

TABLE 1.3: OVERVIEW OF RESULTS FROM CELL WALL POROSITY STUDIES

Plant material	Technique	Pore Size (radius)	Comments	Citation
<i>Raphanus sativus</i> ('radish', root hairs)	Solute exclusion (microscopy)	1.25-1.4 nm in root cells 2.3 - 2.5 nm in paliside	Solutes may have influenced porosity	(Carpita <i>et al.</i> 1979)
<i>Phaseolis vulgaris</i> Isolated cell walls from hypocotyl	Gel-filtration chromatography	40-60 kDa	Used frozen and isolated cell wall material.	(Tepfer and Taylor 1981)
<i>Glycine Max</i> (root cells, grown in suspension culture)	FRAP	3.3 - 4.3 nm		(Baron-Epel <i>et al.</i> 1988)
<i>Triticum aestivum</i> (straw and grain fractions)	Gas adsorption Mercury Porosimetry	1.5 - 2.5 nm	Measurements affected by starch in endosperm	Chesson (1997) (Chesson <i>et al.</i> 1997)

¹FRAP; Fluorescence recovery after photobleaching.

Generally, the suggested pore radius seems to be in the range of 1.2 to 4.3 nm, which is similar to the radius of gyration of the amylase molecule (2.69 nm). However, there is some controversy regarding the methodologies used. For instance, one issue is that the experimental conditions and/or preparation of cell wall material may alter the porosity of the wall. Differences are also likely to exist between the cell wall permeability of different plant tissues, especially considering the known differences in

cell wall composition and structure (*Section 1.2.7.1*). It seems that the porosity of cell walls and the mechanisms that regulate porosity remain unclear. Nevertheless, considering the range of pore-sizes reported, cell wall porosity and permeability to digestive amylase could be a critical factor in determining the bioaccessibility of cell wall encapsulated starch and therefore merits further investigation.

1.2.8 DIGESTION, METABOLISM AND HEALTH

The physical and chemical breakdown of food and its components as it is passed through the gastro-intestinal tract is of direct relevance to understanding the release ('bioaccessibility') of macronutrients such as starch. The postprandial metabolic response to these nutrients also has important implications for health. From an experimental perspective, knowledge of digestive physiology and metabolism is needed to accurately simulate the physiological digestive conditions *in vitro*, and for monitoring the physiological response to food *in vivo*.

1.2.8.1 DIGESTION IN HUMANS AND PHYSIOLOGICAL ASPECTS

An overview of the digestion process in the human gastro-intestinal tract is provided in **Figure 1.13**. Digestion begins in the mouth, where food is mixed with saliva and comes into contact with salivary α -amylase, secreted by the salivary glands (Chen 2009, Bornhorst and Singh 2012). The actions of salivary and pancreatic α -amylase on starch are known to be similar, but it is still a matter of debate as to what extent salivary amylase contributes to total starch breakdown.

The duration of starch exposure to salivary amylase before swallowing is relatively brief, for instance, 27 seconds for bread, (although this varies depending on food properties) compared with the exposure to pancreatic α -amylase (hours) (Dahlqvist and Borgstrom 1961, Butterworth *et al.* 2011, Hoebler *et al.* 1998), although, saliva does have excellent viscosity-reducing effects, which may increase starch susceptibility to enzyme attack (Evans *et al.* 1986). The enzymic digestion of starch in the mouth is facilitated by the mechanical action of mastication, which aids mixing and reduces

particle size, effectively increasing the availability of carbohydrate as the food matrix becomes disrupted. Where intact cells/tissues are present, the shear forces of mastication may cause the cells to rupture, such that the intracellular contents (i.e. starch) become exposed to salivary enzymes. Alternatively, as mentioned previously, individual cells may remain intact and simply separate, such that the intracellular content remains encapsulated by the plant cell wall. Thus, mastication can produce a range of particle size distributions (for example, particles <1 μm to 12.5 mm long sections (as seen with spaghetti, for example), depending on the nature of the ingested food (Hoebler *et al.* 2000).

The physico-chemical transformation of food in the oral phase has effects on subsequent digestion in the gastric phase: Some foods, such as bread, are formed into a bolus, in which the salivary enzymes at the centre of the bolus can be protected from the acidic conditions of the stomach and may remain active throughout the gastric phase. Where foods are swallowed as hard particulates (e.g. peanuts), however, any salivary enzymes residing on the surface of the food particle, are likely to be inactivated by the acidic pH (Rosenblum *et al.* 1988, Fried *et al.* 1987). Although gastric juice itself is acidic (~pH 2.0), digestion in the stomach generally occurs at a higher pH because of the buffering capacity of food (Malagelada *et al.* 1976).

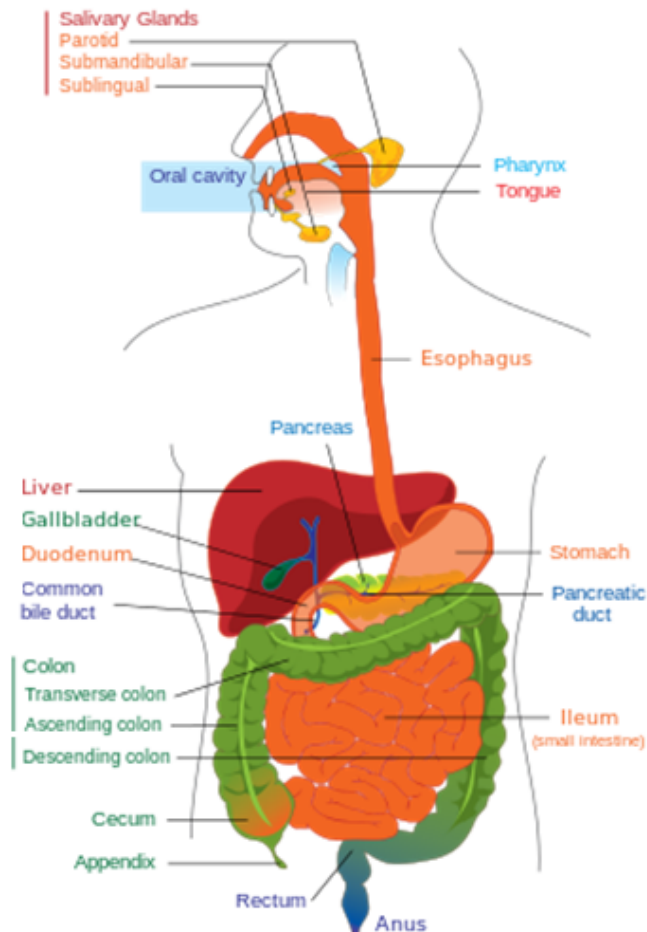
In the stomach, food is mixed with gastric proteases and lipases which may contribute to a weakening of food structure. The shear forces in the lower part of the stomach and 'gastric-sieving' mechanism (i.e. the preferential retention of larger particles) may aid particle-size reduction, but the chyme which leaves the stomach is far from homogeneous, and may, for instance, contain intact plant cells or tissues (Noah *et al.* 1998). After it is expelled from the stomach, chyme is buffered by bicarbonate, mixed with mucin (secreted from the Brunner's glands) and exposed to bile from the gallbladder.

3) SMALL INTESTINE

- Chyme is mixed with pancreatic, biliary and intestinal secretions.
- pH is neutralised by bicarbonate
- Starch digestion by pancreatic amylase and disaccharidases
- Absorption of products (e.g., glucose)

4) COLON

- Fermentation of dietary fibre
- Production and absorption of SCFAs
- Water absorption



1) MASTICATION

- Food is mixed with saliva and broken-down into smaller particles.
- Salivary amylase digestion of starch.

2) GASTRIC DIGESTION

- Bolus is mixed with gastric secretions:
 - HCL
 - Enzymes
 - Mucus
 - Water
- Formation of chyme.
- Acidic pH contributes to digestion
 - Disintegration of bolus
 - Retards salivary amylase activity
- Particle size reduction and 'gastric sieving' mechanism.

FIGURE 1.13: DIGESTION OF CARBOHYDRATE FOODS IN HUMAN GASTRO-INTESTINAL TRACT. Adapted from Grassby *et al.*, 2013

In the duodenum, pancreatic α -amylase digests starch into predominantly maltose, isomaltose, maltotriose, and α -limit dextrans' (see *Section 1.2.6.2*). These products are further digested by di/oligosaccharidases, notably maltase-glucoamylase (MGAM), which hydrolyses α -(1,4)-linkages in maltose and dextrans, and sucrase-isomaltase (SI), which hydrolyses the α -(1,6)-linkages in isomaltose and α -limit dextrans. The resulting glucose is then absorbed from the intestinal mucosa into the portal blood (**Figure 1.14**). When glucose is present at lower concentrations, absorption across the brush-border occurs by active transport, mediated by the sodium-glucose cotransporter (SGLT-1) (Kellett and Brot-Laroche 2005, Sim *et al.* 2008). When luminal glucose concentration is high, for instance after a high glycaemic meal, the GLUT2 transporter moves to the brush-border, providing a second route for glucose absorption (Frayn 2010). These transporters bring sugar across the brush-border into the enterocyte cells of the mucosa. Most of these sugars then exit the cells through the baso-lateral membrane and drain into the hepatic portal vein (Frayn 2010). Thus, absorbed sugars elicit a measurable rise in plasma glucose concentration.

Some starch may remain undigested and/or entrapped in the food matrix by the time the digesta reaches the end of the small intestine (the 'terminal ileum'). This is termed 'resistant starch' and is passed onto the colon along with other undigested components, including non-starch polysaccharides (NSPs) and short chain carbohydrates (all classed as 'dietary fibre'). The colon hosts micro-organisms which have enzymes capable of breaking-down these complex polysaccharides by fermentation. The resulting short chain fatty acids (SCFA), predominantly, acetate, butyrate and propionate, and also isovalerate, valerate and isobutyrate, may be absorbed and metabolised, contributing some dietary energy, i.e. 8.8 kJ/g fully fermentable RS (Cummings and Macfarlane 1997, Asp *et al.* 1996).

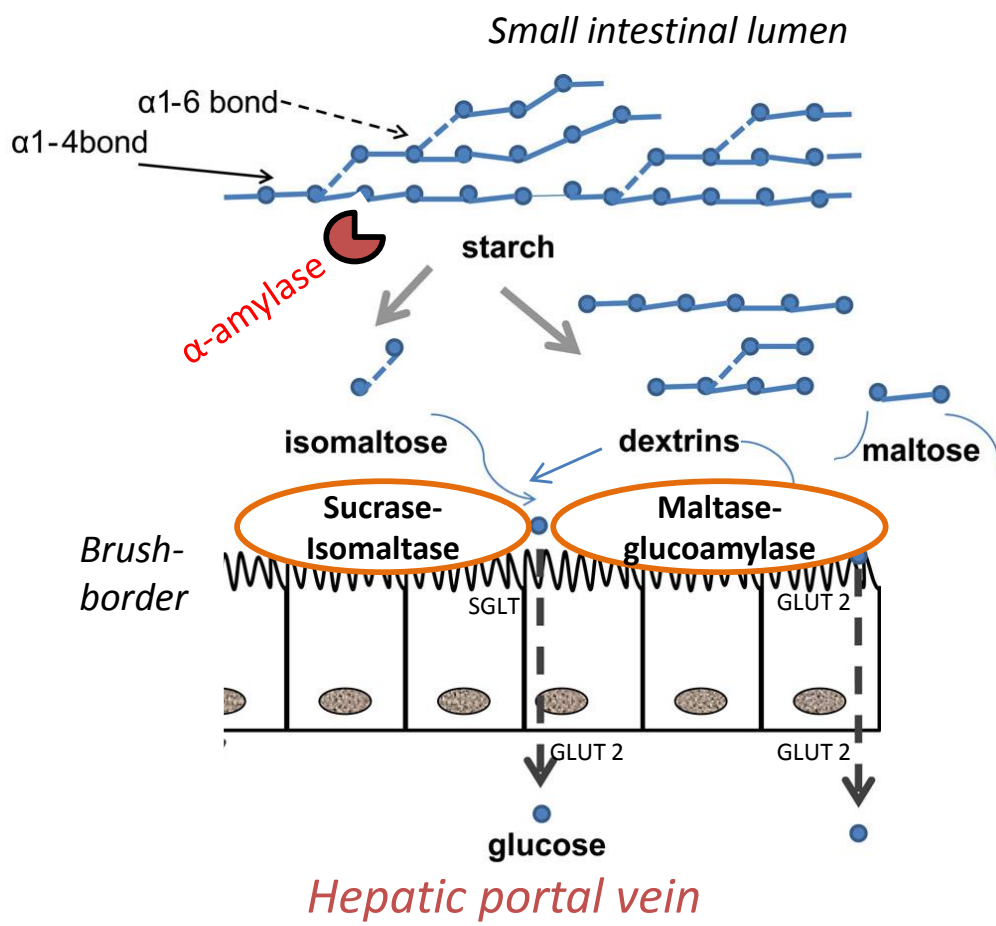


FIGURE 1.14: DIGESTION AND ABSORPTION OF STARCH HYDROLYSIS PRODUCTS. Starch is digested by α -amylase in the small intestinal lumen. The main products are maltose, isomaltose, maltotriose (not shown) and maltodextrins are then broken down into glucose by brush-border enzymes: Sucrase-Isomaltase cleaves α (1,6) and some α (1,4) bonds, Maltase-Glucoamylase cleaves α (1,4) bonds only. The glucose is then absorbed into the enterocyte and transferred to the blood through the basolateral membrane. Adapted from Tappy 2012.

Overall, the secretions of digestive organs, gut motility, and associated feelings of hunger and satiety are regulated by gastro-intestinal hormones ('gut hormones'), which are secreted from enteroendocrine cells (distributed throughout the gastro-intestinal tract) in response to nutrients (Murphy and Bloom 2006, Wu *et al.* 2013). An overview of the major gut hormones and their functions is provided in **Table 1.4**. These gut hormones play a major role in regulating energy homeostasis, and are recognised as interesting targets for the development of new pharmaceutical drugs to prevent or control diabetes and obesity (Murphy and Bloom 2006).

The secretion of insulinotropic or ‘incretin’ hormones (e.g, Glucose-Dependent Insulinotropic Hormone, GIP, and Glucagon-Like Peptide, GLP) is strongly dependent on the rate of glucose absorption into the portal blood (Wu *et al.* 2013). It is therefore likely that starch bioaccessibility plays an important role in influencing gut hormone signalling. Some studies have shown that water-soluble non-starch polysaccharides (e.g., guar gum), which are known to reduce glucose absorption (Ellis *et al.* 1995), decrease post-prandial GIP concentration (Morgan *et al.* 1990). However the effect of fibre on post-prandial gut hormone signalling is still not well understood and it is not known whether the encapsulation of starch within cell walls may affect gut hormone signalling.

TABLE 1.4: OVERVIEW OF MAJOR GASTRO-INTESTINAL HORMONES.

HORMONE ¹	SECRETION	FUNCTION
Ghrelin	X-cells in stomach	Stimulates appetite
Gastrin	G-cells in stomach and duodenum	Stimulates secretion of HCL, pepsinogen and intrinsic factor
CCK	K-cells in duodenum and jejunum	Stimulates pancreatic and bile secretions Inhibits gastric emptying
Secretin	S-cells in duodenum and jejunum	Stimulates secretion of bicarbonate
GIP	K-cells in duodenum and upper jejunum	Releases insulin from pancreatic β -cells
GLP-1	L-cells in distal ileum and colon	Enhances glucose absorption from intestinal lumen Stimulates insulin release from pancreatic β -cells Inhibits food intake
PYY	L-cells in lower ileum and colon	Inhibits gastro-intestinal motility in response to fat in ileal lumen (‘ileal break’)
Somatostatin	D-cells in stomach, intestine and pancreatic islets	Inhibits HCL and pepsinogen secretion Inhibits pancreatic and biliary secretions Inhibits gastrin, secretin, insulin and glucagon release

¹Abbreviations: CCK, cholecystokinin; GIP, Glucose-dependent insulinotropic polypeptide or Gastric inhibitory peptide; GLP-1, Glucagon Like Peptide-1; PYY, Polypeptide YY. Somatostatin was previously known as growth hormone inhibiting hormone (Petersen and Dimaline 2007).

1.2.8.2 GLUCOSE HOMEOSTASIS AND IMPLICATIONS FOR HEALTH

Glucose (released from digestion of starch and other carbohydrates), is an essential energy source for the brain, kidney, medulla and red blood cells. In healthy individuals, the postprandial rise in plasma glucose concentration is normally counteracted predominantly by the hormone insulin, which stimulates the increased utilisation and storage of glucose by tissues, thereby reducing the circulating glucose concentration to maintain homeostasis (**Figure 1.15**).

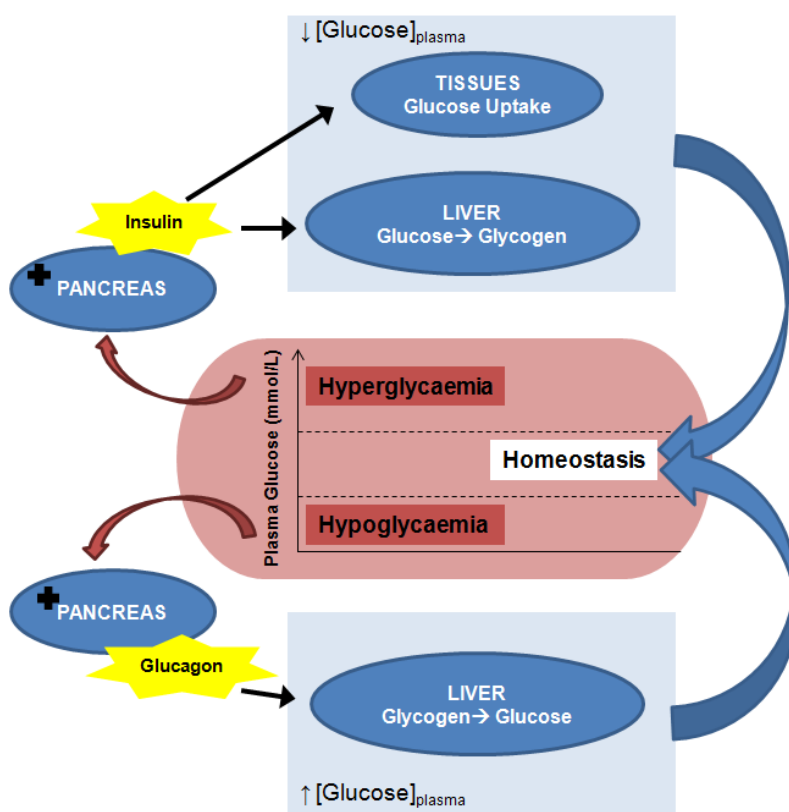


FIGURE 1.15: ROLE OF INSULIN AND GLUCAGON IN GLUCOSE HOMEOSTASIS. When blood (plasma) glucose concentration becomes too high ('hyperglycaemia'), this stimulates the pancreas to release insulin, which acts on tissues and the liver to stimulate glucose uptake, utilisation and storage. When the plasma glucose concentration becomes too low ('hypoglycaemia'), glucagon, released from the pancreas, stimulates the release of glucose from stored glycogen. Thereby, the actions of insulin and glucagon maintain glucose homeostasis (glucose = 4 - 6 mmol.L⁻¹). The action of other hormones, such as growth hormone, adrenaline, and cortisol, which contribute to the regulation of glucose homeostasis, are not shown.

In subjects with insulin resistance the mechanisms involved in maintenance of glucose homeostasis are impaired. The term 'insulin resistance' refers to the failure of insulin, at normal concentrations, to exert its normal effects on target tissues. This condition is associated with impaired glucose tolerance, but also with a range of other metabolic changes that increase the risk of developing coronary heart disease and hypertension. Insulin resistance is a prominent feature of obesity and Type 2 diabetes, and appears to be related to dietary and life-style factors (Wolever 2000). The mechanisms by which insulin resistance develops, however, are not fully understood (Frayn 2010).

In diabetes, there is a problem with the secretion or sensitivity to insulin, such that blood glucose concentrations remain elevated. This is often accompanied by excessive glucagon secretion, which can cause hypoglycaemia (plasma glucose $<3 \text{ mmol.L}^{-1}$). In type 1 (insulin-dependent) diabetes, this occurs because of an inability to synthesise and secrete insulin. Type 2 (non-insulin dependent) diabetes which affects more than 2.9 million people in the UK, develops as a result of a combination of insulin resistance and pancreatic β -cell failure ('Diabetes UK') Consequently, the consumption of foods that are digested *slowly* and tend to elicit a low glycaemic response is encouraged for the dietary management of diabetes (Jenkins *et al.* 2002). The excessive consumption of foods which contain a high proportion of *rapidly* digested starch and/or sugars and elicit prolonged/fluctuating secretions of insulin, on the other hand, seems to be detrimental to glycaemic control (Jenkins *et al.* 2002).

Obesity, which affects ~25% of adults in the UK (2011 data from UK National Statistics) results when caloric intake exceeds energy expenditure, i.e., a 'positive energy balance'. The role of sugars and starch in development and management of obesity are currently inconclusive (Pereira 2006). One view is that because starch is such a major contributor of dietary energy, it is also inevitably implicated in the positive energy balance leading to obesity. Therefore, reducing the consumption of sugar-rich foods and drinks may aid weight loss by a reduction in energy intake (van Dam and Seidell

2007). Similarly, limiting the bioaccessibility of starch in food, for instance by encapsulating starch within plant cell walls, would be expected to reduce energy uptake from food.

While it is recognised that diet provides an important means of preventing and managing these diseases, confusion arises because of the different properties of carbohydrate-foods. The Glycaemic Index (GI), which is calculated from the area under an incremental glycaemic response curve following ingestion of a 50 g carbohydrate load, has been used to document differences in the glycaemic response to a range of carbohydrate foods. Accordingly, foods are often referred to as having a low (≤ 55), medium (56-69) or high (≥ 70) GI (Jenkins *et al.* 1981, Jenkins *et al.* 1984, Brand-Miller 1995, Foster-Powell *et al.* 2002). There are now a number of studies that recommend the use of low GI foods in the dietary management and prevention of obesity, diabetes and cardiovascular disease (Jenkins *et al.* 2002, Wolever *et al.* 1992, Wolever 2000, Brand *et al.*). However, GI labelling of food remains a subject of controversy, partly because of issues and limitations related to the methodology by which GI is determined (see review by (Aziz *et al.* 2013)). An alternative approach could be to measure the rate and extent of starch digestion under simulated conditions *in vitro*, and use this to predict the glycaemic response. However, current digestion models are not yet reliable enough to accurately predict the metabolic response.

1.2.8.3 EXPERIMENTAL DIGESTION MODELS

A range of different methodologies have been used to simulate the *in vivo* digestive environment (Woolnough *et al.* 2008). These range from the simple biochemical digestion models, which use only one or two enzymes (Dona *et al.* 2010) to the more complex multi-compartment systems which attempt to mimic the oral, gastric, duodenal and colonic phases (Bornhorst and Singh 2012, Wickham *et al.* 2012, Rumney and Rowland 1992, Woolnough *et al.* 2008). It has been reported that the rate and extent of starch digestion observed *in vitro* correlates with the *in vivo* glycaemic response (O'Dea

et al. 1981, Granfeldt *et al.* 1992, Englyst *et al.* 1999, Goñi *et al.* 1997, Wolever *et al.* 1988, Seal *et al.* 2003, Van Kempen *et al.* 2010, Weurding *et al.* 2001), suggesting that results obtained *in vitro* are indeed of physiological relevance. However, discrepancies do arise, particularly if the *in vitro* procedure involves de-structuring by severe homogenisation processes in excess of that which occurs *in vivo*.

The simplest biochemical models generally involve incubation of one or more enzymes (usually amylase and/or glucosidase at physiologically relevant concentrations) with a substrate (e.g., isolated starch, flour or homogenised starch-rich food). The digesta is sampled at various points throughout the digestion to monitor the formation of digestion products, or the amount of remaining undigested substrate. These relatively simple models have been particularly valuable in terms of advancing understanding of starch digestion kinetics. For instance, Goñi and colleagues demonstrated that when starch-rich foods such as bread, spaghetti, biscuits, rice, potatoes, potato crisps, and legumes were processed and macerated before they were digested *in vitro*, the resulting digestibility plots could be fitted to a first-order reaction (Goñi *et al.* 1997). This was an important observation, because it demonstrated that enzyme kinetic principles are also applicable to more complex food systems.

One criticism of these simple biochemical digestive models is that they do not simulate the progressive physical breakdown of food structure or the changing biochemical environment that occurs *in vivo* as food moves through the gastro-intestinal tract. In response to this, a number of 'dynamic' or multi-compartment models are currently being developed to simulate physical and biochemical conditions, including the shear stress and mixing conditions and enzyme secretions in the oral, gastric, duodenal and colonic phases of gastro-intestinal digestion. The Dynamic Gastric Model (DGM) at the Institute of Food Research (IFR) is an example of an advanced gastric model. It is a relatively new model, and has been used in conjunction with static models of the oral and intestinal phase to study the survival/degradation of probiotics (Mainville *et al.*

2005, Pitino *et al.* 2010) and pharmaceuticals (Mercuri *et al.* 2011), and the role of viscous fibre in starch digestion (Ballance *et al.* 2013). For practical purposes, the appeal of such multi-compartment models is that they enable samples to be recovered at various stages throughout the simulated gastro-intestinal tract, thereby providing insight into the specific function and contribution of each digestion phase.

In vitro models may be complemented by *in silico* (computer-based) analysis, for instance to explore patterns and relationships which may provide mechanistic insight, and to make predictions about the *in vivo* response (Ellis *et al.* 2007, Van Kempen *et al.* 2010, Ballance *et al.* 2013). In turn, Butterworth *et al.* recently described an enzyme-kinetic analysis method, referred to as the 'Logarithm of Slope' or 'LOS'- method, which allows the release of starch-hydrolysis products to be predicted from the early stages of *in vitro* digestion (Butterworth *et al.* 2012). Overall, novel *in silico* methods may provide relatively easy and low-cost means of studying nutrition and digestion without the demands and ethical constraints of human/animal studies. However, the accuracy and reproducibility of these computer-based techniques in predicting *in vivo* processes has yet to be determined.

1.2.9 PROPOSED ROLE OF CELL WALLS IN STARCH BIOACCESSIBILITY

Understanding the mechanisms by which cell walls limit nutrient bioaccessibility is of interest with regard to predicting and optimising the nutritional value of edible plant tissues.

Cell wall components have previously been shown to limit nutrient bioaccessibility by generating viscosity in the gut lumen (Ellis 1999, Würsch and Pi-Sunyer 1997, Judd and Ellis 2005), however the structural role of intact cell walls in physically encapsulating nutrients has been largely overlooked. Considering that plant cell walls tend to resist digestion in the small intestine, it seems likely that the cell walls may protect the intracellular starch from digestion.

This 'encapsulation' hypothesis is particularly well-supported for leguminous materials. For instance, early *in vitro* studies on leguminous materials have linked the presence of intact cells with a relatively low *in vitro* starch digestibility (Würsch *et al.* 1986, Snow and O'Dea 1981, Tovar *et al.* 1992), and, indeed, such intact, starch-filled cells (e.g., from *Phaseolus vulgaris* L.) have been identified amongst digesta recovered from the end of the small-intestine of human ileostomy volunteers (Noah *et al.* 1998). In another study, the inclusion of undamaged legume cells in mixed meals was reported to lower significantly the postprandial incremental blood glucose and insulin responses in patients with type 2 diabetes (Golay *et al.* 1986). Thus, it seems that starch encapsulated within leguminous cells is protected from digestion in the small intestine and therefore does not elicit a significant glycaemic response (Golay *et al.* 1986). Whether or not cereal endosperm cell walls, which tend to fracture (rather than separate), have a similar protective role is unclear, although it is noteworthy that one study did observe intact, starch-filled cells of barley in ileal effluent (Livesey *et al.* 1995).

An alternative hypothesis is that the food matrix limits the gelatinisation of intracellular starch, for instance by restricting water and/or heat ingress during hydrothermal processing. Evidence for this hypothesis is largely based on qualitative evidence, i.e. microstructural observations of distorted starch granules entrapped within processed food matrices (Würsch *et al.* 1986, Fujimura and Kugimiya 1994), although some studies have attempted to quantify the extent of starch gelatinisation (Champagne *et al.* 1990, Marshall 1992). Considering the large differences between the digestibility of native and hydrothermally processed starch, partial gelatinisation would be expected to have implications for starch digestibility, however, the specific digestibility of this distorted intracellular starch has not yet been studied.

1.2.10 RELEVANCE OF THIS STUDY

From this literature review it is evident that further studies are needed to better understand the many factors that influence starch digestibility and bioaccessibility. Correlations have been observed between fibre content, *in vitro* digestibility and subsequent glycaemia (Wolever *et al.* 1988, Ells *et al.* 2005, Seal *et al.* 2003). However, the underlying mechanisms by which dietary fibre, especially cell wall matrices, affect digestibility, are not well understood (Mann and Cummings 2009, Judd and Ellis 2005, Grassby *et al.* 2013).

Some of the postprandial effects of fibre may be attributed to its capacity to be fermented by micro-organisms in the large intestine, or its role in increasing viscosity and gut transit (Brownlee 2011). However, there is increasing evidence in the literature to suggest that the structural role of fibre, either as intact cell walls or individual polymers, may also be responsible for the differences in digestibility observed in the upper gastrointestinal tract (Bjorck *et al.* 1994, Ellis *et al.* 2004, Mandalari *et al.* 2008). Hence, there is a need to improve our understanding of food structure and material characteristics in studies of digestion.

So far, some progress has been made in terms of understanding the behaviour and properties of isolated food components (e.g. purified cell wall polysaccharides and starches). However the overall structure of the plant tissue, which may remain largely intact after mastication and digestion (Ellis *et al.* 2004), albeit at a reduced particle size, has not yet been studied in a detailed and quantitative way. Furthermore, there is still a lot of uncertainty about how and to what extent food structure is disassembled during digestive transit, which is of fundamental importance in order to improve understanding of nutrient uptake from food. Finally, it also seems that new digestion methodologies are required to enable *in vitro* and/or *in silico* studies of more complex food structures that occur during *in vivo* digestion of real foods.

Here, an effort has been made to overcome some of the methodological limitations of previous studies by using a novel combination of *in vitro*, *in silico* and *in vivo* techniques to compare the digestibility of two contrasting edible plants – chickpea and durum wheat.

1.2.10.1 AIM & OBJECTIVES

The overall aim of this PhD project is to study the role of the cell walls of starch-containing edible plants (cereals and legumes), in influencing the bioaccessibility of starch.

The specific objectives are to:

- i. Compare physico-chemical characteristics of starch-containing tissues of chickpeas (legume) and durum wheat (cereal).
- ii. Establish the mechanisms by which amylase digests starch entrapped in a complex food matrix
- iii. Develop a mathematical *in silico* model of starch digestion, applicable to study starch digestion in heterogeneous plant matrices
- iv. Determine the consequential effects of cell wall encapsulation of starch on the post-prandial glycaemic and insulinaemic responses and the resistant starch content of selected plant foods in ileostomy volunteers
- v. Evaluate the role of plant cell walls in regulating starch bioaccessibility and digestion kinetics, and consequential effects on post-prandial metabolism.

CHAPTER 2

MATERIALS & METHODS

2.1 PLANT MATERIALS

Chickpeas (*C. arietinum* L.; Russian cv., Kabuli type) were donated by Poortman Ltd., London, UK. Durum wheat grains (*Triticum durum* L.; Svevo cv.), were provided by Millbo S.p.A., Trecate, Italy. These raw materials were food-grade, and were subsequently processed into flours of different particle sizes using commercial pilot scale milling techniques. For experimental purposes, starch and intact plant cells were also isolated from these materials, as described below.

2.1.1 STARCHES

Starches were extracted from durum wheat grains and chickpeas using a modification of previously described methods (Vansteelandt and Delcour 1999, Güzel and Sayar 2010). Grains or chickpeas were steeped overnight in ~0.2 (w/v)% sodium bisulphate at 25 °C, and then homogenised using an Ultra-Turrax[®] (IKA T25 digital). The homogenised material was then washed through steel analytical sieves (Labquip Ltd., Penrith, Cumbria, UK) with 250 and 160 µm apertures to exclude any intact tissue or cells. As chickpea endosperm cells are smaller than durum wheat cells, an additional 106 µm sieve was included for chickpea starch extraction to obtain a more homogeneous filtrate. The filtrate was aliquoted into several 50 mL falcon tubes, and centrifuged for 10 min at 1800 x G (Mistral 3000 MSE centrifuge). The collected starch pellet was purified through repeated centrifugation, decantation of supernatants, and re-suspension in 80% (v/v) ethanol (rather than NaOH used in the original methods). Finally, the purified starch was distributed across the bottom of a large plastic container and left to dry uncovered at 22 °C for 2 days prior to storage. With this method, 22% of the starch contained in chickpeas and 37% of the total amount of starch contained in durum wheat grains was extracted.

2.1.2 MILLED FRACTIONS

Milling was performed on two occasions: Milled materials for laboratory use were prepared at The Mill, University of Manchester, Manchester, UK, whereas food-grade milled durum wheat was prepared according to Hazard Analysis and Critical Control Points (HACCP) guidelines at Satake Europe, Bredbury Industrial Estate, Stockport, UK. The equipment available at the two sites differed slightly, but the principles of operation and the materials obtained are comparable.

First, the outer protective layers of the wheat grains or chickpea seeds (i.e. bran and seed coat, respectively) were removed (**Figure 2.1**). Chickpeas were de-hulled manually following a 2 h soak in water, then spread out across a tray and left to dry for 4 days. Durum wheat grains were first colour-sorted (AlphaScan™ AS II 32, Satake Europe Ltd., Stockport) to remove foreign seeds and insects (~1.6% rejected), then de-branned in 200 g batches by abrasion for 2 min in a Satake de-branner, model TM-05C (lab-grade) or TH050 (food-grade).

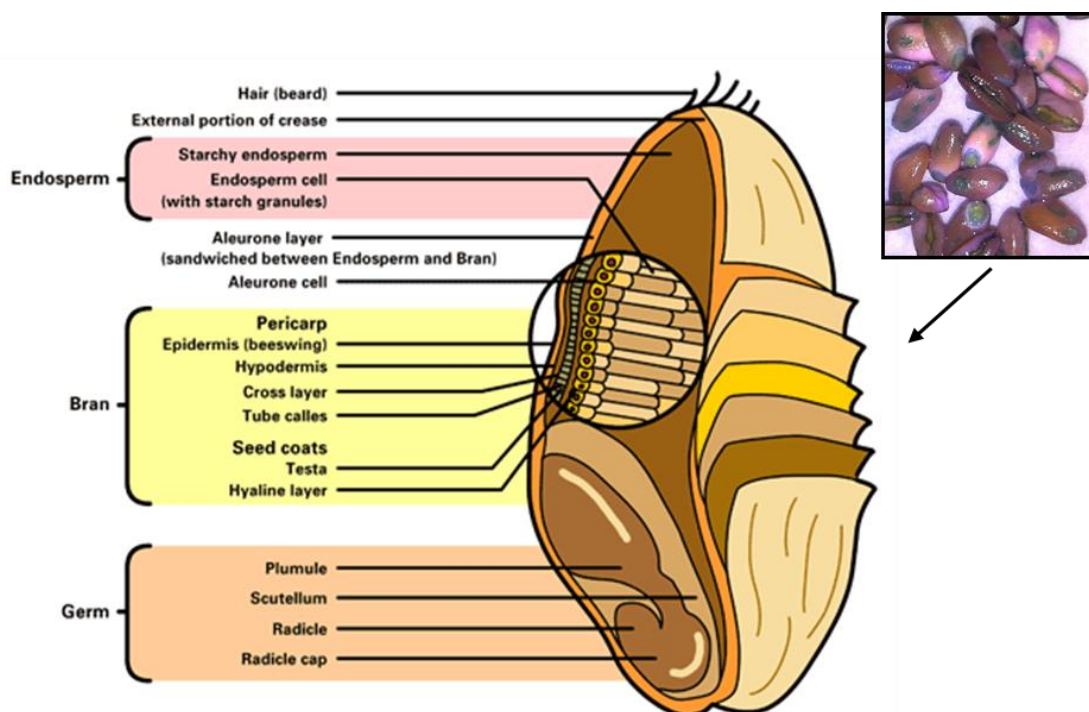


FIGURE 2.1: ILLUSTRATION OF WHEAT GRAIN SHOWING BRAN LAYERS AND PHOTOGRAPH OF DE-BRANNED GRAINS STAINED WITH CICA REAGENT. In the photograph the endosperm is stained pink, aleurone blue and the pericarp and testa stained green. Image adapted from HGCA [online] (2014).

The de-branning treatment removed the majority of the pericarp, testa, and aleurone, resulting in ~15 – 20% mass loss. However, treatment with phenolphthalein (methanolic MG solution CAT-28362-32, 'CICA reagent', Kanto Chemical Co. Inc.), revealed that some non-endospermic tissue remained, particularly in the crease region of the grain (**Figure 2.1**). Further abrasion did not remove the crease, which folds into the centre of the grain, and when extended abrasion was attempted, this caused a greater erosion of endosperm. Therefore, although the milled wheat grains consisted predominantly of endosperm, some residue from other tissues adhering to the endosperm was inevitable.

Next, the de-hulled chickpeas and de-branned durum wheat were milled to obtain a range of particle size fractions. Roller-milling was used, as these type of mills are versatile and offer greater control over milling parameters and therefore of sample materials obtained. The seeds or grains also pass through the mill in less than 30 seconds, such that any heat generation from friction was minimal.

Roller-mills are used in commercial flour production during the first-break, where the endosperm is separated from the bran, and further reduced on reduction rolls to produce flour. The main components of a roller-mill are illustrated in (**Figure 2.2**).

The break-rolls are generally fluted with an asymmetric saw tooth profile, so that by altering the relative roller speed ('differential'), the mill may be operated in one of four dispositions: Sharp-Sharp, Dull-Dull, Sharp-Dull or Dull-Sharp. The disposition determines the working angle of the flutes and thereby the direction and magnitude of breakage forces, with significant effects on the particle size distribution of milled material (Fang and Campbell 2003).

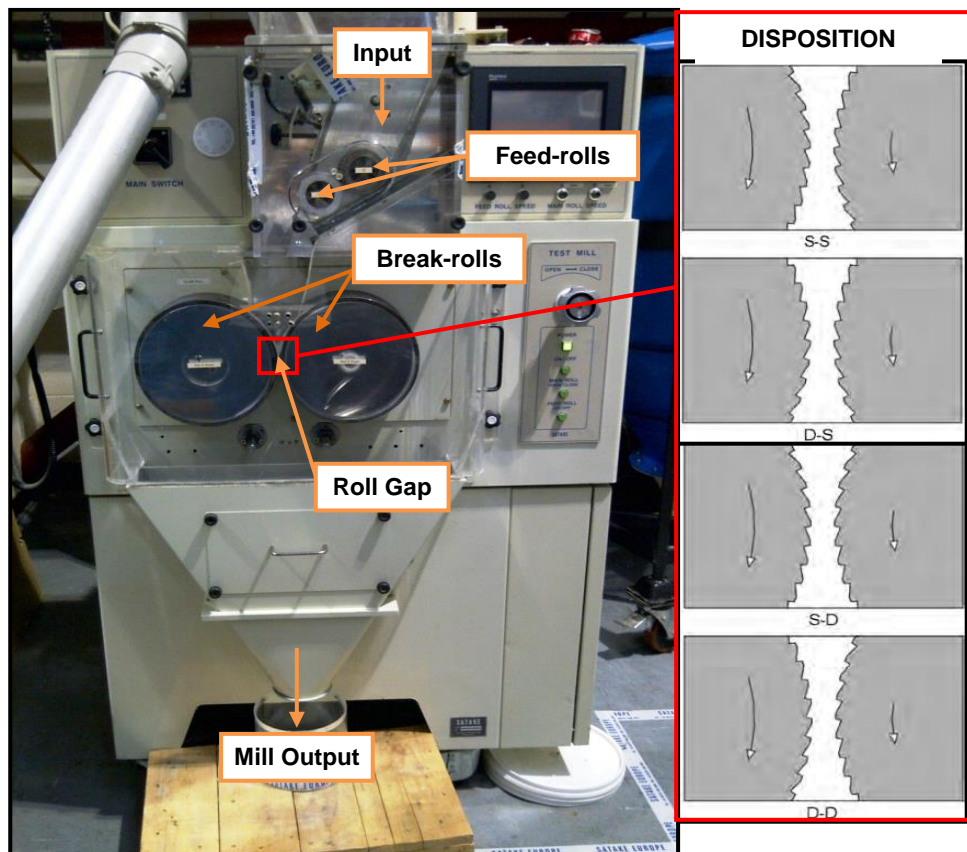


FIGURE 2.2: SATAKE TEST-ROLLER MILL AND DISPOSITION. STR-100 roller-mill, Four dispositions shown: S:S; Sharp to Sharp, D:D; Dull to Sharp, S:D; Sharp to Dull, and D:D; Dull to Dull. Arrows indicate relative roller speed (i.e. larger arrow indicates faster speed). Adapted from Campbell 2007.

The test materials used in the present work were milled using a sharp-sharp disposition was used, because this breaks the bran and endosperm of wheat simultaneously, such that a narrower particle size distribution is achieved. The relative roller speed was set to achieve a range of differentials (between 2.5 and 1.9, roller speed: 222 rpm: 421 - 555 rpm), with the higher differential used to obtain a greater yield of large particles. The distance between the two break rolls ('roll gap') can also be altered to control output particle size, with a larger roll gap generally producing a greater proportion of large particles (Fang and Campbell 2002). Thus, in order to obtain a high yield of target size fractions, the roll gap was progressively reduced (i.e. from 1.7 mm to 0.2 mm) because smaller particles were required. For flour milling, where very fine particles (<0.21 μm) were desired, milled residue from the first-break was re-milled on smooth rolls with a minimal roll gap to achieve a compressive, grinding action (Campbell 2007).

The milled materials were separated, using a selection of analytical sieves, into 10 size fractions ranging from flour (< 0.210 mm) up to 3.15 mm coarse particles. This effectively manipulates the proportion of cell wall encapsulated starch in the milled materials (**Figure 2.3**). The proportion of intact and ruptured cells in these different size fractions was estimated using principles of geometry, as described in *Chapter 3, Section 3.2.2*.

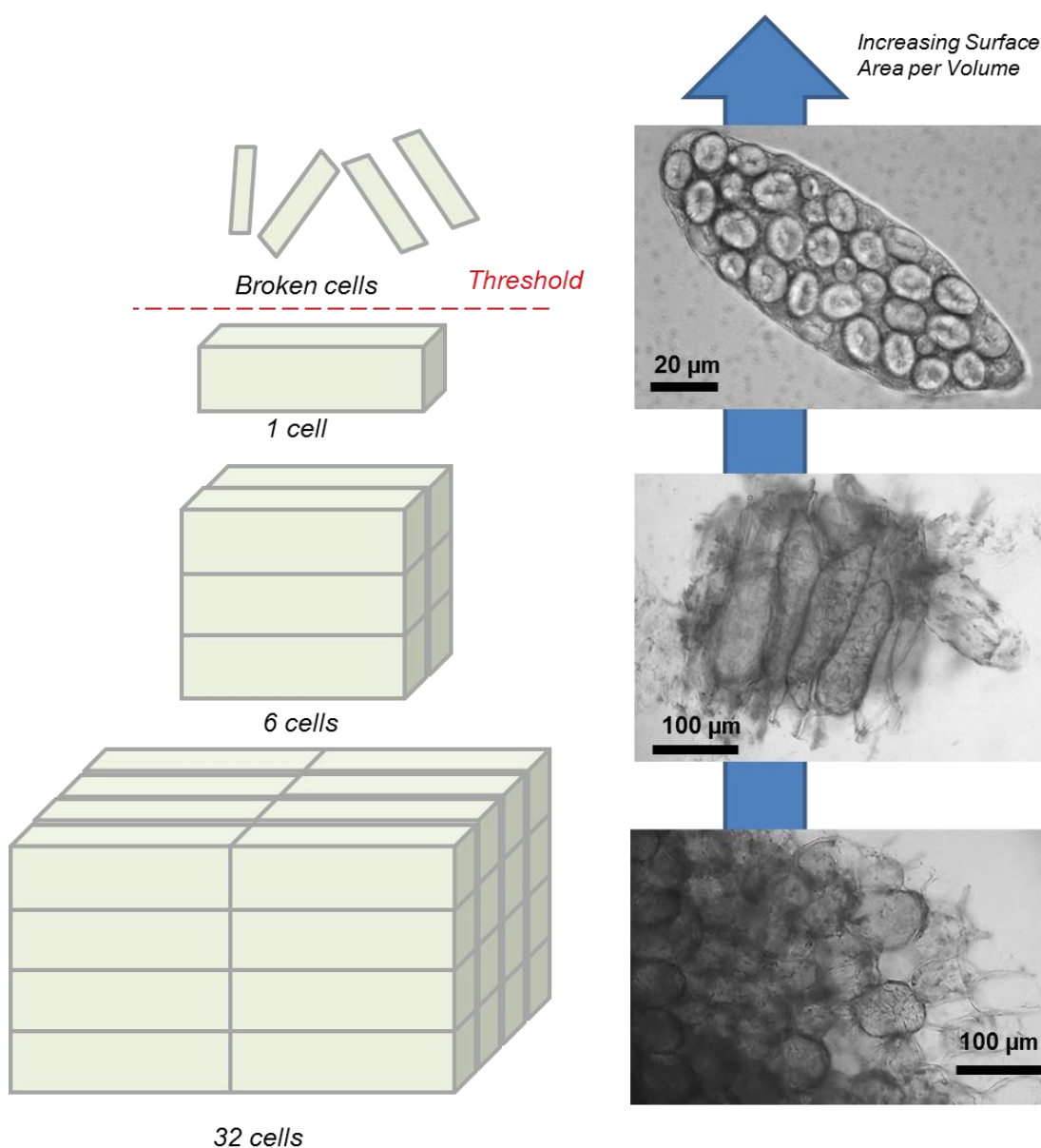


FIGURE 2.3: PARTICLE SIZE AND CELLULAR INTEGRITY. As the particle size decreases, surface area per volume ratio increases, and a greater proportion of the cells in the particle are ruptured (i.e., on the particle surfaces) 'Threshold' indicates the size at which no further reduction in size can be achieved without rupturing all the cells.

2.1.3 SEPARATED CELLS

Separated cells were isolated from de-hulled chickpeas using a hydrothermal treatment. The combination of heat and water is known to cause the pectic polysaccharide in the middle lamella to depolymerise and solubilise. This leads to a weakening of the intercellular adhesions, and thereby enables isolated cells to be obtained. A schematic of the method is provided in **Figure 2.4**.

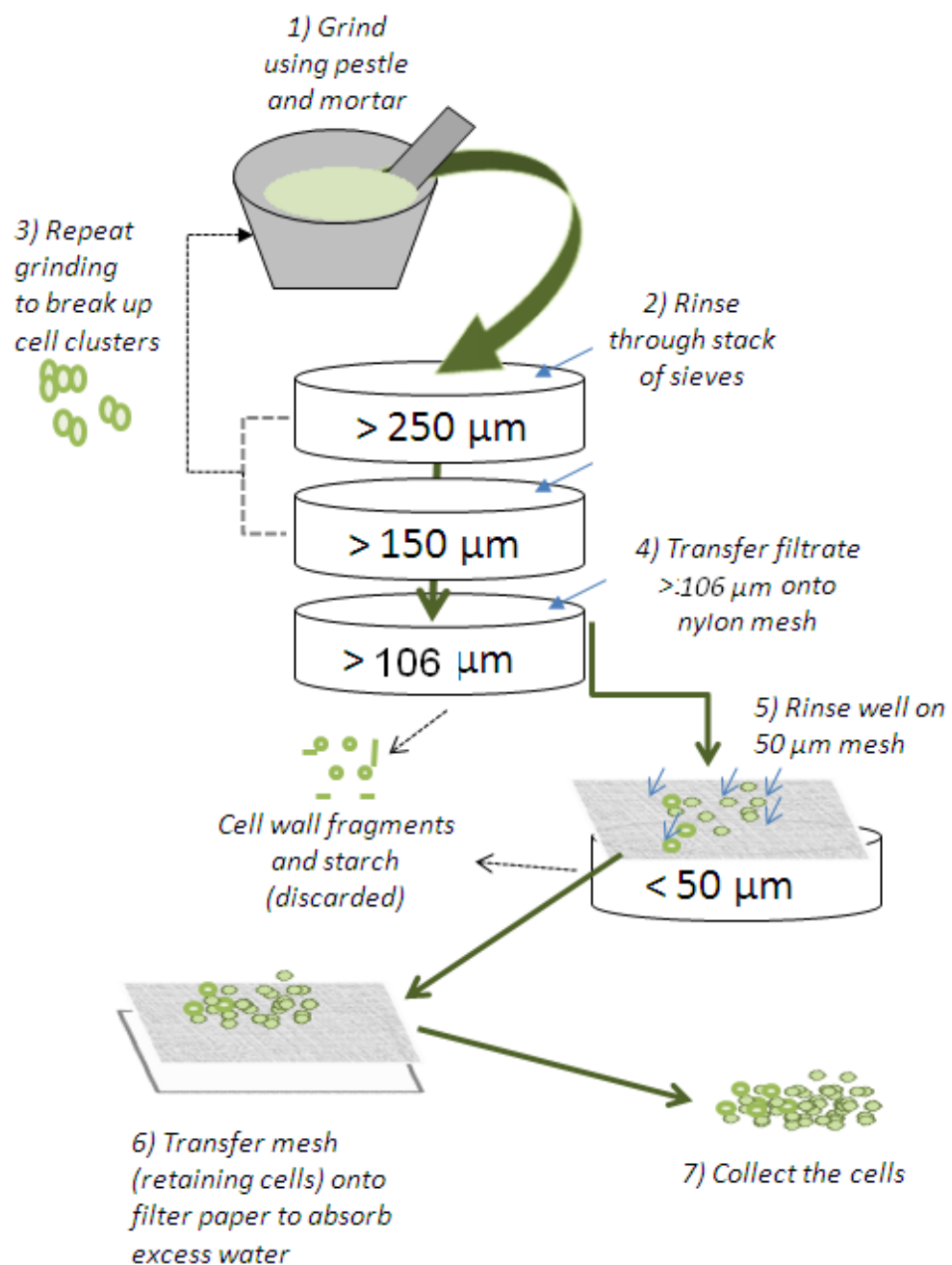


FIGURE 2.4: PREPARATION OF SEPARATED CELLS FROM HYDORTHERMALLY PROCESSED CHICKPEAS.

To prepare separated cells (**Figure 2.4**), de-hulled chickpeas (prepared as described in *Section 2.1.2*) were soaked at room temperature overnight in a large beaker containing 5 times their volume of deionised water. The following day, the hydrated chickpeas were heated to 95 °C and hydrothermally processed for 1 h. Next, the boiling liquor was decanted and the cooked chickpeas were ground with a pestle and mortar and washed through a stack of sieves to break-up any cell clusters. Intact, separated cells are retained on a sieve with 106 µm aperture. The residue on this sieve was rinsed thoroughly with deionised water to exclude cell wall fragments and free starch granules. The cells, retained on the 106 µm sieve, were then transferred onto a nylon mesh with a 50 µm aperture, and rinsed once more. Finally, glass fibre paper (Type A/E Glass, Pall Corp., Michigan) was placed under the mesh to absorb excess water. This left a grainy 'cell paste', which could be weighed into tubes for immediate use in assays ('fresh cells') or allowed to dry to a low moisture state ('dry cells') for storage (**Figure 2.5**).

Quantifying cells by weighing in paste-form was found to be considerably more reproducible than attempting to pipette a suspension of cells. However, the cells are not stable in this form, because the moisture content declines rapidly during storage. Thus, for more permanent storage, the cell paste was distributed across a tray and allowed to dry to a constant weight (~ 9% moisture, as measured by oven drying method; see *Section 2.3.2, page 81*), before storage.

In the low-moisture state, the cells are stable for several months. The form of cells used is specified for each experiment described in subsequent chapters. The yield of cells achieved with this method ranged from 22-55% (recovery of dry weight of de-hulled chickpeas). The highest yields were achieved by repeated grinding of material retained on the sieves with 250 and 150 µm apertures.

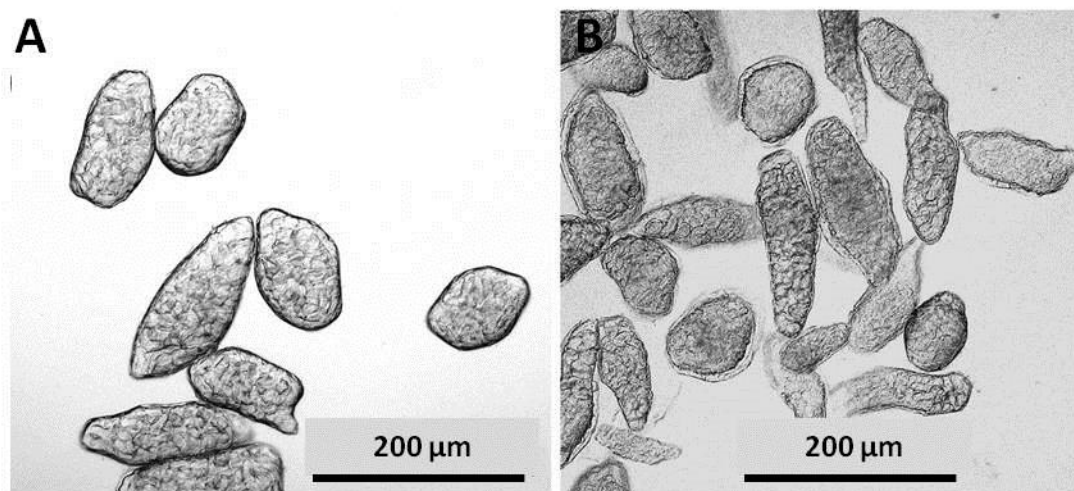


FIGURE 2.5: SEPARATED CELL PREPARATIONS (A) FRESH CELLS AND (B) DRY CELLS. Fresh cells were viewed within 30 min of isolation. Dry cells were re-hydrated in water for ~12 h before viewing. Scale bar = 200 µm.

2.1.4 PROTOPLASTS

A range of attempts were made at creating 'leaky cells' for use as experimental materials. These preliminary experiments included exposing cells to a range of chemical, hydrothermal and mechanical treatments and assessing permeability, but attempts to create leaky cells were largely unsuccessful. Instead, enzymes that degrade the cell wall were used to remove the cell walls completely, leaving the intracellular contents, i.e. the 'protoplasts'.

Protoplasts were obtained using Driselase[®] from *Basidiomycetes* sp. (Sigma-Aldrich Co Ltd., UK). Driselase[®] is a crude extract containing a combination of cell wall degrading carbohydrases, notably; 100 U/g solid cellulase, >10 U/g solid of laminarinase, and ≥ 3 U/g xylanase. Prior to use, driselase[®] was purified using previously described methods (Fry 1988) and the protein content of the purified extract was determined by a bicinchoninic (BCA) assay (Smith *et al.* 1985)) To prepare protoplasts, 125 ± 1 mg of freshly prepared cell paste was suspended in 640 µL sodium acetate buffer 50 mM, pH 5.0, to which was added 160 µL driselase stock (5.43 mg protein.mL⁻¹). This was incubated on a rotary mixer at 37°C for 14 h, which, on microscopical examination, appeared to be sufficient to digest the cell walls. The protoplasts were centrifuged at 12000 x G for 1 min, and the pellet rinsed 3 times with

PBS to remove driselase residue. Next, 700 μL of 100 μM phenylmethanesulfonyl fluoride (PMSF, 5 μL of 100 mM stock in ethanol added to 5 mL PBS) was added to inhibit any residual proteolytic activity. This was mixed on the rotary mixer at 37 °C for 4 h. This was more than double the half-life of PMSF (at pH 7.0, $t_{1/2} = 110$ min). Finally, the sample was centrifuged again 12000 x G for 1 min, and the supernatant replaced with 1 mL fresh PBS. For subsequent digestibility experiments, the protoplasts were immediately re-suspended, and 100 μL 'blank' sample collected, before addition of porcine pancreatic α -amylase, as described in *Chapter 4*.

2.2 CHEMICAL REAGENTS

All chemicals were of the highest available grade and obtained from Sigma-Aldrich Co. Ltd., Poole, Dorset unless otherwise specified. Porcine-pancreatic α -amylase of a high purity (Grade 1-A) was obtained from Sigma-Aldrich Co. Ltd. (A6255, EC 3.2.1.1). The manufacturers state that the enzyme preparation was treated with diisopropyl fluorophosphate (DFP) to inhibit protease activity, and it was supplied in 2.9 M NaCl (with 3 mM CaCl_2). The purity of the enzyme was confirmed by denaturing gel electrophoresis in which the enzyme formed a band at 56 kDa, and no other contaminants were observed (Roder *et al.* 2009). The total protein content (determined by a BCA assay (Smith *et al.* 1985)) and activity (determined by assaying hydrolysis of purified wheat starch) of the enzyme was found to be within the range specified by the manufacturer (1333 U/mg protein). One unit of activity, as defined by the manufacturers, releases 1 mg of maltose from starch in 3 min at 20 °C. This is approximately equivalent to 1 IU at 20 °C (Tahir *et al.* 2010).

Phosphate buffered saline (PBS) was prepared from tablets (Oxoid, Basingstoke, UK) dissolved in deionised water ('dH₂O', from PURELAB Ultra, ELGA) to give a final concentration of 137 mM NaCl, 2.7 mM KCl, 10 mM phosphate, pH 7.4 at 37 °C.

'Total Starch (AA/AMG)' assay kits were obtained from Megazyme International, Ireland. Details of kit components are provided in *Section 2.3.3*. Assay kits used for blood analysis are described in the *Appendix D*.

2.3 CHEMICAL ANALYSIS

This section describes the methods used to determine the composition (e.g., starch, sugar, and moisture content) of the plant materials described in *Section 2.1*. Most of these methods were modified from existing protocols to achieve a higher-throughput, as they were also needed for the analysis of samples collected during various *in vitro* and *in vivo* studies.

2.3.1 PROXIMATE ANALYSIS

Proximate analysis was carried out on milled fractions and separated cells by Premier Analytical Services (High Wycombe, UK) according to in-house methods. The principles behind these proximate analysis methods are described in detail elsewhere (Kirk and Sawyer 1991). In summary, energy values were determined using conversion factors (European commission directive 2008/100/EC). Crude protein was calculated from the nitrogen content of samples using standard conversion factors (in this case $6.25 \times N$). Nitrogen was measured based on the Dumas principle, according to method No.0019 of the Flour Testing Working Group (Anderson and Salmon 1999), in which nitrogenous constituents of the sample are oxidatively combusted (at $850\text{ }^{\circ}\text{C}$ - $1100\text{ }^{\circ}\text{C}$) to nitrogen oxides, and then reduced to gaseous nitrogen and measured using a gas chromatograph with a thermal conductivity detector. Fat was determined by a method similar to the Werner-Schmidt process (Kirk and Sawyer 1991), in which the sample is hydrolysed in a mixture of hot formic and HCL acids, and the liberated fat is extracted into hexane. Dietary fibre was determined gravimetrically based on AOAC 1995 32.1.17, Method 991.43, in which starch and protein is removed by enzyme treatments, and the resulting residue, which is insoluble in 78% ethanol, is determined gravimetrically. Sugars were determined by HPLC (Jones *et al.* 1977). Total ash was determined

gravimetrically following incineration of organic matter at 500 °C (BS 4603:1970). Moisture was determined by oven drying at $102 \pm 1^\circ\text{C}$, (derived from commission directive 79/1067/EEC). Total available carbohydrate was determined 'by difference', meaning that the carbohydrate content is assumed to be what remains in a 100 g sample after subtraction of protein, lipid, ash, fibre, and moisture contents. The starch content is then obtained by subtracting the analysed sugars from the calculated available carbohydrate content.

Due to the accumulated errors associated with the method of estimating carbohydrate 'by difference', the measurement of starch content in the milled and cell samples was also carried out in our laboratory using direct methods (see total starch analysis, *Section 2.3.3*). Moisture analysis was carried out in parallel, as described in the section below.

2.3.2 MOISTURE DETERMINATION

Moisture content was determined using an oven-drying (gravimetric) method, in which the moisture content is determined based on the assumption that all loss of mass results from the evaporation of water during drying. In this method, 30 mL aluminium pans with a screw-top lid (Ampulla Ltd., Hyde) were dried in an oven at $103 \pm 2^\circ\text{C}$ for 16 h. The pans were then transferred to a desiccator containing silica gel, and allowed to cool to room temperature for 30 min. The dry weight of the empty pans and lids was recorded. Wet samples were added to the pans, taking care to break-up any aggregates or big particles. The weight of each wet sample added to the pans was recorded. Samples were then returned to the oven and allowed to dry at $103 \pm 2^\circ\text{C}$ for 16 h (overnight). The following morning, samples were moved to the desiccator and allowed to cool for 30 min before recording the dry weight. All analyses were performed in triplicate. Moisture content was calculated from the difference in wet and dry weight (**Equation 2.1**).

$$\text{Moisture (\%)} = \frac{\text{sample wet weight (g)} - \text{sample dry weight (g)}}{\text{Sample wet weight (g)}} \times 100$$

EQUATION 2.1: CALCULATION OF MOISTURE CONTENT**2.3.3 TOTAL STARCH DETERMINATION**

Total starch determination was performed using a modified version (see **Figure 2.6**) of the Megazyme Total Starch Test (AOAC 996.11 Official Method). This method relies on an enzyme cascade in which amylase and amyloglucosidase (AMG) are used to convert starch into glucose, which in turn, may be determined colorimetrically with a glucose oxidase assay (McCleary *et al.* 1994).

The manufacturer outlines a number of different versions of this test, depending on the nature of the material to be analysed and on the outcome measures required (for instance, available starch, resistant starch, or sugars). Here, the DMSO-format of the test was used, as this method should return the total starch content, including 'resistant starch', i.e. starch which is encapsulated within plant cell walls. However, bearing in mind the vast differences in plant tissue structure and susceptibility to enzyme hydrolysis, some modification of this generic method was required in order to ensure that all the starch contained within the material was converted to glucose for detection. The need for these modifications became apparent, because although the method described by the manufacturer works well for the purified starch standard supplied, it consistently underestimated the starch content of chickpea and durum wheat materials. Upon micro-structural examination, a number of issues were identified, particularly at the solubilisation stage, where intact starch-containing chickpea cells were clearly present after 6 min of treatment with hot DMSO. Thus, a high-throughput, smaller scale version of the protocol was developed, which uses components of the Megazyme Total Starch Assay kit, but with necessary modifications to ensure complete starch conversion to glucose.

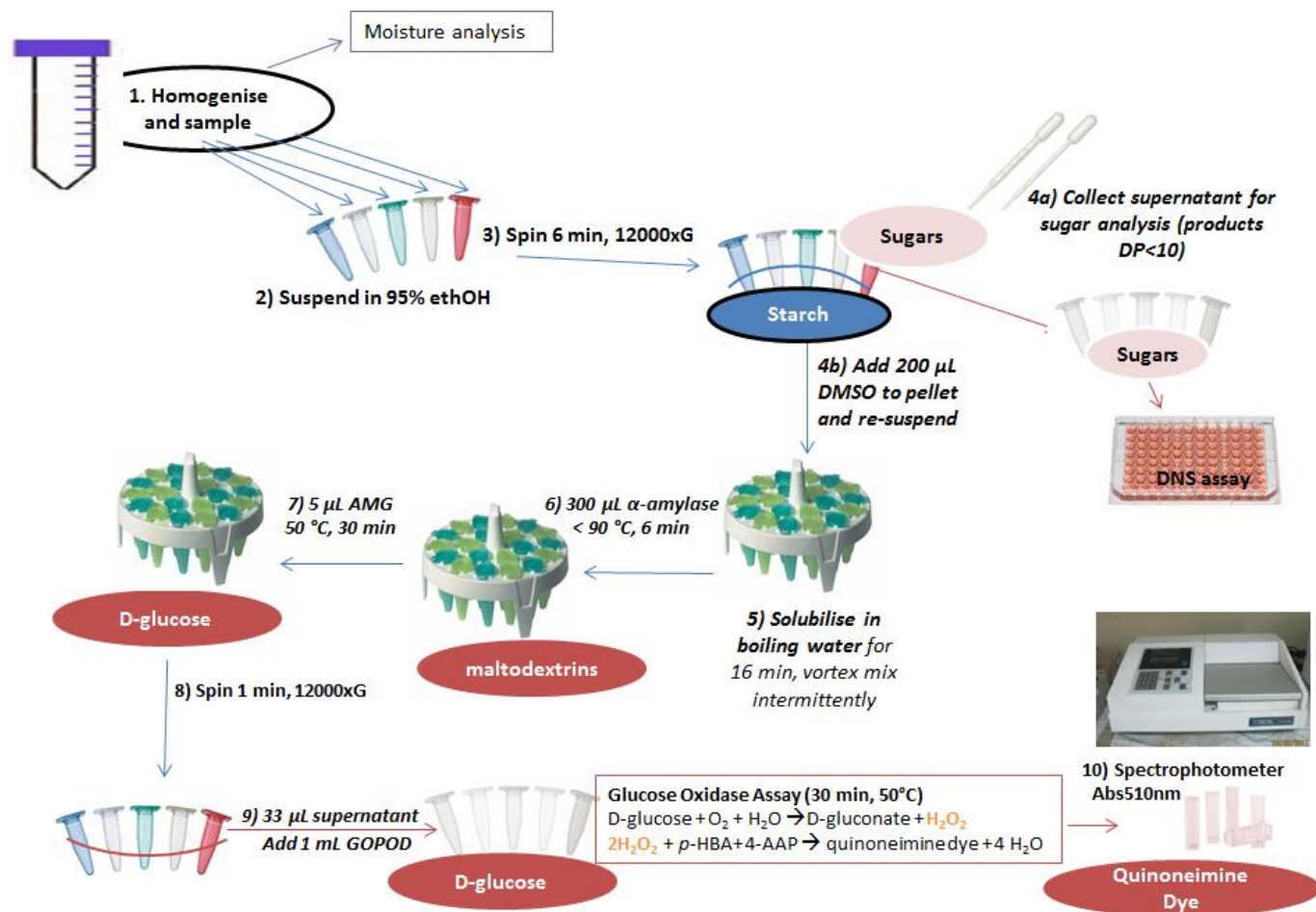


FIGURE 2.6: HIGH-THROUGHPUT TOTAL STARCH DETERMINATION METHOD. Abbreviations: ethOH; ethanol, DMSO; dimethylsulfoxide, AMG; amyloglucosidase, *p*-hba; *p*-hydroxybenzoic acid, 4-AAP; 4-aminoantipyrine, Abs; absorbance, DNS; dinitrosalicylic acid (see Section 2.3.4.1), GOPOD; Glucose oxidase peroxidase.

The modified assay protocol was used to determine the total starch content of chickpea and durum wheat starch, which is present in cells and milled fractions, as well as for the determination of total starch in ileal effluent. One kit is normally sufficient for 100 assays, but initial tests revealed that this method could be scaled down to 1/20th of the original scale without increasing measurement errors, thus conveniently permitting analysis in disposable 1.5 mL tubes (instead of glass test tubes).

First, material to be analysed was ground (for dry plant materials) or homogenised (for wet ileal effluent), then suspended and/or diluted in 95% (v/v) ethanol. Next, 4 x 1 mL aliquots of the homogeneous suspension were taken into 1.5 mL Eppendorf Safe-Lock Tubes™ and centrifuged at 12000 x G for 4 min, to sediment the starch residue, leaving sugar and oligosaccharides with DP<10 in the supernatant. If desired, an aliquot of the supernatant was taken at this stage for subsequent sugar analysis, as described in *Section 2.3.4*. A fine-tip plastic pasteur pipette was then used to remove all the supernatant, leaving the collected starch pellet undisturbed. The starch pellet was then re-suspended in 200 µL DMSO with vigorous mixing. If, at this stage, the pellet did not re-suspend, the procedure was repeated using a more dilute sample (i.e. less than 20% solids) to improve chances of solubilisation.

Tubes containing starch suspensions were then loaded into a Nalgene® (Thermo Scientific) floating rack and placed in a boiling water bath for 16 min, with intermittent vortex mixing, which is longer than specified in the original method, but necessary to ensure complete solubilisation of starch. Next, the boiling water bath was switched-off, and thermostable α-amylase from *Bacillus licheniformis* (53 U/mL on Ceralpha reagent, pH 5.0 and 40°C, diluted 1:30 from stock in 100 mM sodium acetate buffer, pH 5.0 containing 5 mM CaCl₂), was added. Samples were then returned to the water bath (80 - 90 °C) for 6 min to catalyse starch-hydrolysis. The ‘thermostable’ amylase has a higher activity at lower temperatures (temperature optima = 75 °C, temperature stability > 80 °C, as specified by Megazyme Ltd.), and so adding this enzyme after the

temperature of the sample had cooled slightly improved the conversion of starch to maltodextrins.

Samples were then moved to a 50 °C waterbath and allowed to equilibrate before addition of 5 µL amyloglucosidase solution (activity of 3300 U/mL on soluble starch). The samples were returned to the 50 °C waterbath for 30 min, to allow time for conversion of maltodextrin to glucose. Samples were then centrifuged at 12000 x G for 1 min to spin down any residual material (dietary fibre etc.). If necessary, the supernatant was diluted in dH₂O at this stage so that the concentration of glucose in the sample would fall within the working range (0.1 to 1 mg/mL glucose) of the glucose oxidase assay. A 33 µL aliquot of the diluted supernatant was then transferred into 1.5 mL tubes, to which was added 1 mL of GOPOD reagent (Glucose oxidase plus peroxidase and 4-aminoantipyrine in *p*-hydroxybenzoic acid reagent buffer, pH 7.4, with <0.02% w/v sodium azide). Two glucose standards were also included at this stage. Samples and standards were incubated for 30 min at 50 °C, during which colour development occurred. The samples were then allowed to cool to room temperature before decanting into 1mL cuvettes. Finally, the absorbance of samples and standards was read at $\lambda = 510$ nm in a spectrophotometer (CE2041, Cecil Instruments, Cambridge, UK) against the reagent blank (water and GOPOD). The total starch content was then calculated as described in the Megazyme Official method (**Equation 2.2**), accounting for sample moisture to express on a dry weight basis.

$$\text{Starch (mg/mL)} = \Delta Abs \times F \times D \times \frac{162}{180}$$

EQUATION 2.2: CALCULATION OF STARCH CONTENT. ΔAbs is the absorbance read against the reagent blank, F is the conversion from absorbance to mg, D is the dilution factor used to account for dilution of sample at various stages throughout the assay, and $162/180$ is the adjustment from free D-glucose to anhydro D-glucose (as occurs in starch).

2.3.4 SUGAR DETERMINATION

Sugar analysis was carried out using either 3,5-dinitrosalicylic acid reagent (DNS), Glucose Oxidase, or Prussian blue assays (Deng and Tabatabai 1994, Miller 1959). The DNS and Prussian blue methods detect all reducing sugars (e.g. maltose, maltotriose), whereas the glucose oxidase assay measures glucose only.

2.3.4.1 DNS ASSAY

The DNS assay is the least sensitive of the sugar assays used but, it was chosen because of its broad working range (linearity observed between 5.6 and 22 mM maltose). This assay was particularly well-suited for the determination of sugars in ileal effluent (*Chapter 7*), since samples could generally be assayed without the need for further dilution. The assay method, originally developed by Sumner *et al*, is based on the reduction of 3,5-dinitrosalicylic acid to 3-amino-5-nitrosalicylic acid, a highly coloured compound which has an absorption maximum at 458 nm (Sumner and Graham 1921). A limitation of this method is that it does not distinguish between different reducing compounds present. For the purpose of quantifying starch hydrolysis products, it was assumed that all reducing-power originated from reducing-sugars, and that all these oligosaccharides elicited a similar colour change. On this basis, the concentrations of total reducing sugar (expressed as maltose equivalents) were obtained.

Various versions of this method have been used (Miller 1959). Here, the assay method described by Slaughter *et al*, was modified to be performed in a microarray plate (Slaughter 2000): Samples (i.e. an aliquot of ileal effluent suspended in ethanol) were first centrifuged at 12000 x G for 4 min to spin down any starch remnant or other residues. Maltose standards were also included in the assay (2–8 mg/mL). Next, 15 µL of supernatant were transferred into the wells of a 96-well, flat-bottom, clear plate (Nunc[®] MicroWell[™]). A Multipette[®] plus with combitip[®] was then used to add 5 µL of 3M NaOH, to each well and a multi-channel pipette was used to add 20 µL DNS

reagent, consisting of 1.0% (w/v) DNS acid, 1.6% (w/v) NaOH, and 30.0% (w/v) sodium potassium tartrate in dH₂O, to the wells. The microarray plate was then covered with foil to prevent evaporative losses and floated in a waterbath at 90°C for 5 min. The plate was then taken out of the waterbath and allowed to cool for 5 min before addition of 200 µL dH₂O. The sample absorbance at 544 nm was then read in a FluoStar Optima plate reader (BMG Labtech).

2.3.4.2 GLUCOSE OXIDASE

The glucose oxidase assay has already been described, as it is the final stage in the starch analysis procedure outlined in *Section 2.3.3*

2.3.4.3 PRUSSIAN BLUE ASSAY

The Prussian blue assay offers a sensitive colorimetric method for detecting reducing sugars. The colour formation arises as a result of reduction (by reducing sugars) of ferricyanide ions in alkali solution at 100 °C, which results in the formation of ferric ferrocyanide aka 'Prussian blue' (Deng and Tabatabai 1994, Park and Johnson 1949). Due to its extremely high sensitivity to reducing sugar (limit of detection of 1 µM), this was the preferred method for quantification of starch hydrolysis products (mainly maltose and maltotriose) in the enzyme kinetic studies. The assay was modified for this purpose by previous workers. (Slaughter *et al.* 2001, Slaughter *et al.* 2002, Tahir 2008, Warren 2011). For the assays described in this thesis, samples (i.e. supernatant from inactivated aliquots of digesta) were first diluted in dH₂O, which is necessary not only to bring the sugar concentration down to a suitable working range (20 – 100 µM maltose), but also to dilute the effects of any buffers in the original sample, as the assay is incompatible with many common buffers, including PBS. Next, 150 µL of the diluted samples was transferred into 1.5 mL Eppendorf Safe-Lock Tubes™, to which were added 150 µL of Solution A (16 mM KCN, 0.19 M Na₂CO₃ in dH₂O) and 150 µL of Solution B (1.18 mM K₃Fe(Cn)₆ in dH₂O

The tubes were sealed and moved to a Nalgene[®] floating rack, which was then placed in a boiling water bath for 15 min. The samples were allowed to cool for 10 min before addition of 750 μL of Solution C (3.11 mM $\text{NH}_4\text{Fe}(\text{SO}_4)_2$, 0.1% (w/w) SDS and 0.2% (v/v) H_2SO_4 in dH_2O). The samples were left at room temperature for 2.5 h to allow time for colour development, prior to reading the absorbance against a reagent blank reading at 695 nm in a spectrophotometer (CE2041, Cecil Instruments, Cambridge, UK). Maltose standard solutions (20 – 100 μM) were included in every assay, and the concentration of reducing sugar in the samples was calculated from a standard curve and expressed as maltose equivalents.

2.4 MICROSTRUCTURAL ANALYSIS

A number of techniques were used to visualise micro-structural changes during various experiments. Specific details of the microscopy technique (e.g., resins, stains) are provided in each micrograph caption.

2.4.1 LIGHT MICROSCOPY

For some purposes, samples were viewed 'as is', whereas other samples were embedded in resin and sectioned. In general, for visualization of smaller particles, such as starch, flour and cells, the samples were simply suspended in dH_2O , dropped onto a glass slide and covered with a glass cover-slip before viewing. Larger particles, however, required sectioning in order to visualize the internal particle microstructure. These samples were fixed, washed, dehydrated, embedded in resin and cured prior to cutting. The details of the protocol used, i.e. the chemicals and conditions and time the sample was exposed to each treatment solution, was adapted from published protocols (Flint 1994). The entire procedure was carried out under the fume hood, wearing long Marigold Nitrosolve[™] gloves (Marigold Industrial Ltd., Bristol, UK), as this protocol uses some very toxic chemicals. As toxic fumes are released during curing, the oven must be placed in the fume hood for this procedure.

First, samples were immersed in freshly prepared Karnovsky's fixative (1.6% formaldehyde and 2% glutaraldehyde, 0.08 M sodium cacodylate, pH 7.2), ensuring ratio of 1 part sample to at least 10 parts of fixative, and left to fix at room temperature for at least 24 h. Next, the fixative solution was removed and replaced with 0.1 M sodium cacodylate buffer. This treatment with cacodylate was repeated for two 30 min periods to wash off any residual fixative. Some samples were post-fixed at this stage for 1 h in 1% (w/v) osmium tetroxide, prepared in 0.1 M cacodylate buffer, at this stage to provide contrast for electron microscopy. Samples were then dehydrated through a graded ethanol series, in which samples were immersed in 10, 30, 50, 70, 80, 90% and absolute (>99.5% (v/v)) ethanol for 1 h each. Samples were incubated in absolute ethanol for an additional 3 h, with changes of the solution every hour, to ensure all moisture was removed before proceeding. Resin was gradually introduced to the sample through 1 h immersions in increasing concentrations (i.e. 25, 50, 75%) of freshly prepared resin mixture, using either absolute ethanol (for acrylic resin) or propylene oxide (for epoxy resin) as the transition solvent. An overview of the different resins, their components and properties is provided in **Table 2.1**. Spurr resin was used for osmicated samples, whereas LR white (less toxic) was used otherwise.

Samples were infiltrated with the resin mixture for at least 48 h, with at least 4 changes of the resin solution during this period. Larger samples were left in resin for longer to ensure infiltration to the core of the particle. Samples were then embedded in fresh resin using closed capsules (i.e. gelatine or BEEM[®]00 for LR white or an open mould for Spurr resin), prior to oven-curing in the fume hood at 60 ± 2 °C (LR white) or 70 ± 2 °C (Spurr). Samples were then brought to the Centre for Ultra-Structural Imaging (CUI), King's College London, where they were trimmed and sectioned (0.5 – 1.0 μm thickness) on an Ultracut E, Reichert-Jung with a glass knife mounted. Sections were viewed on a Zeiss Axioskop 2 mot *plus* microscope. Images were captured with a Zeiss AxioCam HRc and AxioVision v3.1 microscope software (Carl-Zeiss, UK).

TABLE 2.1: OVERVIEW OF RESINS AND THEIR PROPERTIES

RESIN	Spurr (epoxy)	LR White (acrylic)
Product	Spurr low-viscosity embedding Kit (EM0300, Sigma-Aldrich)	LR White Embedding Kit (62662, Sigma-Aldrich)
Components ¹	<p><u>For a 'Firm' resin mixture:</u></p> 35.6% (w/w) ERL 4221 – <i>epoxide resin</i> 12.4% (w/w) D.E.R 726 – <i>flexibiliser</i> 51.2% (w/w) N.S.S – <i>hardener</i> 0.9% (w/w) D.M.A.E - <i>accelerator</i>	LR White (<i>acrylic resin</i>), prepared in 1.98% (w/w) benzoyl peroxide (<i>catalyst</i>)
Transition Solvent	Propylene Oxide	Ethanol
Curing	70 ± 2 °C for a minimum of 8 h (<i>anaerobic</i>)	60 ± 2°C for a minimum of 24 h (<i>oxygenated</i>)
Properties	+Better penetration into hard materials +Compatible with Osmium, EM, -Toxic	+Better Iodine staining +Easier cutting +Less toxic

¹D.E.R. - Diglycidyl ether of polypropylene glycol; N.S.S. - Nonenyl succinic anhydride; D.M.A.E. – Dimethylaminoethanol.

Some samples were also stained before viewing. Toluidine blue (1%, w/v, with 1%, w/v, sodium borate) was used to stain cell walls purple, or Lugol's iodine (2.5, 5, or 10%, w/v, I₂ with 5, 10 or 20% KI, respectively), which stains amylose a dark blue, and amylopectin red/purple was used to enhance the appearance of starch (**Figure 2.7**). Iodine binds to amylose, giving a dark blue/purple appearance, but as the amylose becomes hydrolysed, the stained starch appears more red/brown (Bailey and Whelan 1961).

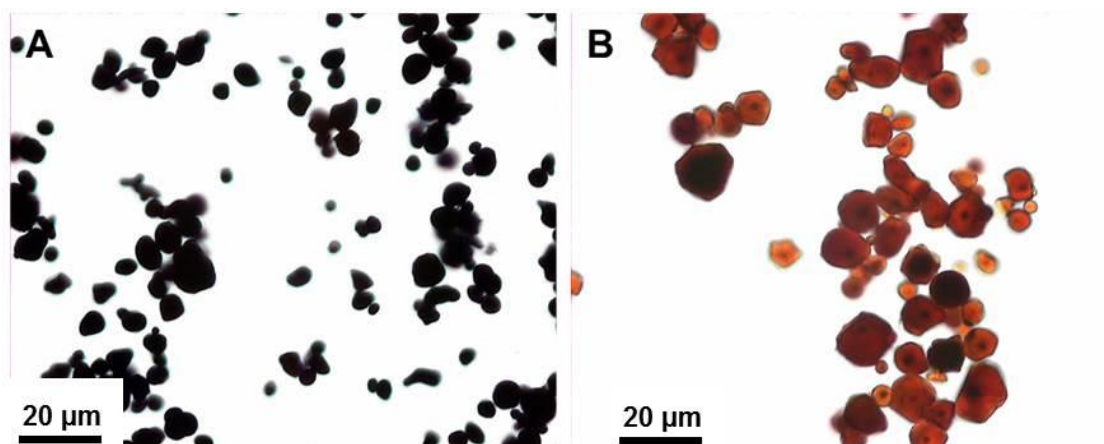


FIGURE 2.7: LIGHT MICROGRAPHS OF IODINE STAINED (A) HIGH AMYLOSE AND (B) HIGH AMYLOPECTIN MAIZE STARCH.

2.4.2 SCANNING ELECTRON MICROSCOPY

Scanning Electron Microscopy (SEM), was carried out at the CUI, King's College London. Dry samples were mounted on double-sided carbon tape on an aluminium stub and coated with gold in a Polaron E5100 sputter coating unit. Samples were viewed on a Hitachi S-3500N scanning electron microscopy (FEI Company, Cambridge, UK) using a 20 KV accelerating voltage.

2.4.3 THERMAL CROSS-POLARISED MICROSCOPY

A polarising microscope (Leitz Dialux ED22 microscope fitted with cross-polarisers and a red 1 (λ) compensator plate (which makes the crystalline regions appear blue and the background pink) was used to observe the degree of birefringence in native and hydrothermally processed materials. Samples were suspended in an excess of dH₂O and sealed between two coverslips (SLS laboratories) with nail polish. In native samples, the characteristic 'Maltese cross' pattern, which results from the long-range ordering of α -glucan chains in the starch granule, could be observed (Wang *et al.* 1998). This Maltese cross disappears during starch gelatinisation, as crystalline regions become more disordered (**Figure 2.8**). Images were acquired using a Qi Imaging QiFastCam camera and Q-capture pro software.

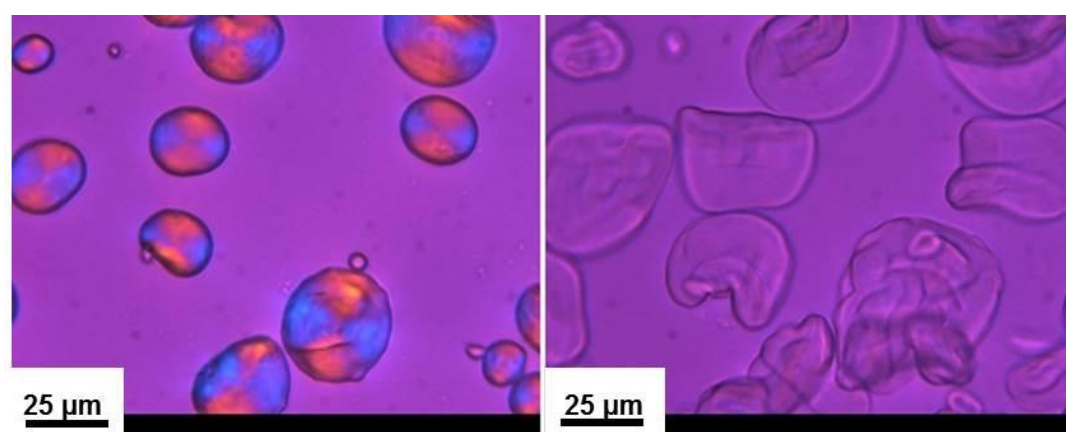


FIGURE 2.8: STARCH GRANULES VIEWED UNDER CROSS-POLARISED LIGHT BEFORE (LEFT) AND AFTER (RIGHT) HYDROTHERMAL TREATMENT. A maltese-cross pattern is evident in native granules, but no longer present in gelatinised starch.

In order to visualize the progressive loss of crystallinity during heating, a Linkam HFS91 heated-stage was connected to the microscope through a TP92 controller. Linksys 32 software (Linkam Scientific Instruments, Surrey, UK) was used to program a heating and image acquisition profile, such that images could be acquired throughout the thermal treatment, thereby enabling the gradual loss of birefringence during gelatinisation to be observed.

2.5 DETERMINATION OF CELL WALL POROSITY

Cell wall pore-size, previously defined as “the Stoke’s radius of a neutral hydrocolloid that is sufficient to prevent its free permeation through the cell wall” (Carpita *et al.* 1979), has been studied in a very limited number of plant materials by observing diffusion of markers (Polyethylene glycol, ‘PEG’ or dextrans) of known size (Carpita *et al.* 1979, Baron-Epel *et al.* 1988). Here, cell wall porosity was studied by observing the diffusion of dextrans or porcine pancreatic α -amylase labelled with fluorescein isothiocyanate (FITC) (**Figure 2.9**). FITC is a derivative of fluorescein, with Excitation/Emission maximum 490/520 nm. Because FITC is relatively small (389.38 g/mol) and reactive (isothiocyanate group) towards amine and sulph-hydryl groups of protein and hydroxyl groups of dextrans, it is particularly well suited for fluorescent labelling of amylase and dextran.

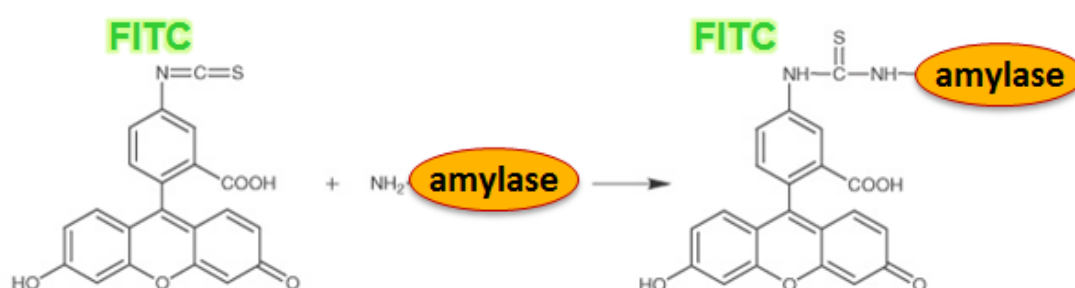


FIGURE 2.9: FLUORESCHEIN ISOTHIOCYANATE (FITC) CONJUGATION TO PROTEIN.The isothiocyanate group of FITC reacts with the amine groups of proteins (e.g., amylase) to form FITC-labelled protein (e.g., FITC-amylase). FITC molecular formula: $C_{21}H_{11}NO_5S$

Dextrans of various molecular weights (4 kDa, 10 kDa, 40 kDa) labelled with FITC, were purchased from Sigma-Aldrich. In these dextrans, the FITC is conjugated randomly to hydroxyl groups at a frequency of 0.003 to 0.02 moles of FITC per mole of glucose (as stated by the manufacturer). The size of these dextrans (R_{HYD} = 1.4, 2.3 and 4.5 nm, respectively) was also specified by the manufacturer in terms of the hydrodynamic radius (R_{HYD}), defined as “*the radius of an equivalent hard sphere diffusing at the same rate*”. R_{HYD} is normally similar to the radius of gyration (R_G), but the latter takes into account the mass of elements and their distance from the particle core.

FITC-amylase was prepared by conjugation of FITC (Isomer I, F7250, Sigma-Aldrich) and porcine-pancreatic α - amylase (A6255, Sigma-Aldrich) according to the protocol provided by the manufacturer. In brief, 50 μ L of 0.69 mg/mL FITC, was incubated with 200 μ L of 5 mg/mL amylase in 0.1 M sodium carbonate-bicarbonate buffer (0.286%, w/v, of $\text{Na}(\text{CO}_3)$ + 0.756%, w/v, of $\text{Na}(\text{HCO}_3)$, pH 9) for 2 h on a rotary mixer at 37 °C. The mixture was then filtered through a chromatography column (height = 10 cm, diameter = 1 cm) loaded with Sephadex[®] G25 (in PBS) to separate the conjugated FITC-amylase from unbound label or enzyme. The first eluent (collected in 1 mL fractions), contained the conjugated FITC-amylase, whereas the later fractions contained un-bound enzyme and label. Spectrophotometry was used to identify FITC-amylase in the eluent and the absorbance at 280 and 495 nm used to calculate the fluorescein to protein ratio (normally approximately 1:1), following the protocol provided by the manufacturer.

Eluent containing FITC-amylase was combined and stored in a dark vial at 4 °C. FITC-amylase activity (determined by assaying the activity on purified starch) was tested the following day, and the FITC-amylase was found to have a lower activity than the pure enzyme. For the purpose of porosity experiments, the size of FITC-amylase was

assumed to be very similar to the known R_G of α -amylase (2.69 nm), because of the relatively small size of the FITC-molecule.

Exact details of porosity experiments are provided in subsequent chapters, but generally involved suspending plant material in buffer or water and incubating with FITC dextran/amylase before viewing on a Zeiss Axioskop 2 mot *plus* microscope, equipped with a Zeiss FT510 Filter Cube (Filter set 10, Excitation 450-490 and Emission 515-585 nm). Images were captured with a Zeiss AxioCam HRc and AxioVision v3.1 microscope software (Carl-Zeiss, UK).

2.6 DIFFERENTIAL SCANNING CALORIMETRY (DSC)

Differential scanning calorimetry (DSC) was used to observe starch gelatinisation in various size fractions of chickpea and durum wheat. DSC involves measuring how a sample's heat capacity changes as a function of temperature when the sample is heated at a constant rate (Gill *et al.* 2010). As starch gelatinisation requires energy to break non-covalent hydrogen bonds, gelatinisation can be observed as an endothermic peak on the DSC. Furthermore, assuming that all energy absorption by the sample is associated with starch gelatinisation, integrating the transition peak provides an indication of starch gelatinisation enthalpy ($\Delta_{gel}H$), which may be expressed as J/g sample, provided that the mass of sample is known. Thus, if the energy required to gelatinise 1 g of pure starch is known, it is possible to estimate the proportion of starch in an unfamiliar sample that has undergone gelatinisation, defined as the 'Terminal Extent of Gelatinisation' (Fukuoka *et al.* 2002).

For the experiments detailed in this thesis, a Multi-Cell DSC (TA Instruments) with a high sample volume capacity was used. This unique instrument enables three samples (solid or liquid) and one reference to be run simultaneously in removable 1 mL capacity Hastelloy[®] ampoules, and has a sensitivity of $<41.8 \mu\text{J}/^\circ\text{C}$, and baseline reproducibility

of $<104.6 \mu\text{J}$ at a heating rate of $1^\circ\text{C}/\text{min}$. It was therefore very well-suited for studies of milled fractions of chickpeas and durum wheat.

The Multi-Cell DSC operates by a heat-flux mechanism, in which hermetically sealed sample pans and the reference pan are heated together in the same adiabatic chamber at a controlled rate, and thermocouples record the difference in energy required to maintain the same heating rate for both samples (**Figure 2.10**). Effectively, changes in heat capacity were recorded as changes in heat flow between the reference and sample crucibles.

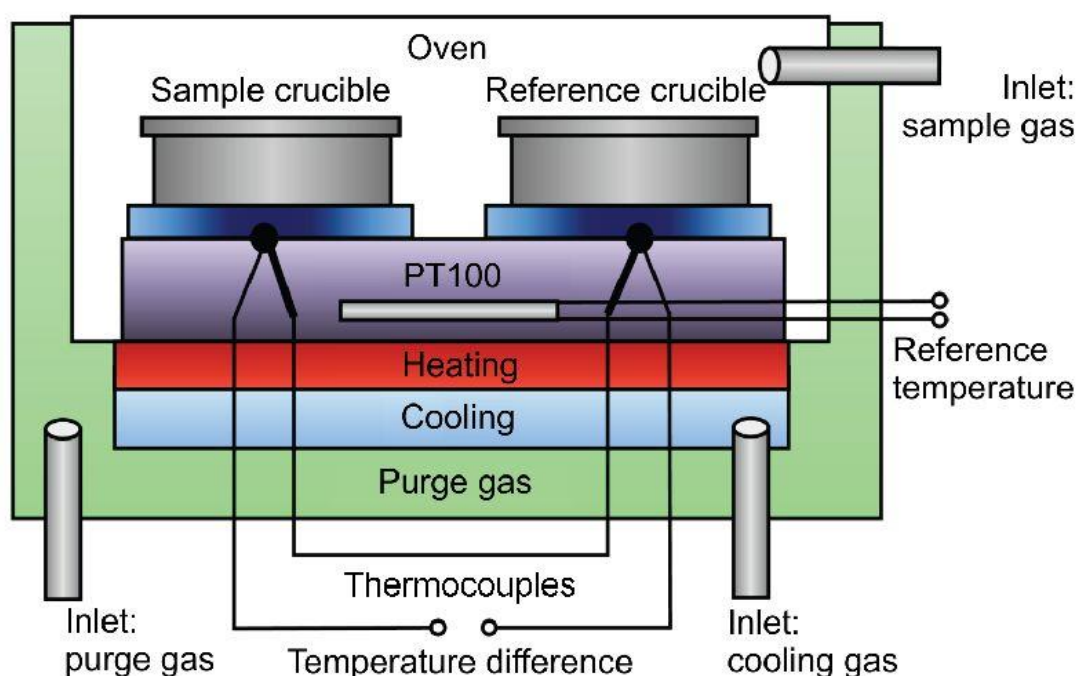


FIGURE 2.10: SCHEMATIC OF A DSC HEAT-FLUX INSTRUMENT. Taken from Steinmann *et al.*, 2013.

When heat flow is plotted against temperature, starch gelatinisation is observed as an endothermic peak. Using commercially available software such as NanoAnalyze or TA Universal Analysis, the onset, peak, and conclusion -temperatures (denoted T_o , T_p , T_c) of starch gelatinisation may be calculated from a DSC trace, as shown in **Figure 2.11** (Bogracheva *et al.* 2002).

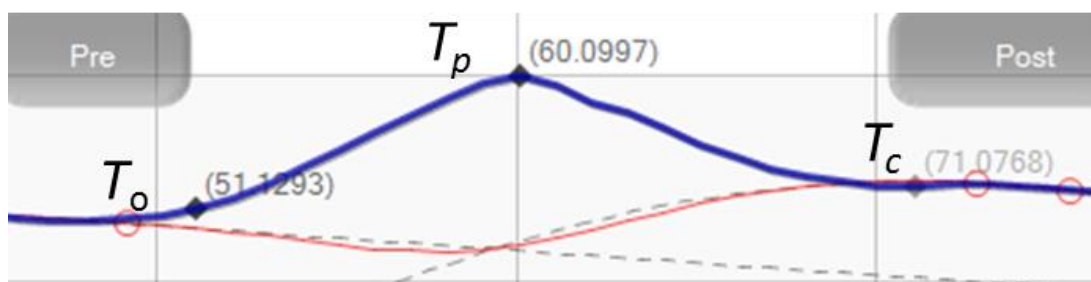


FIGURE 2.11: EXAMPLE THERMOGRAM FOR STARCH GELATINISATION (ENDOTHERM UP) IN MILLED PLANT TISSUE. Showing analysis in NanoAnalyze software with onset (T_o), peak (T_p) and conclusion (T_c) temperatures indicated. The red-line is the baseline and is drawn to represent the heat-flow in starch that has already been gelatinised.

This approach was used to determine the extent of starch gelatinisation in a range of milled fractions of chickpea and durum wheat when heated for a prolonged period in an excess of water. Full details of the DSC run settings are provided in *Chapter 4, Section 4.2.5, page 133*.

2.7 *IN VITRO* DIGESTIBILITY ASSAY

Starch digestibility was determined *in vitro* by incubation with porcine-pancreatic α -amylase (PPA). This assay was intended to represent the initial stage of starch hydrolysis under luminal conditions, and does not account for the contribution of salivary amylase or other digestive enzymes; these were accounted for in the ‘multi-compartmental digestion model’, which is described in the next section. Nevertheless, the ratio of amylase to substrate concentration used in the *in vitro* studies is compatible (Slaughter *et al.* 2001) with the *in vivo* values reported by Dahlqvist and Borgström, who carried out direct measurement of amylase activity at various regions in the small intestine by intubation. They observed that with 50 g carbohydrate, amylase activity ranged from 50-500 IU (at 37°C) (Borgstrom *et al.* 1957).

The exact details (e.g., amount and type of starch or starch-rich materials and the processing conditions) are described in subsequent sections. Generally, test materials were weighed into 50 mL BD Falcon™ tubes (BD Biosciences, Oxford, UK) suspended

in PBS, covered with foil and hydrothermally processed with intermittent stirring with a spatula every 15 min. The tubes were then equilibrated at 37 °C for 15 min on a rotary mixer, and a 'blank' aliquot was taken before addition of sufficient amylase to achieve an incubation concentration of 8 nM enzyme. The tubes were immediately returned to the rotary mixer in the incubator (LEEC Compact Incubator), and taken out 20 s prior to an aliquot collection time point to allow particles to settle before withdrawing an aliquot of the solution. All aliquots were taken into 1.5 mL tubes on ice containing an equal volume of 0.3 M Na₂CO₃, to achieve a 1:2 dilution of the sample aliquot. The strong alkali and cold temperature slows catalysis to a negligible rate and inactivates the amylase to prevent any further digestion of the sample. Aliquots were later centrifuged at 13000 x G to spin down any starch remnants, and the supernatant was transferred into a new set of 1.5 mL tubes and frozen for storage at -20 °C. At a later date, supernatants were de-frosted and analysed for starch hydrolysis products using the Prussian blue method (as described *Section 2.3.4.3*). Digestibility curves were then obtained by plotting the concentration of starch hydrolysis products (expressed as maltose equivalents) against time. Alternatively, digestion was expressed as the percentage of starch that had been digested, assuming all starch can be converted to maltose.

For simplicity, the starch content of digestion mixtures was expressed as a concentration (mg/mL), however, many of the materials used in the digestion mixtures are heterogenous and contain starch entrapped within cells that is not immediately available for digestion. Thus, this notation does not always represent the concentration of substrate that is exposed to enzyme, but reflects the total starch content in a known volume. Unless otherwise specified, experimentally obtained digestibility data were fitted to a bi-phasic first order equation (**Equation 2.3**). This equation is available from the equation library of SigmaPlot 12.0, where it is described as a '4 parameter, double exponential rise to maximum'. The value of all parameters was obtained by iterative Maximum Likelihood Estimation (MLE), unless otherwise specified.

$$y = a(1 - e^{-bx}) + c(1 - e^{-dx})$$

EQUATION 2.3: BI-PHASIC FIRST-ORDER EQUATION In which y is product concentration and x is time. Values of parameters a , b , c , and d were identified by iterative MLE using SigmaPlot 12.0

2.8 MULTI-COMPARTMENT DIGESTION MODEL

The *in vitro* digestibility assay described in the previous section involves only the use of PPA, but under physiological digestion in the human gastro-intestinal tract, other mechanical and biochemical factors may influence the digestion and/or degradation of the food matrix and entrapped starch. Therefore, a multi-compartmental digestion model was used to better simulate the enzymes, mixing and pH changes in the oral, gastric and duodenal digestive environments. This work was carried out at the Institute of Food Research (IFR) in Norwich using patented in-house techniques. Further details of the methodology and instrumentation used are provided in *Chapter 6*.

2.9 LOGARITHM OF SLOPE ANALYSIS

Butterworth *et al* recently described the application of logarithm of slope (LOS) plots, first described by Poulsen and co-workers, to starch hydrolysis data in order to estimate the endpoint product concentration (C_{∞}) and rate constant, k , from data collected during the first hour of *in vitro* digestion (Butterworth *et al.* 2012, Poulsen *et al.* 2003). This approach is based on the theory that product formation from starch hydrolysis over time follows a logarithmic relationship, in which the rate of starch digestion decreases over time, due to the conversion of available substrate (starch) to product. Thus, by plotting the logarithm of the slope (LOS) between various time points of a starch digestibility curve against time, a linear plot with a slope, $-k$, and y-intercept $\ln(C_{\infty}k)$ is obtained. The theory of this analysis is described in more detail in *Chapter 5*, in which this approach is applied to heterogeneous plant tissues of chickpea and durum wheat.

2.10 ILEOSTOMY STUDY

A randomized, single-blind (researcher), dietary intervention study was designed to investigate the effect of particle size on the bioaccessibility of starch in durum wheat, and the consequential effects on postprandial metabolism. This study was carried out in ileostomy subjects and is described in full in *Chapter 7*.

2.11 STATISTICAL AND GRAPHICAL SOFTWARE

Specific details of statistical analyses are provided in subsequent chapters. Data entry and processing was carried out in Microsoft Excel. Graphing, curve-fitting and regression analysis was performed in SigmaPlot 12.0 (© Systat software 2011). Statistical tests were carried out using IBM SPSS Statistics 20.0 (© IBM Corp. 2011).

CHAPTER 3

CHARACTERISATION OF TEST MATERIALS

3.1 INTRODUCTION

Chickpeas and durum wheat are both widely consumed dietary sources of starch, but differ in their glycaemic potential. Chickpeas, like many other pulses, tend to elicit a lower glycaemic response than durum wheat and most other cereals (Foster-Powell *et al.* 2002); however the underlying mechanisms have not yet been thoroughly investigated and explained.

This chapter outlines some of the key structural and chemical characteristics of the test materials (i.e., starch, milled fractions and cells) obtained from chickpeas and durum wheat. Proximate analysis provides an overview of the macronutrient content of these materials, of which the starch content is especially important for the design and interpretation of subsequent digestibility studies. This work is complemented by micro-structural observations, which provide a visual overview of the structural integrity of the tissue and plant cell walls and the presence or absence of ordered α -glucan structures in the encapsulated starch during and after cooking. The potential enzyme inhibitory or stimulatory effect of plant endogenous compounds is assessed by comparison of digestibility of native and hydrothermally processed flour with that of purified starch. Cell wall behaviour (e.g. cell rupture and separation), chemical composition and porosity were also investigated, as these properties are thought to play some role in influencing the digestion process, but do not appear to have been systematically studied.

3.1.1 OBJECTIVES

- i. To characterise the structure and properties of the chickpea and durum wheat materials and the corresponding extracted starches using a range of chemical and physical methods.
- ii. Evaluate the physico-chemical data that can be used to explain the *in vitro* and *in vivo* digestion studies on the test plant materials and extracted starches described in subsequent chapters

3.2 MATERIALS AND METHODS

3.2.1 PLANT MATERIALS

Milled materials, isolated cells and starch were obtained from chickpeas and durum wheat as described in *Section 2.1 page 71*.

3.2.2 GEOMETRIC MODEL OF CELL RUPTURE AS A FUNCTION OF PARTICLE SIZE

A rough geometric approach was used to estimate the number of intact cells in milled macro-particles. Essentially, cells were assumed to be rectangular prisms, and the milled particles were assumed to be cubes. The number of cells that were exposed on the surfaces of the milled particle were assumed to be ruptured, as observed when milled endosperm particles were viewed under the scanning electron microscope (see *Section 3.3.4*).

First, the milled particle dimensions, surface area (**Equation 3.1**) and volume (**Equation 3.2**) were calculated for the different size fractions, assuming that particles were cubes, with side length, s , equal to the median of the sieve aperture range.

$$\text{cell surface area} = cSA = 2(d \times h) + 4(l \times d)$$

$$\text{particle surface area} = pSA = 6 \times s^2$$

EQUATION 3.1: SURFACE AREA OF CELL AND A MACROPARTICLE. In which d , h and l is the depth, height and length; s , is the particle side lengths. Cells are assumed to be rectangular prisms in which $d = h$, and milled particles are assumed to be cubic with side length, s , defined from the median of the sieve aperture range.

$$\text{cell volume} = cV = l \times d \times h$$

$$\text{particle volume} = pV = s^3$$

EQUATION 3.2: VOLUME OF A CELL AND A MACROPARTICLE. In which d , h and l is the depth, height and length; s , is the particle side lengths. Cells are assumed to be rectangular prisms in which $d = h$, and milled particles are assumed to be cubic with side length, s , defined from the median of the sieve aperture range.

Next, cell dimensions were estimated from light micrographs of randomly selected cells (see microscopy method in *Section 3.2.6* and results in

Table 3.5). The total number of cells (assumed to be rectangular prisms) in a cuboid particle ($\#V$) was calculated from the cell volume (cV) (**Equation 3.3**)

$$\#V = \frac{pV}{cV}$$

EQUATION 3.3: NUMBER OF CELLS IN PARTICLE VOLUME. pV is the particle volume, cV is the volume of a cell calculated from cell dimensions ($cV = \text{cell length} \times \text{depth} \times \text{height}$)

The average cell dimensions ($D = \text{length} \times \text{depth} \times \text{height}$) were used to estimate how many cells would fit into the sides of the cubic particle. The number of cells on the particle surfaces ($\#S$) was calculated as shown in **Equation 3.4**

$$\#S = 2(\#D \times \#H) + 4(\#L \times \#D)$$

EQUATION 3.4: NUMBER OF CELLS ON PARTICLE SURFACES. In which $\#S$ is the number of cells on the particle surface and is calculated from the; number of cells in the particle depth ($\#D$), height ($\#H$) and length ($\#L$).

Finally, the proportion of ruptured cells within a milled particle was calculated (**Equation 3.5**). Cells that were not ruptured were taken to be intact.

$$\% \text{ Ruptured} = \frac{\#S}{\#V}$$

EQUATION 3.5: PROPORTION OF RUPTURED CELLS: In which $\#S$ is the number of cells on the particle surface and $\#V$ is the number of cells in the particle volume.

3.2.3 PROXIMATE ANALYSIS

Proximate analysis was performed as described in *Section 2.3.1*, (page 80). In addition to these analyses, moisture and direct 'Total Starch' determinations were performed in our laboratory as described in *Sections 2.3.2* and *2.3.3*, respectively. The starch content measured using the direct 'Total Starch' method was considered more accurate than the 'by difference' values obtained by proximate analysis and was therefore used in subsequent calculations.

3.2.4 STARCH DAMAGE AND AMYLOSE-AMYLOPECTIN RATIO

Starch characterisation was carried out with the assistance of Hamung Patel at King's College London. Starch damage (which can increase starch susceptibility to amylase)

was determined for purified starches by Congo red, as described previously (Slaughter *et al.* 2001). Amylose was determined by the Iodine-binding method (Knutson 2000, Knutson 1986) using the correction factor incorporated by Warren (Warren 2011). Swelling Power was determined gravimetrically from the increase in starch weight after incubation in excess (10 mL with 0.1g starch) water at 60 °C for 30 min (Daramola and Osanyinlusi 2006).

3.2.5 CELL WALL ANALYSIS

Cell wall analysis was determined by a novel high-throughput microarray analysis method at the University of Copenhagen, Denmark. In this method, cell wall glycans are sequentially extracted (with CDTA and NaOH), loaded on microarray plates and probed with monoclonal antibodies or carbohydrate binding modules which bind to specific cell wall components. This method has previously been described in detail (Moller *et al.* 2007, Pedersen *et al.* 2012).

3.2.6 MICROSCOPY

Light micrographs were obtained as described in *Section 2.4.1, (page 88)*. Dimensions (e.g., of cell wall thickness and cell size) were estimated from at least 10 different specimens viewed in various orientations at different magnifications (10x, 20x and 40x). For scanning electron microscopy (SEM), dry samples were mounted, gold sputter-coated and viewed as described in *Section 2.4.2*. Selected samples (indicated in figure captions) were rinsed with deionised water and allowed to dry at room temperature for 1 week before sputter coating and viewing. This was done to remove surface debris and thereby enhance structural features of interest.

3.2.7 ESTIMATION OF CELL WALL POROSITY

In order to assess the porosity of plant cell walls, the diffusion of different size FITC-dextran was observed using fluorescence microscopy (see *Section 2.5, page 92* for details). For these studies, 10 mg of plant material (cells or milled), was suspended in

1.4 mL PBS in amber Eppendorf tubes and hydrothermally processed for 30 min at 90 °C. An aliquot of the suspension was dropped onto a slide and viewed to observe the background level of auto-fluorescence, making note of the exposure time. Next, 20 µL of FITC-dextran solution (0.5 µM, pH 9.0) was added to the tubes. Tubes were inverted 3 times to mix, then left to stand at room temperature for 10 min before viewing for up to 60 min on a fluorescence microscope. The porosity of cell walls was estimated based on whether or not 4, 10 and 40 kDa dextrans (**Table 3.1**) penetrated plant cells.

TABLE 3.1: OVERVIEW OF FITC-DEXTRANS USED IN CELL WALL PORE-SIZE DETERMINATIONS.

DEXTRAN MWT (Da)	R_{HYD} (nm)	Sigma Ref.
4,000	1.4	46944
10,000	2.3	FD-10S
40,000	4.5	FD-40

MWT- molecular weight, as defined by suppliers on product specification sheet. ' R_{HYD} ' is the hydrodynamic radius and is smaller than the effective radius, as dextrans are not necessarily spherical.

3.2.8 GELATINISATION BEHAVIOUR

Samples were suspended in deionised water and sealed with nail polish between two coverslips (to prevent evaporation) and placed on a heatable stage. The progressive loss of birefringence during heating was observed using a microscope connected to the heated stage as described in *Section 2.4.3, page 91*. The stage was heated from 20 to 95 at 1 °C/min, and images captured every 30 seconds. For comparison, the starch gelatinisation point was qualitatively identified as the temperature at which a loss of birefringence was observed during hydrothermal processing. More accurate determinations of starch gelatinisation (i.e. using DSC) are presented in *Chapter 4*.

3.2.9 DIGESTIBILITY ASSAYS OF NATIVE AND PROCESSED STARCH AND FLOURS

Digestibility assays were carried out on native (equilibrated to 37°C in a waterbath for 20 min) and hydrothermally processed (1.5 h at 100°C) starches and flours as described in *Section 2.7, page 96*. The amount of material used in the assay was adjusted such that the incubation mixture contained 3.9 mg/mL starch, and was incubated with 8 nM porcine pancreatic α -amylase. Enzyme-free control runs were also carried out on selected size fractions (0.38, 0.73 and 1.85 mm) to test for the

contribution of endogenous sugars, which may leach out or be actively produced by endogenous enzymes during boiling or incubation on the rotary mixer.

3.3 RESULTS

3.3.1 PROXIMATE ANALYSIS

Proximate analysis data is shown in **Table 3.2** and **Table 3.3** for chickpea and durum wheat materials. For both botanical sources, the milled material (i.e., de-branned or de-hulled and roller-milled) contained less fibre than the whole grain or peas. This reflects the removal of the outer layers (bran and seed coat) of the grains or peas prior to milling. Milled chickpeas contained a greater proportion of protein and dietary fibre, and less starch than milled durum wheat. Chickpea cells contained less protein, fibre and fat, and more starch than the milled chickpeas, which probably arises from a loss of soluble fibre during the cell preparation procedure. For chickpea cell preparations, the starch content (g starch per 100g dry material) varied between batches, but was always greater than in the milled material, because of the loss of fibre during cell isolation. The macronutrient contents of the food-grade and lab-grade batches of milled durum wheat were very similar.

TABLE 3.2: PROXIMATE ANALYSIS DATA OBTAINED FOR RAW CHICKPEA MATERIALS

TEST	WHOLE PEAS	MILLED	CELLS
Energy (kJ/100g)	1366 ± 1.0	1408.3 ± 5.8	1409.7 ± 5.7
Energy (kcal/100g)	325.7 ± 0.3	335.7 ± 1.5	334.3 ± 1.3
Protein (g/100g)	21.7 ± 0.2	23.0 ± 0.0	21.1 ± 0.0
Carbohydrate (g/100g)	35.8 ± 0.1	37.5 ± 0.6	50.0 ± 0.3
-Sugars(g/100g)	2.9 ± 0.0	3.0 ± 0.0	0.1 ± 0.0
-Starch (g/100g)	33.0 ± 0.1	34.6 ± 0.7	49.9 ± 0.3
Fat (g/100g)	5.2 ± 0.1	5.3 ± 0.0	2.4 ± 0.1
Dietary Fibre (g/100g)	24.4 ± 0.1	22.6 ± 0.7	14.0 ± 0.4
Ash (g/100g)	3.1 ± 0.1	2.8 ± 0.0	0.1 ± 0.0
Moisture (g/100g)	9.7 ± 0.0	8.7 ± 0.0	12.3 ± 0.0

Values are shown as mean of triplicates ± SEM, and are expressed on an 'as is' basis; 'Whole peas' had seed-coat intact, 'Milled' chickpeas were de-hulled before milling, and 'Cells' were in a dry form. Carbohydrate is the sum of starch and sugars.

TABLE 3.3: PROXIMATE ANALYSIS DATA OBTAINED FOR RAW DURUM WHEAT MATERIALS

TEST	WHOLE GRAIN	MILLED-Batch 1	MILLED-Batch 2
Energy (kJ/100g)	1445.6 ± 7.3	1490.7 ± 2.4	1498.7 ± 4.7
Energy (kcal/100g)	342 ± 1.5	352.0 ± 0.6	354 ± 1.0
Protein (g/100g)	11 ± 0.1	10.7 ± 0.0	10.9 ± 0.1
Carbohydrate (g/100g)	64.8 ± 0.7	70.2 ± 0.2	71.0 ± 0.3
-Sugars (g/100g)	n/a	0.6 ± 0.0	0.5 ± 0.0
-Starch (g/100g)	n/a	69.6 ± 0.2	70.5 ± 0.3
Fat (g/100g)	2.1 ± 0.1	1.7 ± 0.0	1.7 ± 0.0
Dietary Fibre (g/100g)	9.8 ± 0.6	6.5 ± 0.2	5.2 ± 0.1
Ash (g/100g)	1.6 ± 0.0	0.9 ± 0.1	0.6 ± 0.2
Moisture (g/100g)	10.6 ± 0.1	9.9 ± 0.0	10.5 ± 0.0

Values are shown as mean of triplicates ± SEM, and are expressed on an 'as is' basis; 'Whole grains' had outer layers of the grain present, 'Milled' durum wheat grains were de-branned before milling to remove outer layers of the grain. Batch 2 was prepared in food grade facilities using slightly different equipment to batch 1 (lab grade). Carbohydrate is the sum of starch and sugar.

Using direct analysis methods, the total starch content (means ± standard deviation) of milled chickpea (de-hulled) and durum wheat (de-branned) was found to be 45 ± 1.07 and 71 ± 3.1, respectively, expressed on a g/100 g dry weight basis. No significant differences were observed between the starch content of the different milled fractions. These values were used to calculate the weight of material needed to achieve a specific starch content in subsequent digestibility assays.

3.3.2 STARCH CHARACTERISTICS

A summary of the key characteristics of chickpea and durum wheat starches is provided in **Table 3.4**. Chickpea starch contained a higher proportion of amylose than durum wheat starch, and also had a higher swelling power. Damaged starch accounted for less than 0.1% of the granules examined.

TABLE 3.4: STARCH CHARACTERISTICS

	CHICKPEA STARCH	DURUM WHEAT STARCH
Amylose (% DW)	39.7 ± 2.1	32.8 ± 0.3
Amylopectin (% DW)	60.3 ± 2.1	67.2 ± 0.3
Swelling Power (g/100g DW)	14.4 ± 0.0	9.84 ± 0.7
Gelatinisation Temp. (°C)	65 -80	50 - 70
Starch Damage	<0.1%	<0.1%

Values are mean of triplicates ± SEM. DW; dry weight. Gelatinisation was observed as a loss of birefringence and occurred over the temperature range shown.

3.3.3 STRUCTURAL CHARACTERISTICS OF ISOLATED CELLS

Light micrographs in **Figure 3.1** provide an example of material obtained using the same cell preparation procedure, applied to durum wheat and chickpea. Cell shaped structures were difficult to isolate from durum wheat because of their extreme fragility. The edges of these structures were not well-defined, and it was therefore not clear a 'cell wall' was truly present or if these shapes were just intracellular material held together by the protein matrix.

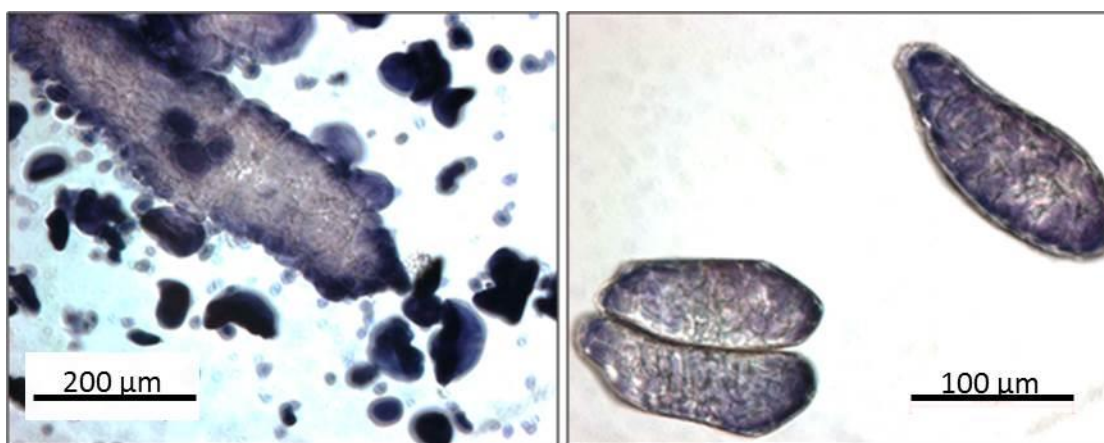


FIGURE 3.1: SEPARATED CELLS OBTAINED FROM DURUM WHEAT (LEFT) AND CHICKPEA (RIGHT). Samples were suspended in deionised water and stained with 2.5% Lugol's iodine immediately before viewing. The difference in scale should be noted.

3.3.4 STRUCTURAL CHARACTERISTICS OF MILLED MATERIALS

Milled materials were examined using various microstructural techniques. Micrographs of *raw* flour (< 0.21 mm) of chickpea and durum wheat are shown alongside the extracted starch in **Figure 3.2**.

The 'flour' represents the smallest particle size fraction that was achieved by milling, and contained no intact cells; only free starch granules, cell wall fragments and other debris (**Figure 3.2 A,B**). These cell wall fragments and impurities were not observed in the purified starches (**Figure 3.2 C,D**).

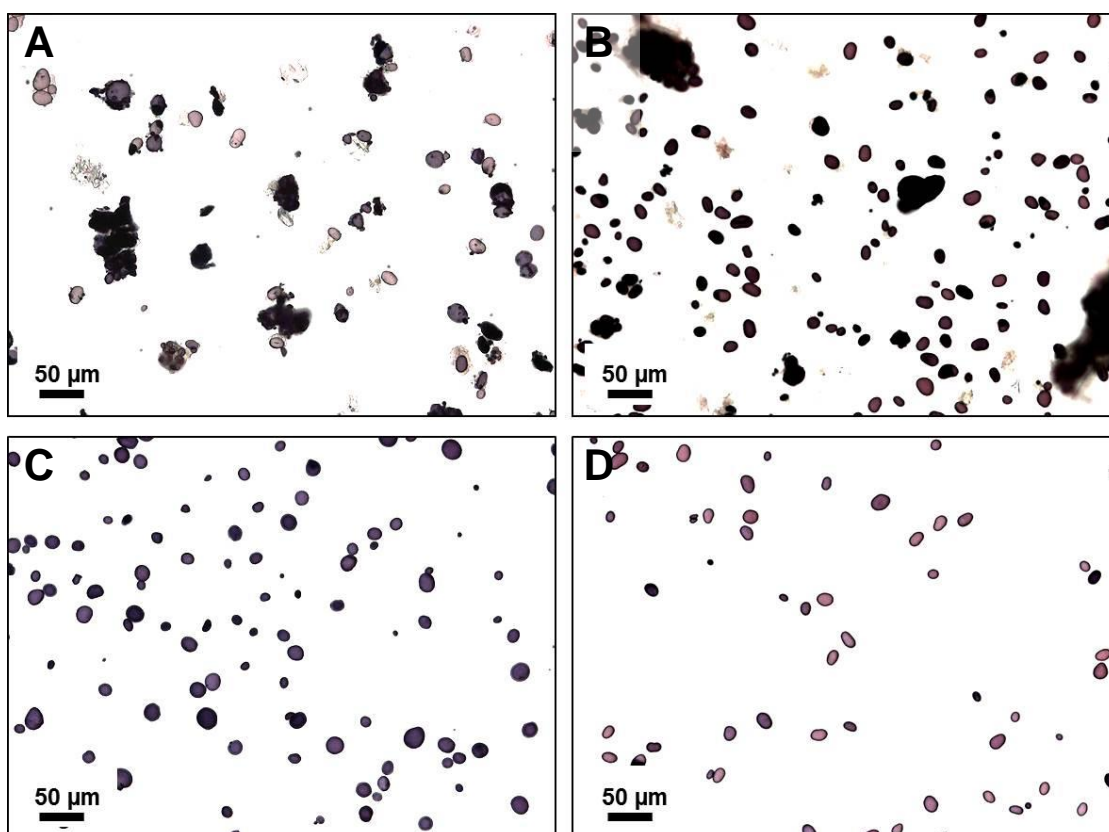


FIGURE 3.2: LIGHT MICROGRAPHS OF NATIVE (A) DURUM WHEAT FLOUR, (B) CHICKPEA FLOUR, (C) DURUM WHEAT STARCH AND (D) CHICKPEA STARCH. Samples were suspended in deionised water and stained with 2.5% Lugol's iodine immediately before viewing.

For the more coarsely milled particles, SEM of *raw* materials (**Figure 3.3**) was used to visualise the surface structure (**Figure 3.3 C,D**) and overall geometry (**Figure 3.3 E,F**).

The fractured surfaces consisted of ruptured cells containing exposed starch granules (*Figure 3.3 A*). In the rinsed chickpea materials, some damaged cells were evident (*Figure 3.3 B*).

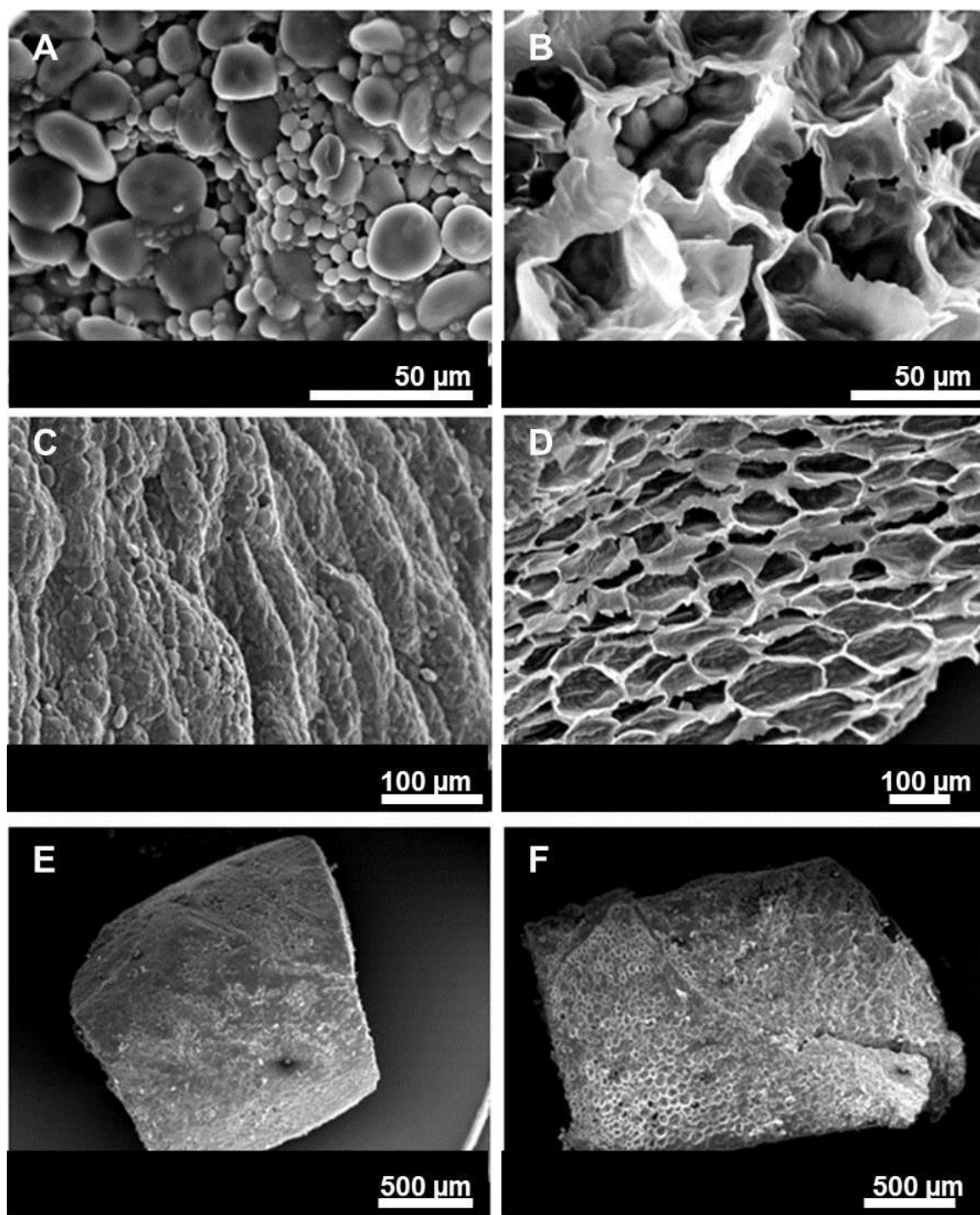


FIGURE 3.3: SEM OF NATIVE MILLED DURUM WHEAT ENDOSPERM (A, C, E) AND CHICKPEA COTYLEDON (B, D, F) SHOWING FRACTURED SURFACES AND PARTICLE GEOMETRY. Particles in Figures A, B, C, D have been rinsed with deionised water prior to viewing. Samples were mounted dry, gold sputter-coated, and viewed on Hitachi S-3500N, at accelerating voltage 20 KV

The structural integrity of the raw macro-particles was largely retained during hydrothermal processing. The micro-structures of *hydrothermally-processed* macro-particles of chickpea and durum wheat are shown in **Figure 3.4**.

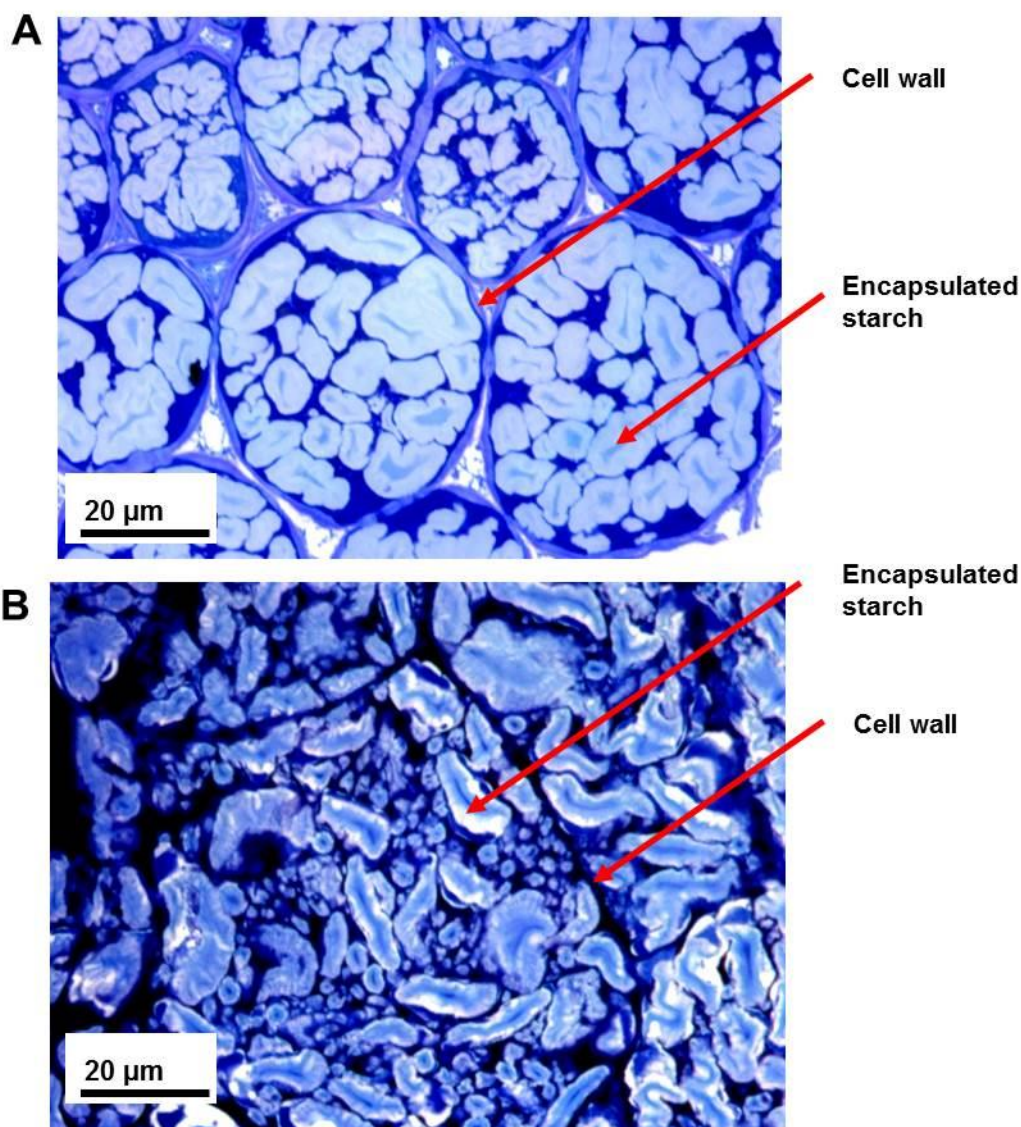


FIGURE 3.4: LIGHT MICROGRAPHS OF HYDROTHERMALLY PROCESSED CHICKPEA (A) AND DURUM WHEAT (B) TISSUE. Samples were boiled for 1.5 h. Cured in Spurr resin. Sections are 0.5 µm thickness and stained with Toluidine blue (1%, w/v).

Some structural differences between hydrothermally processed chickpeas and durum wheat were evident: The chickpea cells appeared rounded, probably due mainly to changes in the pectic materials in the middle-lamella, which is associated with a tendency to cell separate, whereas the durum wheat endosperm cells were more angular **Figure 3.4**.

The chickpea parenchyma cell walls were between 1.0 and 1.7 μm thick, whereas durum wheat endosperm cell walls were thinner (~ 0.3 to $0.8 \mu\text{m}$). The intracellular starch in both tissues appeared swollen, but had a distorted, 'buckled-saddle' shape, which is associated with restricted gelatinisation (Fardet *et al.* 1998, Würsch *et al.* 1986). In durum wheat, which has large (A-size) and small (B-size) starch granules, the larger granules appeared more distorted than the smaller, less swollen granules (**Figure 3.4**). Cell sizes observed under the microscope varied, but the average cell dimensions were $0.14 \times 0.04 \times 0.04 \text{ mm}$ for chickpea cells and $0.25 \times 0.05 \times 0.05 \text{ mm}$ for durum wheat endosperm cells. These cell dimensions were used in calculations based on the geometric model.

3.3.5 GEOMETRIC MODEL: PARTICLE SIZE AND CELLULAR INTEGRITY

Estimated proportions of the number of ruptured and intact cells present in the various milled size fractions are shown in

Table 3.5 for chickpeas and durum wheat. The number of ruptured cells on the particle surface increased with respect to particle size. In the smallest particles, all the cells were ruptured, whereas in the largest particles of chickpea, only 17% of the cells were ruptured (i.e., up to 83% remained intact). The mathematical model was limited in that for the smallest sizes, it suggested that more cells were present on the particle surface than were contained within the total particle volume. As a result, the initial estimates suggested that more than 100% of the cells in the small particles were ruptured, which is not a possible outcome. Therefore, any initial estimates indicating $>100\%$ rupture were adjusted to 100%, to reflect that all the cells were likely to be ruptured. This adjustment is shown in (**Table 3.5**). Although the macro-particle dimensions were the same for chickpeas and durum wheat, different proportions of ruptured/intact cells were estimated because of the different cell dimensions of these botanical species (e.g., durum wheat cells are larger than chickpea cells).

TABLE 3.5: ESTIMATED NUMBER OF CELLS PRESENT IN VARIOUS SIZE FRACTIONS OF MILLED DURUM WHEAT AND CHICKPEA

		MILLED MACRO-PARTICLE CHARACTERISTICS						DURUM WHEAT CELLS ($D = 0.25 \times 0.05 \times 0.05 \text{ mm}$)						
	MIN	-	MAX	s (mm)	$\rho V (\text{mm}^3)$	$\rho SA (\text{mm}^2)$	$\rho SA/PV (\text{mm}^{-1})$	#L	#D	#H	#V	#S	% Ruptured	% Intact
DURUM WHEAT	0.00	-	0.21	0.11	0.0	0.1	57.1	0.4	2.1	2.1	1.9	12.3	100 (*667)	0 (*-567)
	0.25	-	0.50	0.38	0.1	0.8	16.0	1.5	7.5	7.5	84.4	157.5	100 (*187)	0 (*-87)
	0.50	-	0.60	0.55	0.2	1.8	10.9	2.2	11.0	11.0	266.2	338.8	100 (*127)	0 (*-27)
		<i>threshold</i>		0.70	0.3	2.9	8.6	2.8	14.0	14.0	548.8	548.8	100.0	0.0
	0.60	-	0.85	0.73	0.4	3.2	8.3	2.9	14.5	14.5	609.7	588.7	97	3
	0.85	-	1.18	1.02	1.0	6.2	5.9	4.1	20.3	20.3	1673.1	1153.9	69	31
	1.18	-	1.40	1.29	2.1	10.0	4.7	5.2	25.8	25.8	3434.7	1863.8	54	46
	1.40	-	1.70	1.55	3.7	14.4	3.9	6.2	31.0	31.0	5958.2	2690.8	45	55
	1.70	-	2.00	1.85	6.3	20.5	3.2	7.4	37.0	37.0	10130.6	3833.2	38	62
2.00	-	3.15	2.58	17.1	39.8	2.3	10.3	51.5	51.5	27318.2	7426.3	27	73	
		MILLED MACRO-PARTICLE CHARACTERISTICS						CHICKPEA CELLS ($D = 0.14 \times 0.04 \times 0.04 \text{ mm}$)						
	MIN	-	MAX	s (mm)	$\rho V (\text{mm}^3)$	$\rho SA (\text{mm}^2)$	$\rho SA/PV (\text{mm}^{-1})$	#L	#D	#H	#V	#S	% Ruptured	% Intact
CHICKPEA	0.00	-	0.21	0.11	0.0	0.1	57.1	0.8	2.6	2.6	5.2	21.7	100 (*419)	0 (*-319)
	0.25	-	0.50	0.38	0.1	0.8	16.0	2.7	9.4	9.4	235.4	276.2	100 (*117)	0 (*-17)
		<i>threshold</i>		0.44	0.1	1.2	13.6	3.1	11.0	11.0	380.3	380.3	100.0	0.0
	0.50	-	0.60	0.55	0.2	1.8	10.9	3.9	13.8	13.8	742.7	594.2	80	20
	0.60	-	0.85	0.73	0.4	3.2	8.3	5.2	18.1	18.1	1701.2	1032.5	61	39
	0.85	-	1.18	1.02	1.0	6.2	5.9	7.3	25.4	25.4	4668.2	2023.7	43	57
	1.18	-	1.40	1.29	2.1	10.0	4.7	9.2	32.3	32.3	9583.4	3268.8	34	66
	1.40	-	1.70	1.55	3.7	14.4	3.9	11.1	38.8	38.8	16624.4	4719.2	28	72
	1.70	-	2.00	1.85	6.3	20.5	3.2	13.2	46.3	46.3	28266.2	6722.8	24	76
2.00	-	3.15	2.58	17.1	39.8	2.3	18.4	64.4	64.4	76222.6	13024.4	17	83	

ρV is the volume and ρSA is the surface area of a cubic particle with side length, s , #L, #D, #H is the number of cells with dimensions ($D = \text{length} \times \text{depth} \times \text{height}$) that can fit into the side length 's', #V is the number of cells in the ρV , and #S is the number of cells that occupy the particle surface. 'Threshold' indicates the largest possible size at which all cells are ruptured. *Milled materials smaller than this threshold were taken to contain 100% ruptured cells and 0% intact cells (original number shown in brackets).

3.3.6 CELL WALL ANALYSIS

The major pectic and hemi-cellulosic polysaccharides present in chickpea and durum wheat endosperm cell walls are shown in **Table 3.6**. These are typical constituents of Type 1 (chickpea) and Type 2 (durum wheat) cell walls (Brett and Waldron 1996). Both cell wall types also contain cellulose, but this was not measured with the present methodology.

TABLE 3.6: PECTIC AND HEMICELLULOSIC POLYSACCHARIDES IN CHICKPEA AND DURUM WHEAT CELL WALLS

MATERIAL	PECTINS	HEMICELLULOSES
Chickpea (Type I)	Homogalacturonan	Xyloglucan
	Arabinan	Xylan/Arabinoxylan
	Galactan	
	(<i>arabinogalactan 1</i>)	
	Xylogalacturonan	
Durum wheat (Type II)	Arabinan	Xylan/Arabinoxylan
		Feruloylated arabinan

3.3.7 CELL WALL PORE SIZE

Fluorescence micrographs showing the diffusion of FITC-dextran into hydrothermally processed chickpea cells or durum wheat tissue (because isolated durum wheat cells could not be obtained) are presented in **Figure 3.5** and **FIGURE 3.6**, respectively. Both materials were permeable to the smallest dextran (4000 Da, $R_{HYD} = 1.4$ nm). The larger 10 kDa ($R_{HYD} = 2.3$ nm) dextran did not penetrate chickpea cells, but appeared to diffuse progressively into durum wheat tissue, although the cell wall barrier was not well defined in these micrographs. Neither tissue was permeable to 40 kDa dextran ($R_{HYD} = 4.5$ nm).

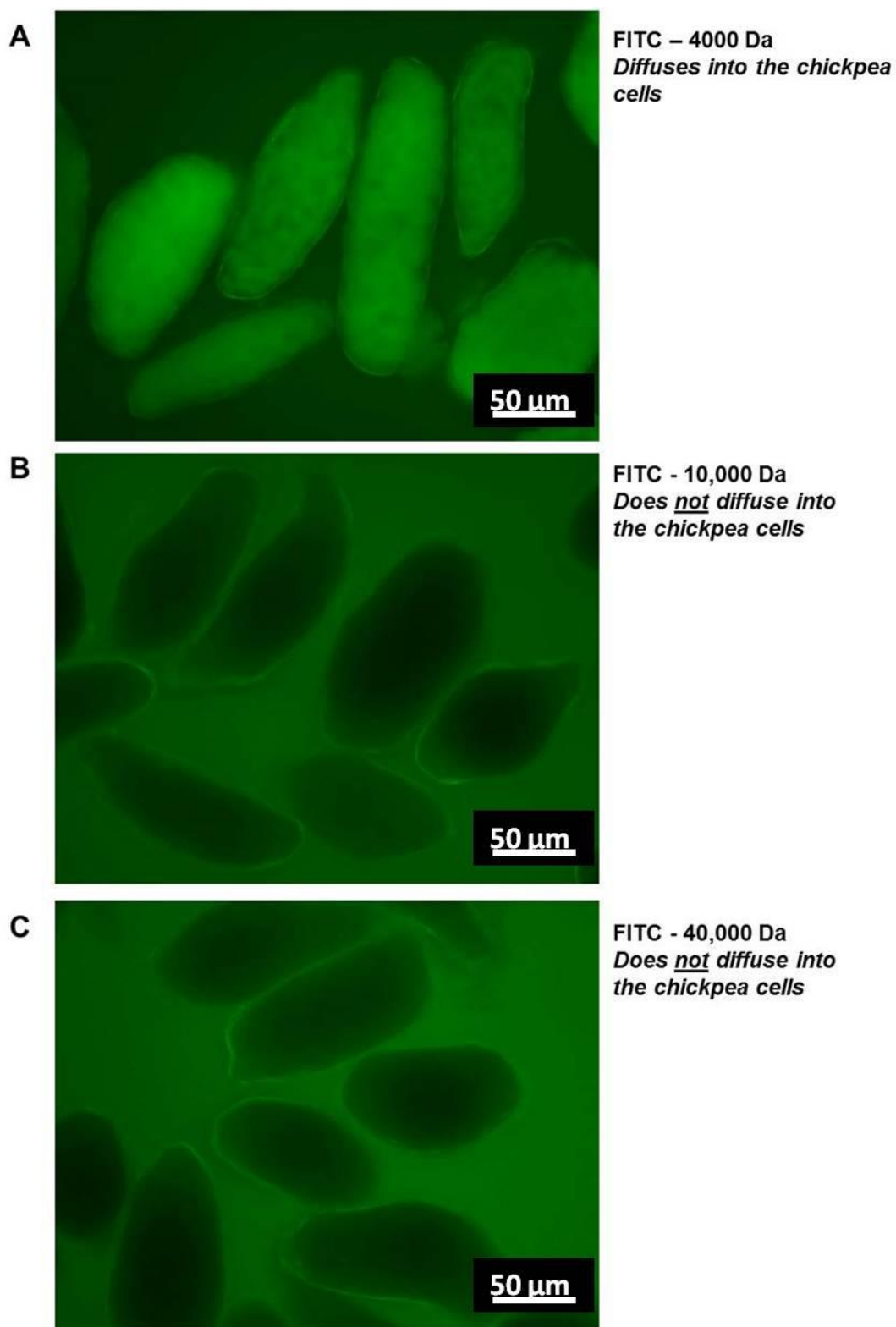


FIGURE 3.5: FLUORESCENCE MICROGRAPHS SHOWING PERMEABILITY OF HYDROTHERMALLY PROCESSED CHICKPEA CELLS TO FITC-DEXTRANS. (A) 4000 Da ($R_{HYD} = 1.4$ nm), (B) 10 000 Da ($R_{HYD} = 2.3$ nm) and (C) 40 000 Da ($R_{HYD} = 4.5$ nm) FITC-dextran.

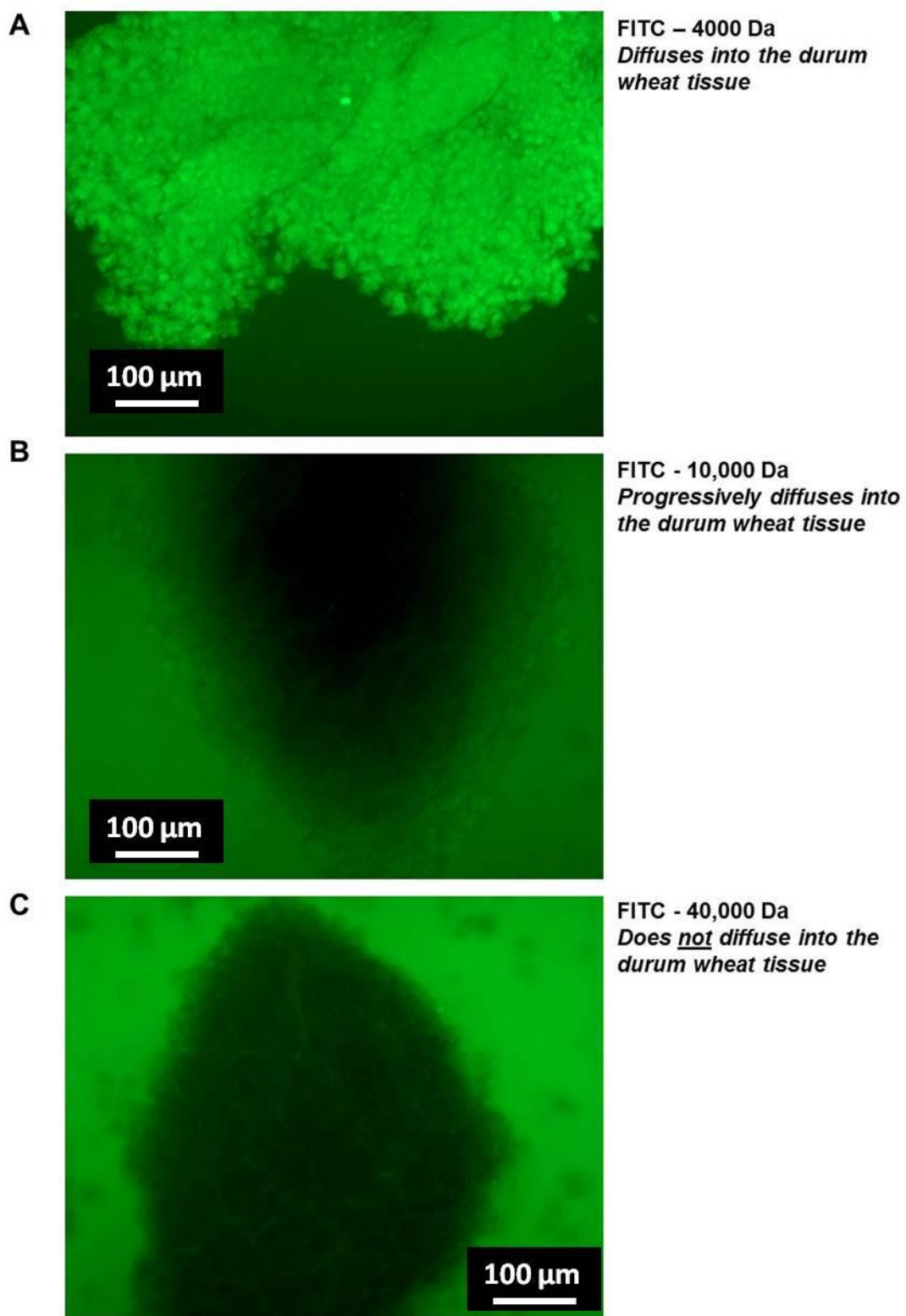


FIGURE 3.6 FLUORESCENCE MICROGRAPHS SHOWING PERMEABILITY OF HYDROTHERMALLY PROCESSED DURUM WHEAT TISSUE TO FITC-DEXTRANS. (A) 4000 Da ($R_{HYD} = 1.4$ nm), (B) 10 000 Da ($R_{HYD} = 2.3$ nm) and (C) 40 000 Da ($R_{HYD} = 4.5$ nm) FITC-dextran. Representative example shown after 1 h incubation, obtained from ~ 0.73 mm particles after hydrothermal processing.

3.3.8 STARCH GELATINISATION BEHAVIOUR

The gelatinisation of purified starches from chickpea and durum wheat was observed as a loss of birefringence during heating (**Figure 3.7**). In the native state, both starches showed the characteristic Maltese cross pattern. As starch was heated, the granules were observed to swell, and an accompanying loss of birefringence occurred between 50 and 70°C in durum wheat starch, and between 65 and 80 °C in chickpea starch.

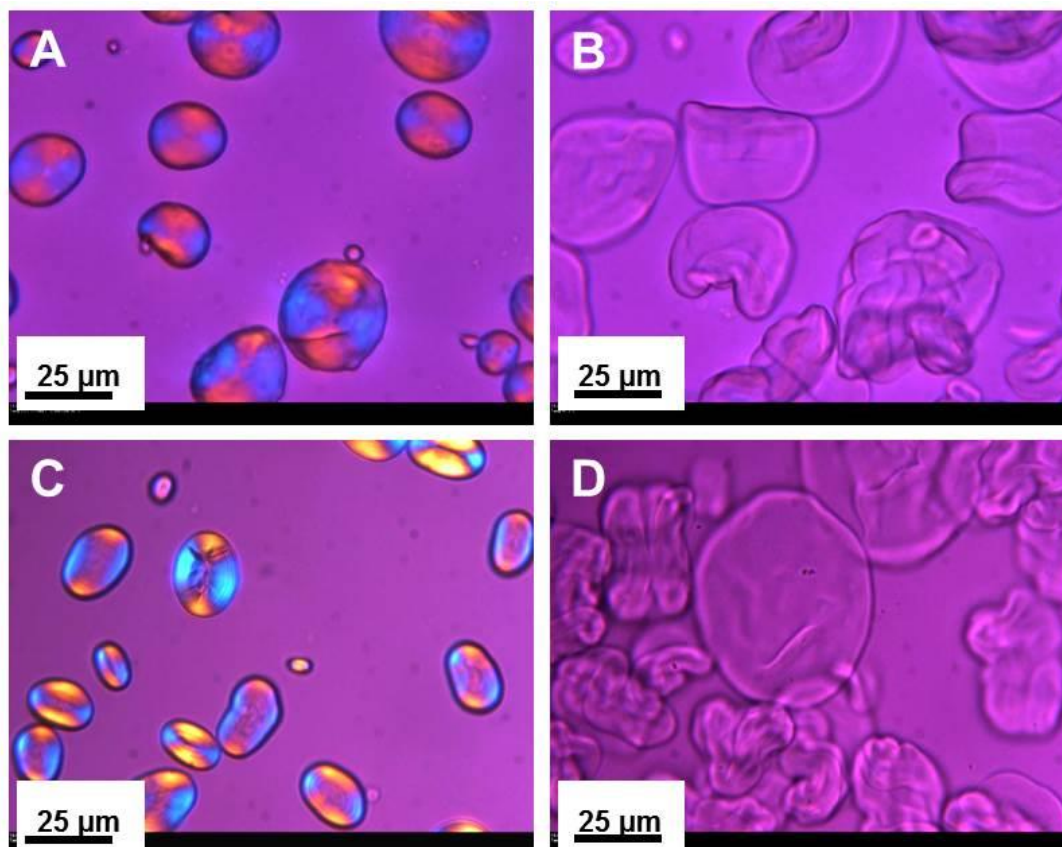


FIGURE 3.7: BI-REFRINGENCE OF PURIFIED STARCHES OF RAW DURUM WHEAT (A) AND CHICKPEA (C) AND HYDROTHERMALLY TREATED DURUM WHEAT (B) AND CHICKPEA (D). Purified starches were hydrothermally processed in deionised water on a heated-stage microscope which heated the samples from 0 to 95 °C at 1°C/min.

The same hydrothermal treatment was applied to milled durum wheat and chickpea, containing some intact cells. Although the micrograph suggests that intracellular durum wheat starch expanded and that consequently, cellular integrity was lost, it was difficult to see the durum wheat cell walls at this magnification.

Thus, the micrograph of durum hydrothermally treated durum wheat may actually be showing just the intracellular matrix, held together in the shape of a cell. Intact cells, were, however, clearly evident in the milled chickpea, but the cell wall encapsulated starch did not fully gelatinise under the heating conditions used (**Figure 3.8**).

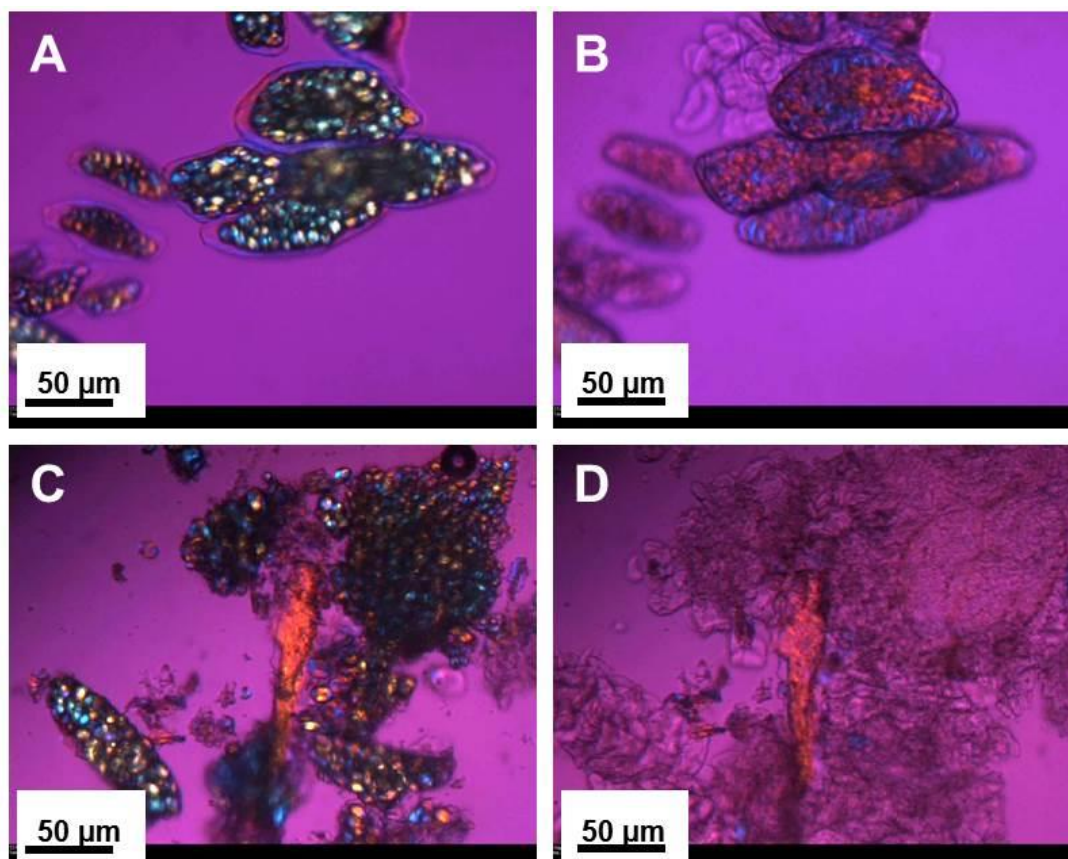


FIGURE 3.8: BIREFRINGENCE OF STARCH IN RAW MILLED CHICKPEA (A) AND DURUM WHEAT (C) AND HYDROTHERMALLY TREATED CHICKPEA (B) AND DURUM WHEAT (D). Milled materials were hydrothermally processed in deionised water on a heated-stage microscope which heated the samples from 0 to 95 °C at 1°C/min.

3.3.9 EFFECT OF ENDOGENOUS COMPOUNDS ON *IN VITRO* DIGESTIBILITY

Enzyme-free control runs performed on native and hydrothermally processed samples revealed that < 350 µM reducing sugar from endogenous sources (expressed as maltose equivalents) was present in the solution during 4 h mixing at 37 °C, and that the concentration of endogenous sugar did not increase over time. To correct for the contribution of endogenous sugars, the amount of reducing sugar detected in the 'blank' aliquots (collected before enzyme addition) was subtracted from all digestibility data.

Preliminary digestibility experiments were carried out on purified starches and flours to provide an indication of interference from endogenous enzymes or inhibitors (expected to be present in the flour fraction, but not in the purified starch) on starch digestibility.

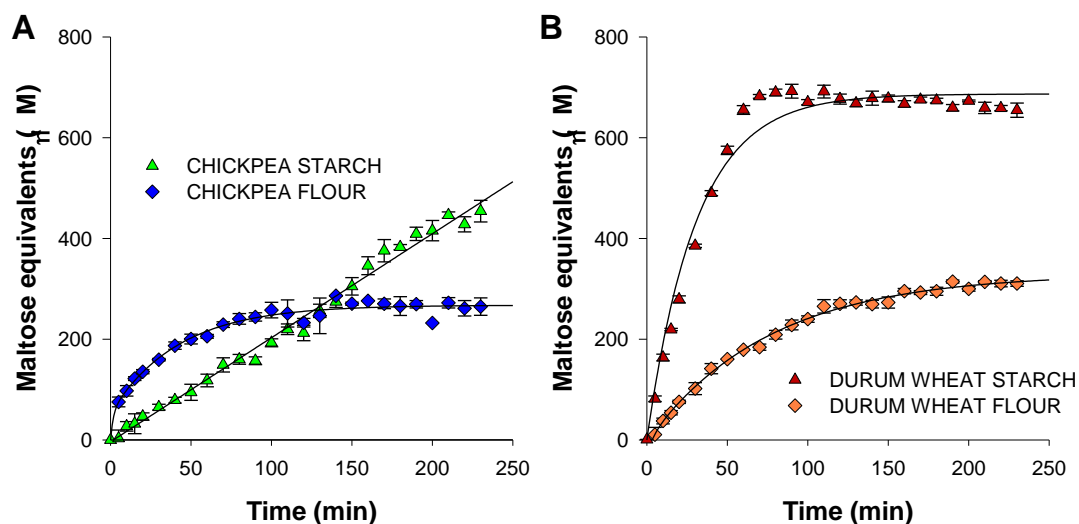


FIGURE 3.9: DIGESTIBILITY CURVES OBTAINED FOR NATIVE STARCH AND FLOUR OF CHICKPEA (A) AND DURUM WHEAT (B). Values are mean of triplicates \pm SEM. Endogenous reducing sugars have been subtracted. Curves were fitted to Equation 2.3, except for chickpea starch, which was fitted to a linear equation.

Comparison of *in vitro* digestibility of **native** chickpea and durum wheat revealed clear differences between starch and flours (i.e. containing cell wall fragments but no encapsulated starch), and between the two botanical sources (**Figure 3.9**). Overall, flours were less digestible than the native starches, which could be explained by amylase inhibition by endogenous compounds. It is not entirely clear why a greater rate of digestion was observed for chickpea flour compared to the purified starch during the first 2 h of digestion, but it is probable that this could reflect a greater degree of starch damage in the milled flour than in the extracted starch.

Once **boiled**, however, these differences between the digestibility of starches and flours of chickpea and durum wheat (**Figure 3.10**) were much less apparent, both in terms of the initial rate and the extent of digestion. This suggests that any endogenous inhibitors of amylase (likely to be present in the flour fraction) were largely inactivated

during hydrothermal processing. As expected, hydrothermal processing of these materials also gave rise to vast increases in the rate and extent of starch digestion, compared with the native materials.

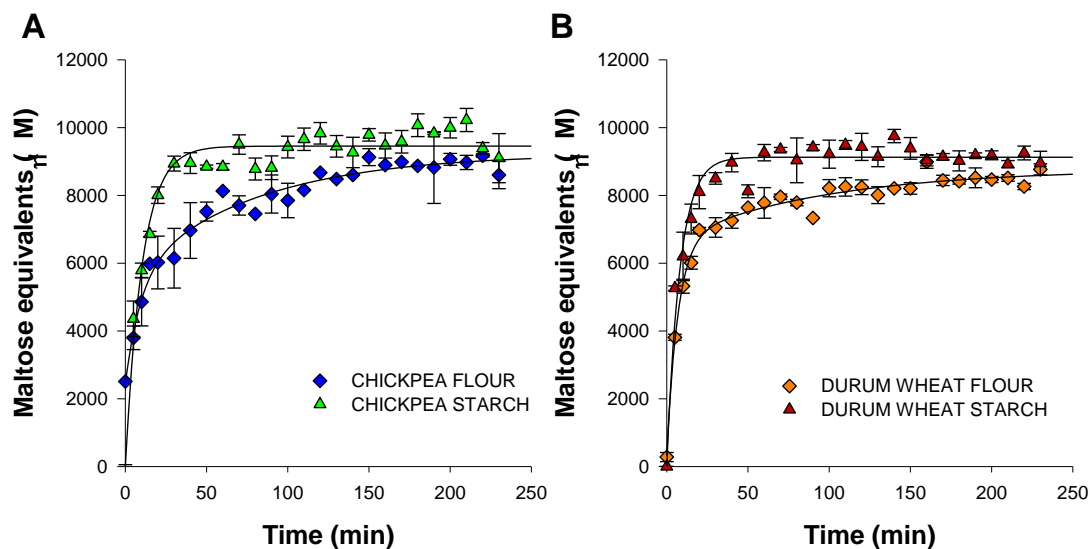


FIGURE 3.10: DIGESTIBILITY OF HYDROTHERMALLY PROCESSED STARCH AND FLOURS OF (A) CHICKPEA AND (B) DURUM WHEAT. Values are mean of triplicates \pm SEM. Endogenous reducing sugars have been subtracted. Curves were fitted to *Equation 2.3*.

3.4 DISCUSSION

The characterisation of isolated cells, extracted starch and milled fractions from durum wheat and chickpea provided insight into their structure, composition and properties. In the preparation of these materials, the outermost ‘fibre-rich’ layers were removed to enable the effect of starch encapsulation in wheat endosperm or chickpea parenchyma cells to be studied more precisely. Proximate analysis data were consistent with the literature on whole chickpeas and grains (McCance and Widdowson 2002). Both test materials had similar energy densities, but the milled chickpeas contained more dietary fibre, protein and fat and less starch, than durum wheat. Because the rate of starch amylolysis is dependent on substrate concentration, in subsequent digestibility experiments, the weight of milled material or amount of extracted starch reacted with enzyme(s) was adjusted so that the starch content was standardised across both botanical sources and for all size fractions.

There were some differences in the characteristics of the native, purified starches extracted from chickpeas and durum wheat: Chickpea starch, for instance, contained more amylose, and had a greater swelling power than durum wheat starch. These different characteristics may have a bearing on the susceptibility of raw/native starches to amylolysis (Tahir *et al.* 2010), and on the behaviour of these materials during hydrothermal processing (Svihus *et al.* 2005). Once gelatinised, however, the digestibility of the purified starches was found to be very similar. This is explained by the more amorphous structure of gelatinised relative to native starches (see *Section 1.2.6.1, page 40*), and is consistent with previous comparisons of digestibility of raw and gelatinised starches obtained from various botanical sources (Slaughter *et al.* 2001). Similarly, the amount of starch damage, which occurs during milling and increases starch swelling and therefore susceptibility to α -amylase, becomes less relevant once the starch is gelatinised. As suggested by previous workers (Buonocore *et al.* 1977, Würsch *et al.* 1986, Frias *et al.* 2000) hydrothermal processing also reduces/eliminates the effects of endogenous inhibitors or enzymes that were seen to alter starch digestibility in the native materials.

In the hydrothermally processed tissues of chickpeas and durum wheat, the cells appeared largely intact, and held together as a tissue, while the starch, evident as distinct granules, remained encapsulated by plant cell walls. Some micro-structural differences were observed between chickpeas and durum wheat, e.g., the cell walls (i.e. a component dietary fibre) of chickpea parenchyma cells were considerably thicker than in durum wheat, which explains the higher fibre content of chickpeas. On average, durum wheat cells are somewhat larger than chickpea cells, although cell size is known to vary considerably, especially in wheat, depending on where in the endosperm the cells are located (Kent and Evers 1994)

Milling provided a suitable means of manipulating the proportion of intact cells present in the hydrothermally processed tissues, without significantly altering the starch

content. Theoretical estimates obtained with the 'geometric model' indicated that the smallest size fraction, the flour, consisted entirely of ruptured cells, whereas in the largest macro-particles ~2.6 mm, up to ~90% of starch was encapsulated within intact cells. Similar geometric principles have previously been used to mathematically predict the release of lipid from ruptured cells of almond cotyledonary tissue (Ellis *et al.* 2007). However, chickpeas and durum wheat have very different tissue structure to almonds and the existing 'Ellis 2007' model could not easily be applied to these materials. The geometric model used in this thesis represents a simplified mathematical model in which the interstitial spaces, corners and cell orientation are not accounted for, and is also based on a number of assumptions (i.e. with regard to particle and cell shape, dimensions, and cell assembly). The values obtained with the geometric model are therefore very rough estimates. Nevertheless, these estimates, although crude, demonstrate the extent to which milling can be used to manipulate the proportion of cell wall encapsulated starch. The theoretical predictions of size-dependant changes in cellular integrity will be compared with experimental data in subsequent chapters.

Of course, manipulating particle size also alters the surface area per volume ratio, which can influence the rate of ingress of digestive enzymes within permeable cereal materials of different sizes (Al-Rabadi *et al.* 2009). Isolated chickpea cells were a desirable control because they have a high surface area per volume ratio, but still contain 100% cell wall encapsulated starch. Chickpea cells were readily obtained from hydrated materials; however isolating cells from durum wheat endosperm, which has a tendency to fracture, proved more difficult. None of the chemical, mechanical and thermal treatments applied allowed intact cells to be obtained without compromising the structural integrity of the cell walls and intra-cellular starch.

The isolation of chickpea cells resulted in significant losses of dietary fibre (35.5% reduction from milled to cells, dry weight basis). Comparison of preliminary cell wall analysis (*data not shown*) of raw and hydrothermally processed (1.5 h) chickpeas

suggested losses (solubilisation) of pectins (e.g., homogalacturonan and galactan) and xyloglucan (hemi-cellulose) following boiling. Indeed, homogalacturonans are most abundant in the middle lamella, and are subject to de-polymerisation during hydrothermal processing (Jarvis *et al.* 2003). Although the composition of raw chickpea cells cannot be taken to directly match the components of milled chickpeas, similar fibre losses are likely to occur when the milled materials are hydrothermally processed prior to *in vitro* digestion. Thus, the cellular integrity of isolated cells is likely to be fairly representative of the cells contained within the hydrothermally processed tissues.

With regard to other cell wall components, different polysaccharides were identified in durum wheat and chickpeas. Durum wheat endosperm, like other Type 2 cell walls, contained relatively high proportions of arabinoxylan, whereas chickpea cell walls, like other dicot Type 1 cell walls, contained relatively high proportions of the pectic polysaccharides homogalacturonan, arabinan and galactan (Brett and Waldron 1996). The semi-quantitative analysis methodology used did not allow the relative proportions of cellulose, hemicelluloses and pectic polysaccharides in the cell walls of these materials to be determined. Considering the literature on similar plant materials (see *Section 1.2.7, page 48*), it is very likely that chickpea cell walls consist predominantly of pectin and cellulose, whereas cell walls of durum wheat endosperm consist predominantly of one hemicellulose (i.e., the arabinoxylan fraction).

The cell wall porosity studies provided novel insights into the permeability of the chickpea and durum wheat cell walls to molecules of relevant size (e.g., similar to digestive enzymes). Chickpea cells were found to have a lower pore size and excluded smaller dextrans than durum wheat. This is particularly relevant considering the reported values for the radius of gyration (2.69 nm) and dimensions ($a = 5.63$, $b = 8.78$ and $c = 10.34$ nm) of amylase, as it suggests that the pore size of chickpeas (< 2.3 nm) would exclude amylase (Simon *et al.* 1974, Payan *et al.* 1980). This would be expected to limit starch bioaccessibility. Results obtained with coarsely milled durum wheat were

difficult to interpret, because the cell wall barrier was not clearly defined under the light microscope, yet the 10 kDa FITC-dextran ($R_{HYD} = 2.3 \text{ nm}$) did appear to diffuse progressively into the tissue.

However, it is important to note that the R_{HYD} of dextrans does not exactly reflect pore size (radius), because these dextrans are unlikely to be perfectly spherical. It is therefore difficult to predict accurately whether amylase will be able to penetrate cell walls based on this data. The next chapter (*Chapter 4*) will describe further studies of amylase diffusion and consider the potential role of cell walls as physical barriers to starch digestion.

Observing the different behaviour of starch encapsulated within chickpea cells during hydrothermal processing (i.e., on a heated stage microscope fitted with cross-polarizers) also provided some evidence with regard to the potential role of cell walls in limiting starch bioaccessibility. When milled material containing intact cells was heated, encapsulated chickpea starch began to swell, but retained birefringence (a characteristic of pre-gelatinised starch), and the cell walls did not seem to give way to the pressure of expanding starch granules. Pressure exerted by intracellular starch granules is believed to facilitate cell separation (Jarvis *et al.* 2003), and in some potato varieties, the swelling of starch causes the cells to rupture (Shomer 1995). Potatoes starch has a much greater swelling power (~1159% at 95 °C) than chickpea (~12% at 90°C) and wheat starch (18-26% at 100°C), probably as a result of the high phosphate content (Noda *et al.* 2007, Singh *et al.* 2003, Singh *et al.* 1982). Nevertheless, it is possible that the highly resilient chickpea cell walls hindered the swelling of starch and therefore impeded starch gelatinisation.

In durum wheat, the role of the cell walls in influencing starch gelatinisation was difficult to interpret using heated stage microscopy, because of the difficulty in obtaining intact cells from durum wheat. At first sight, the durum wheat cells seemed to rupture as the starch granules expanded. However, the cell wall could not be easily identified in the

micrographs, and the starch-rich material perceived as a durum wheat endosperm cell could also have been intracellular contents, held together by the cytoskeleton. Certainly the vast majority of cells appeared intact in the light micrographs of tissue sectioned from hydrothermally processed durum wheat. These micrographs did, however, depict intracellular starch granules with a distorted shape, which is thought to arise from restricted starch gelatinisation (Würsch *et al.* 1986, Fujimura and Kugimiya 1994). These effects were investigated in further experiments reported in **Chapter 4**.

3.5 CONCLUSIONS

In this chapter, the physico-chemical properties of starch, milled size-fractions, and separated cells of chickpeas and durum wheat were compared. No differences were observed between the digestibility of hydrothermally processed starches and flours (i.e., no intact cells) obtained from chickpea and durum wheat. However, the cell wall properties differ markedly. Chickpea parenchyma cells have thick, less permeable, Type I, pectin and xyloglucan-rich cell walls, and the tissue tends to separate when hydrated. Durum wheat endosperm cells (Type II walls) have thinner walls, composed predominantly of arabinoxylans and the tissue tends to fracture. In chickpea cotyledonous tissue, the starch encapsulated by cell walls appeared to resist swelling and gelatinisation, and the chickpea cell walls were impermeable to dextrans of smaller size than α -amylase. This provided initial evidence that cell wall encapsulation of starch may influence starch bioaccessibility. Overall, the properties observed are consistent with the expected differences between cereals and pulses, and justifies the selection of these materials for further comparative studies. It is not known, however, to what extent the properties of chickpeas and durum wheat apply to other pulses and cereals. This is an area that warrants further investigation.

CHAPTER 4

IN VITRO STRUCTURE-FUNCTION STUDIES

4.1 INTRODUCTION

Accumulating evidence suggests that food structure plays an important role in influencing starch bioaccessibility and the post-prandial blood glucose response (Singh *et al.* 2010, Jarvi *et al.* 1995, Parada and Aguilera 2011, Bjorck *et al.* 1994, Read *et al.* 1986). The structure-function studies described in this chapter were carried out to examine how cell walls influence the rate and extent of starch digestion and to explore the underlying mechanisms.

It is currently unclear by what mechanism cell wall encapsulation influences digestion kinetics and glycaemia. Progress in this area has not been helped by the tendency of many researchers to use digestion methodologies that involve excessive de-structuring (e.g., maceration, homogenisation and grinding that ruptures many cells) prior to *in vitro* digestion (Woolnough *et al.* 2008). Furthermore, published studies often provide limited structural descriptions of experimental materials, which makes it difficult to interpret the reported results. There also appears to be some confusion about the role of 'fibre content' and fibre in the form of plant cell walls that physically encapsulate nutrients (Brownlee 2011, Mann and Cummings 2009). This thesis is focussed on the latter.

Across the literature, two mechanisms by which encapsulating cell walls limiting nutrient (starch) bioaccessibility are widely alluded to: i) plant cell walls may act as barriers to digestive enzymes and/or, ii) they may restrict gelatinisation of intracellular starch, which lowers susceptibility to amylolysis, with consequences therefore for restricting starch bioaccessibility and digestion. These mechanisms are not mutually exclusive and so both may contribute to a limitation of starch bioaccessibility.

Evidence for the *cell wall barrier mechanism* appears to be based largely on qualitative data, including microstructural observations of undigested starch in leguminous cells (Noah *et al.* 1998, Würsch *et al.* 1986), rather than studies on cell wall properties, such

as fracture mechanics and permeability. To the authors' knowledge, no published studies have actually determined the permeability to digestive enzymes of hydrothermally processed chickpea parenchyma and durum wheat endosperm cell walls, or indeed any similar plant tissues. Addressing this question may provide fundamental insights into digestion mechanisms.

With regard to studies of the proposed effects on *starch swelling and gelatinisation*, these originate largely from observations of 'buckled-saddle' shaped starch granules (see *Section 1.2.9, page 66*), that have been observed in various hydrothermally processed foods (Fardet *et al.* 1998, Würsch *et al.* 1986, Fujimura and Kugimiya 1994), but are also supported by DSC studies which have demonstrated an increase in the extent of starch gelatinisation with increasing disruption of physical structure (Champagne *et al.* 1990, Marshall 1992). It has been suggested that when starch is entrapped in a food matrix or in plant cells, the heat, water or space required for granular swelling and gelatinisation is limited, resulting in partially swollen granules with a distorted shape (Würsch *et al.* 1986). It is likely that these granules retain some of the ordered structure of native starch, and would therefore be expected to be less susceptible to α -amylase than starch which has fully gelatinised (Roder *et al.* 2009, Slaughter *et al.* 2001).

Thus, the existing data is largely qualitative and there is a lack of direct evidence for both the proposed 'barrier'- and 'restricted gelatinisation'- mechanisms. The characterisation work presented in the previous chapter provided some initial evidence (see *Sections 3.3.7 and 3.3.8, from page 114*), on cell wall permeability and birefringence during hydrothermal processing to support both the barrier- and restricted gelatinisation- hypotheses. The studies described in this chapter were designed to explore these mechanisms further. A broader combination of techniques was used to gain additional insight into the consequential effects on digestion kinetics.

4.1.1 OBJECTIVES

- a) Determine the effects of cell wall encapsulation on *in vitro* digestion kinetics
- b) Examine the proposed role of cell walls in impeding intracellular starch gelatinisation and/or amylase access.
- c) Gain insight into the underlying mechanisms of digestion in edible plant tissues (chickpea and durum wheat) with contrasting cell wall properties.

4.2 MATERIALS AND METHODS

4.2.1 PLANT MATERIALS

Milled materials, freshly prepared isolated cells, protoplasts and starch were obtained from chickpeas and durum wheat as described in *Section 2.1 page 71*. These materials were similar in composition, but differed in structure, i.e. they contained different proportions of plant cell wall encapsulated starch. Theoretical estimates of the proportion of intact or ruptured cells in each milled size fraction were obtained using the Geometric Model (*Chapter 3, Section 3.2.2, page 102*), and are shown in **Table 4.1**.

TABLE 4.1: OVERVIEW OF MILLED SIZE FRACTIONS

Size range (mm)	s (mm)	SA:V (mm ⁻¹)	DURUM WHEAT		CHICKPEAS	
			Ruptured Cells (%)	Intact Cells (%)	Ruptured Cells (%)	Intact Cells (%)
0.00 - 0.21	0.11	57.1	100	0	100	0
0.25 - 0.50	0.38	16.0	100	0	100	0
0.50 - 0.60	0.55	10.9	100	0	80	20
0.60 - 0.85	0.73	8.3	97	3	61	39
0.85 - 1.18	1.02	5.9	69	31	43	57
1.18 - 1.40	1.29	4.7	54	46	34	66
1.40 - 1.70	1.55	3.9	45	55	28	72
1.70 - 2.00	1.85	3.2	38	62	24	76
2.00 - 3.15	2.58	2.3	27	73	17	83

Size range defined based on sieve aperture. *s*; median sieve aperture range and taken to be the side length of a milled particle. SA:V; surface area per volume, calculated from *s* assuming cuboid particles. Intact Cells (%) is the proportion of the cells that are structurally intact, and contain cell wall encapsulated starch, and was obtained through geometrical estimation as described in *Section 3.2.2*.

The exact starch content of all materials was determined by Total Starch analysis, as described in *Section 2.3.3*.

4.2.2 DIGESTIBILITY ASSAYS

Two different digestibility studies were carried out:

In the first study, digestibility assays were performed on materials with varying degrees of cellular integrity (milled fractions, isolated cells, and protoplasts) to gain insight into the effect of cell wall encapsulation on starch digestion kinetics.

In the second study, digestibility assays were performed on coarsely milled materials that were *homogenised after boiling* to explore the proposed role of cell walls as barriers to digestion and/or as restrictors of starch gelatinisation. This was more of a preliminary experiment to explore the underlying mechanisms by which cell walls may influence digestion.

The experimental digestibility procedures used were modified slightly for each of these different purposes, as detailed in the sections below.

4.2.2.1 EXPERIMENT I: EFFECT OF CELL WALL ENCAPSULATION ON STARCH DIGESTION KINETICS

This experiment was performed on hydrothermally processed (85 min in a boiling water bath) milled endosperm (size fractions: $s = <0.21, 0.38, 0.55$ and 1.85 mm), extracted starch, isolated cells and protoplasts. The isolated cells and protoplasts were obtained (see *Sections 2.1.3* and *2.1.4*) from the hydrothermal processed tissues. All materials were kept at 37 °C prior to the assay. The starch digestibilities of these materials were assayed, as described in *Section 2.7, page 96*. The same assay procedure was used for all materials, but, due to batch-batch variability in the starch content of cell paste and protoplasts, the amount of material weighed out (which was based on previous starch determinations) resulted in digestion mixtures that were later found (i.e. when the total starch content of each specific batch was performed) to differ slightly in starch content. Thus, the final digestion mixtures contained 8 nM amylase with the following amounts of substrate: 3.9 mg/mL starch for all the milled fractions and extracted starch,

2.2 mg/mL starch for the freshly prepared separated cells, or 12.5 mg/mL starch for the protoplasts and parallel assay on intact cells.

4.2.2.2 EXPERIMENT II: RUPTURING CELLS AFTER HYDROTHERMAL PROCESSING

In this digestibility experiment, the tissue structure was disrupted (i.e., homogenised to release encapsulated starch) after hydrothermal processing, and then digested with α -amylase. The digestibility of the homogenised materials was compared with structurally intact particles, that had been processed and handled under exactly the same conditions, but that had not been subjected to de-structuring step. For this purpose, the concentration of plant material was increased (relative to previous experiments) during the hydrothermal processing stage, and the duration of processing was reduced, to achieve a 'porridge' that was more easily homogenised.

Coarsely milled particles ($s = 1.85$ mm) of chickpea (3.15 g) and durum wheat (2.10 g) were weighed into 50 mL Falcon tubes. The weight used was selected based on the known starch content of these materials, such that all tubes contained the same amount (1.26 ± 0.2 g) of starch.

For hydrothermal processing, the tissue was left to soak in 7 mL of PBS at room temperature overnight (chickpeas) or for 50 min (durum wheat), before boiling for 40 min (chickpeas) or 10 min (durum wheat). The tubes were equilibrated at 37°C for 10 min, before homogenisation treatment. Samples were homogenised for 30 s at 16.4×10^3 rpm using an IKA T25 Digital UltraTurrax®. The UltraTurrax® probe was rinsed into each tube with an additional 3 mL of buffer, to minimize starch loss and cross-contamination between tubes. Tubes were returned to the water bath to equilibrate at 37°C for an additional 5 min. PBS (30 mL, warmed to 37°C) was then added and the tubes mixed. 'Blank' aliquots of the solution (200 μ L) were taken, and then α -amylase was added to start the assay. Under these conditions, the suspension of plant material (~ 30 mg.mL⁻¹ starch) was incubated with 69 nM α -amylase, which is a proportionate increase from the enzyme to substrate ratio used in the digestibility experiment

described in the previous section (*Section 4.2.2.1*). Due to the difficulty in sampling the heterogeneous digestion mixture, tubes were taken out of the incubator to allow particles to settle 20 s before collecting an aliquot of the surrounding solution. Aliquots were collected at regular intervals over 6 h, and analysed for reducing sugar by the Prussian blue assay method (*Section 2.3.4.3, page 87*)

4.2.3 MICROSCOPY

For micro-structural observations of processed and digested materials, ‘microscopy sampling tubes’ were included in the aforementioned digestibility experiments. Samples were taken from these tubes immediately before addition of enzyme, and again throughout the enzyme-incubation period. These samples were immediately immersed in Karnovsky’s fixative to prevent further structural changes post-sampling. Homogenised samples, cells and protoplasts consisted of small particulate material and could be stained (as specified in the figure captions) and viewed under the light microscope without further processing, whereas the more coarsely milled particles were embedded in resin (LR white) and sectioned as described in *Section 2.4.1*, prior to viewing.

4.2.4 FITC-AMYLASE DIFFUSION

Cell wall permeability studies were carried out using FITC-amylase, prepared as described in *Section 2.5, page 92*. The permeability of cell walls to FITC-amylase was assessed following the principles used to estimate cell wall porosity in the previous chapter, but with slight changes to the methodology. For these experiments, 20 μL of FITC-amylase (0.17 mg/mL in PBS) were added to material suspended in PBS (50 mg plant material in 300 μL PBS), inverted once, then left for 2 min before pipetting onto a microscopy slide for examination by fluorescence microscopy. Diffusion was monitored for up to 1 h, with micrographs captured throughout.

4.2.5 DIFFERENTIAL SCANNING CALORIMETRY AND OBSERVATIONS OF BIREFRINGENCE

Differential scanning calorimetry (DSC) was used to determine quantitatively the extent to which starch gelatinised in plant tissues with variable degrees of structural integrity. DSC analysis was performed using a Multi-Cell DSC (TA Instruments) according to principles described previously (*Section 2.6, page 94*).

Starch or milled material was weighed into 1.0 mL capacity inert hastelloy[®] ampoules, to which was added 1.0 g de-gassed, deionised water. The weight of milled material added was adjusted (on the basis of measured starch content) so that all pans contained approximately 50 mg starch and 1 g water (sufficient to meet gelatinisation requirements). A pan containing only water was also included as a reference sample. Pans were hermetically sealed and gently shaken before loading into the DSC. The position of each sample (3 per run) was alternated between replicate runs, and all runs were performed in at least triplicate. Prior to heating, the instrument was equilibrated for 2.5 h at 22 °C, during which time the materials were effectively soaked. The pans were then heated from 20 °C to 90 °C at 1°C.min⁻¹, held at 90 °C for a further 10 min, then cooled back to 20 °C in a chamber constantly purged with nitrogen at a flow rate of 50 mL.min⁻¹. The relatively slow heating rate in excess aqueous solution ensures that the gelatinisation process is 'quasi-equilibrium'. To check for reversible transitions and baseline deviations, the cooled samples were immediately re-heated a second time; however no transition was observed on the second heating.

Peak integration and estimation of gelatinisation parameters (*Section 2.6*) was performed using NanoAnalyze Data Analysis software (version 2.2.0, TA Instruments 2005[®]) following principles described elsewhere (Bogracheva *et al.* 2002). As an indicator of the extent of gelatinisation, the Terminal Extent of Gelatinisation (TEG) was calculated from measured gelatinisation enthalpies as shown in **Equation 4.1**. This equation was based on that of Fukuoka *et al*, except that the correction for residual

enthalpy was excluded, because no enthalpy change was observed on the second heating cycle (Fukuoka *et al.* 2002). This estimation of TEG requires the starch content of the sample to be known, and is based on the assumption that any energy absorbed by the sample upon heating is associated only with gelatinisation of starch.

$$TEG (\%) = \frac{\Delta_{gel}H \text{ of milled material}}{\Delta_{gel}H_{sp} \text{ of purified starch}} \times 100$$

EQUATION 4.1: TERMINAL EXTENT OF GELATINISATION TEG is the terminal extent of gelatinisation and is the enthalpy associated with gelatinisation of 1 g of material ($\Delta_{gel}H \text{ J.g}^{-1}$), divided by the specific enthalpy associated with gelatinisation of 1 g of purified starch in excess water conditions ($\Delta_{gel}H_{sp} \text{ J.g}^{-1}$).

For selected samples, birefringence was also assessed (as described in *Section 2.4.3*) in samples recovered from the DSC pans after each run.

4.3 RESULTS

4.3.1 EFFECT OF ALTERING THE PROPORTION OF ENCAPSULATED STARCH ON DIGESTIBILITY

A particle-size dependent effect on starch bioaccessibility was clearly observed in the hydrothermally processed milled fractions. The larger particles (i.e., containing more cell wall encapsulated starch) were the least digestible (**Figure 4.1**). Differences in the pattern of digestion were also observed between the two botanical sources. In chickpea materials, cell wall encapsulation of starch seemed to mainly limit the *extent* of starch digestion, whereas in durum wheat, the predominant effect was on digestion *rate*. Eventually, a similar amount of starch was digested in all durum wheat fractions, irrespective of particle size. The extent of starch digestion in chickpea fractions, on the other hand, differed greatly between size fractions, and digestion reached a plateau within the first hour of digestion. These differences in starch bioaccessibility suggest that chickpea cell walls hinder amylase access to a greater extent than do cell walls of wheat.

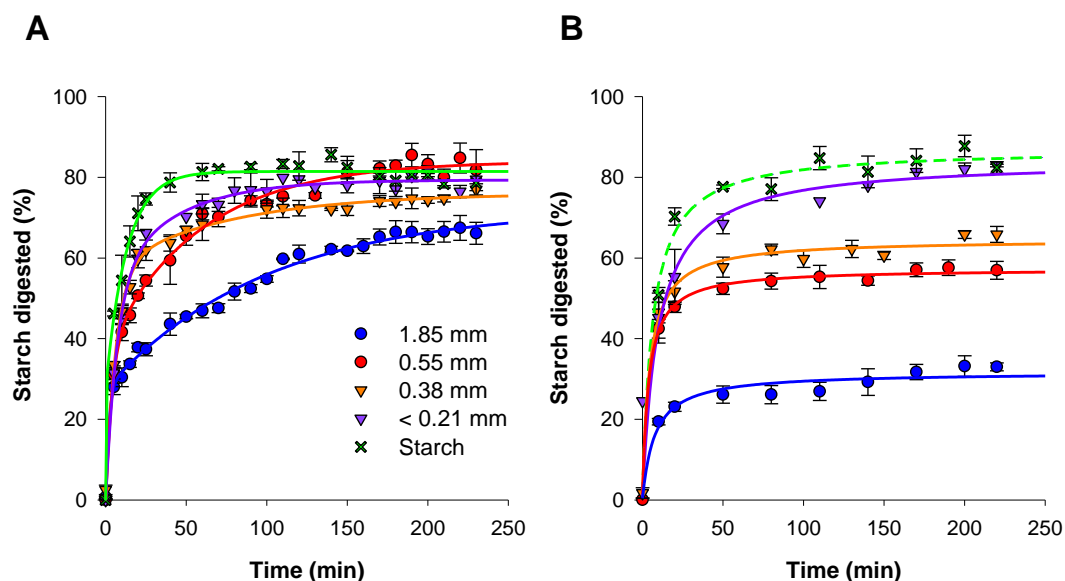


FIGURE 4.1: EFFECT OF MILLING ON STARCH DIGESTIBILITY IN HYDROTHERMALLY PROCESSED DURUM WHEAT (A) AND CHICKPEA (B). Values are mean of triplicates, error bars are SEM. The legend indicates median particle size and applies to both panels. Curves were fitted to *Equation 2.3*.

Digestibility assays were then performed on hydrothermally processed separated chickpea cells (~140 μm), which have a similar particle size to flour, but consist almost exclusively of starch that is encapsulated by plant cell walls. As shown in **Figure 4.2**, less than 0.1% of the starch in these cell preparations was digested. This strongly indicates that encapsulating cell walls play a major role in limiting the extent of digestion in chickpea materials.

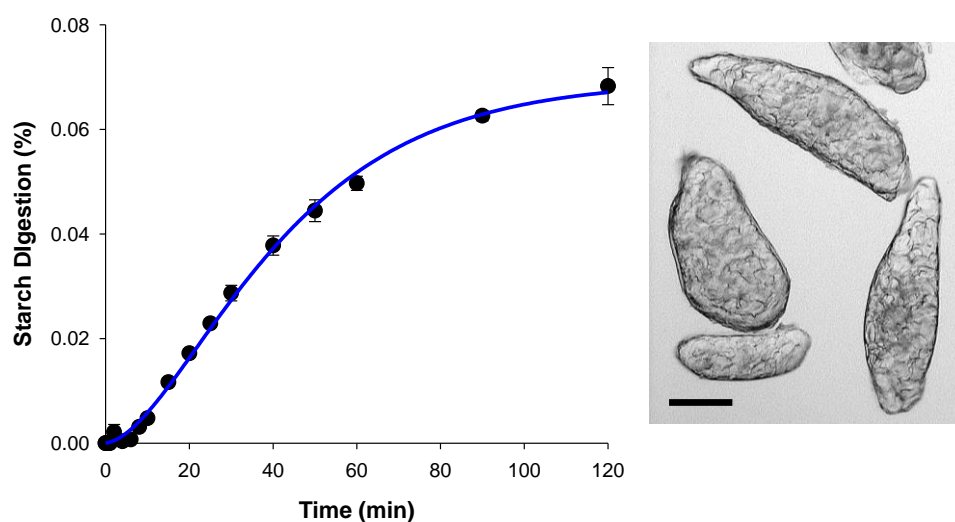


FIGURE 4.2: DIGESTIBILITY CURVE SHOWING LIMITED STARCH DIGESTION IN HYDROTHERMALLY PROCESSED SEPARATED CHICKPEA CELLS. Values are mean of triplicates with error bars as SEM. Curves were fitted to *Equation 2.3*. Light micrograph shows hydrothermally processed chickpea cells (not stained). Scalebar = 50 μm

The cell walls were successfully degraded by driselase treatment (see light micrographs of protoplast compared to intact cells in **Figure 4.3**). Digestibility curves obtained for driselase treated cells (i.e. cell wall barrier removed) and the intact cell control are shown in **Figure 4.3**. After 120 min incubation with α -amylase, only 0.11% of the starch in protoplasts and ~0.08% of the starch in intact cells had been digested. This would suggest that the intracellular starch was not very susceptible to amylase hydrolysis; however, some starch retrogradation is likely to have occurred during the preparation of these protoplasts. Additionally, some starch digestion seemed to have occurred during incubation with driselase, prior to addition of amylase (i.e., y-intercept = 0.06% starch). Therefore, it is unlikely that the limited digestibility of these protoplasts truly represents the digestibility of intracellular starch in freshly boiled plant tissues.

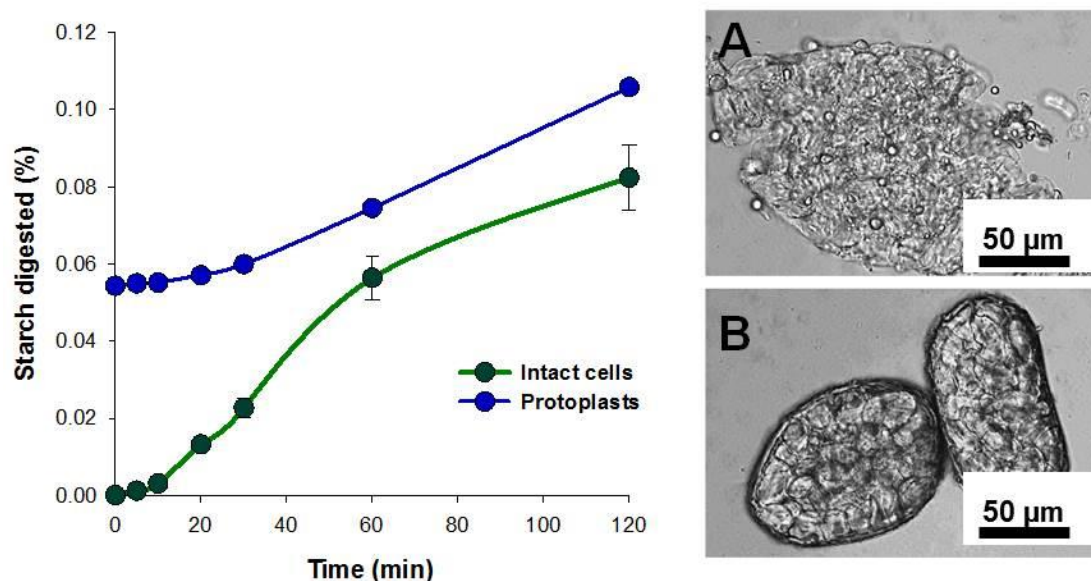


FIGURE 4.3: DIGESTIBILITY CURVES AND LIGHT MICROGRAPHS OF INTACT CELLS AND PROTOPLASTS.

Micrographs were captured before addition of α -amylase. Protoplasts (A) were prepared by treating with driselase to digest cell wall. Cells (B) were prepared in parallel, but PBS was added in place of driselase. The y-intercept represents the amount of reducing sugars released (presumably from starch) prior to incubation with α -amylase.

4.3.2 CELL WALL PERMEABILITY TO FITC-AMYLASE

The fluorescence micrographs in **Figure 4.4** show the localisation of FITC-amylose when incubated with chickpeas cells and milled durum wheat (isolated cells could not be obtained from durum wheat). FITC-amylose did not penetrate the intact chickpea cells, but did bind to starch from ruptured cells. FITC-amylose was not observed to penetrate towards the core of the milled durum wheat particle. However, the FITC-amylose was found to bind to starch exposed on the fractured surfaces of the milled particle, and probably prevented its ingress into the particle. It is therefore not clear if this result necessarily reflects endosperm cell wall permeability.

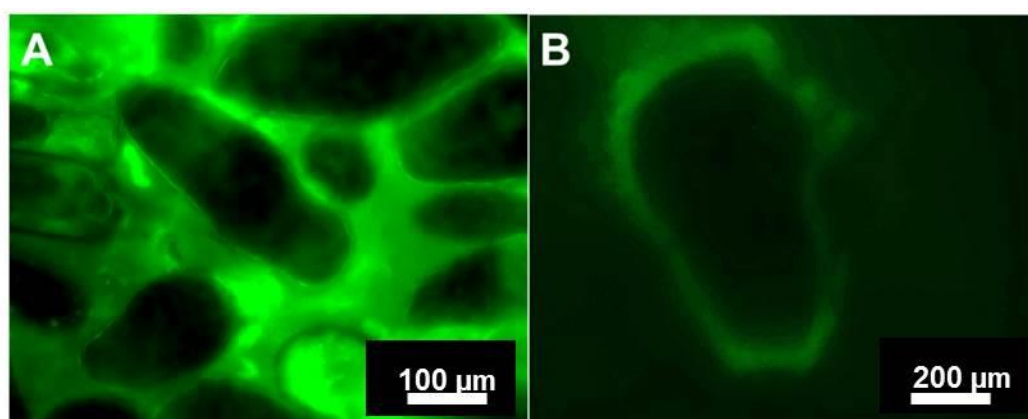


FIGURE 4.4: HYDROTHERMALLY PROCESSED CHICKPEA CELLS (A) AND MILLED DURUM WHEAT PARTICLE (B) WITH FITC-AMYLASE. Micrographs represent typical patterns observed after 30 min incubation with FITC-amylose. FITC-amylose did not penetrate intact chickpea cells, and adhered to the ruptured cells on the surface of the milled particle. Readers should note the difference in scale and that panel A shows cells, whereas panel B shows one milled particle composed of several intact cells.

4.3.3 STARCH DIGESTIBILITY IN HOMOGENISED MATERIALS

Digestibility curves were obtained for intact particles (i.e., non-homogenised control) and for macro-particles that were homogenised (to release the encapsulated starch) after hydrothermal processing. Comparison of the digestibility curves (**Figure 4.6** and **Figure 4.7**) and accompanying micrographs (**Figure 4.5** and **Figure 4.8** for durum wheat and chickpea, provides insight into the proposed role of the plant cell walls as barriers or restrictors of gelatinisation, and its implications for the rate and extent of starch digestion.

In **durum wheat**, the homogenisation disrupted the tissue structure and released nearly all the starch encapsulated within the hydrothermally processed macro-particles (**Figure 4.5A**). After 6 h *in vitro* digestion, many of the starch granules appeared eroded, except for some dark-staining granules (**Figure 4.5B**).

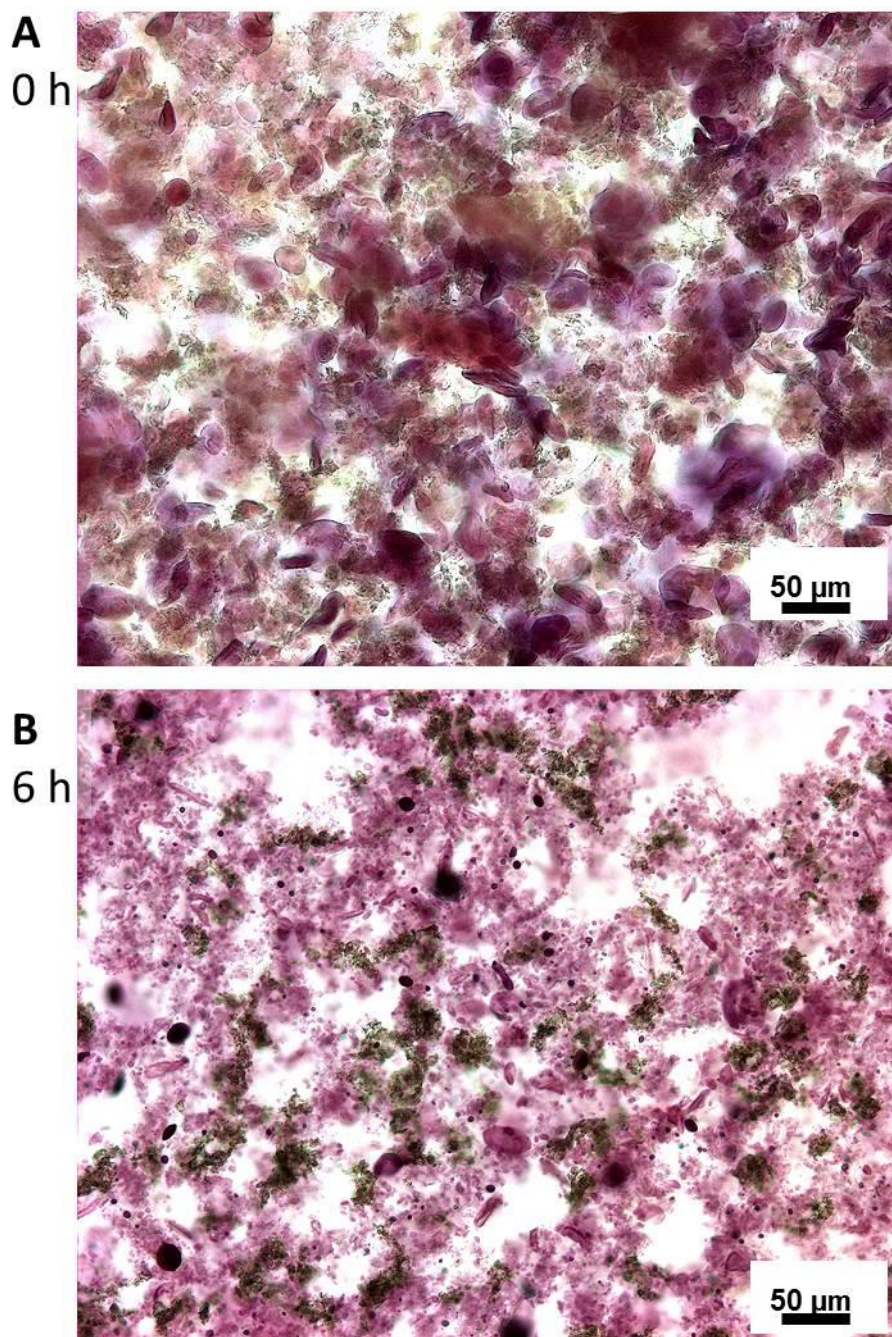


FIGURE 4.5: LIGHT MICROGRAPHS OF HOMOGENISED MACROPARTICLES OF HYDROTHERMALLY PROCESSED DURUM WHEAT BEFORE (A) AND AFTER 6 H *IN VITRO* DIGESTION (B). Stained with 2.5% Lugol's iodine solution. Homogenisation ruptured the majority of the cells. After digestion, starch granules were visibly eroded. Scale bars (50 and 20 µm in panel A and B, respectively) are shown in the bottom right corner. Both images are the same scale.

Homogenisation of hydrothermally processed durum wheat particles also increased the rate of starch digestion during the first 60 min compared to that of the intact macro-particles, i.e, in which the starch was encapsulated by cell walls (**Figure 4.6**). This supports the view that cell wall barriers delay starch hydrolysis by limiting amylase access.

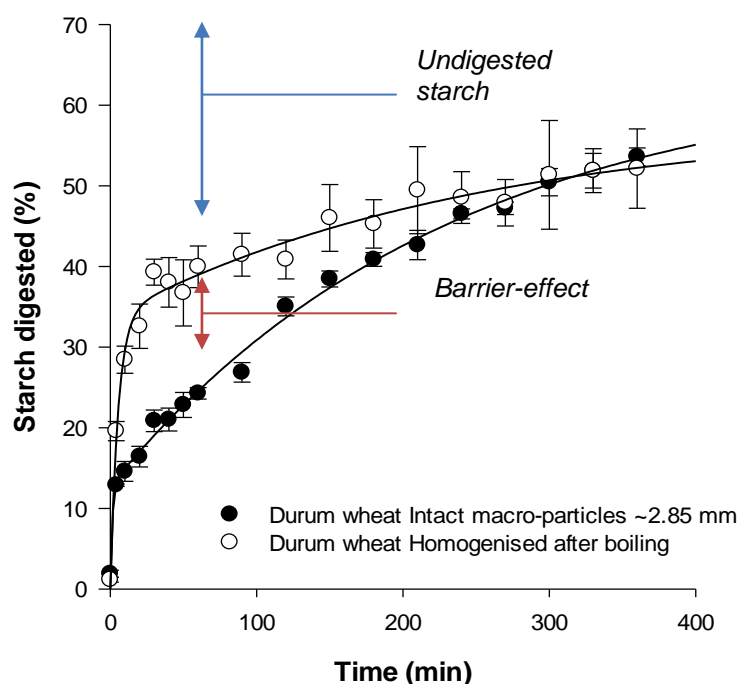


FIGURE 4.6: EFFECT OF HOMOGENISATION AFTER BOILING ON THE RATE AND EXTENT OF STARCH DIGESTION IN DURUM WHEAT. Values shown as mean of quadruplicates with error bars as SEM. 'Barrier-effect' is defined as an increase in digestibility resulting from homogenisation. 'Undigested starch' represents starch that is less susceptible to amylolysis, perhaps as a result of restricted swelling and incomplete gelatinisation.

After 6 h of digestion, approximately 50% of the starch had been digested, irrespective of structural integrity **Figure 4.6**. This is ~30% less than reported for hydrothermally processed flour (see **Figure 4.1**), in which the starch was not encapsulated by cell walls during processing. This suggests that starch that is encapsulated within cell walls during hydrothermal processing is less susceptible to amylolysis than 'free' starch, perhaps because the cell walls impose restrictions on starch gelatinisation. On the basis of the first-order digestibility curves fitted to the experimental data, both homogenised and intact materials would be expected to continue to be digested further, but at a slow rate.

Digestibility curves obtained for hydrothermally processed intact and homogenised macro-particles of chickpea are shown in **Figure 4.7**. Homogenisation nearly doubled the extent of starch digestion, but the treatment did not completely disrupt the chickpea tissue structure, and many intact cells containing encapsulated starch remained after homogenisation (**Figure 4.8A**). As a result, the barrier effect (indicated in **Figure 4.7**) is likely to be underestimated. Nevertheless, the micrograph of starch-filled, intact chickpea cells after 6 h of *in vitro* digestion (**Figure 4.8B**), indicates that chickpea cell walls are effective enzyme barriers, that limit the extent of starch digestion. Accordingly, the measured starch hydrolysis occurs with starch released by homogenisation or starch that is already available on the fractured surfaces of milled particles.

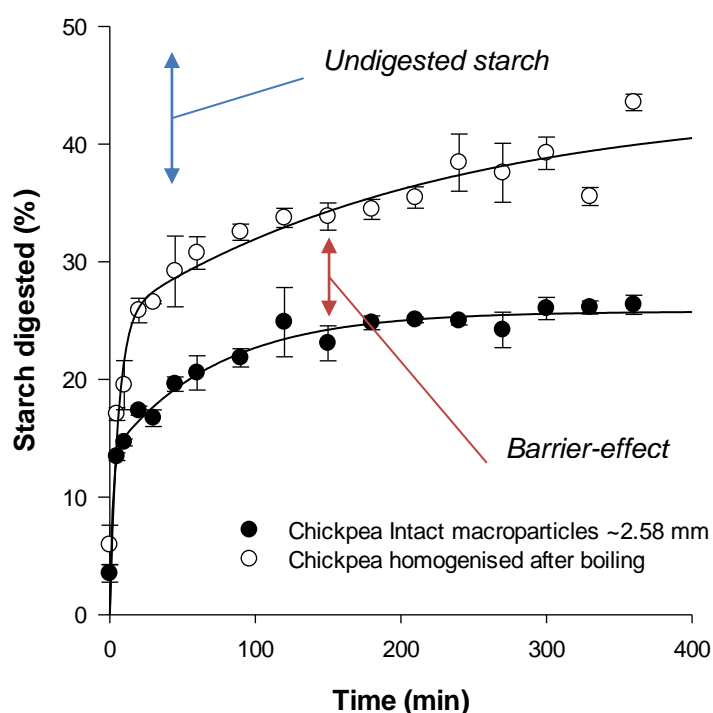


FIGURE 4.7: EFFECT OF HOMOGENISATION AFTER BOILING ON THE RATE AND EXTENT OF STARCH DIGESTION IN CHICKPEA. Values shown as mean of quadruplicates with error bars as SEM. 'Barrier-effect' is defined as an increase in digestibility resulting from homogenisation. 'Undigested starch' represents starch that is less susceptible to amylolysis, perhaps as a result of restricted swelling and incomplete gelatinisation.

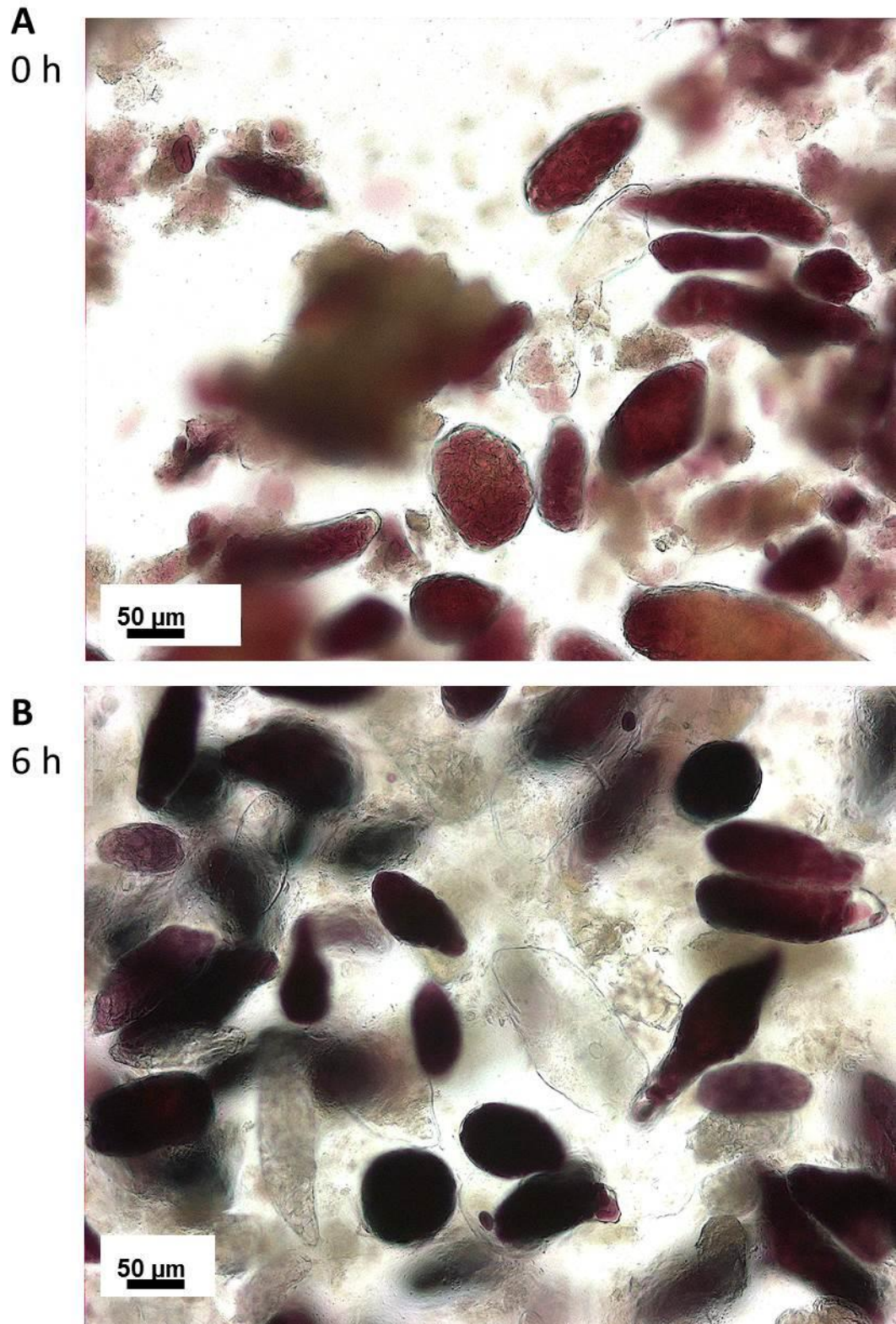


FIGURE 4.8: LIGHT MICROGRAPHS OF HOMOGENISED MACROPARTICLES OF HYDROTHERMALLY PROCESSED CHICKPEA BEFORE (A) AND AFTER 6 H *IN VITRO* DIGESTION (B). Stained with 2.5% Lugol's iodine solution. Homogenisation ruptured some, but not all, cells (A). After digestion (B), a large number of intact, starch containing cells remained.

4.3.4 EXTENT OF STARCH GELATINISATION

The effect of plant cell walls in restricting the gelatinisation of encapsulated starch was investigated quantitatively using DSC. Representative endotherms are shown for each milled size fraction (containing variable proportions of cell wall encapsulated starch) and 'pure' starch in **Figure 4.9**. Peaks of milled chickpea generally appeared narrower than those of durum wheat, although larger size fractions of durum wheat elicit notably broader peaks. This was reflected in the gelatinisation parameters (shown in **Table 4.2**).

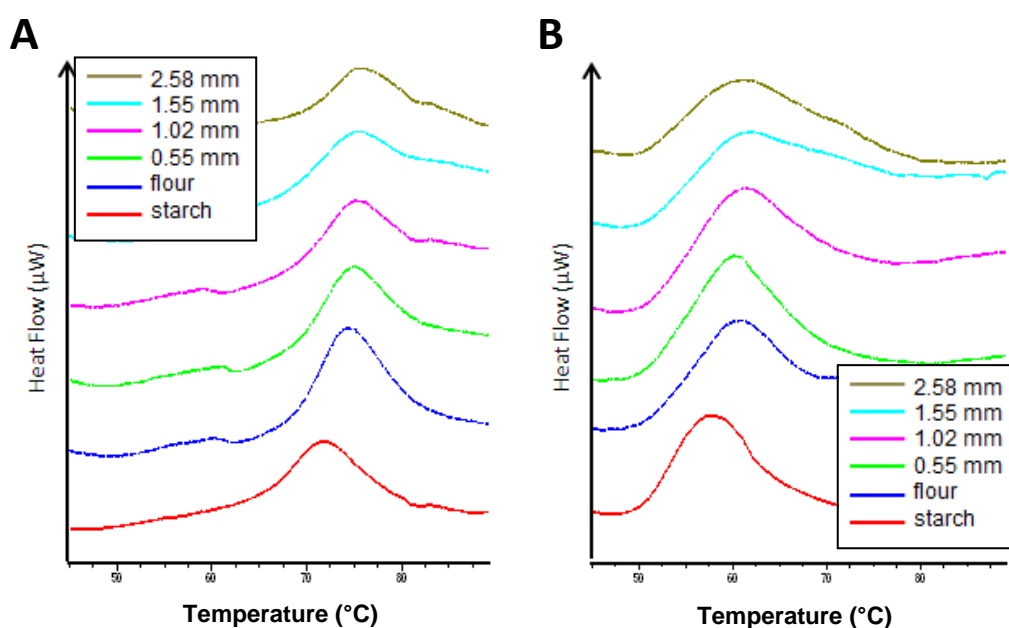


FIGURE 4.9: GELATINISATION ENDOTHERMS OF VARIOUS MILLED SIZE FRACTIONS OF CHICKPEA (A) AND DURUM WHEAT (B). Legend indicates median particle sizes, 'flour' refer to particles < 0.21 mm. Y-axis indicates heat flow (μW), but the plots are offset to order endotherms by particle size.

Chickpea starch gelatinised at a higher temperature ($T_p = 71.7\text{ }^\circ\text{C}$) than durum wheat starch ($T_p = 57.0\text{ }^\circ\text{C}$). However, the $\Delta_{gel}H_{sp}$ ($\sim 9.6\text{ J/g starch}$) and TEG values ($\sim 96\%$) of the two purified starches were not significantly different ($P > 0.05$, paired t-test) between the two botanical sources. The gelatinisation transition occurred at a higher temperature (2 - 3 °C) in flour than in purified starch, suggesting that the presence of cell wall fragments and/or other non-starch components may delay starch gelatinisation.

In the larger macro-particles, in which a proportion of starch is encapsulated by plant cell walls, the $\Delta_{gel}H$ and TEG values (**Table 4.2**) of chickpea materials were significantly lower than those of durum wheat, and were strongly influenced by particle size ($P < 0.001$, paired t-test, $r^2 = 0.91$), as shown in **Figure 4.10**. This suggests that the structural integrity (e.g., encapsulating cell walls or particle size) of chickpea tissue imposes some restrictions on starch gelatinisation. None of the gelatinisation parameters obtained for durum wheat materials in these DSC runs correlated with size.

TABLE 4.2: GELATINISATION PARAMETERS OF SIZE FRACTIONS OF CHICKPEA AND DURUM WHEAT

	Size (mm)	Ruptured Cells (%)	T_o (°C)	T_p (°C)	T_c (°C)	$\Delta_{gel}H$ (J/g starch)	TEG (%)
CHICKPEA	Starch	100	62.7 ± 0.3	71.7 ± 0.4	82.4 ± 0.4	9.6 ± 0.0	96.4 ± 0.3
	<0.21	100	67.0 ± 0.4	74.0 ± 0.0	84.0 ± 0.0	8.7 ± 0.4	87.2 ± 4.1
	0.55	80	66.7 ± 0.3	75.0 ± 0.0	83.0 ± 0.0	6.1 ± 0.4	61.2 ± 3.6
	1.02	43	67.0 ± 0.6	75.0 ± 0.0	83.0 ± 0.0	5.1 ± 0.3	50.7 ± 2.9
	1.55	28	68.3 ± 0.0	75.0 ± 0.5	83.0 ± 0.0	3.9 ± 0.2	38.6 ± 0.4
	2.58	17	68.3 ± 0.9	75.3 ± 0.3	82.3 ± 0.3	3.3 ± 0.3	33.2 ± 2.5
DURUM WHEAT	Starch	100	49.0 ± 0.0	57.0 ± 0.0	69.4 ± 0.9	9.5 ± 0.2	95.2 ± 2.3
	<0.21	100	51.4 ± 0.3	60.0 ± 0.0	72.0 ± 0.6	10.0 ± 0.3	100.4 ± 3.4
	0.55	100	49.1 ± 0.0	60.4 ± 0.3	73.1 ± 1.2	9.9 ± 0.4	98.5 ± 4.1
	1.02	69	50.8 ± 0.3	60.4 ± 0.3	72.8 ± 0.7	9.6 ± 0.2	96.2 ± 2.3
	1.55	45	50.4 ± 0.7	59.4 ± 0.7	71.7 ± 0.3	9.7 ± 0.1	97.3 ± 1.2
	2.58	27	50.7 ± 0.9	61.0 ± 0.6	75.4 ± 1.3	8.1 ± 0.5	81.2 ± 5.4

Values are mean of triplicate runs ± SEM. Onset (T_o), peak (T_p) and concluding (T_c) temperatures of gelatinisation are shown. $\Delta_{gel}H$ is the enthalpy change associated with the gelatinisation of 1 g of starch. TEG is the terminal extent of gelatinisation, expressed as% of starch.

A plot of TEG against particle size for both materials highlights the differences in gelatinisation behaviour of chickpea and durum wheat tissues heated under identical conditions (**Figure 4.10**). In milled chickpea materials, the extent of gelatinisation (TEG) increased with decreasing particle size (i.e. greater proportion of cells on the fractured surface), whereas in durum wheat, nearly all (> 95%) of the starch contained within milled macro-particles gelatinised, regardless of size, although the largest size fraction of durum wheat did have a lower TEG (81.2 ± 5.4% starch gelatinised). Birefringence was observed in chickpea materials recovered from the DSC, but not in wheat materials (**Figure 4.10**).

A large standard error was observed for the largest size fraction of durum wheat, and the DSC measurement was repeated several times due to difficulties in obtaining reproducible endotherms. Thus, there is some uncertainty about this value.

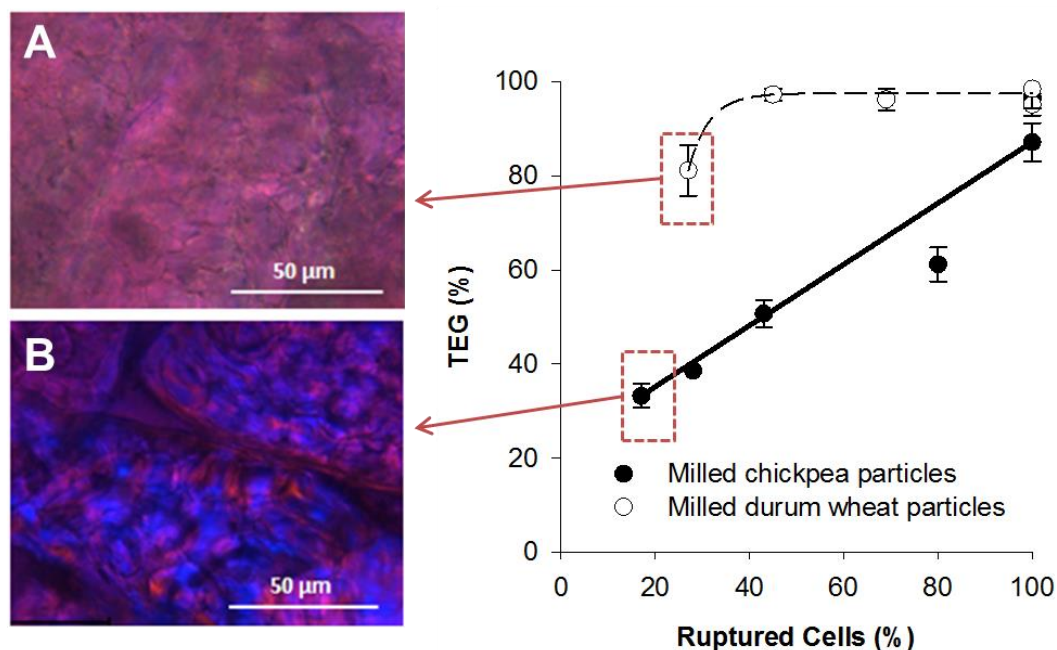


FIGURE 4.10: EFFECT OF CELL WALL ENCAPSULATION ON THE EXTENT OF STARCH GELATINISATION AS OBSERVED BY DSC FOR MILLED CHICKPEA AND DURUM WHEAT. *TEG*; terminal extent of gelatinisation, i.e. the proportion of starch which is gelatinised. Particle size is expressed in term of the proportion of ruptured cells in each fraction. Insets are micrographs of the largest particles recovered after DSC viewed under cross-polarised light; (A) no birefringence in wheat, (B) birefringence in chickpeas.

4.4 DISCUSSION

The structure-function studies presented in the chapter have provided new insights into the extent to which food structure (cellular integrity) influences starch digestion kinetics. The first digestibility experiments demonstrated that larger particles were digested at a reduced rate and/or to a lesser extent. This was not surprising, and has, for instance, been reported for hammer- and cryo- milled sorghum samples in a recent study (Mahasukhonthachat *et al.* 2010). Rather, the novel aspect of this digestibility data was that different kinetic effects were observed between chickpeas and durum wheat when the same size-manipulation was performed. This provided the first evidence that the effect of particle size on digestion kinetics was not simply a result of the available

surface area per volume, but also resulted from some inherent differences in the structural characteristics of these botanically different materials.

For durum wheat materials, increasing the particle size reduced the *rate* of starch digestion, but eventually, a similar extent of digestion was reached for all size-fractions. This implies that α -amylase is able to access the same amount of starch in all size fractions. When durum wheat cells were ruptured by homogenisation after boiling, this increased the rate of starch digestion. These results suggest that the durum wheat endosperm cell walls delay α -amylase access to starch, and thereby delay the release of starch hydrolysis products during digestion. This finding is consistent with an earlier study of digestion kinetics and enzyme ingress in other cereal sources, namely sorghum and barley (Al-Rabadi *et al.* 2009).

For chickpea materials, increasing particle size limited both the rate and also the *extent* of starch digestion: This will be demonstrated further in the next chapter. When freshly prepared isolated chickpea cells were incubated with α -amylase, the extent of starch digestion was remarkably low (less than 0.1%). Like the smallest milled particles, chickpea cell preparations also have a large surface area per volume and contain similar amounts of starch and fibre. The difference between cell preparations and flour was that in the cell preparations the vast majority of the starch was encapsulated by cell walls, whereas in the flour the cells were ruptured and the starch exposed. Hence, this supports previous suggestions that cellular integrity is a major determinant of starch bioaccessibility (Snow and O'Dea 1981, Würsch *et al.* 1986, Tovar *et al.* 1992).

These interpretations of digestibility data were consistent with the observations of cell wall permeability to FITC-amylase. Intact chickpea cells did not appear to be penetrated by FITC-amylase, and it seems that, under the experimental conditions of the present study, the chickpea cell walls act as physical barriers that hinder enzyme access. The experiment was less successful with durum wheat, however, because intact, isolated cells could not be obtained from durum wheat (*see Section 3.3.3 page*

108). Instead, the permeability experiment was attempted using milled durum wheat material. With this material; however, the FITC-amylase seemed to bind to starch exposed on fractured surfaces, and did not penetrate the material further during the 1 h period of observation. To overcome this problem, attempts were made at removing the surface starch using water at high pressure. SEM (*data not shown*) indicated that this technique worked very well for milled chickpeas, but for durum wheat particles the starch was more tightly embedded on the fractured surfaces and could not be removed. Although the methodology used in the permeability studies requires some further development to overcome some of these issues, these studies have revealed some very interesting differences between the cell wall properties of chickpeas and durum wheat.

Evidence was also presented in this chapter that supported the importance of the role played by cell walls in limiting the gelatinisation of intracellular starch: The extent of starch gelatinisation (TEG) correlated well with the estimated proportion of ruptured cells. This finding is compatible with the observations of birefringence on heated stage microscopy presented in *Chapter 3*, which showed that starch encapsulated within chickpea cells did not lose birefringence on heating (i.e. did not gelatinise). Hence, cell walls appear to limit the gelatinisation of encapsulated starch in chickpeas, and potentially other pulses (Fujimura and Kugimiya 1994, Würsch *et al.* 1986, Oyman 2007). The DSC runs on matched fractions of durum wheat, however, indicated that nearly all the starch underwent gelatinisation. This differs from a previous DSC experiment on milled rice (Marshall 1992), although this discrepancy is probably explained by the different nature of the botanical material used, and the different processing conditions that these materials were subjected to.

With regard to the possible factors that are responsible for hindering starch gelatinisation in these materials, a number of elements need to be considered. Studies on purified starches have demonstrated that the extent of gelatinisation can be

manipulated by controlling water availability, heating conditions, and the presence of non-starch components during processing (Bogracheva *et al.* 2002, Perry and Donald 2002, Roder *et al.* 2009, Fukuoka *et al.* 2002). During the DSC runs, durum wheat starch gelatinised at a lower temperature than chickpea starch, but considering the slow heating rate and modern instrumentation used, it is unlikely that heat transfer was the limiting factor in starch gelatinisation. The slightly higher gelatinisation onset observed for milled materials compared to the purified starches could be explained by the presence of starch-granule associated proteins and lipids (SGAP and SGAL) as well as other components of the (intra)cellular matrix (Debet and Gidley 2006, Tester and Morrison 1990). However, within each plant species, these non-starch components, which are likely to be present in all milled fractions, do not account for the particle size dependant restrictions on starch gelatinisation in chickpea samples.

Another explanation is that the 'soaking' time was sufficient to hydrate starch in wheat, but not chickpeas. For food preparation purposes, durum wheat semolina (similar to the smaller fractions of milled endosperm used in this experiment) is normally boiled for 20 min, whereas whole dry chickpeas require 1-2 h. Whole chickpeas are also often pre-soaked for 4-12 h to reduce subsequent cooking time (Clemente *et al.* 1998). The time required to cook chickpeas depends on a range of factors, especially the permeability and thickness of the seed coat, which limits the rate of cotyledon hydration (Sayar *et al.* 2001). Bearing in mind that the chickpeas used in these experiments were de-hulled and milled to a smaller particle size (<3.2 mm) than whole peas (>5 mm), the 2 h pre-soak incorporated in the DSC run was expected to provide sufficient time for hydration. Another discrepancy is that, in the heated stage experiments on *isolated chickpea cells* (presented in Chapter 3, Section 3.3.8, page 105), which were freshly prepared and had more time to hydrate, intracellular starch retained birefringent properties after processing. In these cells, the distance for water ingress is considerably less (i.e. a single cell wall barrier) than in the milled macro-particles (i.e.,

several cell layers), and therefore limitations on water availability seemed less likely with this material.

Of course, a longer hydration time may not necessarily lead to an even distribution of water within a heterogeneous plant tissue. This could be investigated further, for instance using NMR to study the distribution of water in tissue during hydration (Stapley *et al.* 1997). An alternative, and perhaps more likely hypothesis is that the cell walls of chickpeas impose *spatial* restrictions on intracellular starch swelling (as mentioned in the previous chapter), and thereby prevent the water ingress required for starch gelatinisation. Accordingly, differences between chickpeas and durum wheat may be explained by differences in cell wall resilience or starch swelling power. For instance, durum wheat endosperm cell walls are considerably thinner, and perhaps less resilient than chickpea walls. Durum wheat starch also has a lower swelling power **Table 3.4** and may therefore require less space to hydrate than chickpea starch.

In order to study the structure and properties of the intracellular starch without the complicating effects of the cell walls, numerous attempts were made at creating new experimental materials, e.g., 'leaky cells' or 'protoplasts'. Preliminary attempts were made at manipulating cell wall permeability by subjecting cells to a range of treatments which have been suggested by various mechanisms to influence cell wall porosity. None of these treatments were found to increase chickpea cell wall permeability, and the idea of obtaining 'leaky cells' was abandoned, yet it was still interesting to observe the remarkably resilient behaviour of chickpeas

Subsequently, driselase was identified as a treatment capable of digesting the chickpea cell walls, leaving the intracellular material, 'protoplast', exposed. However, this technique was not satisfactory for the preparation of material for enzyme assays for a number of reasons; Firstly, some starch retrogradation probably occurred during the long preparation procedure (~19 h total), and so the protoplasts were not truly representative of intracellular starch in freshly prepared cells. Secondly, the protoplasts

obtained were very fragile, and difficult to manipulate. Large variations in the extent of cell wall degradation and protoplast integrity were also observed between preparations and between cells within the same batch. Thirdly, the driselase extract contained enzymes and enzyme inhibitors with the potential to interfere with measurements of starch digestibility by porcine pancreatic α -amylase. The idea of using protoplasts as experimental materials was therefore abandoned at this stage. Nevertheless, the described protocol for preparation of protoplasts provides a foundation for future work.

Overall, identifying the predominant mechanism by which cell walls influence bioaccessibility, was difficult. It seems that plant cell walls may restrict starch bioaccessibility both by acting as physical barriers to digestive enzymes, and also by restricting the gelatinisation of intracellular starch. The mechanism that will have the largest impact on starch digestion kinetics appears to depend on the processing conditions used. Certainly, if the cell wall barrier is not permeable to digestive enzymes, the digestibility of the starch encapsulated within cells becomes irrelevant. Therefore, the permeability of the cell wall barrier merits further investigation. Irrespective of mechanism, these experiments clearly showed that the *physical encapsulation* of starch by cell walls significantly limits starch bioaccessibility. This will be described further in subsequent chapters.

4.5 CONCLUSIONS

Cell walls that physically encapsulate starch imposed major restrictions on the rate and/or extent of starch bioaccessibility. The effects observed may be attributed to cell walls acting as physical barriers to digestive enzymes, and also to the limited gelatinisation of cell wall encapsulated starch during hydrothermal processing. Starch encapsulated within chickpea cells escaped digestion, whereas starch encapsulated within durum wheat cells was digested at a slower rate. Overall, the results presented in this chapter provide clear evidence for the role of cell wall encapsulation in limiting starch bioaccessibility.

CHAPTER 5

A PREDICTIVE MODEL OF STARCH DIGESTION

5.1 INTRODUCTION

In the previous chapter (*Chapter 4*), the encapsulation of starch within plant cell walls was reported to reduce significantly the rate and extent of starch digestion, with likely consequences for post-prandial glycaemia. Although *in vitro* studies provide a popular and cost-effective means of predicting postprandial outcomes (e.g., glycaemic responses), current methodologies (including those used in *Chapter 4*) generally require the rate and extent of starch digestion to be established by running assays to completion (Woolnough *et al.* 2008). This approach is tedious, and can introduce inaccuracies due to product inhibition and enzyme inactivation (Butterworth *et al.* 2012). A new and improved approach to studying *in vitro* starch digestibility is therefore needed. This chapter presents work associated with the development and application of a new *in silico* model of starch digestion.

Mathematical modelling is a valuable research tool for studying nutrient bioaccessibility and digestion. Recognising the important role of food structure in influencing bioaccessibility, researchers are developing 'geometric' models which use theoretical principles of geometry to predict nutrient release (Monro *et al.* 2011, Ellis *et al.* 2007). A very simplistic geometric model was described in *Chapter 3, Section 3.2.2*, but there are several other geometric models that are more elaborate and take into account finer structural details such as interstitial spaces and particle erosion during digestion. Such models therefore provide a better representation of food structure. The disadvantage of the geometric approach, however, is that these models are entirely specific: They represent the properties of one food material (e.g., almonds) when processed in a particular way, and may not be applicable, therefore, to the wide range of food materials consumed in a normal diet.

An alternative approach is to determine the digestibility of starch in various food products, and use this to predict postprandial outcomes (Woolnough *et al.* 2008). One popular method is to classify starch-sources into so-called rapidly and slowly digested

fractions (Englyst *et al.* 1992). This method, referred to as the 'Englyst-system', involves measuring the extent of digestion with amylase at arbitrary time points: starch which is digested within 20 min is described as 'rapidly digested starch' (RDS), whereas starch digested between 20 and 120 min (SDS) is 'slowly digested starch'. There are however, some fundamental issues with this system. Since it is already known that starch amylolysis follows a (pseudo) first-order kinetic reaction (Goñi *et al.* 1997), the arbitrary division of starch into RDS and SDS on the basis of a slowing in amylolysis rate as the reaction proceeds is unsound. The rate naturally becomes slower because the concentration of substrate falls continuously as the reaction proceeds (Butterworth *et al.* 2012). Hence, the Englyst system appears to be based on a misunderstanding of starch digestion kinetics, and is therefore of questionable value for mechanistic studies.

Instead, a more rigorous means of identifying starch fractions digested at different rates may be adopted from the enzyme-kinetic literature. Starch amylolysis is a first-order process (Goñi *et al.* 1997) and has already been studied using Michaelis-Menten kinetics (Slaughter *et al.* 2001, Tahir *et al.* 2010, Dona *et al.* 2010). The Michaelis-Menten approach provides useful quantitative information about starch hydrolysis, but this approach is not suitable for application to heterogeneous plant materials where the substrate availability is not known. A number of workers have fitted first-order curves to starch digestibility data obtained from heterogeneous food materials to estimate the extent of starch digestion (Goñi *et al.* 1997, Al-Rabadi *et al.* 2009, Mahasukhonthachat *et al.* 2010). However, this approach requires relatively lengthy periods of digestion with α -amylase and is associated with inaccuracies because of loss of enzyme activity and product inhibition. Butterworth *et al.* recently described the novel application of Logarithm of Slope (LOS) analysis to study starch amylolysis (Butterworth *et al.* 2012, Poulsen *et al.* 2003). LOS analysis involves plotting the 'logarithm of slope' of first-order digestibility data (i.e. product formation over time) to obtain the rate constant, k , and end-point product concentration, C_{∞} (Butterworth *et al.* 2012, Poulsen *et al.* 2003).

LOS plots have a number of attributes which make them particularly well suited for mechanistic studies of starch hydrolysis. Firstly, because digestibility plots are very sensitive to changes in slope (i.e. digestibility rate), taking the logarithm of the slope of digestibility data can reveal changes in the digestibility constant as the reaction proceeds. Secondly, LOS plots enable the endpoint product concentration, and therefore the total amount of digestible starch, to be predicted from initial digestibility data without the need for prolonged assays in which the endpoint values have to be assumed. Thirdly, the rate constant, k , is independent of substrate concentration, and can therefore be used for universal comparisons of digestibility, provided that the amount of enzyme used is known. Overall, this approach provides an effective means of determining values of parameters in the first-order equation using only data collected from the *early stages* of digestion, and therefore has potential to form the basis of a novel predictive model of starch amylolysis.

LOS analysis has previously been applied to digestibility curves of purified starches and homogenised foods (Butterworth *et al.* 2012, Goñi *et al.* 1997). However, it has not yet been applied to more complex food structures, e.g., containing starch encapsulated by cell walls, that are likely to be present in the small intestine post-mastication (Noah *et al.* 1998, Livesey *et al.* 1995). The application of LOS plots to digestibility data obtained from milled chickpeas and durum wheat, i.e., containing variable proportions of intact cells, may provide a valuable means of elucidating the mechanisms by which cell walls influence amylolysis.

5.1.1 OBJECTIVES

- a) Apply LOS analysis to digestibility data obtained from heterogeneous starch-rich plant materials
- b) Use LOS analysis to identify and quantify nutritionally important starch fractions present in these materials

- c) Develop a predictive model of starch digestion in which the value of all parameters may be estimated from LOS plots.
- d) Evaluate the performance of this model in predicting the rate and extent of release of starch hydrolysis products from heterogeneous food materials (i.e. plant tissues)
- e) Deduce mechanisms of starch digestion in the materials studied and make predictions about the post-prandial glycaemic response for investigation in subsequent chapters.

5.2 METHODS

5.2.1 PLANT MATERIALS

Milled materials and starch were obtained from chickpeas and durum wheat as described in *Section 2.1, page 71*. The proportion of intact cells in each of the milled fractions (*Table 4.1, page 129*) was estimated using the Geometric Model (see *Chapter 3, Section 3.2.2, page 102*). The total starch content (means \pm SD) of milled chickpea (de-hulled) and durum wheat (de-branned) was 45 ± 1.07 and 71 ± 3.1 , respectively, expressed on a g/100 g dry weight basis.

5.2.2 DIGESTIBILITY ASSAYS

Digestibility assays were performed as described in *Section 2.7, page 96*. These experiments were similar to those described in *Section 4.2.2.1*, but the assay was run for 60 min of digestion only, during which a large number of aliquots were collected to obtain sufficient information for application of the LOS method.

In brief; milled materials and starches were weighed out into tubes, so that each tube contained 117 mg of starch. Next, 30 mL of phosphate buffered saline (PBS) was added, and the tubes were hydrothermally processed in a boiling water bath for 85 min with intermittent stirring. Once processed, the suspensions were equilibrated in a water bath at 37 °C for 20 min, and then incubated with 8 nM α -amylase (in PBS, pH 7.4) on

a rotary mixer at 37 °C. Aliquots of the digestion mixture were taken at predetermined time points for subsequent quantification of starch hydrolysis products by the Prussian blue assay (*Section 2.3.4.3*). For improved sampling (compared to *Chapter 4*), the tubes were taken out of the rotary mixer 20 s prior to aliquot collection. This allowed larger particles to settle and improved sampling precision and reproducibility.

To test for endogenous reducing sugars or enzyme activity, the addition of amylase was omitted from control assays. The amount of reducing sugar freshly produced in these controls was found to be negligible; subsequently, endogenous sugar was accounted for by subtraction of blank values taken for each assay prior to enzyme addition.

5.2.3 THEORY OF LOS ANALYSIS

The LOS procedure and mathematical basis has been described previously (Butterworth *et al.* 2012, Poulsen *et al.* 2003), but a brief overview of key principles is provided in this section.

It is well established that starch amylolysis follows a first-order equation (**Equation 5.1**) (Goñi *et al.* 1997).

$$C_t = C_\infty (1 - e^{-kt})$$

EQUATION 5.1: FIRST-ORDER EQUATION In which C_t is the concentration of product at a given time (t), C_∞ is the concentration of product at the end of the reaction, and k is the digestibility rate constant

The linear form of the equation can be used to plot starch digestibility data, but requires accurate values of k and C_∞ to be known. Many workers attempt to obtain these values by running *in vitro* digestibility experiments until the reaction end-point is reached. This process often requires assaying over several hours, and can give inaccurate values. This problem may be overcome by expressing the linear equation in a different form, such that the value of k and C_∞ can be readily obtained from Logarithm of Slope (LOS) plots.

Firstly, differentiation of **Equation 5.1** gives an equation which represents the slope of a first order digestibility plot (**Equation 5.2**).

$$\frac{dC}{dt} = C_{\infty} k e^{-kt}$$

EQUATION 5.2: DERIVED FIRST-ORDER EQUATION

When expressed in logarithmic form (**Equation 5.3**), this gives a linear plot where the slope, $-k$, is equal to the pseudo first-order rate constant, and the value of C_{∞} may be calculated from the y-intercept:

$$\ln\left(\frac{dC}{dt}\right) = \ln(C_{\infty}k) - kt$$

EQUATION 5.3: LOGARITHMIC FORM OF THE DIFFERENTIATED FIRST-ORDER EQUATION

Values of the variables in equation (**Equation 5.3**), may be obtained graphically by plotting the change in the slope between adjacent data points of a digestibility curve against the time interval to obtain a LOS plot, for which linear regression enables the slope and y-intercept to be estimated (**Figure 5.1**)

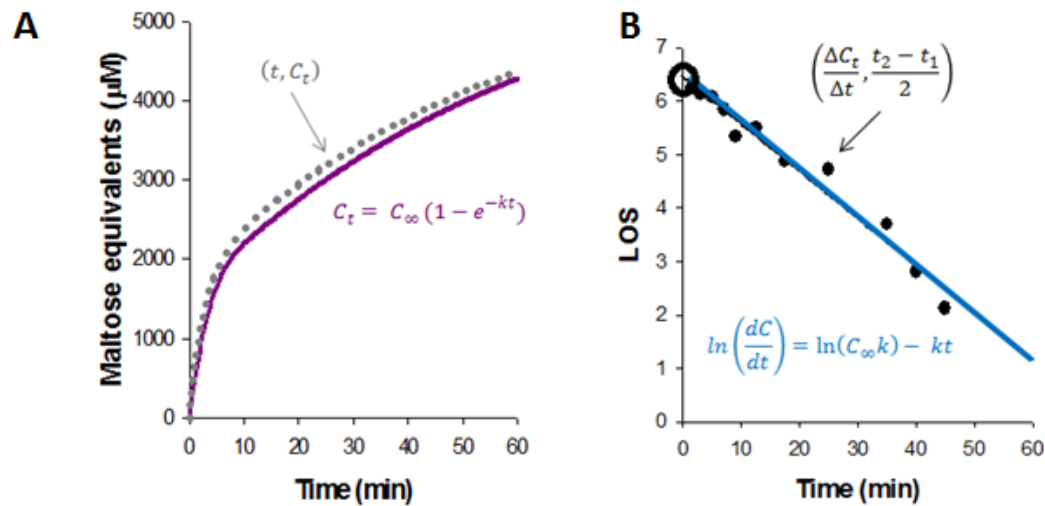


FIGURE 5.1: SCHEMATIC SHOWING HOW LOS PLOTS (B) ARE OBTAINED FROM DIGESTIBILITY PLOTS (A). The Cartesian co-ordinates (x, y) and regression equations are shown for each plot. C_t is the concentration of product (i.e. maltose) at a specific time point, t . The circle highlights the y-intercept, from which C_{∞} can be obtained. The rate constant, k , is obtained from the slope.

This LOS method has previously provided very good estimates of the total extent of digestion in gelatinised starches and homogenised foods where starch digestion occurs by a single-phase process (Butterworth *et al.* 2012). However, in foods containing starch fractions that are digested at different rates, discontinuities in the LOS plots signify that digestion occurs in two or more phases, in which the slope of each distinct linear phase provides a digestibility constant, denoted $k_1, k_2 \dots$ etc. Hence, starch digestion in complex plant foods may be described by more than one k -value. For the materials examined here, these two processes were found (by residual analysis, to represent *consecutive*, rather than *simultaneous*, first-order reactions. This implies that the rapid phase is considered to have become negligible by the time represented by the intersection of the different phases in the LOS plot, i.e. where the slower phase commences (**Equation 5.4**).

Some modification of the first-order equation was required to accommodate for the two consecutive digestion phases (see **Equation 5.4**). With the use of time identifiers, the total product formed at the end of the first phase (C_{int}) must be added to the product formed during the second phase to represent total starch digestion. The value of C_{int} may be determined computationally from **Equation 5.4**, letting $t = t_{int}$ using substituted values for $C_{1\infty}$ and k_1 .

$$C(t) = \begin{cases} C_{1\infty}(1 - e^{-k_1 t}), & \text{if } t \leq t_{int} \\ C_{int} + C_{2\infty}(1 - e^{-k_2 \times (t - t_{int})}), & \text{if } t \geq t_{int} \end{cases}$$

EQUATION 5.4: TWO-PHASE EQUATION. When the LOS plot consists of a single linear phase, t_{int} does not exist, and only the first part of this equation applies.

5.2.4 MATHEMATICAL MODEL

The validity of using the LOS method to predict the rate and extent of starch digestion was examined by re-inserting the LOS plot estimates for parameters ($C_{1\infty}, k_1, C_{2\infty}, k_2, C_{int}$ and t_{int}) into **Equation 5.1** or **Equation 5.4** depending on whether one or two distinct rates were observed in the LOS plot, respectively. This enabled a ‘model-fit’ to

be computed. For comparison purposes, a 'best-fit' to experimental data was also obtained using iterative Maximum Likelihood Estimation, MLE, of the parameters ($C_{1\infty}$, k_1 , $C_{2\infty}$, k_2 , C_{int} and t_{int}). Hence, the '**model-fit**' refers to curves computed using LOS-estimated values for parameters in the first-order equation, whereas the '**best-fit**' refers to curves obtained by an iterative process with no constraints on the values of the parameters in the same equation.

This curve-fitting procedure was performed on triplicate values obtained for experimental data from 10 different particle sizes of durum wheat and chickpea tissue (including the purified starch equivalent). Predicted and residual values, coefficients of determination (R^2), and standard error of the estimate (SEE) were obtained as part of the curve-fitting procedure and are indicators of 'goodness-of-fit'.

Residual values represent the distance between the predicted and experimental data points, and were used to evaluate the performance of the model in accurately predicting the concentration of product over time. Experimental outliers (for instance, values outside 2 standard deviations of the mean), were not excluded from the regression or residual analysis.

5.2.5 HYDROLYSIS INDEX

The extent of starch digestion in the initial 90 min of digestion has previously been reported to provide the best correlation with the glycaemic index (Goñi *et al.* 1997). Conventionally, the hydrolysis index is obtained from the area under an experimentally obtained digestibility curve (Granfeldt *et al.* 1992). Here, the area under model-computed *predictive* digestibility curves was calculated using the area under curve (AUC) macro in SigmaPlot to obtain the hydrolysis index, denoted HI_{AUC90} . Values obtained using this method were compared with values obtained algebraically (denoted $HI_C(t=90)$), in which the proportion of starch digested at 90 min was obtained by substituting $t = 90$ min into **Equation 5.1** or **Equation 5.4** and solving for $C_{t=90}$.

5.2.6 STATISTICAL AND GRAPHICAL ANALYSIS

All data are presented as mean values \pm SEM, unless otherwise specified. Repeated Measures Analysis of Variance (ANOVA) was used to compare experimentally obtained digestibility curves, with time as a 'within-sample' factor, and particle size and botanical source as 'between-sample' factors. Tukey's *post-hoc* analysis was carried out to identify homogenous subsets among particle sizes. Statistically significant differences were accepted at $P < 0.05$. The analysis was performed in IBM SPSS Statistics 20.0 (© IBM Corp. 2011). All model-fitting and regression analysis was performed in SigmaPlot 12.0 (© Systat software 2011), by entering **Equation 5.1** or **Equation 5.4** as user-defined equations, in which parameters were either defined based on LOS estimates, or, for best-fit regression, allowed to vary.

5.3 RESULTS

5.3.1 EXPERIMENTAL DIGESTIBILITY CURVES

Experimentally obtained digestibility curves obtained for the 10 fractions of different sizes are shown for hydrothermally processed chickpea and durum wheat in **Figure 5.2**. Digestibility curves of starches and flours were not significantly different. A clear particle size-dependant effect was observed; with large differences in the extent of digestion at 60 min. Particle size had a greater effect on the extent of starch digestion in chickpea materials than in durum wheat.

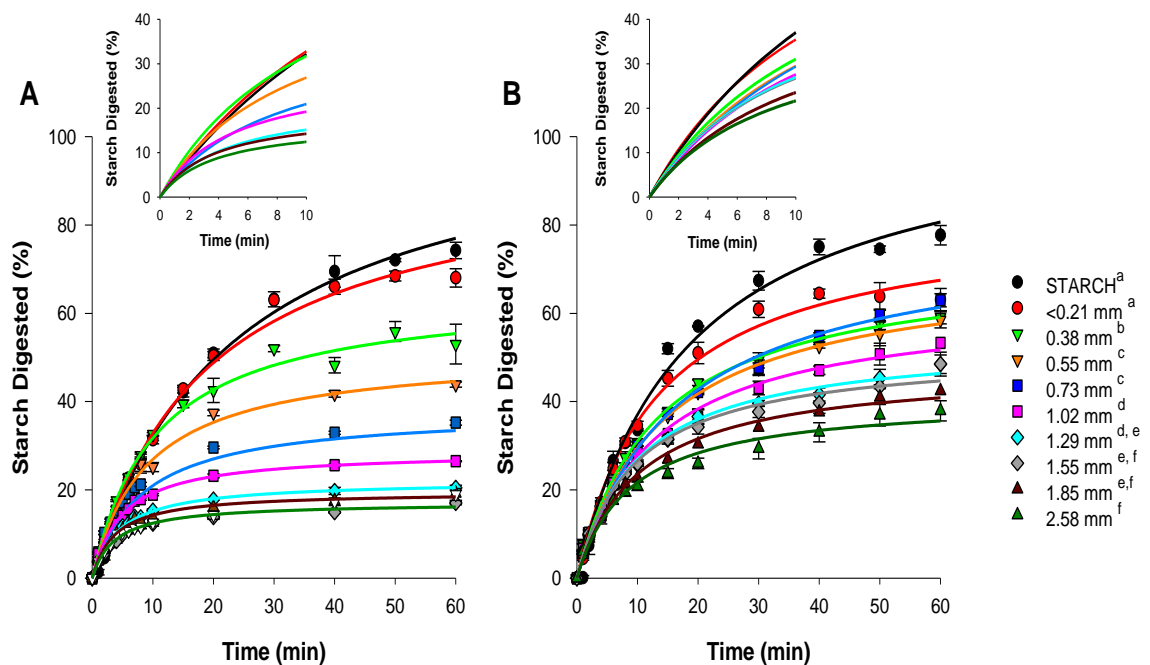


FIGURE 5.2: DIGESTIBILITY CURVES OBTAINED FOR MILLED SIZE FRACTIONS AND STARCHES OF HYDROTHERMALLY PROCESSED CHICKPEA (LEFT) AND DURUM WHEAT (RIGHT). Values are mean of triplicates \pm SEM. Regression line shows best fit to experimental data. Inserts show data from initial 10 min. Legend applies to all panels and different superscript letters indicate significant differences ($P < 0.05$) between curves for chickpea and durum wheat, as determined by Tukey's *post-hoc* analysis. Particle size is defined on the basis of material retention in sieves of known aperture.

5.3.2 LOS PLOTS

LOS plots obtained for starches and flours are shown in **Figure 5.3**. These linear plots ($r^2 > 0.9$) indicate that starch digestion occurs by a single-phase process and may be described by **Equation 5.1** in which the values of k and C_∞ are estimated from the slope and y-intercept of the LOS plot, respectively.

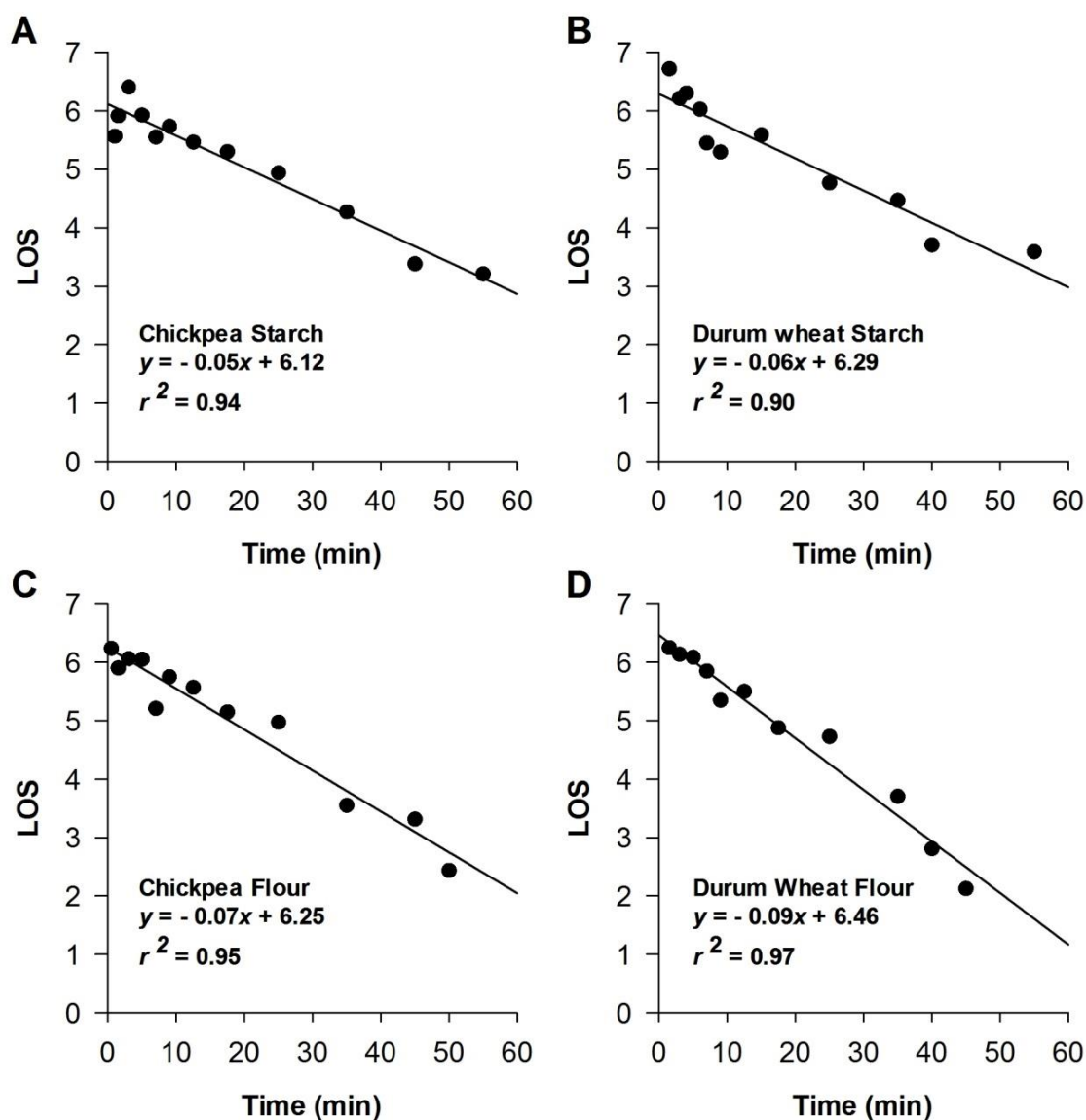


FIGURE 5.3: LOS PLOTS OBTAINED FOR HYDROTHERMALLY PROCESSED STARCHES AND FLOURS REVEAL A SINGLE PHASE OF DIGESTION. (A) Chickpea starch; (B) durum wheat starch; (C) chickpea flour; (D) durum wheat flour. Flour refers to milled particles with diameter < 0.21 mm, and contains no intact cells.

In contrast, LOS plots of digestibility data obtained for larger size fractions revealed two-linear phases, as shown for selected sizes in **Figure 5.4**. Each digestion phase is characterised by a C_{∞} and k - value, in which k is obtained from the slope of each linear phase, $C_{1\infty}$ is obtained from the y-intercept, and $C_{2\infty}$ was obtained from the intersection between the two linear phases. Biphasic LOS plots were observed for all chickpea fractions > 0.50 mm, whereas only the largest (>1.18 mm) particles of durum wheat displayed this behaviour. The values of parameters for **Equation 5.1** or **Equation 5.4** estimated from the LOS plots are shown in **Table 5.1**. The rate constant of the first reaction, k_1 , was always greater than the second. For chickpeas, the value of k_1 increased with particle size, whereas for durum wheat, the value of k_1 did not appear to be influenced by size. The rate constant of the second phase, k_2 , was similar for all milled fractions ($k_2 = 0.06 \pm 0.006 \text{ min}^{-1}$ for chickpea and $0.05 \pm 0.006 \text{ min}^{-1}$ for durum wheat), and is comparable to the single rate constant obtained where digestion occurs as a single-phase process, i.e. starch, flour and smaller size-fractions (**Figure 5.3**).

The intersection represents the point at which the slower phase becomes the predominant reaction, and seemed to occur after 7 to 15 min of digestion, with no obvious trend with particle size. The total extent of digestion ('*Total C_{∞}* ', which is the sum of $C_{1\infty}$ and $C_{2\infty}$) was reduced by increasing particle size. The largest reductions were observed for chickpea materials, where *Total C_{∞}* decreased by up to 49% (i.e. from flour to larger macro-particles), whereas in durum wheat a 14% reduction was observed.

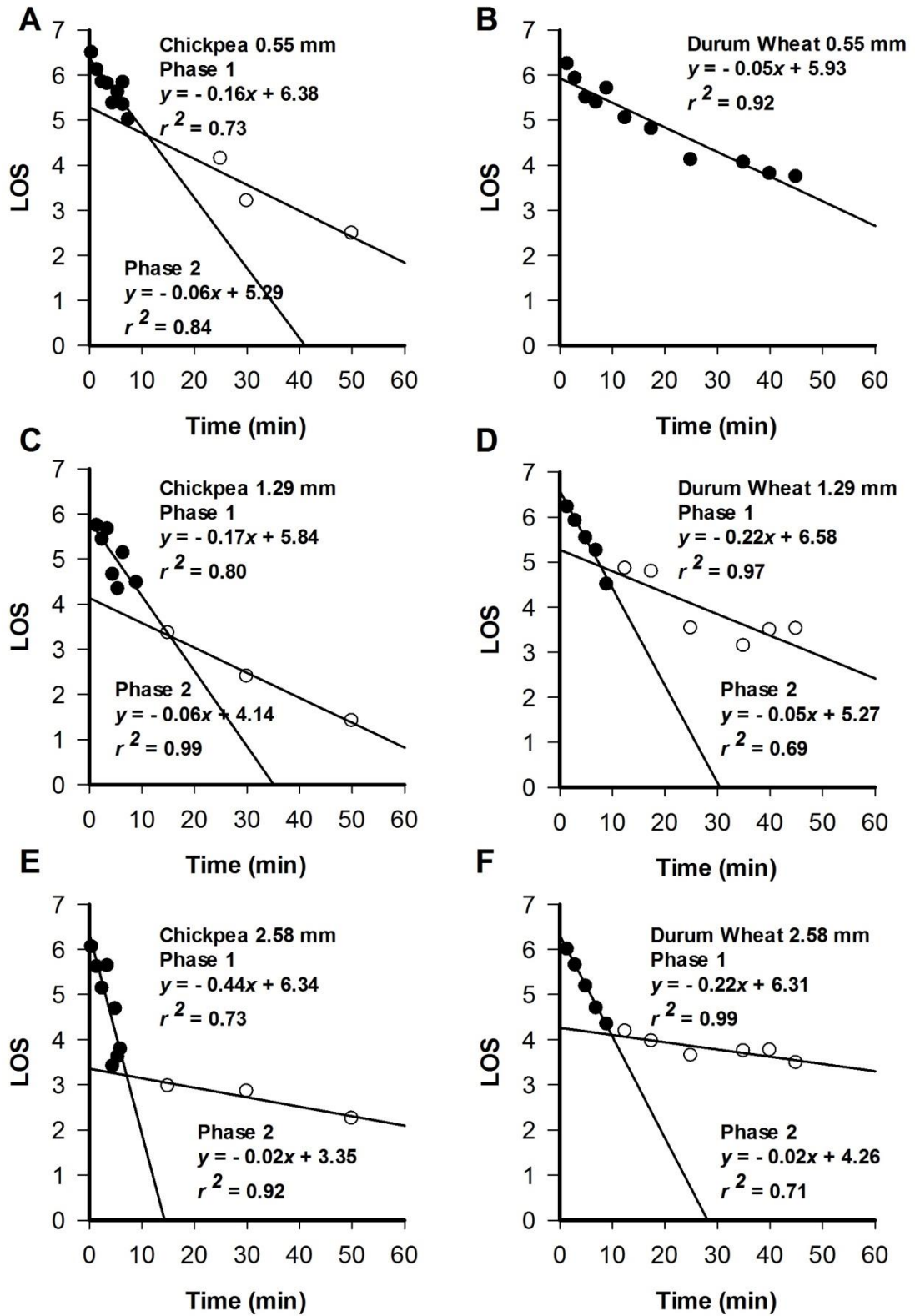


FIGURE 5.4: LOS PLOTS OBTAINED FOR VARIOUS HYDROTHERMALLY PROCESSED MILLED FRACTIONS SHOWING ONE OR MORE PHASES OF DIGESTION. (A) Chickpea 0.55 mm; (B) durum wheat 0.55 mm; (C) chickpea 1.29 mm; (D) durum wheat 1.29 mm; (E) chickpea 2.58 mm; (F) durum wheat 2.58 mm.

TABLE 5.1: VALUES OF VARIABLES ESTIMATED FROM LOS ANALYSIS FOR ALL SIZE FRACTIONS OF HYDROTHERMALLY PROCESSED CHICKPEA AND DURUM WHEAT

CHICKPEA							
Size (mm)	RAPID PHASE		SINGLE OR SLOWER PHASE		INTERSECTION		TOTAL
	$C_{1\infty}$ (%)	k_1 (min ⁻¹)	$C_{2\infty}$ (%)	k_2 (min ⁻¹)	t_{int} (min)	C_{int} (%)	C_{∞} (%)
Starch	-	-	73.5*	0.05*	-	-	73.5*
0.11	-	-	64.7*	0.07*	-	-	64.7*
0.38	-	-	51.7*	0.09*	-	-	51.7*
0.55	33.2	0.16	15.9	0.06	11.1	27.3	49.1
0.73	27.4	0.16	12.2	0.05	12.4	23.7	39.6
1.02	19.5	0.26	9.0	0.06	8.5	17.4	28.5
1.29	18.2	0.17	4.3	0.06	15.3	16.8	22.5
1.55	12.4	0.32	3.3	0.07	9.2	11.7	15.7
1.85	13.6	0.32	6.0	0.08	6.8	12.1	19.5
2.58	11.3	0.44	10.3	0.02	7.1	10.8	21.6

DURUM WHEAT							
Size (mm)	RAPID PHASE		SINGLE OR SLOWER PHASE		INTERSECTION		TOTAL
	$C_{1\infty}$ (%)	k_1 (min ⁻¹)	$C_{2\infty}$ (%)	k_2 (min ⁻¹)	t_{int} (min)	C_{int} (%)	C_{∞} (%)
Starch	-	-	78.9*	0.06*	-	-	78.9
0.11	-	-	63.7*	0.09*	-	-	63.7
0.38	-	-	58.9*	0.05*	-	-	58.9
0.55	-	-	60.7*	0.05*	-	-	60.7
0.73	-	-	59.5*	0.05*	-	-	59.5
1.02	-	-	52.0*	0.05*	-	-	52.0
1.29	29.4	0.22	24.9	0.05	7.8	23.9	54.3
1.55	30.0	0.17	21.5	0.04	11.2	25.5	51.5
1.85	23.8	0.16	25.7	0.03	9.5	18.8	49.5
2.58	21.6	0.22	33.0	0.02	9.8	19.2	54.6

Values are estimated from LOS plots with one- or two- phases

* Indicates that digestion occurred by a single-phase process, and that no rapid phase was observed.

C_{∞} is the extent of starch digestion for each digestive phase. *Total* C_{∞} is the sum of $C_{1\infty}$ and $C_{2\infty}$ and represents the total extent of starch digestion. k is the rate constant of each phase. C_{int} is the extent of starch digestion at the time of intersection, t_{int} .

The estimated values for $C_{1\infty}$ and $C_{2\infty}$ provide an indication of the contribution of each digestion phase to the total starch breakdown, and are represented graphically in **Figure 5.5**. In durum wheat materials, the contribution of each phase to total starch breakdown was more or less equal, whereas in chickpea size fractions, the rapid phase, where it exists, contributed considerably more.

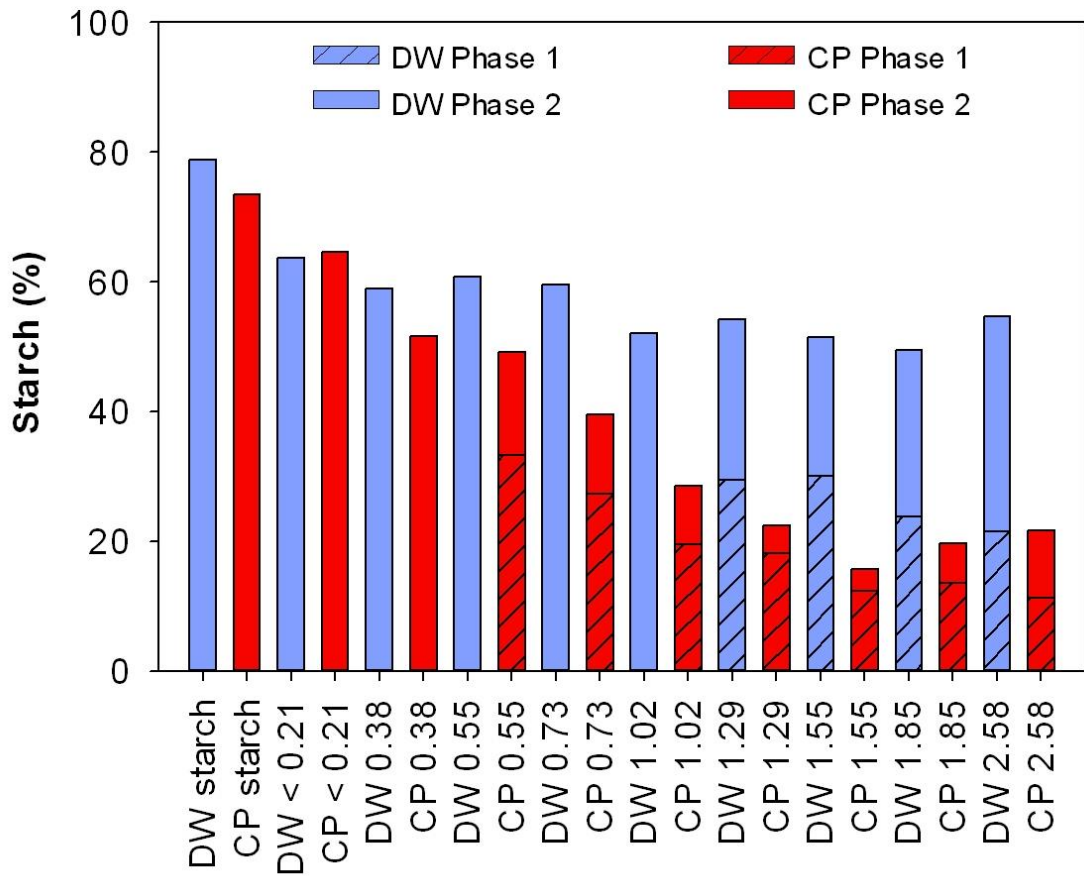


FIGURE 5.5: CONTRIBUTION OF EACH REACTION PHASE TO TOTAL STARCH BREAKDOWN FOR VARIOUS SIZE FRACTIONS OF CHICKPEA (CP) AND DURUM WHEAT (DW). Contributions are expressed as a percentage of total starch content, and are based on estimated values for C_{∞} , where digestion occurs as a single phase, or from $C_{1\infty}$ and $C_{2\infty}$ for two-phase reactions. Single phase reactions are coloured as phase 2.

5.3.3 RESIDUAL ANALYSIS OF MODEL PERFORMANCE

Residual plots were used to test for systematic deviations in model performance. Time and size-resolved residual plots are shown in **Figure 5.6**. No correlation was evident between the size of the residual error and digestion time and particle size. This indicated that the model performance was independent of particle size or digestion time.

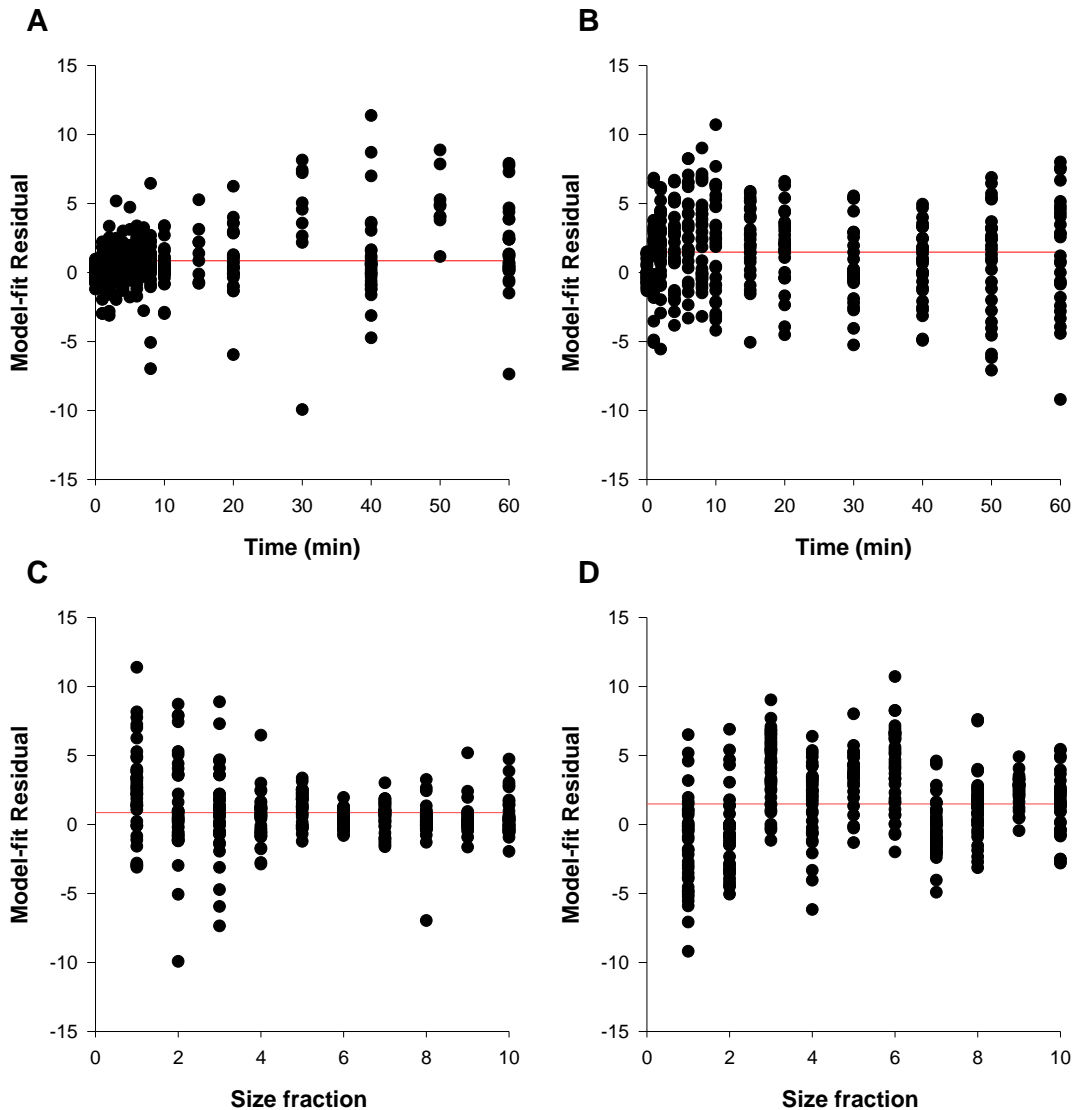


FIGURE 5.6: TIME AND SIZE RESOLVED RESIDUAL PLOTS FOR CHICKPEA AND DURUM WHEAT. Time-resolved plots for (A) chickpea and (B) durum wheat and size-resolved plots for (C) chickpea and (D) durum wheat. Values are residuals (expressed as % starch digested) for all data points obtained across all size fractions, ordered by time or size. Mean line is shown in red.

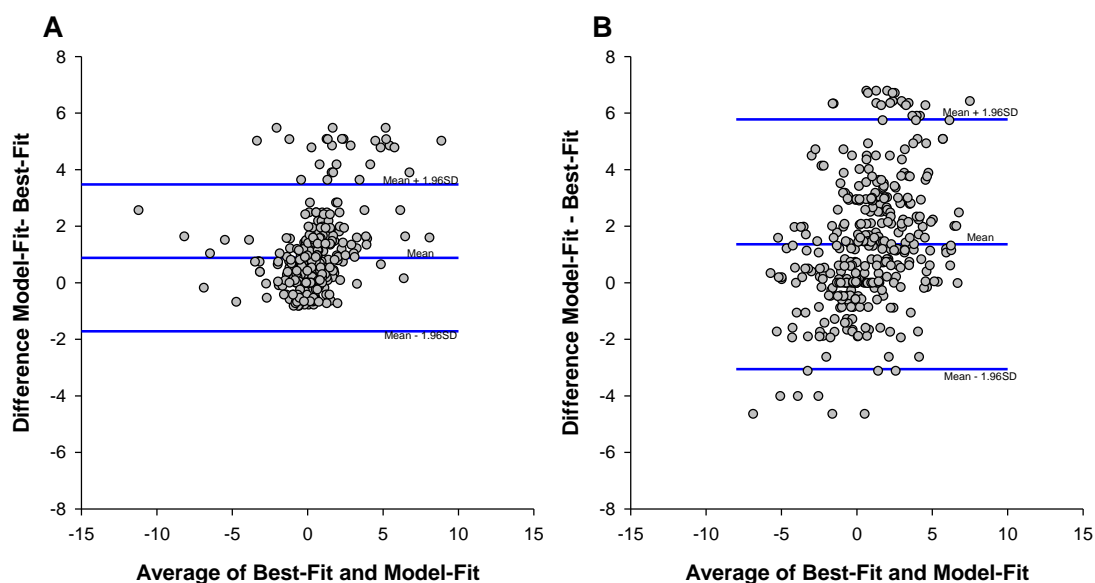


FIGURE 5.7: BLAND-ALTMAN PLOTS OF (A) CHICKPEA AND (B) DURUM WHEAT. Data points are residual values, expressed as % starch digested. Blue lines show mean (which indicates bias) and upper and lower limits of agreement (defined as mean \pm 1.96 SD). Chickpea; mean = 0.98, SD = 1.47). Durum wheat; mean = 1.36, SD = 2.25.

No evidence of systematic bias was observed in the Bland-Altman residual plots (**Figure 5.7**) as the majority of residual data points appear to be arranged in a fairly symmetrical, radial pattern around the origin. The mean residual values were positive for both materials, indicating that the model is more likely to slightly overestimate (rather than underestimate) starch digestion.

The error associated with the model-fitting to experimental data obtained for each size fraction is reflected in the SEE and R^2 values (**Table 5.2**) and is portrayed graphically for a representative example in **Figure 5.8A**. The mean residual values and SDs observed were low (1.65 ± 3.5 for durum wheat and 0.95 ± 2.4 for chickpea, expressed as % starch digested), indicating a very good fit to the experimental data (**Figure 5.8B**). Overall, the model provided an excellent fit to experimental data, which suggests that LOS plots provide a suitable means of estimating the parameters of **Equation 5.4**.

TABLE 5.2: REGRESSION ANALYSIS OF MODEL-FIT AND BEST-FIT TO EXPERIMENTAL DATA OBTAINED FOR VARIOUS SIZE FRACTIONS OF CHICKPEA AND DURUM WHEAT

Size (mm)	CHICKPEA				DURUM WHEAT			
	BEST FIT ¹		MODEL FIT ²		BEST FIT ¹		MODEL FIT ²	
	R^2	SEE (%)	R^2	SEE (%)	R^2	SEE (%)	R^2	SEE (%)
Starch	0.99	2.35	0.98	4.21	0.99	3.15	0.98	3.79
0.11	0.99	2.86	0.98	3.81	0.99	2.57	0.98	2.90
0.38	0.97	3.06	0.97	3.21	0.99	2.16	0.94	4.88
0.55	0.99	1.70	0.98	1.78	0.99	2.28	0.97	3.27
0.73	0.99	0.77	0.97	1.84	0.99	2.49	0.96	4.03
1.02	0.99	0.60	0.99	0.75	0.99	2.94	0.90	5.22
1.29	0.99	0.68	0.96	1.26	0.97	2.13	0.98	2.08
1.55	0.92	1.46	0.90	1.54	0.98	2.48	0.97	2.66
1.85	0.95	1.37	0.94	1.41	0.99	1.14	0.96	2.94
2.58	0.95	1.24	0.92	1.52	0.97	2.34	0.95	2.66

¹'Best-fit' refers to curve-fitting to the first-order equation by an iterative process.

²'Model-fit' refers to curve-fitting in which value of parameters was estimated from LOS plots.

SEE is expressed as % starch digested; R^2 is the coefficient of determination. A perfect fit is characterised by $R^2 = 1$ and SEE = 0.

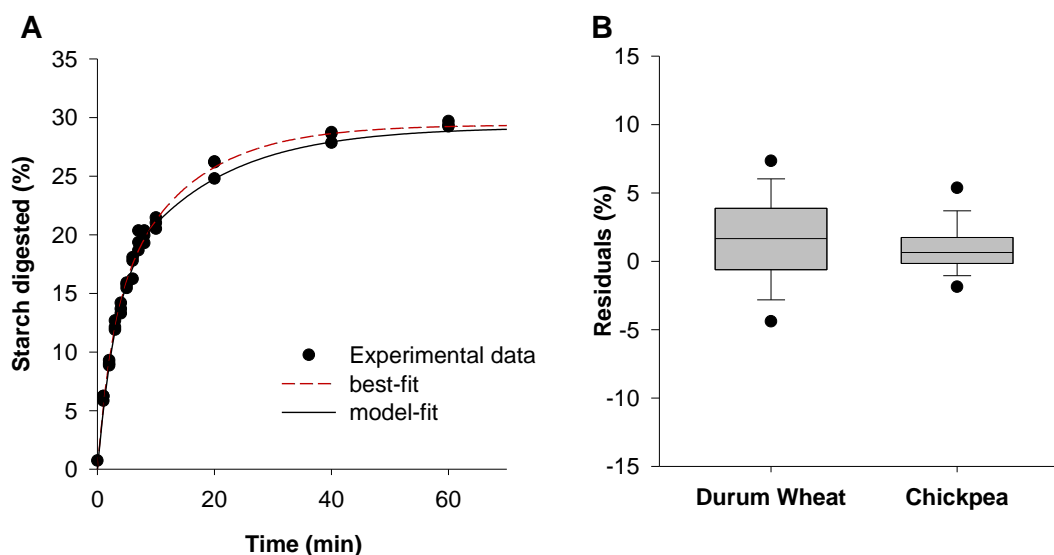


FIGURE 5.8: EXAMPLE OF (A) MODEL COMPUTED DIGESTIBILITY CURVE SHOWN ALONGSIDE A BEST-FIT TO EXPERIMENTAL DATA AND (B) BOX-PLOT OF POOLED RESIDUALS. Data points are experimentally obtained replicate values from a digestibility assay of chickpea, size 1.02 mm. The model-fit was obtained by substitution of LOS estimated values into Equation 3 ($R^2 = 0.991$, SEE = 0.85). The best-fit was obtained by maximum likelihood estimation (MLE) regression of experimental data ($R^2 = 0.995$, SEE = 0.64). The box-plot (B) shows pooled residuals for size fractions of durum wheat and chickpea. Quartiles: 10th to 90th. Values outside this range are represented by a single dot.

5.3.4 ANALYSIS OF STARCH DIGESTION MECHANISMS FROM COMPUTED CURVES

Model computed curves were used to examine potential relationships which influence starch digestion kinetics. Firstly, hydrolysis index (HI) values were obtained for all size fractions of chickpea and durum wheat (**Table 5.3**). These values were obtained from model-computed curves ($t \leq 90$ min) using both the conventional AUC method and algebraically by substitution of $t = 90$ into **Equation 5.4**. The HI values obtained using these two methods were similar for durum wheat materials. However, for chickpeas, HI estimated using the AUC method gave rise to larger values than the algebraic method. This reflects the shape of the digestibility curves (**Figure 5.2**), as the endpoint of starch digestion was generally reached before 90 min in chickpeas, but not for larger size fractions of durum wheat. As expected, a broad range of HI values were observed for the different size fractions.

TABLE 5.3: HYDROLYSIS INDEX CALCULATED IN TWO DIFFERENT WAYS

Size (mm)	CHICKPEAS			DURUM WHEAT		
	Ruptured Cells (%)	HI _{AUC90}	HI _{C(t=90)}	Ruptured Cells (%)	HI _{AUC90}	HI _{C(t=90)}
starch	N/A	100.0	100.0	N/A	100.0	100.0
0.11	100	94.9	88.5	100	88.3	81.1
0.38	100	79.4	70.9	100	74.2	74.4
0.55	80	65.6	59.1	100	76.6	76.8
0.73	61	54.1	48.9	97	75.2	75.2
1.02	43	41.0	36.1	69	64.8	65.6
1.29	34	33.0	28.8	54	63.7	76.0
1.55	28	24.1	20.5	45	58.4	58.2
1.85	24	28.7	24.7	38	52.0	54.2
2.58	17	27.1	26.4	27	49.8	55.0

Hydrolysis Index values expressed as % starch digested, in which maximum digestion is achieved on purified starches. HI was obtained either from the area under the predicted digestibility curve for 90 min (HI_{AUC90}), or by substitution of 90 min for t in **Equation 5.4** to predict the extent of starch digestion at 90 min (HI_{C(t)=90}).

To explore this particle-size effect further, HI was plotted against the estimated proportion of ruptured cells on the surfaces of milled size fractions (**Figure 5.9**). The HI was linearly related to the proportion of ruptured cells on the fractured surface, and HI values were similar for the size fractions in which all cells were ruptured.

Theoretically, the y-intercept represents the extent of starch digestion if all starch is encapsulated within cell walls. Accordingly, the plot suggests that 40% of the starch in intact durum wheat cells and 13% of the starch in intact chickpea cells would be digested. This is consistent with the expectation that durum wheat cell walls are more permeable than durum wheat.

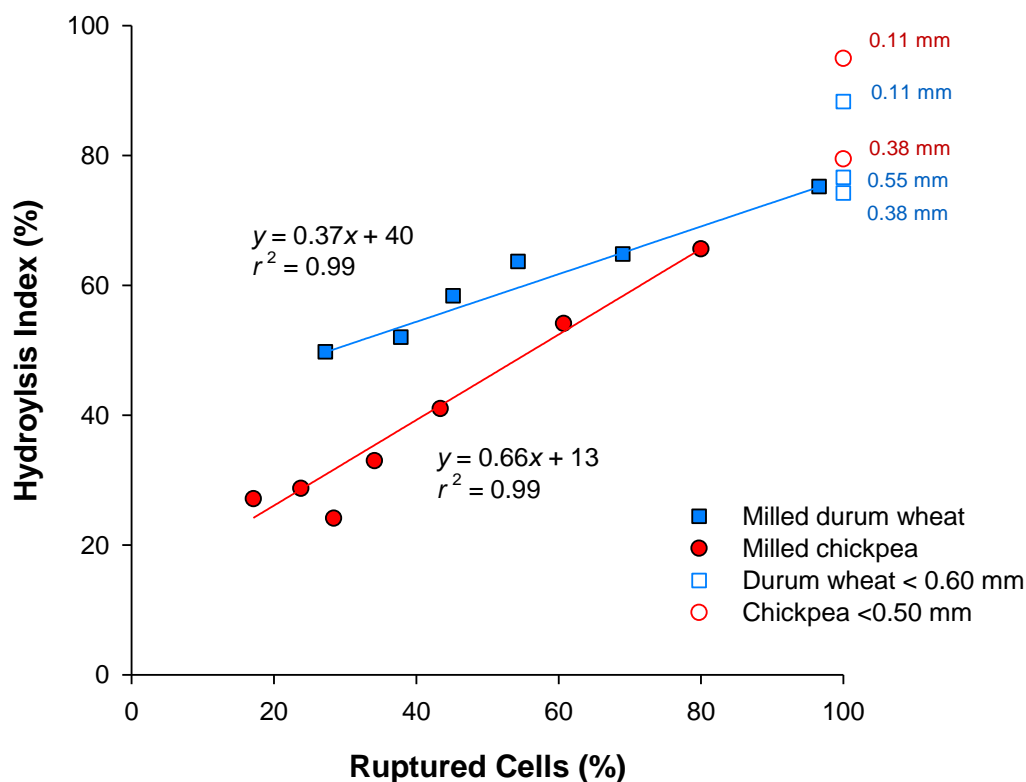


FIGURE 5.9: EFFECT OF CELLULAR INTEGRITY ON STARCH HYDROLYSIS INDEX. Values shown were calculated from the AUC of predictive digestibility curves at 90 min. Linear regression reveals a strong correlation between proportion of ruptured cells in each milled size fraction (*Table 4.1, page 129*) and the hydrolysis index. Data from durum wheat fractions smaller than 0.60 mm (i.e. sizes: 0.55, 0.38 and 0.11 mm) and chickpeas fractions smaller than 0.50 mm (i.e. sizes 0.38 and 0.11 mm) are shown as open squares and circles, and were excluded from the regression analysis, because all these fractions consisted of 100% ruptured cells.

Cell wall encapsulation may also limit starch bioaccessibility by preventing complete gelatinisation of intracellular starch. The DSC runs in *Chapter 4*, showed that particle size also influenced the terminal extent of gelatinisation (TEG) in chickpeas. Interestingly, a plot of TEG against the total extent of starch digestion ('Total C_{∞} ') also reveals a strong linear relationship **Figure 5.10**. This is consistent with the expectation that restricted starch gelatinisation may be a key mechanism responsible for the limited starch bioaccessibility, although these results should be interpreted cautiously, because TEG and *Total C_{∞}* are both independently influenced by particle size.

Nevertheless, **Figure 5.9** and **Figure 5.10** provide examples of how this *in silico* model can be used to explore and predict the effect of factors suspected to influence digestion kinetics.

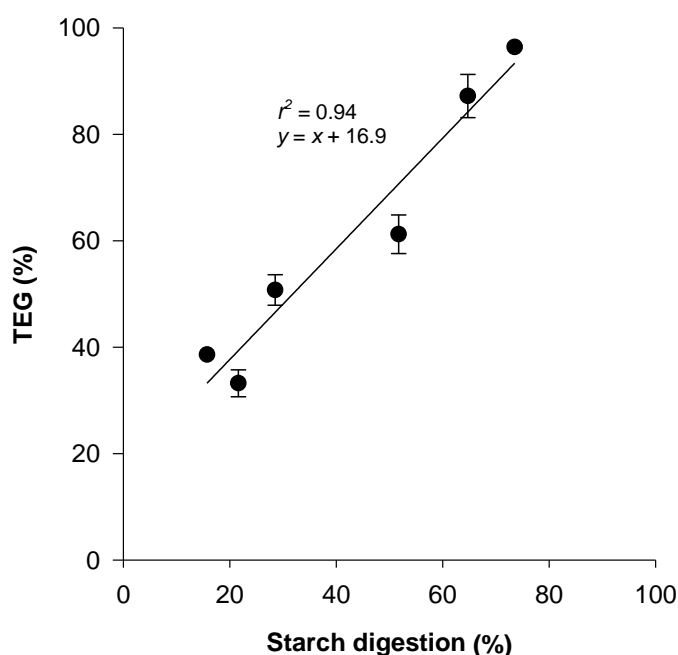


FIGURE 5.10: CORRELATION BETWEEN EXTENT OF STARCH DIGESTION AND GELATINISATION IN CHICKPEA SIZE FRACTIONS. Starch digestion is based on *Total C_{∞}* , as shown in *Table 5.1*. TEG is the terminal extent of gelatinisation, determined for selected size fractions by differential scanning calorimetry as described in *Chapter 4*, section 4.2.5, page 133.

5.4 DISCUSSION

The strong correlation between the predictive digestibility curves and experimental data confirmed that the estimates of C_{∞} and k obtained from LOS plots are valid predictors, and that the equations developed provided a representative description of the processes leading to the release of starch hydrolysis products. Previously, LOS analysis of digestibility curves obtained for hydrothermally-processed starches, and homogenised food products revealed that these materials, which are unlikely to contain high proportions of encapsulated starch, followed a *single-phase* amylolysis process (Butterworth *et al.* 2012, Goñi *et al.* 1997). Using the Englyst classification system, however, these food materials would be subdivided into RDS and SDS, even though the slower rate in the later stages of amylolysis is a natural consequence of the fall in the concentration of available substrate and is not indicative (as already explained) of *intrinsic* differences in rate. This example demonstrates the questionable value of the existing starch classification system, which results from a misinterpretation of starch digestibility data.

In the present study, discontinuities were clearly evident in the LOS plots of materials that contained cell wall encapsulated starch, indicating that amylolysis in these materials did occur in *two phases*. The adaptation of the familiar first-order equation to reflect the *consecutive* biphasic nature of starch digestion in heterogeneous materials provided an excellent description of the release of starch hydrolysis product from hydrothermally processed milled chickpea and durum wheat.

The curves obtained using this bi-phasic model enabled some further exploration of digestion mechanisms. Certainly, the effect of particle size on the extent of starch digestion (C_{∞}) in chickpea and durum wheat materials is consistent with observations from previous chapters. It seems likely, especially given the consecutive nature of these first-order reactions, that the first phase of the LOS plot represents hydrolysis of accessible starch on the fractured surface, whereas the second phase represents less

digestible or less available starch in the underlying cell layers. Accordingly, the observation that in chickpeas, the rapid reaction was responsible for majority of total starch breakdown (i.e. $C_{1\infty}$ vs. $C_{2\infty}$), whereas in durum wheat the two reactions contributed fairly equally, is consistent with the expectation that starch encapsulated by durum wheat cell walls is more accessible to α -amylase than in chickpeas. This was supported further by the strong correlation observed between the HI and estimated proportion of ruptured cells.

There may, however, be other contributing factors which limit starch bioaccessibility. The total extent of starch digestion (Total C_{∞}) suggested incomplete digestion of the starch present in the various milled fractions and also for the purified starch. This could result from a limitation of the assay methodology used, or it may be that some of the starch is enzyme-resistant. Although this appears to be a common phenomenon that has been reported elsewhere (Debet and Gidley 2007), the underlying reasons why 100% starch digestion is not observed *in vitro*, even with a relatively pure starch substrate, remain unclear.

Other researchers have observed that a single-first order reaction does not always provide a suitable description of starch amylolysis, and reported that bi-phasic equations provided a better fit to the data (Weurding *et al.* 2001). Such findings should be interpreted cautiously; however, because, increasing the number of variables in an equation inevitably increases the likelihood of obtaining a good fit to an experimental curve. Furthermore, the use of an iterative process to find values for the variables in these equations provides very limited insight into the mechanisms responsible for producing multiple phase reactions. In the present study, the parameters obtained using the LOS model are based on the well-established properties of first-order reactions, and therefore provide confidence from a scientific viewpoint. Indeed, the various k and C_{∞} values obtained from the LOS plots were used directly to define

parameters of the two-phase consecutive model, which was then found to provide an excellent description of experimental data.

One unexpected finding was that a higher rate constant was observed for the larger macro-particles than was observed by the action of amylase on the purified starch alone. This was surprising, because the rate constant is an inherent property of the enzyme, independent of substrate concentration, and the greatest activity would be expected on the most available substrate (in this case believed to be the purified starches). A number of possibilities were considered in an effort to explain this conundrum. First and foremost, an increase in rate suggests that an activator may be present. Chloride and calcium are both known activators of α -amylase, and plant tissue does contain these compounds. However considering that the enzyme, which has a high affinity (20 pmol.L^{-1}) for calcium, was supplied in $3 \text{ mmol.L}^{-1} \text{ CaCl}_2$, and $2.9 \text{ mol.L}^{-1} \text{ NaCl}$, and that assays were performed in PBS, which has a high concentration of chloride ($137 \text{ mmol.L}^{-1} \text{ NaCl}$ and $2.7 \text{ mmol.L}^{-1} \text{ KCl}$), any further stimulation of the enzyme by these ions seems unlikely (D'Amico *et al.* 2006, Stein *et al.* 1964). Plant materials are also known to contain endogenous enzymes, which could contribute to the overall release of reducing sugar. However, enzyme-free control runs (*data not shown*) did not reveal any increase in reducing sugars concentration over time, and it seems unlikely that these endogenous enzymes would not be de-natured by 85 min of hydrothermal processing.

Phenolic compounds, which are found in wheat and chickpeas, are reported to inhibit the action of α -amylase (Sreerama *et al.* 2009, Barron *et al.* 2007). Paradoxically, however, a recent paper indicates that a polyphenolic compound (i.e. lignin) is an even more effective activator of α -amylase than chloride (Zhang *et al.* 2013). Furthermore, lignins with a larger molecular weight were found to be considerably more potent stimulators of α -amylase (Zhang *et al.* 2013). This could potentially explain why amylase activity appeared to be greater on starch-rich plant tissue than on purified

starch. Alternatively, the rapid phase may represent hydrolysis of readily digested linear amylose, which leaches out from starch granules during hydrothermal processing (Tester and Morrison 1990). Accordingly, the value of $C_{1\infty}$ could represent the leached amylose portion of starch. This is a very interesting hypothesis which warrants further investigation.

5.5 CONCLUSIONS

Starch digestion in heterogeneous plant materials can be modelled using values estimated from LOS analysis of initial digestibility data, without the need for lengthy incubations. LOS plots thereby provide a rapid and rigorous means of identifying nutritionally relevant starch fraction, and are particularly valuable for mechanistic studies.

The application of this novel method to *in vitro* digestibility data obtained for various size fractions of chickpea and durum wheat suggests that when a proportion of the starch is encapsulated by plant cell walls, digestion occurs in two consecutive phases, each described by a first-order process. The first-phase is thought to represent digestion of more accessible starch in ruptured cells on the particle surfaces, whereas the second phase represents digestion of less accessible (i.e. cell wall encapsulated) or less digestible (i.e. pre-gelatinised) starch in the underlying cell layers. Application of this method to first-order digestibility data thereby provided support for the proposed role of cell walls in limiting the rate and extent of starch digestion. Although the observed mathematical relationships alone are not enough to define the underlying mechanisms, LOS analysis is useful for providing insights into digestion kinetics, and for making predictions about nutrient bioaccessibility. The predicted Hydrolysis Index will be compared to the *in vivo* glycaemic response to selected wheat materials in *Chapter 7*.

CHAPTER 6

DIGESTIBILITY STUDIES IN A MULTI-COMPARTMENTAL GUT MODEL

6.1 INTRODUCTION

The *in vitro* starch digestibility data presented in previous chapters was generated from a simple model of amylolysis involving the action of one enzyme, porcine pancreatic α -amylase. However, amylolysis in the small-intestinal lumen is only one of a series of stages that lead to the release of nutrients from food during digestion. *In vivo*, the physical and biochemical disassembly of starch-rich food matrices in the mouth and stomach may increase subsequent susceptibility to α -amylase in the duodenum. Multi-compartment models comprising oral, gastric and duodenal conditions are therefore believed to provide better predictions of *in vivo* digestion outcomes (Woolnough *et al.* 2008).

The Dynamic Gastric Model (DGM) at the Institute of Food Research (IFR), Norwich, is an advanced *in vitro* model (see **Figure 6.1**) that simulates the gastric processing of the human stomach both from a mechanical (e.g., antral contractions) and biochemical (e.g., enzyme breakdown) aspect (Wickham *et al.* 2012). The mixing of food in the DGM is claimed to resemble closely that of the human stomach, and has been developed using MRI imaging (Vardakou *et al.* 2011, Wickham *et al.* 2012)

At the IFR, the DGM model is used in conjunction with simulated salivary fluid (representing the oral phase of digestion) and the Static Intestinal Model (SIM), which simulates the biochemical conditions of the duodenum. These models aim to provide an accurate and reproducible representation of physiological digestive conditions and allow for frequent sampling, and thereby enable the specific effects of the oral, gastric and duodenal conditions to be determined. As shown in *Chapter 4*, chickpea cells appear to be particularly resistant to digestion with α -amylase. However, the effect of biochemical and physical factors present under more physiological digestive conditions remained unclear. Therefore, the DGM and SIM were used to provide an improved assessment of the bioaccessibility of starch encapsulated within chickpea cells.

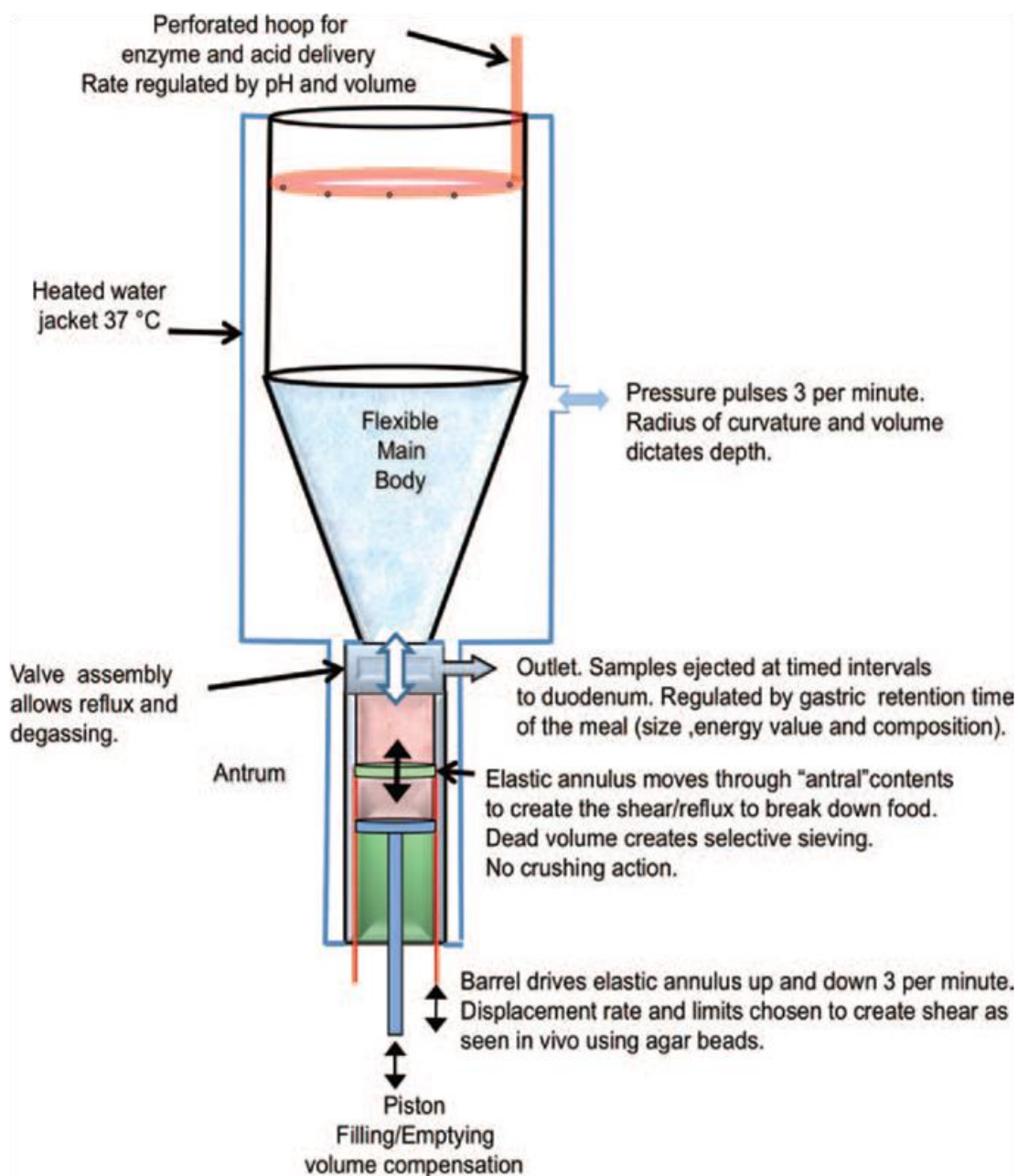


FIGURE 6.1: DGM MECHANICS. Taken from (Wickham *et al.* 2012)

6.1.1 OBJECTIVE

The purpose of these experiments was to assess the effect of simulated oral, gastric and duodenal digestive environment on cellular integrity and starch digestibility.

NOTE: A parallel study using wheat porridge prepared from various milled size fractions is currently ongoing at the Institute of Food Research (IFR). The expected results from the ongoing work may contribute towards the interpretation of other findings reported within this thesis.

6.2 MATERIALS AND METHODS

6.2.1 TEST MEALS

To examine the role of cell wall encapsulation; the digestion of two porridges with different amounts of encapsulated starch was compared. '**Porridge-O**' was prepared from intact chickpea cells, and contained a greater proportion of cell wall encapsulated starch than '**Porridge-F**', which was prepared from freeze-milled cells.

TABLE 6.1: NUTRIENT COMPOSITION OF CHICKPEA PORRIDGE

Energy (kJ)	986.8
Energy (kcal)	234.0
Protein (g)	14.8
Carbohydrate (g)	35.0
Total sugars (g)	0.1
Starch (g)	34.9
Fat (g)	1.7
Dietary Fibre (g)	9.8
Ash (g)	0.1
Moisture (g)	288.6

¹One portion = 350g

Proximate analysis and energy values determined as described in *Section 2.3.1*.

The chickpea cells used to make these porridges were prepared using the hydrothermal cell separation procedure described in *Section 2.1.3 (page 76)*, and the cells were stored in a dry form (48.2 g starch and 10 g moisture/100 g) prior to porridge preparation. For **Porridge-F**, the dry chickpea cells were subjected to 2 x 30 min of freeze-milling at 10 cycles per second (6970D Freezer/Mill[®], SPEX SamplePrep L.L.C., Stanmore, Middlesex, UK). This caused some of the cells to rupture and release their intracellular starch.

To prepare the porridge meals, 70 g dry chickpea cells (either freeze-milled or intact cells), were soaked in 180 mL water overnight and then cooked for 20 min with the addition of another 170 mL water. After cooking, the total weight of the porridge was readjusted to 350 g by the addition of water to make up for evaporative losses. The portion size represents a typical meal for human consumption in terms of nutrition and volume. The nutrient composition of this porridge is shown in **Table 6.1**, and was used for DGM programming purposes. However, direct measurement of starch content (using Total Starch analysis, see *Section 2.3.3*) indicated that the porridge contained 33.6 g starch. This value is more accurate than starch obtained 'by difference' (listed in **Table 6.1**) and was used for subsequent calculations, although the values are reasonably close.

6.2.2 DIGESTION PROTOCOL

Test meals (350 g) were passed through a multi-compartmental model which simulated oral, gastric and duodenal digestive conditions (**Figure 6.2**). The simulated gastric, hepatic and pancreatic secretions used in this protocol represent physiological conditions (Wickham *et al.* 2012, Vardakou *et al.* 2011, Lentner 1981). The methods used to prepare the various secretions have been described elsewhere (Pitino *et al.* 2010).

For the oral phase, 348 g of chickpea porridge was mixed with 20 mL distilled water, 10 mL Simulated Salivary Fluid (SSF, containing 0.15M NaCl, 3 mM urea, pH 6.9) and 1 mL of human salivary α -amylase (HSA, 900 U, Sigma, UK, dissolved in SSF). After 10 min, a 2 g sample was collected to represent the effect of the simulated oral digestion phase.

The remaining 377 g mixture was added to the DGM, which was already primed with 20 mL acidified salt solution (58 mM NaCl, 30 mM KCL, 0.5 mM CaCl_2 , 0.864 mM NaH_2PO_4 , and 10 mM HCL), simulating the fasted contents of the human stomach. Physiological additions of simulated gastric secretions containing 9000 U/mL porcine mucosal pepsin and 60 U/mL gastric lipase analogue from *Rhizopus oryzae* (Amano Enzyme Inc., Nagoya, Japan), and 0.127 mM lecithin liposomes (Mandalari *et al.* 2008) in an acidified salt solution, occurred throughout gastric digestion. Gastric samples were expelled from the DGM every 10 min over a 60 min period.

Each gastric sample was immediately weighed, neutralised with 1 M NaOH and re-weighed. Next, for the SIM, 30 g of each neutralised gastric sample was transferred into individual bottles containing 3.75 mL of so-called 'hepatic mix' and 11.25 mL of designated 'pancreatic mix', and placed on an orbital shaker (170 rpm) at 37 °C to represent the duodenal digestion phase. The hepatic mix contained lecithin (6.5 mM, from Lipid Products, Surrey, UK), cholesterol (4 mM), sodium taurocholate (12.5 mM) and sodium glycodeoxycholate (12.5mM) in a salt solution of NaCl (146 mM), CaCl_2

(2.6 mM) and KCl (4.8 mM) and was prepared fresh for each run. The pancreatic mix contained pancreatic lipase (590 U/mL), porcine co-lipase (3.2 µg/mL), porcine trypsin (11 U/mL), bovine α-chymotrypsin (24 U/mL), and porcine α-amylase (300 U/mL) in a solution of NaCl (125 mM), CaCl₂ (0.6 mM), MgCl₂ (0.3 mM) and ZnSO₄ · 7H₂O (4.1 µM).

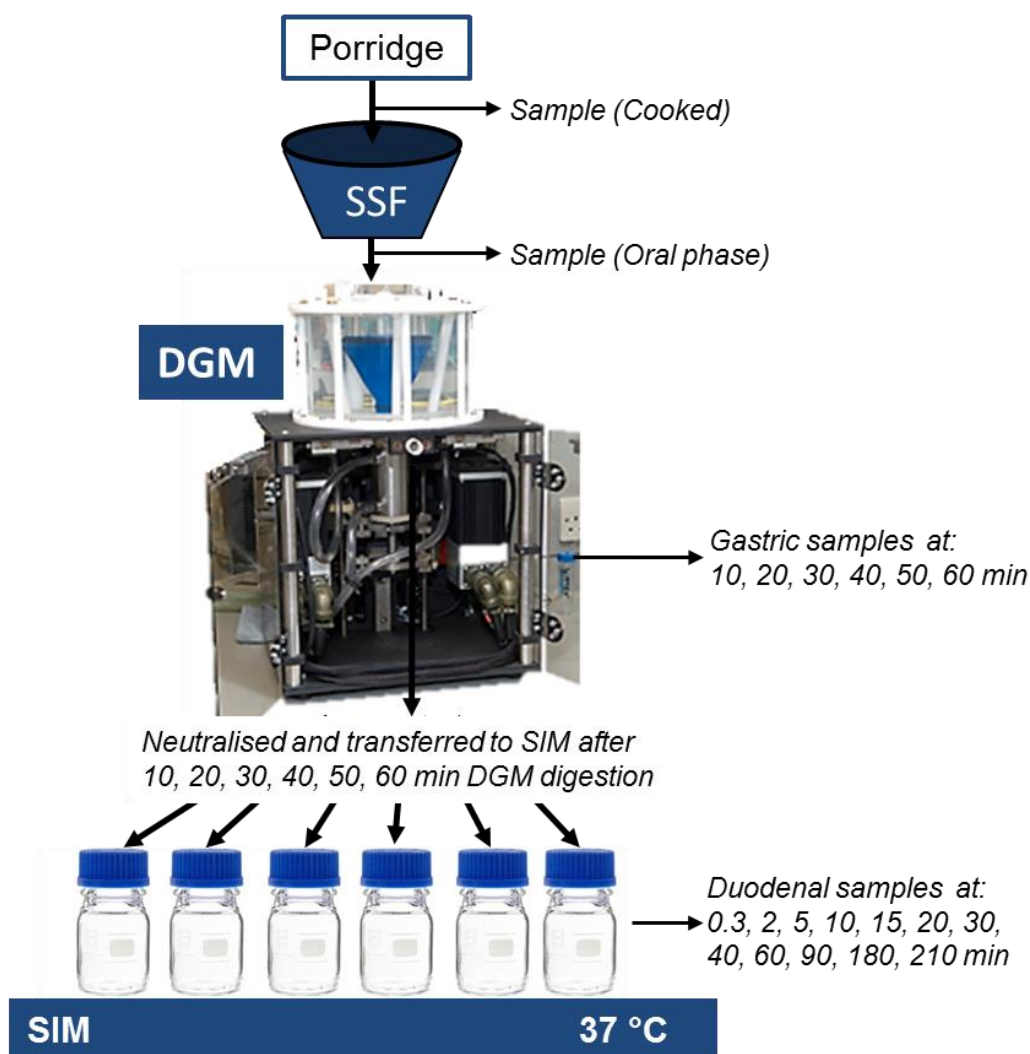


FIGURE 6.2: OVERVIEW OF MULTI-COMPARTMENT DIGESTION SYSTEM. Test meals (porridge) were treated with simulated salivary fluid (SSF) to represent the oral phase of digestion, then transferred into the dynamic gastric model (DGM). Samples expelled from the DGM at 10 min intervals were neutralised before continued digestion in the static intestinal model (SIM). Samples were collected and sub-samples taken for analysis of starch, sugar, dry matter and for examination by microscopy as indicated.

Overall, 1 x cooked sample, 1 x orally processed sample, 6 x gastric samples, and 72 (i.e. 6 x 12) duodenal samples were collected per run (**Table 6.2**). *Porridge-O* was run through the digestion protocol twice, but only one run was carried out with *Porridge-F*.

TABLE 6.2: OVERVIEW OF SAMPLE COLLECTION FROM THE GASTRIC AND DUODENAL MODELS

Duodenal Sampling - a delay of 4 mins is built in for manipulations
 Table below includes baseline t = 0 samples

Time (min)	G1	G2	G3	G4	G5	G6	
0							
1							
2							
3							
4							
5							
6							
7							
8							
9							
10	sample						
14	S1, t=0					G1 coming off	
16	S2					G1D1	
19	S3					G1D2	
20						G1D3	
24	S4	sample				G2 coming off	
26		S1, t=0				G1D4, G2D1	
29	S5	S2				G2D2	
30		S3				G1D5, G2D3	
34	S6	S4	sample			G3 coming off	
36			S1, t=0			G1D6, G2D4, G3D1	
39		S5	S2			G3D2	
40			S3			G2D5, G3D3	
44	S7	S6	S4	sample		G4 coming off	
46				S1, t=0		G1D7, G2D6, G3D4, G4D1	
49			S5	S2		G4D2	
50				S3		G3D5, G4D3	
54	S8	S7	S6	S4	sample	G5 coming off	
56					S1, t=0	G1D8, G2D7, G3D6, G4D4, G5D1	
59				S5	S2	G5D2	
60					S3	G4D5, G5D3	
64		S8	S7	S6	S4	sample	G6 coming off
66						S1, t=0	G2D8, G3D7, G4D6, G5D4, G6D1
69					S5	S2	G6D2
74	S9		S8	S7	S6	S3	G5D5, G6D3
79						S4	G1D9, G3D8, G4D7, G5D6, G6D4
84		S9		S8	S7	S5	G6D5
94			S9	S8	S7	S6	G2D9, G4D8, G5D7, G6D6
104	S10			S9	S8	S7	G3D9, G5D8, G6D7
114		S10			S9	S8	G1D10, G4D9, G6D8
124			S10			S9	G2D10, G5D9
134				S10			G3D10, G6D9
144					S10		G4D10
154						S10	G6D10
194	S11						G1D11
204		S11					G2D11
214			S11				G3D11
224	S12			S11			G1D12, G4D11
234		S12			S11		G2D12, G5D11
244			S12			S11	G3D12, G6D11
254				S12			G4D12
264					S12		G5D12
274						S12	G6D12

Total 72 samples

Blocked samples - Additional samples taken for microscopy

6.2.3 SAMPLE COLLECTION AND ANALYSIS

Samples were collected for analysis of starch, sugar, dry matter and examination by microscopy at key stages throughout the digestion procedure (**Figure 6.2** and **Table 6.2**). The first sample was collected after cooking, and another sample was collected after treatment with artificial saliva. Gastric samples were collected after 10, 20, 30, 40, 50 and 60 min of DGM digestion. Subsequently, samples were collected from the SIM after 0.3, 2, 5, 10, 15, 20, 30, 40, 60, 90, 180 and 210 min incubation with pancreatic and hepatic mix.

For starch and sugar analysis, a 2 mL aliquot of the digesta was taken into 8 mL of 80% ethanol to inactivate any residual enzyme activity. These samples were stored at 4 °C prior to total starch and reducing sugar analysis (DNS assay, see *Section 2.3.4.1*). Samples for microscopy were placed immediately into Karnovsky's fixative and later processed and embedded in LR resin as described in *Section 2.4.1*. Samples for analysis of dry matter were frozen (-20 °C) in plastic pots and analysed by oven-drying (*Section 2.3.2*).

6.2.4 DATA ANALYSIS

The amount of sugar measured in the digested samples was corrected for dilutions occurring throughout the digestion procedure, and expressed as a percentage of starch digested, assuming the main product of hydrolysed starch is maltose, and that all reducing power originates from maltose. Data from gastric digestion of *Porridge-O* is shown for both runs.

Starch digestibility in the duodenal phase was plotted as the average data obtained from all six gastric samples, with error bars showing the range of values obtained (standard deviation). For *Porridge-O*, data (n=12) from the two runs was pooled and averaged, as similar trends and values were observed for both runs in the duodenal phase. Logarithm of Slope (LOS) analysis (described in *Chapter 5*) was applied to the experimental data to identify and quantify starch fractions present. This analysis was

applied to averaged plots (i.e. average duodenal digestibility of six gastric samples), which followed similar starch digestion profiles, regardless of gastric retention time. This helped to overcome difficulties with scattered data, and enabled the effect of freeze-milling on starch digestion kinetics (k and C_{∞}) to be examined. The effect of gastric retention time on subsequent starch digestion kinetics, however, could not easily be determined using LOS analysis, because of the limited and scattered data obtained for some samples.

Primary data analysis was carried out using Microsoft Excel 2010 and SigmaPlot v12.0 was used for curve fitting.

6.3 RESULTS

Micro-structural observations (**Figure 6.3**) revealed that freeze-milling of chickpea cells was not sufficient for rupturing the vast majority of chickpea cells. Nevertheless, a difference in starch digestibility was observed between the two porridge meals, as described below.

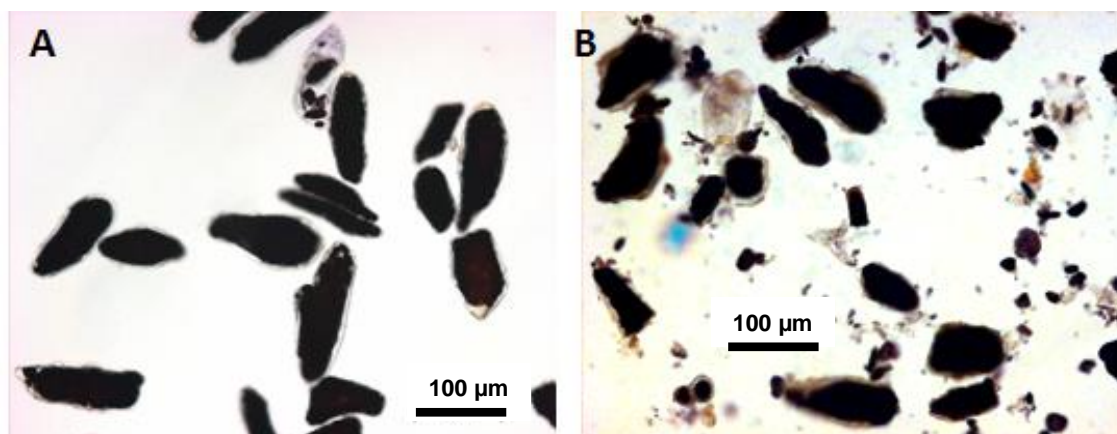


FIGURE 6.3: LIGHT MICROGRAPHS OF (A) PORRIDGE-O AND (B) PORRIDGE-F AFTER COOKING. Intact, starch-filled cells are present in both porridges. The vast majority of cells in *Porridge-O* appeared intact (A). freeze-milling ruptured some cells (B), although many intact cells remain. Free starch and intracellular starch granules are stained dark with 10% Lugol's iodine. Scale bar is 100 µm.

An overview is provided in **Figure 6.4** of the extent of starch digestion in the cooked, oral and various gastric samples for *Porridge-O* and *Porridge-F*. Overall, a small amount of reducing sugar was released during cooking, and during the oral and gastric simulated digestion. The amount of reducing sugar released in the gastric phase was twice as high for the *Porridge-O* than for *Porridge-F*. Nevertheless, the amount of reducing sugar released accounted for less than 2% of the total starch present in the porridge meals, and the concentration of reducing sugar remained fairly constant between 10 and 60 min of gastric incubation (as shown in **Figure 6.4**) suggesting only a negligible amount of starch digestion occurred in the gastric phase (by salivary amylase).

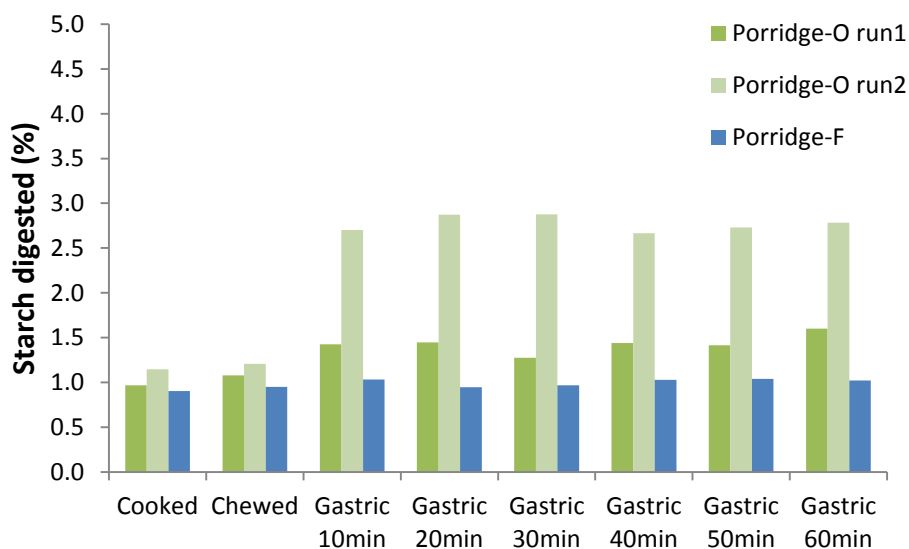


FIGURE 6.4: STARCH BREAKDOWN FROM CHICKPEA PORRIDGE MEALS DIGESTED IN ORAL AND GASTRIC PHASES. Data for *Porridge-O* is shown for both runs. Data for *Porridge-F* is from one run. Starch digestion is expressed as a percentage of the total amount of starch in the original meal.

Gastric digestion had no apparent effects on cellular integrity (**Figure 6.5**). The vast majority of cells appeared to be intact, and contained starch throughout gastric digestion. No cell wall swelling was observed.

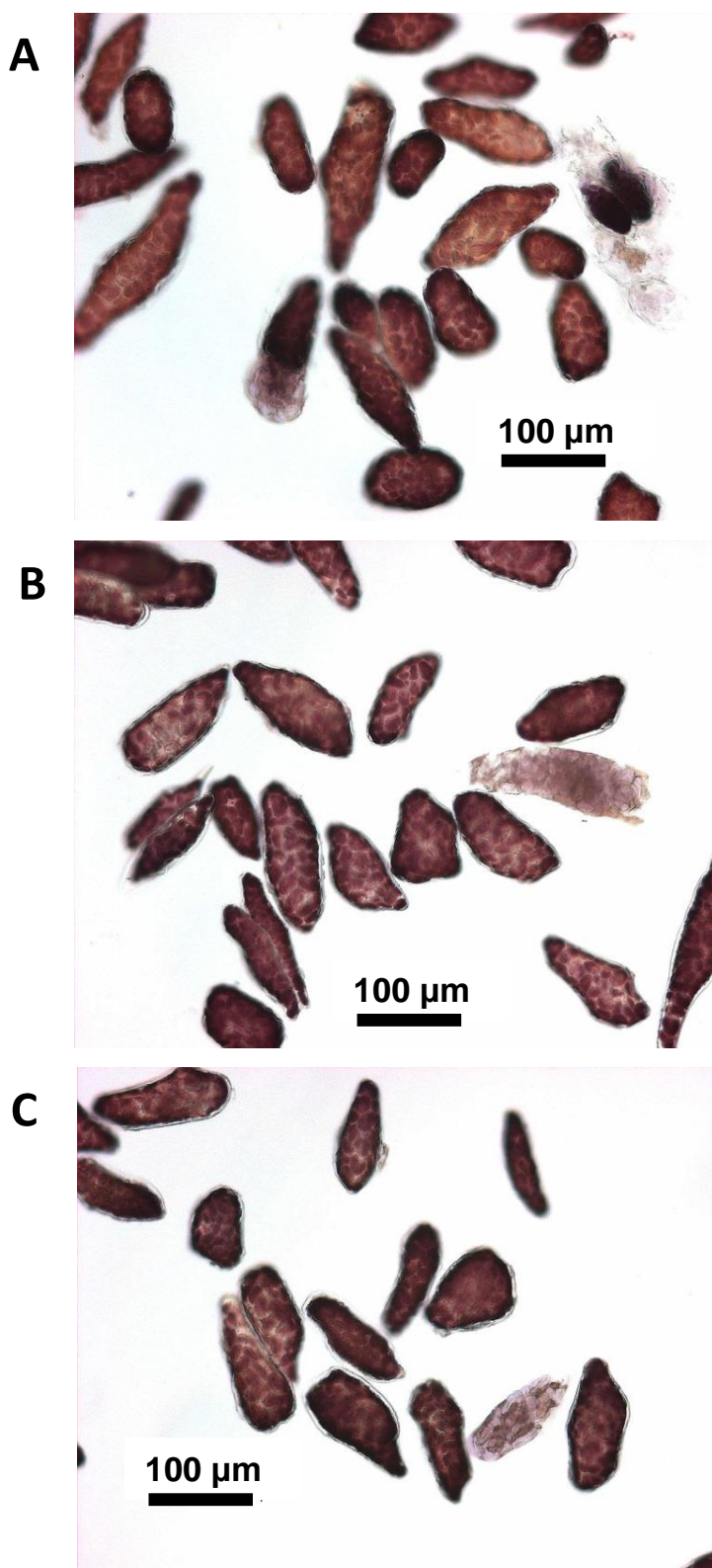


FIGURE 6.5: EFFECT OF GASTRIC RETENTION TIME ON CHICKPEA CELLS FROM PORRIDGE-O AFTER A) 10MIN, B) 30 AND C) 50 MIN GASTRIC RETENTION TIME. Intracellular starch is stained with 2.5% Lugol's iodine. No changes in cellular integrity or starch amyolysis were observed during gastric digestion.

At the end of simulated duodenal digestion, the majority of cells were still intact and contained encapsulated starch, regardless of whether or not the cells had been subjected to freeze-milling treatment before digestion (**Figure 6.6**). Some cells appeared to stain weakly with Lugol's iodine, which could indicate that the intracellular starch had been digested (not shown). However, when a higher concentration of iodine was used, this effect was no longer observed (**Figure 6.6**). Cellular integrity appeared unaffected by digestion, and no cell wall swelling was observed.

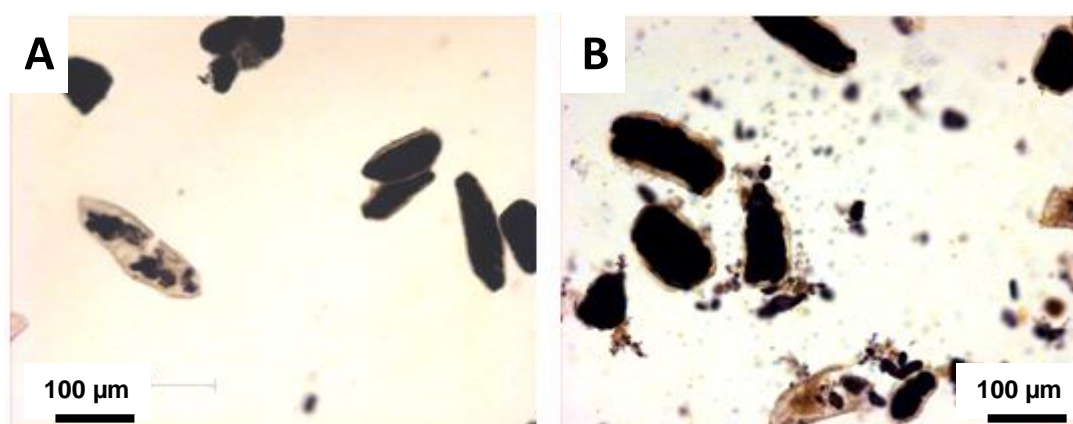


FIGURE 6.6: MATERIAL RECOVERED AT END OF DUODENAL DIGESTION OF (A) PORRIDGE-O AND (B) PORRIDGE-F. Starch stained with 10% Lugol's iodine. Scalebar = 100 µm.

The total extent of starch digestion at the end of the entire digestion regime is shown in **Figure 6.7**. Less than ~10% of the starch in *Porridge-O* was digested, whereas for *Porridge-F*, the freeze-milling treatment increased the extent of starch digestion to ~26%. The gastric phase had no major effects on the total extent of duodenal digestion, although a slight reduction in the total extent of digestion was observed for samples that were retained in the gastric phase for a longer period (see **Figure 6.7**). This effect was more pronounced in *Porridge-F* than in *Porridge-O*, and could reflect the retention of larger particles (intact cells) in the DGM.

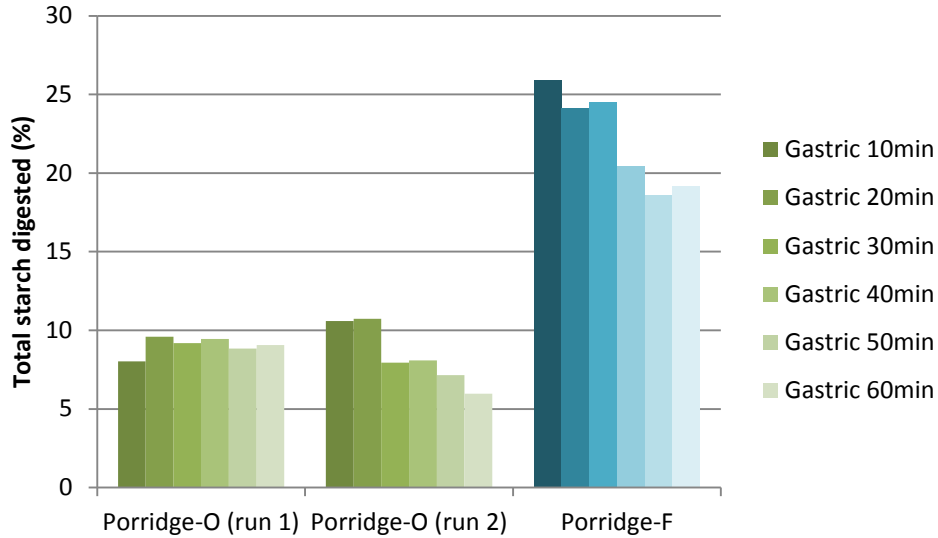


FIGURE 6.7: TOTAL EXTENT OF STARCH DIGESTION AFTER VARIOUS GASTRIC RETENTION TIMES FOR PORRIDGE-O AND PORRIDGE-F. Values for *Porridge-O* are shown for two runs, *Porridge-F* values are from one run. Comparison of the averaged duodenal starch digestibility curves (**Figure 6.8**) obtained for two porridge types revealed different patterns of duodenal digestion. Freeze-milling clearly increased the rate and the extent of starch digestion, as *Porridge-O* was digested at a considerably slower rate than *Porridge-F*.

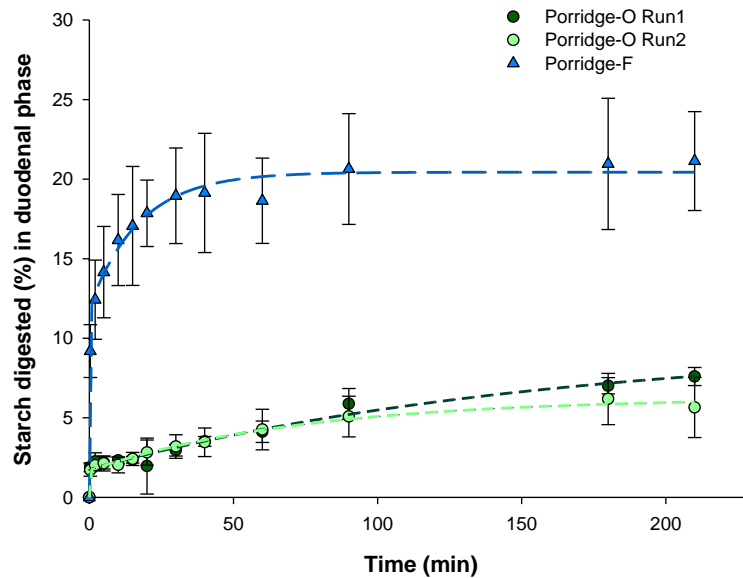


FIGURE 6.8: DUODENAL STARCH DIGESTIBILITY CURVES OBTAINED FOR PORRIDGE-O AND PORRIDGE-F. The curves shown are averaged from duodenal digestion of samples collected after 6 different gastric incubation times. For *Porridge-O* the average of six samples is shown for each replicate run of the simulated DGM and SIM digestion protocol, for *Porridge-F* this is the average of six samples collected from one run. Error bars are standard deviations of this pooled data and represent variation associated with gastric retention time.

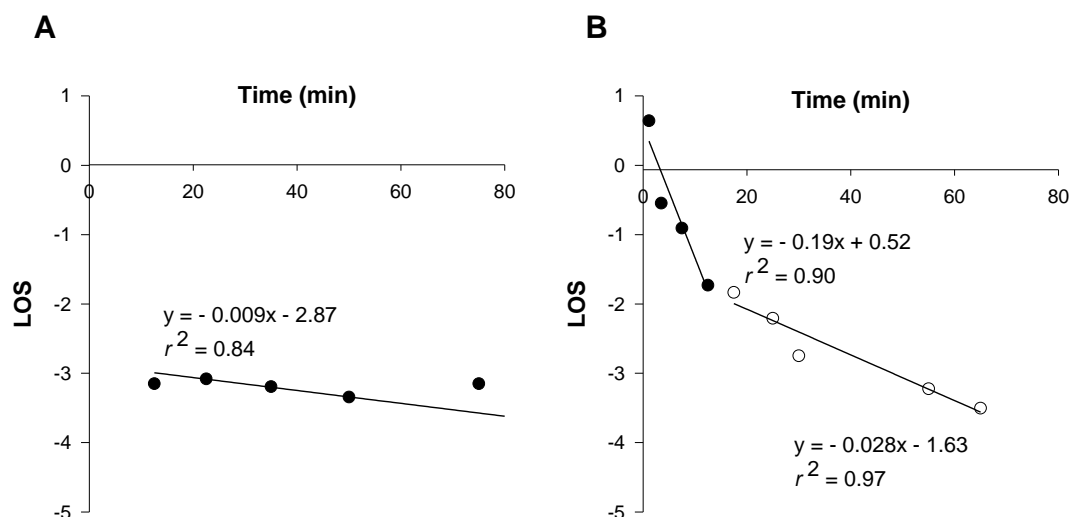


FIGURE 6.9: LOS PLOTS OF DUODENAL STARCH DIGESTIBILITY CURVES FOR (A) PORRIDGE-O AND (B) PORRIDGE-F. It should be noted that for porridges, an initial rapid digestion phase also occurs during the initial 20 s of digestion. However this is not shown because only one time point was collected over this period and a log of slope (LOS) can therefore not be calculated.

LOS analysis was applied to the averaged duodenal digestibility plots (shown in **Figure 6.8**), to examine the effect of freeze-milling (increased cell rupture) on starch digestion kinetics. LOS plots obtained for *Porridge-O* (**Figure 6.9A**), suggested that all starch digestion occurred by a single, slow process. The LOS plot obtained for *Porridge-F* (**Figure 6.9B**) indicated that digestion occurred in two-phases, reflecting the presence of starch fractions with different bioaccessibility (i.e. starch from ruptured vs. intact cells). However, when a model curve was computed on this basis, this consistently underestimated digestion rate and extent, indicating that some starch digestion was not accounted for (*data not shown*). Closer examination of these computed curves suggested that the digestion profile underestimated starch digestion by approximately the amount of starch that had been digested after 20 s. Therefore, the equations were adapted to account for the extent of starch digestion measured after 20 s. This was done by addition of product formed $C_{t=0.3}$, after 20 s (0.3 min). This adjustment generated model-curves that provided an excellent fit to the experimental data (**Figure 6.10**).

TABLE 6.3: PARAMETERS OF DUODENAL STARCH DIGESTIBILITY ESTIMATED FROM LOS PLOTS

	<i>Rapid Phase</i>			<i>Slower Phase</i>		<i>Total C_∞ (%)</i>
	<i>C_{t=0.3} (%)</i>	<i>k₁ (min⁻¹)</i>	<i>C_{1∞} (%)</i>	<i>k₂ (min⁻¹)</i>	<i>C_{2∞} (%)</i>	
<i>Porridge-O</i>	1.5	<i>n/a</i>	<i>n/a</i>	0.009	6.7	8.2
<i>Porridge-F</i>	9.2	0.188	8.97	0.033	4.76	22.9

$C_{t=0.3}$ is the extent (%) of starch digested after 20s; k_1 and k_2 are rate constants. $C_{1\infty}$ and $C_{2\infty}$ represent the extent of starch digestion after each phase. Total C_{∞} is the sum of $C_{t=0.3}$, $C_{1\infty}$ and $C_{2\infty}$, and is the total extent of starch digestion at the end of digestion. *n/a*; not applicable.

LOS analysis indicated that starch was digested at a greater rate and to a greater extent in *Porridge-F*, which was prepared from freeze-milled cells (**Table 6.3**). This indicates that freeze-milling did increase starch bioaccessibility in the duodenal phase, however a large proportion (~77%) of starch still remained undigested.

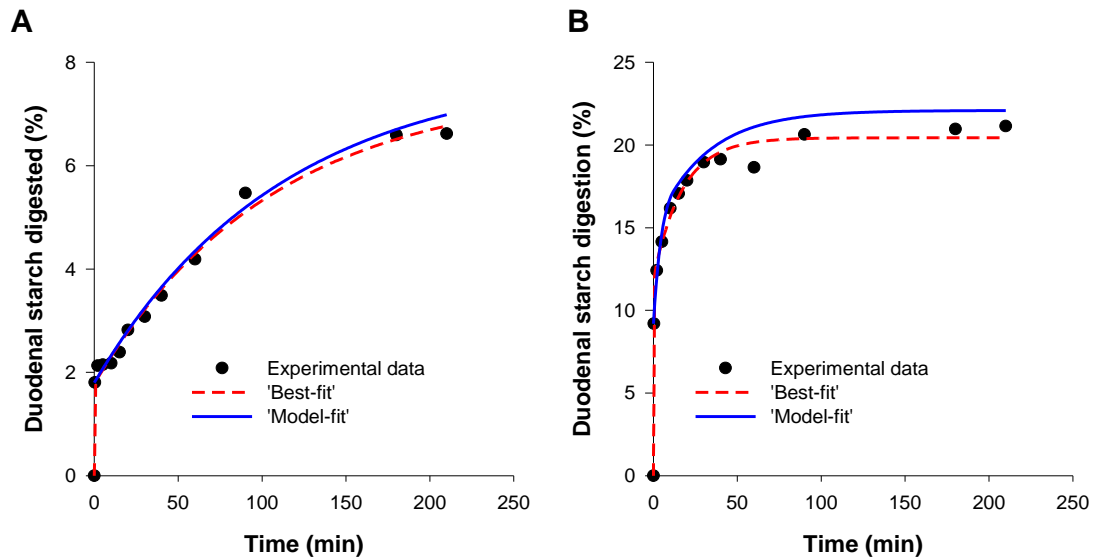


FIGURE 6.10: EXPERIMENTALLY OBTAINED AND MODEL-COMPUTED DUODENAL STARCH DIGESTIBILITY CURVES FOR (A) PORRIDGE-O AND (B) PORRIDGE-F. Best-fit' to experimental data fitted to double first-order equation with variables obtained by Maximum Likelihood Estimation (SEE < 0.7, $R^2 > 0.99$). Model-fit; fitted to two-phase model using variables estimated from LOS plots (SEE = 0.6, $R^2 = 0.92$ for *Porridge-O* and SEE = 3.5, $R^2 = 0.77$ for *Porridge-F*). The difference in scale reflecting a marked difference in the digestion rates of the porridge samples should be noted.

6.4 DISCUSSION

This study has provided insight into the role of oral, gastric and duodenal digestion phases in influencing chickpea cellular integrity and the consequential effects on starch digestion kinetics. Although freeze-milling only ruptured some of the chickpea cells in *Porridge-F*, this was sufficient to increase the rate and extent of starch digestion in the duodenal phase. Certainly, this work demonstrated that cellular integrity was largely retained during the oral, gastric and duodenal phases of digestion.

Microscopy was used to assess the effect of different digestion phases on cellular integrity. Intact cells were the predominant component of samples collected at all stages of the digestion procedure, with no visible increase in cell rupture or swelling with prolonged digestion time. Considering that chickpea cells resisted freeze-milling, a severe physical treatment, it was not surprising that the majority of the cells appeared intact after the more gentle mixing in the gastric and duodenal digestion models. This finding is consistent with *in vivo* studies showing that intact, starch-filled cells from white beans (*Phaseolus vulgaris* L.), which also have a tendency to cell separate, may be recovered in human ileal effluent (Noah *et al.* 1998). The mechanical effects of mastication ('chewing') were omitted in this model, yet it is unlikely that a simulated chewing action would have increased cell rupture, because of the tendency of hydrated chickpea cells to separate. In fact, micrographs of chewed whole, cooked chickpeas and hummus revealed that these foods contain a very high proportion of intact cells, also after *in vivo* mastication (images not shown).

With regard to digestion, the addition of salivary α -amylase in the oral phase caused very limited starch digestion. The total release of reducing sugars (starch hydrolysis products) in the oral and gastric phases together accounted for ~1% of the starch present. In the gastric phase, an initial increase in reducing sugars was detected within the first 10 min for *Porridge-O*, but not for *Porridge-F*. This is illustrated in **Figure 6.4** which shows an apparent increase, albeit a modest one, in starch digestion in the early

gastric phase. However, in view of the fact that no such increase was observed for *Porridge-F*, and that only negligible amounts of reducing sugars were released by salivary amylase in the oral phase (i.e. 'chewed' sample), it seems more likely that the reducing sugars or other reducing compounds originated from sources other than starch. For instance, gastric conditions may have initiated the release of water-soluble, cell wall components (e.g., phenolic compounds such as tannins), which may also contribute to reducing power. The presence or solubility of these components could have been affected by the freeze-milling treatment of cells used to prepare *Porridge-F*, giving rise to differences between the two test meals. Alternatively, in terms of the relatively small differences between the two meals and the very low concentration of reducing sugars released, this effect could also have resulted from experimental error, for instance due to the difficulties in sampling from a heterogeneous mixture which makes it difficult to obtain reliable replicate data. An enzyme-free control run of these samples through the digestion regime would have provided further insight.

The limited release of starch hydrolysis products observed in the simulated oral and gastric phases is not compatible with previous work showing that salivary α -amylase is a major contributor of starch digestion *in vivo* (Hoebler *et al.* 1998). The current results are more consistent with the view that salivary α -amylase plays a relatively minor role in total starch breakdown (Woolnough *et al.* 2010). However, there are some methodological issues with the various studies of salivary amylase and oral digestion, e.g., in terms of the concentration of saliva used, and the literature must be interpreted cautiously (Butterworth *et al.*, 2011). One major consideration in comparing the effects on chickpeas porridges to previously studied foods is the contrasting properties of the materials examined. Bolus formation and disintegration, for instance, are highly complex processes, and depend on a range of physico-chemical factors, including food micro- and macro- structure (Bornhorst and Singh 2012). The formation of some foods into a bolus during mastication is likely to protect salivary enzymes from the acidic secretions of the stomach (Rosenblum *et al.* 1988). The bolus may thereby minimise

inactivation of salivary α -amylase during gastric transit and enable the salivary enzyme to contribute to starch hydrolysis in the small intestine (Fried *et al.* 1987). Chickpea cells, however, have a tendency to separate in an aqueous environment (Brett and Waldron 1996), and would therefore be less effective at forming a protective bolus. This could potentially leave any swallowed salivary α -amylase exposed to the gastric juices, which, at pH below 3.8, would be expected to reduce enzyme activity (Fried *et al.* 1987, Rosenblum *et al.* 1988). Furthermore, irrespective of bolus formation, the results presented in *Chapter 4* showed that chickpea cell walls act as barriers to porcine pancreatic α -amylase, which has a similar structure to salivary α -amylase. Hence, the limited digestion of starch encapsulated within chickpea cells by the salivary enzyme was not surprising.

Although starch digestion in the oral and gastric phases did not contribute significantly to total starch digestion, the pre-treatment of meals in these different conditions appeared to have consequences for subsequent starch amylolysis in the duodenal model. A slight reduction (up to ~5%) in the overall extent of starch digestion (i.e. cumulative effects of oral, gastric and duodenal stages) with prolonged gastric retention time was observed. This effect was evident for both test meals, but the magnitude of the reduction was greater after *Porridge-F*, prepared from freeze-milled cells, than *Porridge-O*, prepared from intact cells (**Figure 6.7**). This could be attributed to the preferential retention of larger particles, e.g., intact cells with very limited starch bioaccessibility, in the model stomach. The first material expelled from the DGM may therefore have contained a higher proportion of relatively smaller particles with more available substrate e.g., ruptured cells and free starch granules. This is a physiological phenomenon known as 'gastric sieving' and has been reported elsewhere, but generally for larger particles of 1-2 mm (Kong and Singh 2008). It is unclear if this effect also differentiates between smaller particles (intact cells ~0.2 mm vs. starch granules ~0.03 mm).

The down-ward trend in starch digestibility with increased gastric retention time is also interesting with regard to the suggestion that gastric proteases increase starch bioaccessibility (Jenkins *et al.* 1987). It seems that proteases are more likely to have an effect where a dense protein matrix is the predominant obstacle to amylase hydrolysis of starch (e.g., pasta) (Fardet *et al.* 1998, Woolnough *et al.* 2008). For the chickpea porridges used in this study, the cell walls seem to be the predominant barriers, and in fact, appear to hinder protease access also and therefore prevent intracellular protein digestion (Melito and Tovar 1995).

With regard to the cell wall barrier mechanism, the application of LOS analysis indicated that the majority of starch digested in *Porridge-F* occurred during the rapid phase, which probably represents digestion of available starch, released from the cells ruptured by freeze-milling. Unfortunately, it was not possible to quantify the ratio of ruptured to encapsulated cells in freeze-milled samples, but on the basis of 'ball-park' estimate from microscopy observations, it seems reasonable that the released starch accounts for up to 25% of total starch in *Porridge-F*.

For *Porridge-O*, in which majority of the starch was encapsulated by intact cell walls, some starch digestion still occurred, but predominantly at a relatively slower rate. This could indicate that the encapsulated starch is accessible to the enzyme, but perhaps structurally resistant to digestion (i.e. starch that has resistant properties such as retrograded starch). Retrogradation of starch would not be unexpected considering that the processing methods used in the preparation of these leguminous cells included prolonged storage following hydrothermal treatment.

Overall, the total extent of starch digestion observed for the porridge prepared from intact cells was higher than that observed previously (*Figure 4.2, page 135*), which suggests that the other enzymes and secretion of the oral, gastric and duodenal phases of digestion contribute to increased starch bioaccessibility. Nevertheless, only ~10% of the starch in the porridge prepared from intact cells was digested,

demonstrating clearly the resilience of chickpea cells, and supporting their potential for use as very low glycaemic index ingredients. Comparison of results obtained with chickpea meals with the literature on cereal foods exemplifies how the behaviour of different food materials can influence their susceptibility to oral, gastric and duodenal digestion, and is of great relevance to the future development of simple and complex *in vitro* models (Woolnough *et al.* 2008).

6.5 CONCLUSIONS

Chickpeas appear to remain intact during simulated gastric and duodenal digestion, and the cell wall encapsulated starch is largely undigested. The starch contained in *Porridge-F*, prepared from freeze-milled cells, was digested at a greater rate and to a greater extent. This supports the suggestion that it is the physical encapsulation of starch by plant cell walls that limits starch bioaccessibility in chickpeas. Although the overall extent of starch digestion observed following oral, gastric and duodenal conditions was higher than that observed with α -amylase only (*Chapter 4*), the total extent of bioaccessible starch in both porridge meals remained very low. Thus, these chickpea cells would be expected to elicit a low glycaemic response *in vivo*.

CHAPTER 7

IN VIVO EFFECTS ON POSTPRANDIAL METABOLISM

7.1 INTRODUCTION

The results of *in vitro* studies presented in *Chapters 4, 5 and 6* of this thesis indicate that the physical encapsulation of starch by plant cell walls can significantly reduce the rate at which starch hydrolysis products are released during digestion. Thus, intact plant cell walls would be expected to limit the rate at which glucose becomes available for absorption *in vivo*, and thereby attenuate the glycaemic response (Jenkins *et al.* 1982, Wolever *et al.* 1988). The consumption of foods which elicit a low glycaemic response has been associated with a reduced risk of developing diseases such as diabetes and cardiovascular disease (Jenkins *et al.* 2002, Wolever *et al.* 1992), and so the consumption of cell wall encapsulated starch may be of potential benefit to public health. Moreover, if a considerable proportion of the starch encapsulated within plant cells passes through the small intestine undigested, its fermentation by colonic microorganisms could also be beneficial in maintaining colonic health (Asp *et al.* 1996). The metabolic effects would, however, depend on the behaviour and integrity of endosperm cells during *in vivo* digestive transit, which has not been widely studied and could potentially differ from previous *in vitro* observations.

This chapter describes the results of a human dietary intervention study performed in ileostomy subjects to determine the effects of cell wall encapsulation on the extent of starch digestion and post-prandial metabolic responses, notably glycaemia and insulinaemia. Wheat was selected for these studies because it is currently used as an ingredient in a broader range of food products than chickpeas, and also because similar studies have already been performed on pulses (Noah *et al.* 1998, Golay *et al.* 1986).

7.1.1 NUTRIENT ABSORPTION AND POST-PRANDIAL METABOLISM

Following ingestion of a starch-rich meal, products of starch hydrolysis in the intestinal lumen (especially in the duodenum), are converted to glucose by mucosal (enterocyte) disaccharidases and absorbed into the hepatic portal vein, which carries this nutrient-

rich blood to the liver (Frayn 2010). The most direct means of measuring glucose absorption is therefore to catheterise the portal vein and monitor increases in glucose concentration; however, this is a very invasive procedure (Van Kempen *et al.* 2010, Ellis *et al.* 1995). A more common and less-invasive method is to measure post-prandial changes in glucose concentration in peripheral venous blood, which can, for instance, be drawn from a venous cannula in the forearm, as was done in the present study (Parada and Aguilera 2011, Jenkins *et al.* 1984).

The concentration of glucose in the peripheral blood is maintained within homeostatic limits by endocrine mechanisms, and reflects the balance between the rate of entry into plasma (e.g., nutrient absorption and mobilisation of stores) and the rate of removal (e.g., uptake by glycolytic tissues). Nevertheless, the absorption of glucose can be deduced from changes in peripheral concentrations (Horwitz *et al.* 1975), especially when the concentration of other hormones and markers of post-prandial metabolism are considered as well.

An overview of the main hormones involved in post-prandial glucose metabolism, gastro-intestinal motility and satiety is provided in **Figure 7.1**. Insulin is known as the primary hormone which acts to lower glucose concentration in the hyperglycaemic state, but other hormones, particularly Glucose-dependent Insulinotropic Peptide (GIP), promote insulin release in a glucose concentration dependant manner, and therefore also plays a role in glucose metabolism (Murphy and Bloom 2006). Cholecystokinin (CCK), Glucagon-like peptide (GLP-1) and Polypeptide YY (PYY) also play a role in influencing the digestion of food and the postprandial state, for instance by regulating gastro-intestinal motility and satiety (Wu *et al.* 2013). These hormones are secreted from enteroendocrine cells in response to the presence of nutrients such as glucose and fatty acids in the gastro-intestinal lumen, and their effects are mediated by actions on various targets, including the pancreas, gall bladder and vagal nerves (Murphy and Bloom 2006, Wu *et al.* 2013).

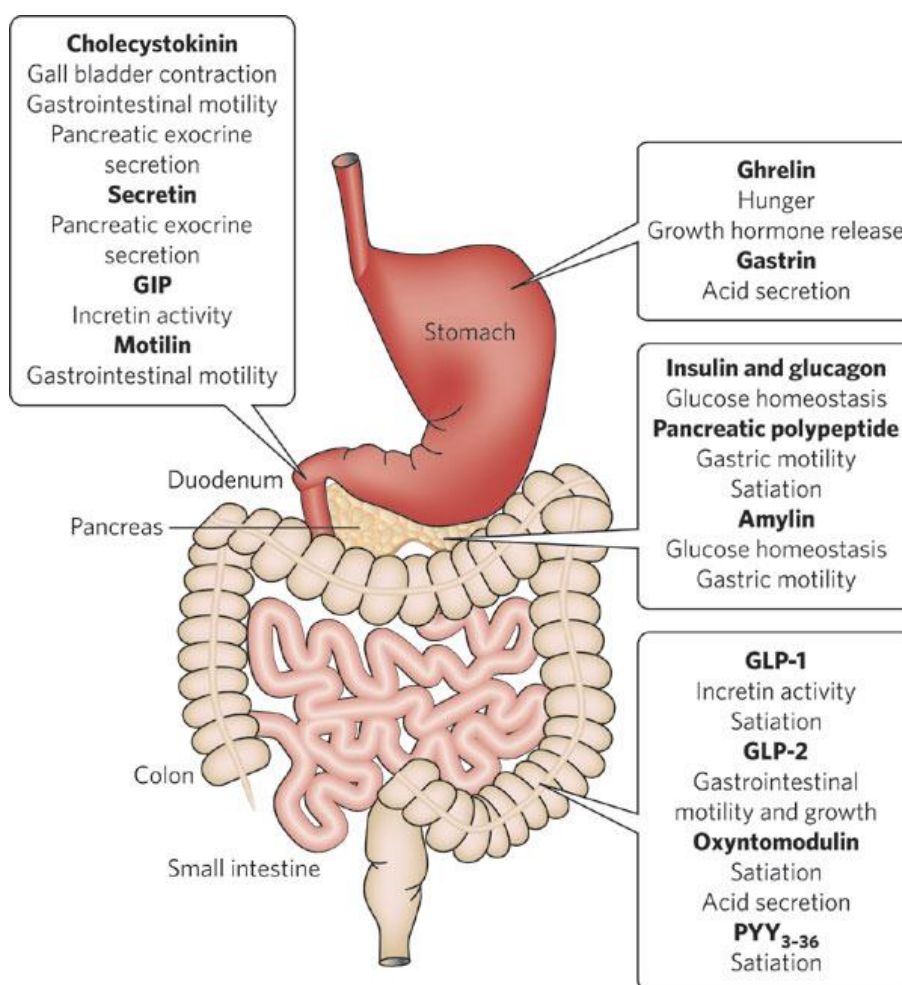


FIGURE 7.1: GUT HORMONES AND THEIR MAIN FUNCTIONS. Abbreviations: GIP, glucose-dependent insulinotropic peptide; GLP-1, GLP-2, glucagon like peptide -1 and -2; PYY, polypeptide YY. Taken from (Murphy and Bloom 2006).

Enteroendocrine cells are present throughout the entire gastrointestinal tract, but different regions of the gut tend to have higher concentrations of certain cell types: GIP and CCK are secreted from K- and I- cells (respectively) located predominantly in the upper small-intestine, whereas GLP-1 and PYY are both secreted from L-cells in the lower small intestine (ileum) and in the colon. Thus, the stimulation of the various cells is dependent on meal transit (Wu *et al.* 2013).

In the present work, the hormones CCK, GLP-1, GIP and PYY were measured, and are referred to as 'gut hormones'. In addition, C-peptide was measured as a useful marker of insulin secretion; C-peptide is cleaved from pro-insulin, and is secreted from the pancreas in equimolar amounts to insulin, but the metabolic clearance of C-peptide is

slower than insulin, and occurs at a constant rate, independent of meal ingestion, and is therefore a better marker of insulin release than insulin *per se* (Ellis *et al.* 1995, Horwitz *et al.* 1975).

The insulin and gut hormone responses to a predominantly carbohydrate meal may also elicit secondary effects on lipid metabolism. For instance, insulin and GIP suppress the mobilisation of fatty acids from lipolysis in adipose tissue, and a reduction in plasma non-esterified fatty acids (NEFA) concentrations can normally be observed following a carbohydrate-rich meal (Frayn 2010). Like glucose, NEFA, can be used as an energy source for muscle metabolism, and so the reduction of circulating NEFA promotes the utilisation of absorbed glucose after a meal (Saltiel and Kahn 2001). Insulin also promotes lipogenesis in adipose tissue, which involves the removal of lipoproteins that contain triacylglycerol (TAG) from the peripheral blood circulation and the storage of TAG within adipocytes. By this mechanism, circulating TAG concentrations would be reduced; however, the net-effect on TAG is more complex, because TAG may also simultaneously enter the blood from dietary or hepatic sources (Frayn 2010). The relationships between glycaemia, insulinaemia and lipaemia are not fully understood, but are likely to be of relevance with regard to understanding how the consumption of low glycaemic index foods can reduce the risk of cardiovascular disease (Jenkins *et al.* 2002, Ginsberg *et al.* 2005). For this reason, the postprandial concentrations of TAG and NEFA in peripheral blood were also measured in this study.

7.1.2 DIGESTION OF STARCH-RICH FOODS IN THE GASTRO-INTESTINAL TRACT

Although a number of post-prandial studies have reported that food structure influences the glycaemic and insulinaemic responses (Parada and Aguilera 2011, Jarvi *et al.* 1995, Golay *et al.* 1986), these previous studies rarely provide insight into the underlying mechanisms occurring in the gastrointestinal tract. Currently there is a limited understanding of how foods are digested and structurally disassembled during digestive transit to release the nutrients that give rise to these metabolic responses.

This information is of fundamental importance in view of the marked differences in starch digestibility that can arise from manipulating food structure, e.g., particle size, as shown in *Chapters 4 and 5*.

One important aspect of digestion which influences the metabolic response is where in the gastrointestinal tract nutrients (i.e. starch hydrolysis products) become available for absorption. For instance, when starch is digested by pancreatic α -amylase and mucosal disaccharidases in the small-intestine, the digestion products (i.e. glucose) are rapidly absorbed into the portal blood, and elicit a postprandial rise in the peripheral blood glucose concentration.

Starch which is not bioaccessible in the small intestine remains undigested and does not contribute metabolic energy until it reaches the colon. This type of starch is often referred to as 'resistant starch' or RS. The colon, however, hosts micro-organisms that are capable of digesting resistant starch and cell wall material. Hence, resistant starch is eventually digested in the colon, where it is broken down into short chain fatty acids, including butyrate, an important fuel for colonocytes (Cummings and Macfarlane 1968). These products of colonic starch fermentation contribute only a relatively minor amount (8.8 KJ/g fully fermentable RS) of energy to the host, compared with the ~16 KJ/g glucose absorbed in the small intestine, and are believed to be beneficial to human health (Cummings and Macfarlane 1991, Asp *et al.* 1996)

7.1.3 THE ILEOSTOMY MODEL

Measuring the amount of undigested starch in the faeces is not an accurate means of measuring the metabolic energy contribution of starch (Livesey *et al.* 2000). Rather, the examination of ileal effluent (i.e. digesta which leaves the small intestine) allows a distinction to be made between nutrient absorption in the small intestine, and the amount of unabsorbed nutrients which enter the large intestine as fermentation substrates.

The 'ileostomy model' (*Figure 7.2*) makes use of subjects who have undergone an operation to divert digesta from the small intestine out through a 'stoma' in the gut wall and into an external bag.

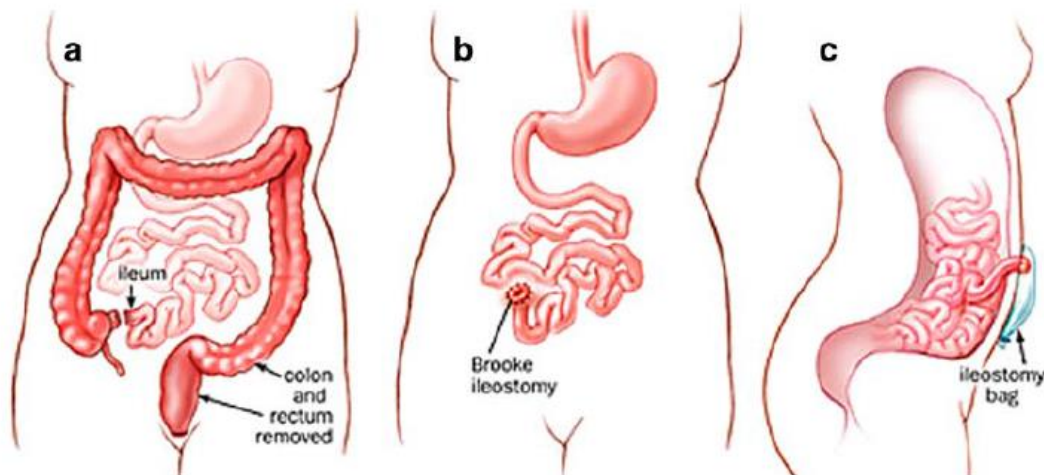


FIGURE 7.2: PHYSIOLOGICAL ASPECTS OF AN ILEOSTOMY. a) protocolectomy b) ileostomy and c) side-view showing ileostomy bag. The small intestine is formed into a stoma ('opening') (b), such that ileal effluent is diverted into an external ileostomy bag (c), rather than passing into the colon. Image reproduced from M'Koma *et al.*, 2007.

Patients normally undergo a protocolectomy because they suffer from chronic diseases of the colon, but may still have a healthy, normal-functioning upper gastro-intestinal tract after the operation (Andersson 1992). Hence, the ileostomy model provides a non-invasive means of recovering ileal effluent from human volunteers with a healthy small intestine.

The ileostomy model has a number of advantages: Firstly, it is particularly convenient for dietary intervention studies, due to the relatively rapid transit of a food to the terminal ileum, which means that all excreted meal components can generally be recovered within 24 h (Englyst and Cummings 1986). Secondly, unlike faecal excretion, ileal output is fairly consistent, with low day-to-day variations within individuals (Andersson 1992). Thirdly, despite the lack of an ileo-caecal valve and part of the distal ileum (usually ~5 – 10 cm), individuals with ileostomies appear to have similar transit

and ileal break mechanism to healthy, 'normal' individuals with a complete gastro-intestinal tract (Malagelada *et al.* 1984, Soper *et al.* 1990).

Although the ileostomy model is considered the 'gold-standard' for determination of resistant starch content, the model is not without limitations. Ileostomy subjects may have different microflora to those with a complete gastro-intestinal tract, and may also have a greater number of bacteria colonising the ileum (Ruseler-van-Embden *et al.* 1991, Finegold *et al.* 1970). The large differences observed between the ileal output of individuals is also difficult with regard to devising a standardised sampling protocol and also for outcome measures. This may be overcome using a repeated-measures design, in which the same subjects' responses to different dietary interventions are compared. Another issue is that sugars are known to result from the degradation of resistant starch in the external ileostomy bag, i.e. by bacterial glycosidase or residual pancreatic enzymes, and may lead to an underestimation of resistant starch (Ruseler-van-Embden *et al.* 1991, Layer *et al.* 1986). The summation of starch and sugar in ileal effluent may account for some of this degradation, and was therefore used to describe resistant starch in this study. Indeed, well-designed ileostomy studies have found a good agreement between *in vitro* and *in vivo* measurements of resistant starch (Silvester *et al.* 1995, Englyst and Cummings 1985, Muir and O'Dea 1993).

Overall, the ileostomy model has been widely used to study resistant starch and fibre, whereas postprandial studies (i.e. peripheral blood measurements) have been used to assess the metabolic response. Here, the analysis of ileal effluent and peripheral blood were considered together to provide novel insight into the relationship between the rate and extent of digestion, the metabolic response, and the amount of resistant starch delivered to the colon.

Unlike previous studies of food structure and glycaemia, which have used highly complex, heterogeneous test foods such as breads, flapjacks or other mixed meals (Golay *et al.* 1986, Holm and Bjorck 1992, Livesey *et al.* 1995), this study was carried

out using relatively simple porridge test meals prepared from well-characterised milled materials (as shown in previous chapters). These test meals were also designed to be consumed without prior-mastication, in order to gain novel insight into the degree of structural degradation that occurs in the stomach and small intestine.

7.1.4 HYPOTHESIS

On the basis of the different rates of release of starch hydrolysis products observed *in vitro*, it was hypothesised that a food made with coarse particles of wheat (i.e. containing a high proportion of encapsulated starch) would elicit a lower glycaemic and insulinaemic response than the same food made with wheat flour (i.e. containing no encapsulated starch). It was also hypothesised that the amount of resistant starch excreted at the terminal ileum would be similar for both test meals, reflecting the similar extent of starch digestion observed *in vitro*.

7.1.5 OBJECTIVES

An ileostomy study was designed to:

- a) Determine the effects of test foods containing variable amounts of encapsulated wheat starch on the post-prandial rise in blood glucose, insulin, C-peptide, TAG, NEFA and gut hormones GIP, GLP-1, PYY and CCK
- b) Determine the effects of test foods containing variable amounts of encapsulated wheat starch on the extent of digestion by measuring starch loss in the terminal ileum
- c) Examine the microstructural characteristics of the digested test foods with a special focus on the structural degradation (i.e. cellular integrity) of non-masticated foods during digestive transit through the stomach to the terminal ileum.

7.2 METHODS

7.2.1 ETHICAL CONSIDERATIONS

The study was approved by the National Research Ethics Service (South East Coast, Kent Ethics Committee, REC reference 12/LO/1016) and registered with www.isrctn.org. The International Standard Randomised Control Trial Number was ISRCTN40517475. The study was also approved by the Department of Research and Development (R&D), Guy's and St Thomas' NHS Foundation Trust (registration number RJ112/N237). Informed consent was obtained prior to enrolment on the study (see screening *Section*). Participants were informed that they were free to withdraw from the study at any point. Each participant was assigned an identification number at screening. Confidential information was kept in a secure locker and on a password protected encrypted hard drive, and was only accessible to designated researchers working on the trial (in accordance with the Data Protection Act 1988). All samples and data were labelled with an identification number to ensure anonymity. All samples were handled, transported and disposed of in accordance with the Human Tissue Act (2011). Participants were reimbursed for their time and travel expenses upon completion of the study. The use of the Clinical Research Facilities was authorised by an independent Scientific Advisory Board prior to commencement of the study. Screening and study day visits took place at the Clinical Research Facilities (CRF) at St Thomas' Hospital, London.

7.2.2 STUDY DESIGN

A single-blind (researcher-blind), randomized cross-over dietary intervention study was carried out in order to compare the ileal output and post-prandial metabolic responses to wheat porridge meals containing different amounts of cell wall encapsulation of starch. In this study, each subject attended on two occasions (at least one week apart) the Clinical Research Facilities (CRF), St Thomas' Hospital, London. During these

visits, subjects consumed the test meals in a randomly allocated order, and blood and ileal effluent was collected to assess the response to these meals.

Readers should note the original study design involved studies of starch and lipid bioaccessibility in the same subject cohort. Thus, the original study had two branches; Study 1 (lipid bioaccessibility in almond muffins) and Study 2 (starch bioaccessibility in wheat). However, Study 1 was terminated because the almond meals were not well-tolerated by the ileostomy subjects. Only results from Study 2 are described in this thesis.

7.2.2.1 POWER CALCULATION

An *a-priori* power calculation was carried out to estimate the number of subjects needed for the study. Because no similar study has previously been carried out, the power calculation was based on the ~30% difference in the hydrolysis index (up to 90 min) observed between coarse particles (1.85 mm) and flour (0.11 mm) in *Chapter 5*, because the HI generally correlates well with the glycaemic response (Goñi *et al.* 1997). The calculation was carried out using a standard deviation of 38%, as reported in a similar study for bread (Kristensen *et al.* 2010).

This power calculation (performed using G-Power[®] 3.1.2 software) predicted that 12 subjects would give 86% power to detect a significant difference ($P < 0.05$) in the area under the plasma glucose curves ($t = 90$ min) between the two test meals.

7.2.3 SUBJECTS

Male and female volunteers between the ages of 20 and 76 who had undergone a proctocolectomy and were stable for at least 12 month post-operation were recruited through the Ileostomy Association, London, and through an article published in the Securicare patient magazine (Edwards *et al.* 2013). Volunteers who expressed an interest in taking part in the study were sent a participant information sheet (approved by South East Coast Kent Ethical Committee) and were asked to complete two pre-

screening questionnaires about their general health and dietary habits. The participant information sheet explains the study in 'layman's terms' and is provided in *Appendix A: 'Participant information sheet'*.

Those volunteers who were likely to be eligible to participate in the study were invited to attend a screening visit which involved anthropometric measurements, blood analysis, and a medical examination to assess eligibility (*Appendix B: 'Subject screening process'*). Fasting plasma glucose concentration, BMI, blood pressure, liver function and blood cell counts were confirmed to be within prescribed limits before subjects were enrolled onto the study. To be included on the study the subjects needed to be healthy, with no history of diabetes or signs of diagnosed gastro-intestinal condition (apart from the ileostomy), and this was confirmed by means of history and a medical examination. Subjects not meeting the entry criteria were excluded at this stage.

Exclusion criteria included; Body Mass Index (BMI) of $< 20 \text{ kg.m}^{-2}$ or $> 35 \text{ kg.m}^{-2}$, fasted glucose $>7 \text{ mmol.L}^{-1}$, plasma cholesterol $>7.8 \text{ mmol.L}^{-1}$, or plasma triacylglycerides $>3 \text{ mmol.L}^{-1}$.

The usual dietary habits of individual subjects were assessed from a three-day diet diary (provided at screening), and the nutrient intake was analysed using NetWisp v.3.0 (©Tinuviel Software, United Kingdom).

7.2.4 TEST MEALS

Full details of the preparation of the test meals are provided in *Appendix C: 'Preparation of test meals'*. In brief, the test meals were a smooth or coarse porridge, prepared by hydrothermally processing small or large milled particles (see *Section 2.1.2*) of durum wheat endosperm in water and seasoning with low-sugar blackcurrant flavouring. The same amount of flavouring was added to each meal, to prevent any confounding effects.

'Smooth porridge' was prepared from ~0.11 mm particles (no encapsulated starch).

'Coarse porridge' was prepared from ~1.85 mm particles (62% encapsulated starch).

An overview of the ingredients and nutrients in each test meal is provided in **Table 7.1**. All test meals were prepared fresh and served immediately to minimise starch retrogradation. The liquid component of the meal was standardised at 449 mL using a convenient look-up table which specified the volume of drinking water required to account for differences in evaporative losses. Subjects were instructed to swallow the porridge without chewing, and consumed the meals within the allocated 15 min time-frame.

TABLE 7.1: TEST MEAL NUTRITIONAL CHARACTERISTICS

	SMOOTH PORRIDGE	COARSE PORRIDGE
INGREDIENTS (per 604 g serving) ¹		
Fine durum wheat (g)	77	0
Coarse durum wheat (g)	0	77
Jam (g) ²	17	17
Jelly (g) ²	61	61
Added Water (g)	449	449
NUTRIENTS (per 604 g serving) ¹		
Energy (kJ)	1239	1239
Energy (kcal)	293	293
Protein (g)	9.3	9.3
Carbohydrate (g)	57.7	57.7
of which starch (g)	55.4	55.4
of which sugars (g)	2.4	2.4
Fat (g)	1.6	1.6
Saturated fat (g)	0.02	0.02
Fibre (g)	5.2	5.2
Salt (g)	0.15	0.15
Moisture (g) ¹	459	459

¹ Portion size and moisture content include the glass of water served with the meal ²Flavouring (jam + jelly) provided 7.5 g carbohydrate of which 5.4 g starch and 2.1 g sugar, and 0.6 g fibre (32 kcal), per serving.

An overview of the test meal characteristics is provided in **Table 7.2**. Both porridge meals contained 55.4 g starch but differed in their expected starch bioaccessibility, because they contained contrasting proportions of cell wall encapsulated starch.

TABLE 7.2: CHARACTERISTICS OF DURUM WHEAT PARTICLES USED IN TEST MEALS

	SMOOTH PORRIDGE	COARSE PORRIDGE
STRUCTURE	(no encapsulated starch)	(encapsulated starch)
Median particle size (mm)	0.11	1.85
Particle size range (mm)	0.00 - 0.21	1.70 - 2.00
Intact Cells (%)	0	62
Ruptured Cells (%)	~100	38
<i>IN VITRO</i> DIGESTIBILITY		
Total C _∞ (% digestible starch)	63.7	49.5
HI ₉₀ (%)	100	67
Digestion kinetics	Rapid (mono-phasic)	Slow (bi-phasic)

The proportion of intact cells was estimated by geometric means, as described in *Chapter 3*

Total C_∞ is the proportion of total starch that was digested *in vitro*, and was determined in *Chapter 5*

HI₉₀ (%) is the extent of starch hydrolysis after 90 min, relative to smooth porridge (100%).

7.2.4.1 RANDOMIZATION AND BLINDING

A double-blind study was not possible as the different test meals (porridge made from large or small particles) could easily be identified on the basis of their physical appearance. A single-blind approach was used, in which each test meal was assigned a blinding code (A or B) by a researcher independent to the study. This code was subsequently used as an identifier such that the researcher performing the analysis was blinded to avoid experimenter's bias. Due to the nature of the methods required for the preparation of the test meal, an additional, un-blinded researcher was required to prepare the porridge.

The order in which volunteers received dietary intervention A or B was randomly assigned using a random number generator (Microsoft Excel 2007). All participants received each intervention once.

7.2.5 STUDY PROTOCOL, SAMPLE COLLECTION AND ANALYSIS

An overview of the sample collection time points and meal times during a study visit day is provided in **Figure 7.3**.

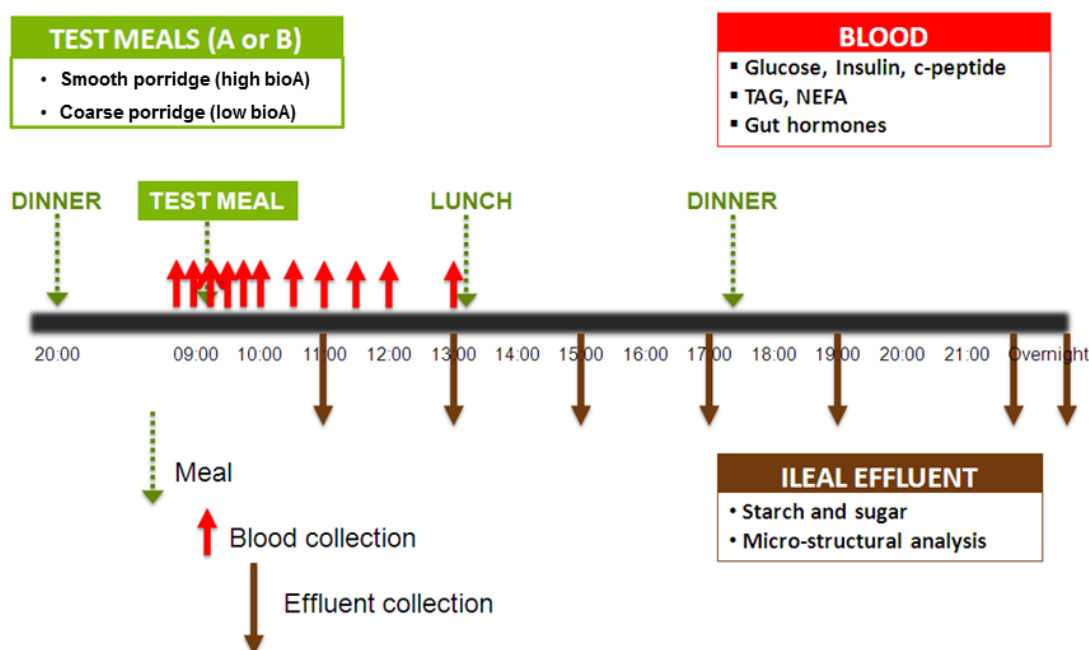


FIGURE 7.3: BLOOD AND EFFLUENT COLLECTION TIME POINTS AND MEAL TIMES. Blood samples were collected at regular intervals up to 4 h and ileal effluent was collected every 2 h. Overnight samples were collected at variable time points between 10 h and 24 h, at the subjects' convenience. To inhibit enzymic and chemical deterioration of carbohydrates (e.g. starch) and other nutrients in the effluent samples were preserved in ethanol or by freezing at the time of collection. Abbreviations: bioA - bioaccessibility; TAG- triacylglycerol; NEFA- non-esterified fatty acids;

Full details of blood sample handling, processing and analysis are provided in *Appendix D: 'Blood sample collection, processing and analysis'*. In brief, subjects consumed the test meal at 0 h. Bloods were collected from a venous cannula on the forearm at -15, 0, 15, 30, 45, 60, 90, 120, 150, 180, and 240 min and dispensed (using a syringe) into various 4 mL BD vacutainers® preloaded with different additives (see *Table D1 in Appendix D*). These blood samples were centrifuged and aliquoted for storage and later analysed for glucose, insulin, C-peptide, TAG, NEFA, GIP, GLP-1, CCK, and PYY. Glucose (glucose oxidase ILTest™ kit), TAG (triglycerides ILTest™ kit) and NEFA (Randox NEFA kit), were determined at King's College London using colorimetric assay methods on an iLab 650 Autoanalyser. Insulin, C-peptide and gut hormones (GIP, GLP-1, CCK, and PYY) were analysed by GSTS pathology using chemiluminescence- or immunoassays. These methods are described further in *Appendix D*.

Full details of the collection, handling and analysis of ileal effluent are provided in *Appendix E: 'Ileal effluent sample collection, processing and analysis'*. Essentially, subjects were required to empty or replace their ileostomy pouch shortly before consuming the test meals. Ileal effluent was collected thereafter every 2 h and overnight, and was immediately sub-sampled into tubes loaded with 8 mL ethanol for starch and total reducing sugars (maltose equivalents) determination, into 2.1 mL cryotubes for moisture determination, and into vials with Karnovsky's fixative for microscopy. Wherever possible, the effluent was blended with a hand-blender before sub-samples for starch, sugar and moisture analysis were taken (microscopy samples were taken before blending). Moisture samples were immediately frozen and stored at -80°C prior to analysis using oven-drying method (*Section 2.3.2, page 81*). Samples for starch and sugar analyses were stored in ethanol at 4°C and analysed using high-throughput versions of the Total Starch and DNS assays (*Section 2.3.3 and 2.3.4.1*). Microscopy samples were fixed, dehydrated, cured in LR white resin, sectioned and stained (*Section 2.4.1*).

The overnight effluent samples were collected by the subjects during the night, and immediately placed between 4 pre-cooled eutectic freezer blocks in a polystyrene box for rapid freezing to minimise sample degradation (see *Appendix E*). Overnight samples were de-frosted, sub-sampled and analysed as described above.

7.2.6 MEALS PROVIDED DURING STUDY VISITS

The pooled average nutrient content (calculated from the nutrient declaration on food packaging) of the meals provided during the study visits is shown in **Table 7.3** together with the nutrient content of the test meal. It is noteworthy that subjects were required to eat an identical menu for each study visit; however, this menu was not standardised across all subjects because of differences in dietary requirements and/or preferences. An overview of the different meal options is provided in *Appendix F: 'Meal options for study visit menu'*

The test meal provided a total of 57.7 g of carbohydrate (55.4 starch, 2.4 g sugars). Lunch was provided immediately after the last blood collection and 4 h effluent sample, and consisted of a leafy salad with a protein-rich topping. Dinner meals consisted of mashed potato, which contains a starch that is readily digested and absorbed (Englyst and Cummings 1987), with beef, chicken or fish topping, and were served with a high-calorie dessert (360 – 420 kcal/portion). A low-fibre ready meal was also provided for the evening before the study visits.

TABLE 7.3: NUTRIENT INTAKE DURING STUDY VISIT

	TEST MEAL	LUNCH	DINNER	DESSERT	DAILY INTAKE
Calories (kcal)	293.	621	607	389	1910
Protein (g)	9.3	41.2	34.8	5.2	90.5
Carbohydrate (g)	57.7	45.3	67.6	35.9	206.5
of which starch (g)	55.4	3.9	39.5	9.8	108.6
of which sugars (g)	2.4	41.34	28.1	26.1	97.9
Fat (g)	1.6	29.5	19.7	25.2	76.0
Saturated fat (g)	0.0	13.2	11.1	14.6	38.9
Fibre (g)	5.2	3.1	11.8	2.2	22.4
Salt (g)	0.2	2.4	2.3	0.1	5

Values shown are g per portion and are the average values for the range of meal options provided. Side dishes and drinks are included.

Subjects were advised to sip a total of 1 L water within the first 4 h of the visit, and another 1 L before leaving the facilities, however some deviations occurred depending on each individuals habits and perceived stoma function, and this was monitored.

7.2.7 DATA PROCESSING AND STATISTICAL ANALYSIS

All data was found to be normally distributed (Shapiro-Wilk, $P > 0.05$). Primary data processing was performed in Microsoft Excel 2007. Postprandial blood concentrations were converted to incremental values by subtracting the fasted concentrations. Mean transit time (MTT) was calculated from the starch content of ileal effluent as shown in **Equation 7.1** (Englyst and Cummings 1985):

$$MTT (h) = \frac{\sum_0^N (\text{Starch in sample } x \text{ } t)}{\text{Total starch recovered}}$$

EQUATION 7.1: CALCULATION OF MEAN TRANSIT TIME. *MTT* is calculated from the starch recovered in each sample at a collection time point, *t*. Adapted from (Englyst and Cummings 1985).

Graphs were created in SigmaPlot 12.0, and statistical analysis was performed using SPSS. Incremental areas under the curve (iAUC) were calculated using the macro available in SigmaPlot 12.0. Repeated Measures Analysis of Variance (ANOVA) was performed with time as the 'within' factor and test meal as the 'between' factor. Student's paired t-tests (two-tailed) were used as a *post-hoc* analysis to identify significantly different values between the two meals when there was a significant diet x time effect. Statistically significant effects were accepted at the 95% level.

7.3 RESULTS

7.3.1 SUBJECT DETAILS

The flow of study participants through the study is shown in **Figure 7.4**. Out of the 13 participants enrolled ('allocated') on the starch study (study 2), 9 completed both visits: Two volunteers (one male and one female) experienced an adverse reaction on the almond branch (study 1) of the study which affected their participation in the starch study. Numbers were further reduced after the first starch study visit, because one male volunteer was found to have abnormally high fasted glucose concentration ($>7\text{mmol.L}^{-1}$), despite having a normal value at screening, and was therefore excluded. During the second and final visit, another male experienced illness potentially associated with the study meals, and decided to withdraw from the study.

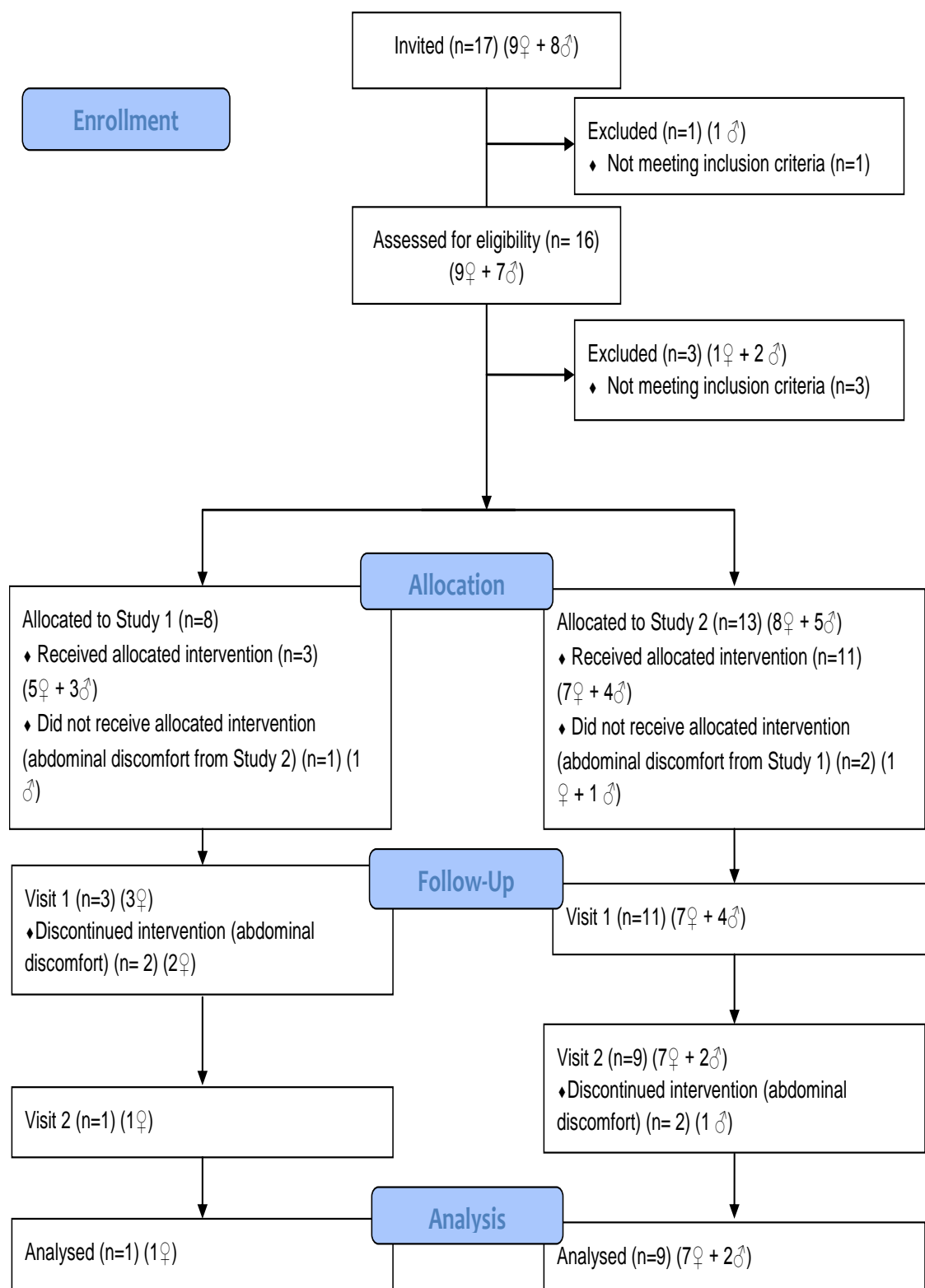


FIGURE 7.4: CONSORT DIAGRAM. ‘Invited’ refers to subjects invited to screening. Volunteers (female, ♀ and male ♂) were excluded on the basis of inclusion/exclusion criteria as outlined in *Section 7.2.3*. Study 2 refers to the starch bioaccessibility study described in this chapter, whereas Study 1 refers to a parallel study on lipid bioaccessibility that was later discontinued.

Although the number of drop-outs were slightly higher than the anticipated 20% drop-out rate, a retrospective power calculation confirmed that the final sample size (n=9) provided reasonable statistical power (>74%) to detect postprandial differences in glucose and insulin responses following the two different test meals.

Details of the nine subjects included in the study are shown in **Table 7.4**. All had undergone a colectomy for ulcerative colitis, pure colonic form of Crohn's disease, or lower bowel cancer, at least one year prior to taking part in the study, and had a healthy small bowel with well-functioning ileostomies with < 10 cm intestine removed. The cohort covered a broad age range (20 – 76 y), but because of the drop-out and exclusions of enrolled male subjects throughout the study, the final cohort had more females (7) than males (2). Dietary intake, blood pressure, BMI, fasted plasma glucose, triglycerides (TAG) and cholesterol concentrations were all within normal range, and the subjects were of good health.

TABLE 7.4: CHARACTERISTICS OF THE NINE SUBJECTS INCLUDED IN THE STUDY

	MEAN ± SD
Age (years)	47.8 ± 18.0
BMI (kg/m²)	23.9 ± 3.9
Waist (cm)	83.3 ± 11.8
Hip (cm)	100.7 ± 6.9
Systolic Blood Pressure (mmHg)	110.3 ± 16.1
Diastolic Blood Pressure (mmHg)	70.3 ± 9.2
Pulse (beats.min⁻¹)	69.1 ± 12.3
Plasma Glucose (mmol.L⁻¹)	5.1 ± 0.7
Plasma Triacylglycerides (mmol.L⁻¹)	1.0 ± 0.4
Plasma Cholesterol (mmol.L⁻¹)	4.9 ± 0.9
Dietary Intake	
Energy (MJ/d)	8.01 ± 3.26
Energy (kcal/d)	1938 ± 765
Protein (g/d)	96.3 ± 53.8
Carbohydrate (g/d)	191.1 ± 80.3
of which starch (g/d)	98.3 ± 49.3
of which sugars (g/d)	89.8 ± 43.2
Fat (g/d)	78.5 ± 32.6
of which saturates (g/d)	26.8 ± 10.7

n = 9, of which 7 females + 2 males . Dietary intake as analysed by NetWisp 3.0 (Tinuviel® software).

All values are mean ± standard deviation

7.3.2 POST-PRANDIAL RESPONSES MEASURED IN PERIPHERAL BLOOD

The post-prandial blood response provides an indication of the rate and extent of nutrient absorption (e.g., glucose) into the blood, and is likely to reflect the rate at which nutrients are released from food (i.e. become available for absorption or 'bioaccessible') during luminal digestion.

7.3.2.1 EFFECTS ON GLUCOSE, INSULIN AND C-PEPTIDE

The pooled mean (\pm SEM) of fasted glucose, insulin and C-peptide concentrations measured from visits 1 and 2 was 5.4 ± 0.15 mmol.L⁻¹, 44 ± 7 pmol.L⁻¹, 683 ± 54 pmol.L⁻¹, respectively. The fasted values were within normal range, and did not differ significantly between the two occasions on which the subjects received the test meals. The changes in plasma glucose, insulin and C-peptide concentrations after the test meals are shown in **Figure 7.5**, with insets showing the incremental area under the curve (iAUC) over 120 min.

The pattern of the post-prandial glucose, insulin and C-peptide curves differed significantly after the two test meals (meal x time; $P < 0.05$, ANOVA). The smooth porridge (55.4 g starch), which consists of highly bioaccessible starch, elicited a rapid and large glycaemic response, in which glucose concentrations dropped below fasted concentrations 150 min after ingestion of the test meal. In contrast, the coarse porridge, made with low bioaccessible starch (i.e. intact cells), elicited a smaller rise in blood glucose and insulin concentrations, and the glucose levels remained above fasted levels throughout the entire 4 h period.

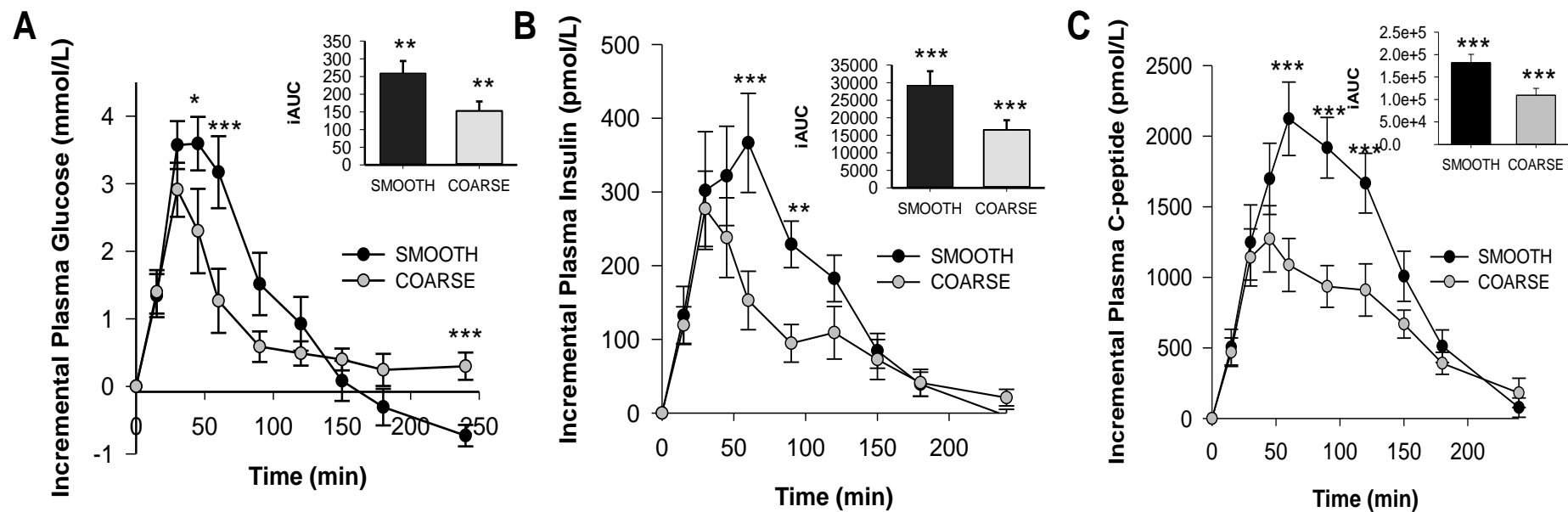


FIGURE 7.5: INCREMENTAL GLUCOSE (A), INSULIN (B) AND C-PEPTIDE (C) RESPONSE AFTER SMOOTH AND COARSE PORRIDGE TEST MEALS. Each meal provided 55.4 g starch. Values are mean deviations from baseline \pm SEM ($n=9$) and were analysed by ANOVA, with meal and time (0-240 min) as factors. Meal, time, and meal \times time effects were significant for glucose, insulin and C-peptide responses ($P<0.05$). Time-points at which values differed significantly between the two meals are annotated with an asterisk; $*P < 0.05$, $**P < 0.01$ and $***P < 0.001$ (paired Students t-test). Insets show iAUC (0 -120 min)

The key parameters of the glycaemic and insulinaemic responses to each test meal are compared in **Table 7.5**.

TABLE 7.5: KEY PARAMETERS OF THE GLYCAEMIC AND INSULINAEMIC RESPONSE TO TEST MEALS

	Smooth Porridge	Coarse Porridge	P-value	Difference (%)
Glucose				
Fasted (mmol.L ⁻¹)	5.3 ± 0.2	5.4 ± 0.3	0.367	
Time to Peak (min)	42 ± 4	33 ± 3	0.095	
Peak Maximum (mmol.L ⁻¹)	9.6 ± 0.4	8.5 ± 0.4	0.009*	11%
iPeak (mmol.L ⁻¹)	4.3 ± 0.4	3.1 ± 0.4	0.004**	28%
iAUC90 (mmol.L ⁻¹ .min ⁻¹)	222.5 ± 24.5	156.0 ± 19.0	0.003**	30%
iAUC120 (mmol.L ⁻¹ .min ⁻¹)	259.2 ± 34.4	173.3 ± 18.6	0.006**	33%
Insulin				
Fasted (pmol.L ⁻¹)	39 ± 11	48 ± 10	0.084	
Time to Peak (min)	63 ± 9	47 ± 13	0.375	
Peak Maximum (pmol.L ⁻¹)	491 ± 75	371 ± 49	0.091	
iPeak (pmol.L ⁻¹)	451 ± 66	322 ± 42	0.000***	29%
iAUC120 (pmol.L ⁻¹ .min ⁻¹)	29205 ± 4025	16534 ± 2742	0.001***	43%
iAUC240 (pmol.L ⁻¹ .min ⁻¹)	36125 ± 3144	22469 ± 3886	0.061	38%
C-peptide				
Fasted (pmol.L ⁻¹)	646 ± 79	720 ± 75	0.327	
Time to Peak (min)	73 ± 10	62 ± 13	0.486	
PeakMaximum (pmol.L ⁻¹)	3050 ± 212	2230 ± 208	0.000*	27%
iPeak (pmol.L ⁻¹)	2404 ± 189	1510 ± 177	0.000***	37%
iAUC120 (pmol.L ⁻¹ .min ⁻¹)	182017 ± 18580	109399 ± 15406	0.001***	40%
iAUC240 (pmol.L ⁻¹ .min ⁻¹)	262587 ± 25586	166093 ± 22327	0.003**	37%

Values shown are means ± SEM (n=9). 'iPeak' is the maximum change from fasted values. 'iAUC' is the incremental area under the curve for specified time period. P-values indicate differences between test meals as determined by paired t-test. Significant differences are indicated; *P < 0.05, **P < 0.01 and ***P < 0.001. 'Difference' is the % reduction in values observed from smooth to coarse porridge and is shown where significant differences were observed.

In most subjects, plasma glucose and insulin concentrations generally reached peak values within 60 min of receiving the test meals. The peak concentrations of glucose and insulin were significantly higher (28% and 29%) after smooth compared to coarse porridge. The iAUC for glucose was measured between 0 and 120 min, due to the negative incremental values observed after this time point, and also between 0 and 90 min, because this provides for useful comparison to starch hydrolysis index values obtained *in vitro*. After 120 min, the glucose iAUC was 33% lower and the insulin iAUC 43% lower after consumption of coarse porridge compared to smooth porridge. These glycaemic differences are compatible with the 33% difference between the two test

meals' Hydrolysis Index (**Table 7.2**), obtained from *in vitro* and *in silico* studies (*Chapter 5*). The differences in the glycaemic responses to the different test meals is therefore likely to reflect the higher proportion of bioaccessible starch in the smooth porridge, which contained no intact cells, compared to the coarse porridge which contained intact cells.

7.3.2.2 EFFECTS ON TAG AND NEFA

The pooled mean (\pm SEM) of fasted TAG and NEFA concentrations measured from visits 1 and 2 was 1.17 ± 0.07 mmol.L⁻¹ and 0.58 ± 0.05 mmol.L⁻¹, respectively. The fasted values were within normal range and did not differ significantly between the two occasions on which the subjects received the test meals. The changes in plasma TAG and NEFA concentrations after the test meals are shown in **Figure 7.6**.

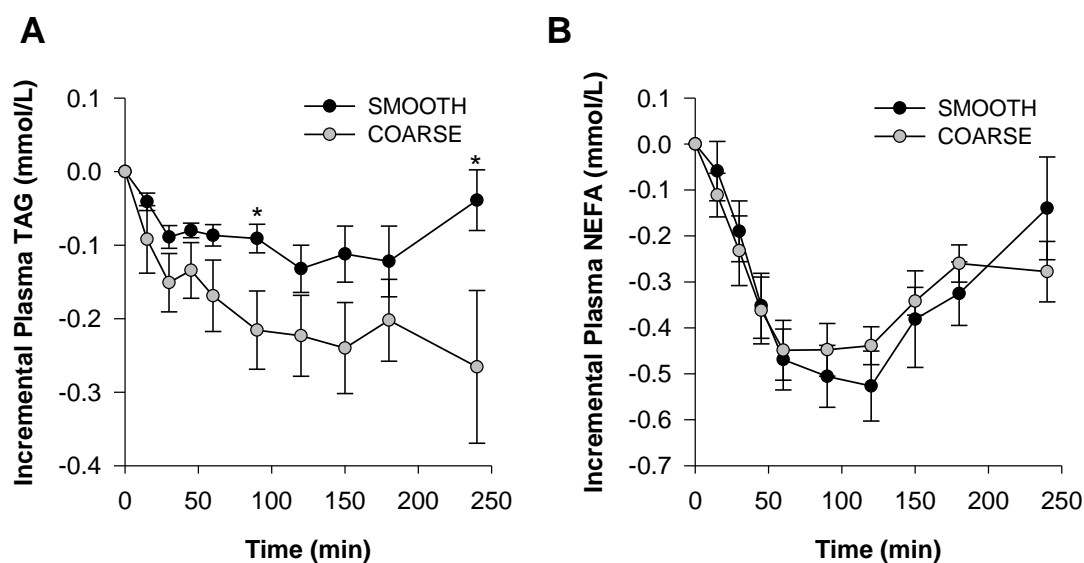


FIGURE 7.6: INCREMENTAL TAG (A) AND NEFA (B) RESPONSE TO SMOOTH AND COARSE PORRIDGE TEST MEALS. Each meal provided 1.56g fat. Values are mean deviations from baseline \pm SEM (n=9) and were analysed by ANOVA, with meal and time (0-240 min) as factors. Effect of time was highly significant TAG (P=0.04) and NEFA (P<0.001), but overall meal and meal x time effects were not significant. Time-points at which values differed significantly between the two meals are annotated with an asterisk; *P < 0.05, as determined by paired t-test.

Plasma NEFA concentrations decreased linearly from fasted concentrations within the first 60 min, then gradually increased again towards the end of the 4 h time period. A gradual reduction in plasma TAG was also observed. These time-effects were significant ($P < 0.01$), demonstrating that the administration of low-fat, high-carbohydrate meals caused significant differences in postprandial changes in lipid metabolism. These effects are probably associated with insulin stimulated mechanisms which cause a net-reduction in TAG and NEFA concentrations in peripheral blood.

Statistical analysis showed that the test meals (1.56 g fat), had no effect on the pattern of the response curves (meal x time effect; $P = 0.100$ for TAG and $P = 0.249$ for NEFA), however there was a tendency for a lower TAG response following the coarse porridge (**Figure 7.6A.**)

Average values for parameters of the lipaemic response are provided in **Table 7.6.**

TABLE 7.6: KEY PARAMETERS OF THE LIPAEMIC RESPONSE TO TEST MEALS

	Smooth Porridge	Coarse Porridge	P-value
TAG			
Fasted (mmol.L ⁻¹)	1.13 ± 0.11	1.21 ± 0.07	0.281
Time to Peak (min)	102 ± 23	157 ± 22	0.270
Peak Minimum (mmol.L ⁻¹)	0.94 ± 0.12	0.86 ± 0.10	0.422
iPeak (mmol.L ⁻¹)	-0.19 ± 0.03	-0.34 ± 0.09	0.083
iAUC240 (mmol.L ⁻¹ .min ⁻¹)	21.83 ± 5.30	46.9 ± 12.32	0.004**
NEFA			
Fasted (mmol.L ⁻¹)	0.61 ± 0.07	0.56 ± 0.06	0.414
Time to Peak (min)	120 ± 10	93 ± 13	0.021*
Peak Minimum (mmol.L ⁻¹)	0.06 ± 0.01	0.07 ± 0.01	0.402
iPeak (mmol.L ⁻¹)	-0.55 ± 0.07	-0.49 ± 0.06	0.255
iAUC240 (mmol.L ⁻¹ .min ⁻¹)	80.8 ± 15.6	77.6 ± 9.1	0.808

Values shown are means ± SEM (n=9). 'iPeak' is the maximum change from fasted values, and negative numbers indicate a reduction. 'iAUC' is the incremental area under the curve for the specified time period. Significant differences between test meals as determined by Student's paired t-test are indicated; *P < 0.05, **P < 0.01.

TAG and NEFA concentrations both decreased from fasted values after consumption of the test meals (**Figure 7.6**). The greater reduction in circulating TAG concentrations (**Table 7.6**; iAUC 240 min for TAG, paired-test, $P < 0.01$) was observed after coarse

porridge compared with smooth porridge, and probably reflects the net-effect of insulin, which was secreted to a greater extent in response to smooth porridge, compared with coarse porridge.

7.3.2.3 EFFECTS ON GUT HORMONES

The changes in GIP, GLP-1, PYY and CCK concentrations in peripheral blood after ingestion of the test meals are shown in **Figure 7.7**.

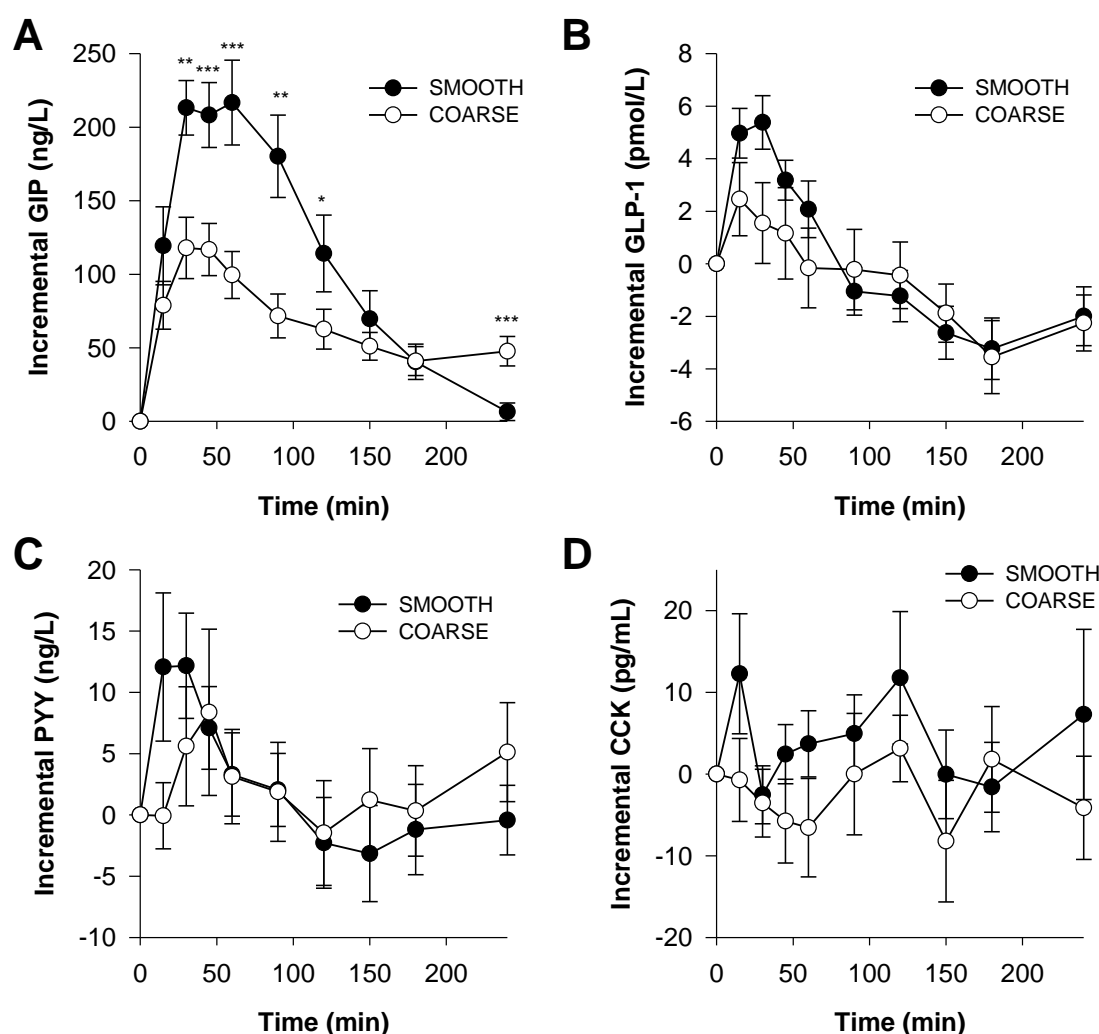


FIGURE 7.7: CHANGES IN PLASMA GUT HORMONES AFTER SMOOTH AND COARSE PORRIDGE MEALS.

Values are mean deviations from baseline \pm SEM. **(A)** GIP; Glucose-dependent Insulinotropic Polypeptide (n=8), **(B)** GLP-1; Glucagon-Like Peptide-1 (n=7), **(C)** PYY; Peptide YY (n=7), **(D)** CCK; Cholecystokinin (n=8). ANOVA: Significant time (4 h) and meal \times time effects (4 h), respectively for GIP ($P < 0.001$, $P < 0.001$), GLP-1 ($P < 0.001$, $P = 0.009$), and PYY ($P = 0.002$, $P = 0.053$), but not CCK. Meal effect was significant for GIP only ($P = 0.024$). Time-points at which values differed significantly between the two meals; * $P < 0.05$, ** $P < 0.01$ and *** $P < 0.001$ (paired t-test).

The concentrations of GIP, GLP-1 and PYY all increased rapidly following consumption of the test meals (**Figure 7.7**). After ~90 min, GLP-1 and PYY dropped below fasted concentrations. The concentration of GIP also began to decline after ~60 min, but remained elevated above fasting concentrations for the entire 240 min period over which blood samples were collected. Average values for parameters of the endocrine ('gut hormone') response are provided in **Table 7.7**. Interestingly, the smooth porridge elicited a significantly larger GIP response, almost double (81% higher *iPeak* value) than that elicited by the coarse porridge. The peak PYY concentration was also reached significantly earlier after consumption of smooth porridge (28 min) compared with coarse porridge (129 min).

TABLE 7.7: KEY PARAMETERS OF THE GUT HORMONE RESPONSE TO TEST MEALS

	Smooth Porridge	Coarse Porridge	P-value
GIP (n=7)			
Fasted (ng.L ⁻¹)	32 ± 6.9	37.7 ± 7.3	0.295
Time to Peak (min)	45 ± 6	34 ± 3	0.140
Peak Maximum (ng.L ⁻¹)	266.2 ± 26.4	166.9 ± 19.7	0.000***
<i>iPeak</i> (ng.L ⁻¹)	234.2 ± 26.1	129.2 ± 18.4	0.000***
GLP-1 (n=8)			
Fasted (pmol.L ⁻¹)	12.5 ± 2.5	13.0 ± 2.7	0.741
Time to Peak (min)	32 ± 5	53 ± 15	0.245
Peak Maximum (pmol.L ⁻¹)	18.5 ± 2.4	17.0 ± 2.5	0.338
<i>iPeak</i> (pmol.L ⁻¹)	6.0 ± 0.9	4.0 ± 1.8	0.210
PYY (n=7)			
Fasted (ng.L ⁻¹)	50.9 ± 3.6	49.2 ± 3.2	0.569
Time to Peak (min)	28 ± 5	129 ± 34	0.030*
Peak Maximum (ng.L ⁻¹)	66.9 ± 5.6	65.0 ± 6.1	0.827
<i>iPeak</i> (ng.L ⁻¹)	16.0 ± 5.3	15.7 ± 4.9	0.970
CCK (n=8)			
Fasted (pg.mL ⁻¹)	65.5 ± 12.1	73.0 ± 14.5	0.523
Time to Peak (min)	133 ± 21	118 ± 22	0.465
Peak Maximum (pg.mL ⁻¹)	87.5 ± 16.3	85.4 ± 13.9	0.753
<i>iPeak</i> (pg.mL ⁻¹)	22.0 ± 8.2	12.4 ± 4.7	0.415

Values shown are means ± SEM (n=9). 'n' is the number of subjects. 'iPeak' is the maximum change from fasted values, and negative numbers indicate a reduction. Significant differences between test meals as determined by Student's paired t-test are indicated; *P < 0.05, ***P < 0.001.

Out of the 9 subjects that completed the study, gut hormone data is shown for only 7 or 8 subjects. The explanation for this is that the samples for gut hormone analyses could not be collected from one subject because of difficulty in drawing enough blood at the specified time points. On primary data processing, a set of GIP data from one subject and PYY data from another subject were identified as outliers (outside >2 SD of the mean). Because of the repeated measures design, it was necessary to exclude the GIP or PYY data obtained following both meals for these subjects from the statistical analyses.

7.3.3 ILEAL OUTPUT & MEAL TRANSIT

An overview of ileal output (shown for 0-10 h, 'daytime', only) following the two test meals is provided in **Table 7.8**. The smooth and coarse porridges (55.4 g starch) did not appear to have any significant effects on the total amount of ileal output, meal transit time, or on the amount of resistant starch excreted (paired t-test, $P>0.05$), although it is noteworthy that large variations were observed between visits and between individuals.

TABLE 7.8: OUTCOME MEASURES IN ILEAL EFFLUENT AFTER CONSUMPTION OF SMOOTH AND COARSE PORRIDGE TEST MEALS

	SMOOTH PORRIDGE	COARSE PORRIDGE
Total effluent (g/d)	359 ± 255	309 ± 210
Moisture content of effluent (g/100g)	92 ± 2	91.3 ± 2
Total dry matter (g/d)	22 ± 7	24 ± 7
Total Resistant Starch (g/d)	3.0 ± 1.1	2.9 ± 1.2
of which starch (g/d)	2.4 ± 0.9	1.9 ± 0.8
of which sugar (g/d)	0.6 ± 0.4	1.0 ± 0.9
Mean Transit Time (h)¹	6.0 ± 0.9	6.4 ± 0.6

Values are mean ± SD

¹MTT calculated as described in (Englyst and Cummings 1985)

Test meal had no significant effects on the parameters listed ($P>0.05$, paired t-test).

On average, a total of 359 g or 309 g of ileal effluent (fresh weight) was excreted over the 10 h day-time collection period after consumption of smooth or coarse porridge, respectively. Large differences were observed in the fresh weight output of study participants, with the amount collected at each time point ranging from 0 to 429 g, and the total daily output ranged from 129 - 924 g between study participants. The dry matter output, however, was less variable.

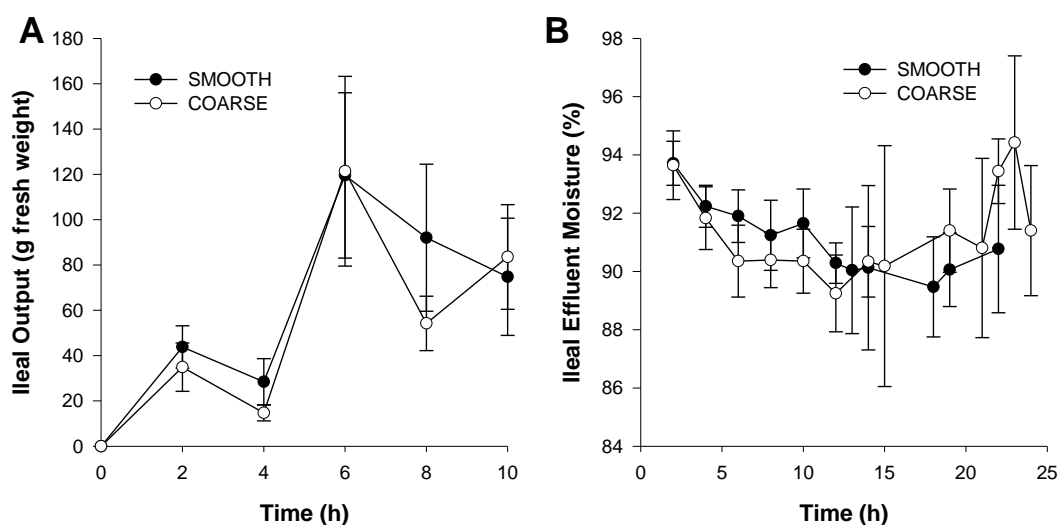


FIGURE 7.8: DAY-TIME EXCRETION OF FRESH WEIGHT (A) AND THE MOISTURE CONTENT OF ILEAL EFFLUENT OVER 24H AFTER CONSUMPTION OF SMOOTH AND COARSE PORRIDGE. Values are mean \pm SEM. Samples collected overnight (between 10-24 h) were collected at different time points at each subject's convenience. Only the data where 3 or more samples were collected at similar time-points is shown.

Moisture determinations revealed that ileal effluent contained between 83 and 98 g water /100 g. A time-effect (**Figure 7.8**) was also observed, in which the moisture content was highest at 2 h (mean = 93.7%), then decreased throughout the day, and then increased again overnight.

Accounting for the variable moisture content of ileal effluent samples, dry matter output during the day ranged from 12.7 to 39.0 g, and was excreted in similar pattern for all participants (**Figure 7.9A**), peaking at 6.7 h. Because samples were collected at the subject's convenience between 12 and 24 h, the ileal output collected over the entire 24 h period is represented cumulatively in **Figure 7.9B**. Overnight sample collection

frequency was highly variable, with some participants waking to empty their ileostomy bag up to 5 times during the night whereas others could manage the night with only 1 collection.

Over the entire 24 h period, on average ~45 g dry matter was excreted, of which 6.0 g (13%) consisted of starch and sugar, and up to 22.3 g (~50%) may have originated from dietary fibre provided during the study visit (refer to **Table 7.3**). As for the remaining 16.7 g (37%) of dry matter, microscopy (*Section 7.3.5*) suggests that this originates from a meal consumed the previous day and/or from endogenous sources, e.g., mucus (Åman *et al.* 1995).

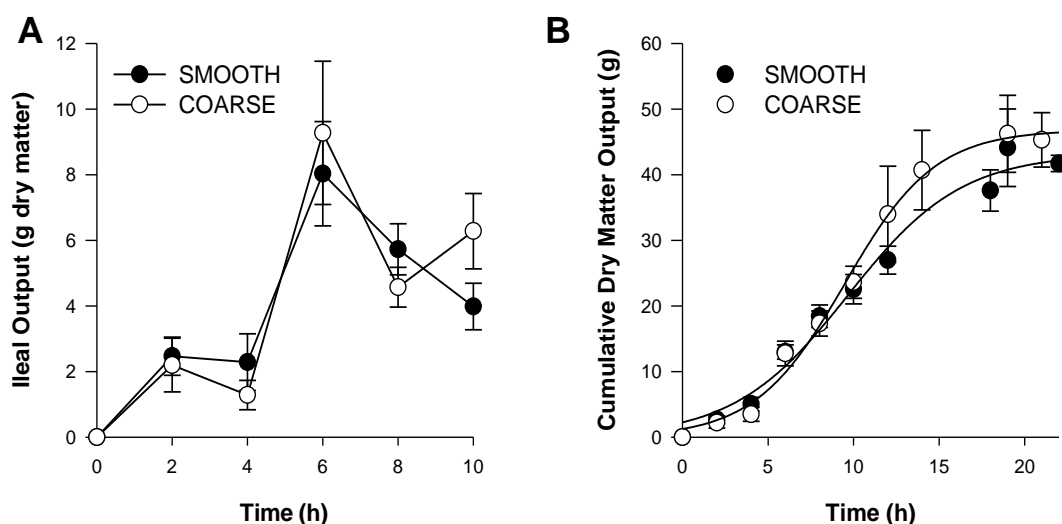


FIGURE 7.9: DAY-TIME EXCRETION OF DRY MATTER AND CUMULATIVE DRY MATTER OUTPUT OVER 24H.

Values are mean \pm SEM. Differences between test meals are not significant ($p > 0.05$, as analysed by ANOVA).

7.3.4 STARCH AND SUGAR RECOVERY

Excretion of resistant starch, defined as the sum of starch and sugar recovered at terminal ileum, followed a similar trend as dry matter (compare **Figure 7.9** and **Figure 7.10**), and no differences were found between the two test meals (ANOVA on starch, sugar and resistant starch; meal and meal \times time effects were not significant, $P > 0.05$). The total amount of resistant (undigested) starch in the effluent produced from the two meals, during day collection, was found to be ~3 g, and accounts for ~6% of the starch in the original test meals. The amount of resistant starch recovered over the entire 24 h

collection period, estimated from cumulative data, was much higher (~5.5 g) amounted to ~9.9 (%). However, microscopy (Section 7.3.5) suggested that the starch recovered overnight may have originated from the evening meal.

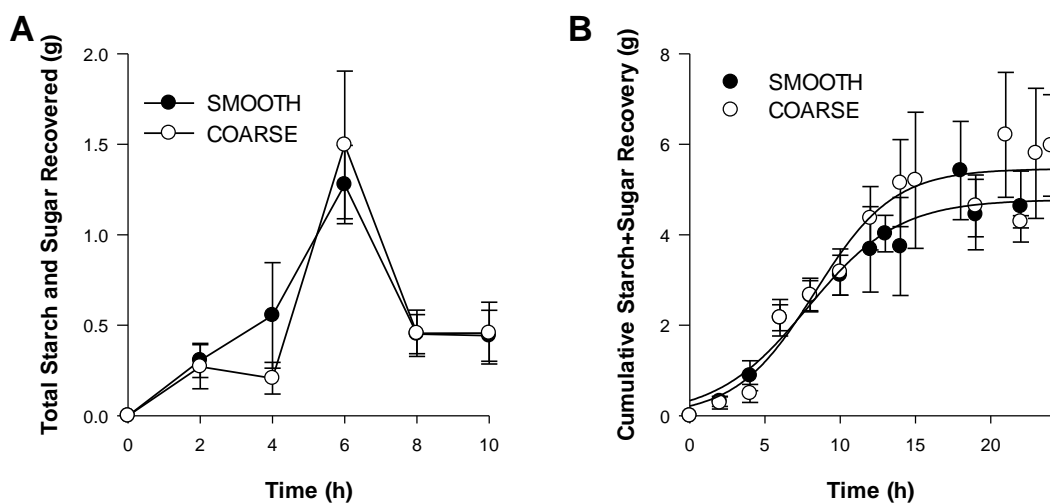


FIGURE 7.10: DAY-TIME EXCRETION OF STARCH AND CUMULATIVE STARCH EXCRETION OVER 24H. Values are mean \pm SEM. Differences between test meals are not significant as analysed by ANOVA.

The general pattern of starch and sugar recovery at the terminal ileum is shown in **Figure 7.11**. The maximum output of starch and sugar occurred at 6 h, and coincides with peak dry matter output. Although non-significant, **Figure 7.11.A** shows a tendency for a greater starch recovery at 4 and 6 h after ingestion of the smooth porridge (i.e. no encapsulated starch), Similarly, **Figure 7.11B** shows a tendency for greater sugar recovery at 6 h following ingestion of the coarse porridge, which contained a greater proportion of cell wall encapsulated starch, however, again this effect was also not significant ($P = 0.056$, paired t-test). When starch and sugar was summed to give the resistant starch excretion (**Figure 7.10**), these apparent differences were reduced. Overall, the test meals had no significant effects on the recovery of starch and sugar in ileal effluent.

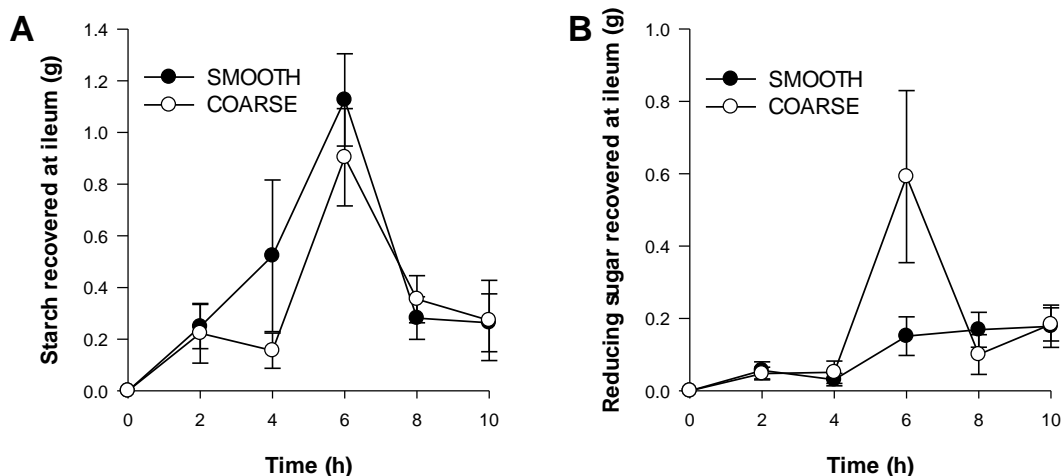


FIGURE 7.11: STARCH AND SUGAR RECOVERED AT TERMINAL ILEUM DURING DAY-TIME COLLECTION.

Values are mean \pm SEM. Differences between test meals are not significant.

7.3.5 MICRO-STRUCTURAL OBSERVATIONS

A similar mean transit time was observed for meal A and B (**Table 7.8**), with peak recovery of the test meal at 6 h. The first sample, collected at 2 h, was normally liquid and contained particles of wheat. For most participants, these first samples did not contain any residue from the evening meal, with the exception of two participants, in which this sample also contained some residue (i.e. pea) from a meal taken the day before the visit. Generally, coarse particles of wheat endosperm were only evident in samples recovered from the terminal ileum within 10 h, although some of the outer layers of the wheat grain (pericarp, testa and aleurone layers) were present.

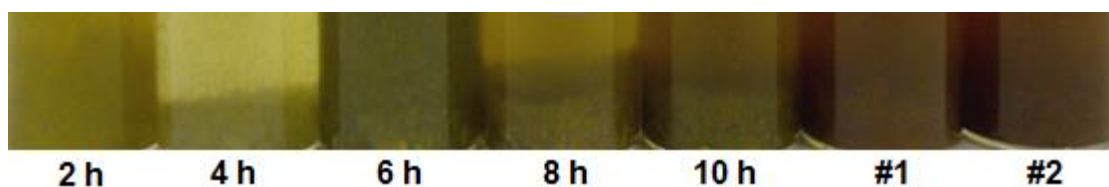


FIGURE 7.12: COLOUR CHANGE OF ILEAL EFFLUENT OVER TIME. Photograph of microscopy samples of ileal effluent in glass vials containing fixative. The colour changed from yellow, to green to brown throughout the collection period. Samples #1 and #2 were collected overnight.

The colour and consistency (**Figure 7.12**) of ileal effluent followed a predictable trend. Generally, the first collections had a more liquid or mucous-based consistency,

whereas after lunch the effluent became green and fibrous. The overnight collections were brown or darker. These changes correspond well with the unabsorbed meal components identified in these samples. For instance, the green colour probably originates from the lunch meal (i.e. chlorophyll), as leaves and seeds from the lunch meal were evident in the first collection after lunch (6 h), and thereafter.

Undigested starch was observed in the ileal effluent after both meals and constitutes the 'resistant starch' measured in the biochemical assays (**Figure 7.13**).

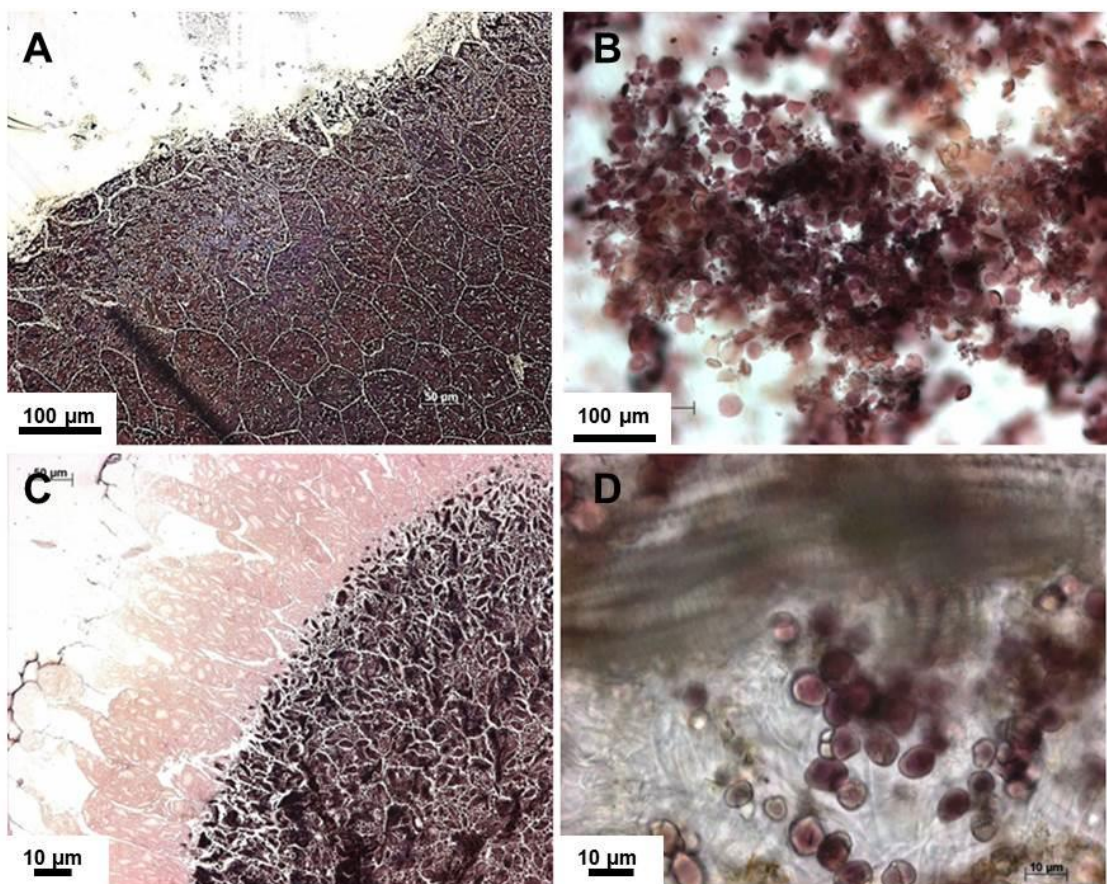


FIGURE 7.13: WHEAT ENDOSPERM SPECIMENS OF COARSE AND SMOOTH PORRIDGE, BEFORE AND AFTER DIGESTIVE TRANSIT. (A) Undigested coarse (A) and smooth (B) porridge, digested coarse (C) and smooth (D) porridge recovered from ileal effluent. All are stained with 2.5% Lugol's iodine. The differences in scale should be noted.

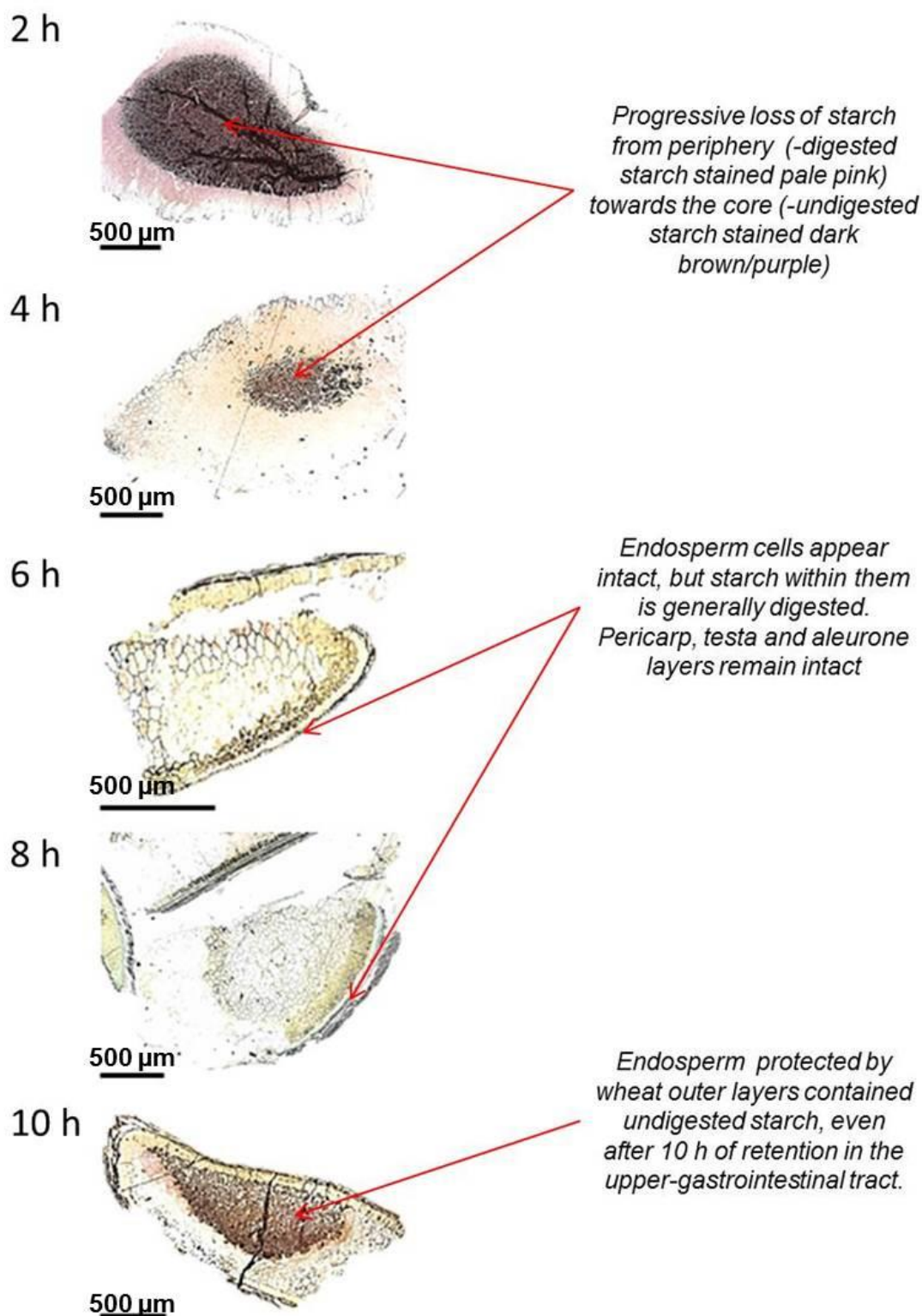


FIGURE 7.14: WHEAT PARTICLES FROM COARSE PORRIDGE RECOVERED FROM ILEAL EFFLUENT AT DIFFERENT TIME POINTS (2 TO 10 H). Scale bar = 0.5 mm, shown in bottom left corner of each panel. Readers should note the difference in scale. Samples were embedded in LR White resin and stained with 2.5% Lugol's iodine.

Examples of the microstructure of wheat particles recovered from the terminal ileum following ingestion of the coarse porridge are shown in **Figure 7.14**. Intact particles of durum wheat ~1 – 2 mm diameter were evident in all samples collected throughout the day. In many of these particles, the starch in the outermost cell layers did not stain strongly with iodine, which indicated that starch in these cells had been digested. Some cells containing undigested starch were present in the centre of the particle, and stained a dark purple with iodine. The outermost layers of the wheat grain appeared largely unaffected by digestive transit, and may have provided a barrier to starch digestive enzymes (i.e. amylase) **Figure 7.14**. Closer examination of the edge of these particles **Figure 7.15** revealed that some of the empty cells along the endosperm particle edge had collapsed; suggesting that the loss or digestion of intracellular starch compromises the structural integrity of the wheat matrix.

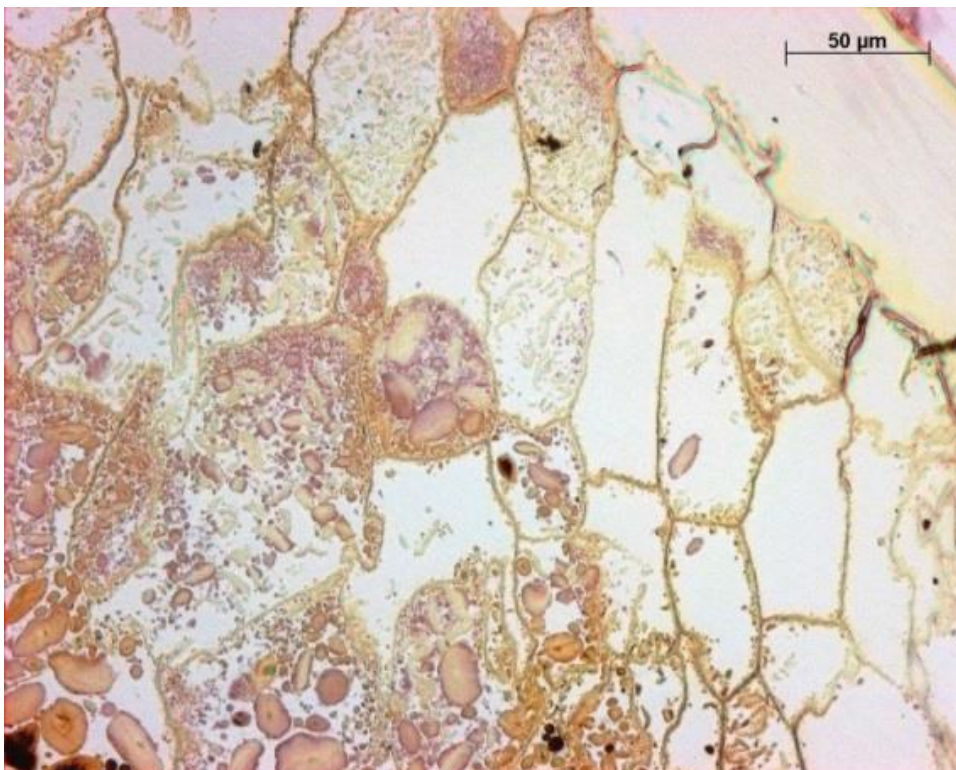


FIGURE 7.15: DIGESTED EDGE OF WHEAT ENDOSPERM MACRO-PARTICLE RECOVERED IN ILEAL EFFLUENT. Stained with 2.5% Lugol's iodine.

A number of other plant food materials (e.g., pea cells, carrots, leaves, xylem tissues and seeds) were recovered in the ileal effluent. The micrographs in **Figure 7.16** provide further evidence for the role of cell walls in limiting the bioaccessibility of starch and other nutrients (e.g., β -carotene, iron).

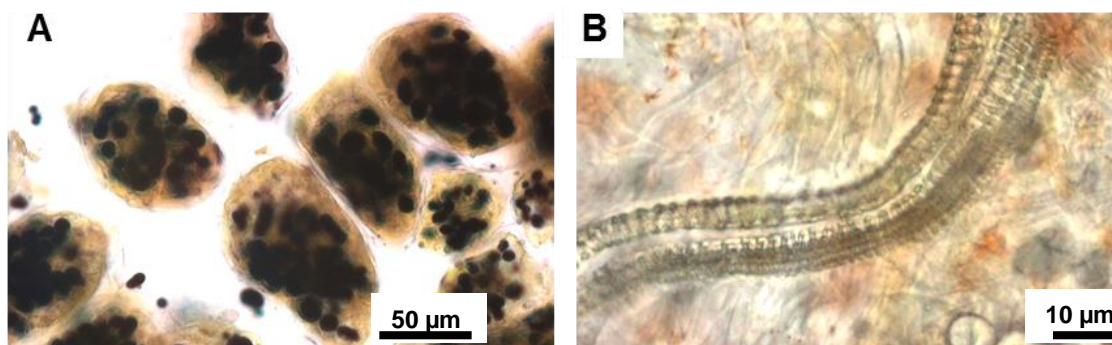


FIGURE 7.16: EDIBLE PLANT MATERIALS RECOVERED IN ILEAL EFFLUENT. (A) Intact, starch-filled pea cells stained with 2.5 % Lugol's iodine. (B) Carrot tissue (not stained) showing xylem and β -carotene (orange colour).

7.4 DISCUSSION

This unique post-prandial ileostomy study was designed to investigate the effects of cell wall encapsulation on the post-prandial metabolic response (primarily glycaemia and insulinaemia), and also to provide some insight into the structural and biochemical breakdown of endosperm during digestion. The test meals were formulated to have a near-identical nutrient composition, but differed in particle size and expected starch bioaccessibility. Unlike many previous studies of food structure and glycaemia (Golay *et al.* 1986, Holm and Bjorck 1992, Kristensen *et al.* 2010), these relatively simple test meals were prepared from durum wheat endosperm materials that had already been extensively studied *in vitro*, e.g., in terms of their digestibility and physico-chemical characteristics. The meals were designed so that they could be swallowed without prior mastication, thereby allowing the effect of the stomach and small intestine on food structure to be studied.

As predicted, the low bioaccessibility meal (coarse porridge, ~62% intact cells) evoked a significantly attenuated glycaemic response compared with the high bioaccessibility

meal (smooth porridge). The markedly reduced iAUC between 0 and 120 min for glucose (33%) and insulin (43%) after the coarse porridge was consistent with the predicted 33% difference in the extent of starch hydrolysis observed *in vitro* after 90 min digestion with porcine pancreatic α -amylase. The attenuated C-peptide response (40% lower iAUC between 0 and 120 min) following the coarse porridge compared with the smooth porridge is indicative of attenuated insulin secretion and probably reflects more gradual release and absorption of glucose from the coarse particles. Overall, the results are consistent with the hypothesis that the physical encapsulation of starch within plant cell walls significantly delays the rate of release of starch hydrolysis products during luminal digestion, and thereby attenuates glycaemia. Furthermore, the magnitude of the reduction in glycaemia and insulinaemia that was achieved by manipulating the proportion of encapsulated starch is considerably greater than has been achieved in some previous by manipulating the soluble fibre component of bread (Holm and Bjorck 1992). Thus, incorporation of coarse endosperm particles containing cell wall encapsulated starch into food products provides a new means of lowering the glycaemic response to food and may be beneficial in the dietary prevention and management of diabetes, obesity and cardiovascular disease.

The insulinaemic response to the starch-rich test meals (1.56 g fat) also appeared to have secondary effects on lipid metabolism. The observed reductions in post-prandial TAG and NEFA concentrations probably reflect the net-effect of insulin-mediated uptake of fatty acids and inhibition of lipolysis in adipose tissue (Robinson 1973, Ginsberg *et al.* 2005). Although no significant differences were observed between the two meals at the 95% confidence level, it was interesting to note that the smooth porridge, which elicited the greatest insulin response, was associated with higher concentrations of TAG than the coarse porridge. This is paradoxical, because the test-meal contained very little fat, and because insulin is known to promote lipogenesis (e.g., TAG storage in adipose tissue) (Frayn 2010). There have, however, been some studies which suggest that the intake of a single high-glycaemic meal can induce

hypertriglyceridaemia, possibly by slowing chylomicron clearance, i.e. slowing the removal of TAG from the blood (Parks 2001). However, the mechanisms leading to this phenomenon, known as 'carbohydrate-induced hypertriglyceridemia' are not fully understood. Further studies are needed to elucidate the complex interactions between glycaemia, insulinaemia, lipaemia and the aetiology of diet-related disease (Jenkins *et al.* 2002, Parks 2001).

As mentioned previously (*Section 7.1.1*), the presence of nutrients in the duodenum after a meal triggers other endocrine mechanisms with implications for digestion and health. The observed post-prandial rise in gut hormones PYY, GLP-1 and GIP and the fluctuating CCK concentration is consistent with their known effects on digestion (*Section 7.1.1*). The underlying mechanisms are not yet fully understood, but generally it seems that the presence of carbohydrate and fat in the small intestine, and the absorption of these nutrients into the blood, stimulates K-and L-cells of the small intestine to release GIP and GLP-1, respectively. These gut hormones encourage the release of insulin from pancreatic β -cells in a glucose dependant manner and promote insulin sensitivity (Meier and Nauck 2004). In this study, the magnitude of the GIP post-prandial response was significantly larger after the smooth porridge meal compared with the coarse porridge. This coincides with the larger glycaemic and insulinaemic responses associated with this test meal, as would be expected considering that GIP is released in response to increased luminal glucose concentration, and has a primary role in stimulating insulin release (Murphy and Bloom 2006).

As to how ileostomy subjects compare to healthy subjects, this is not quite clear. The obvious difference between ileostomy subjects and 'healthy or normal' subjects is that in an ileostomy subject, the large intestine is not involved in digestion. The absence of a functioning large intestine could attenuate the PYY and GLP-1 response to food, because the endocrine L-cells that secrete these hormones are most abundant in the large intestine (Wu *et al.* 2013). However, a recent review of this topic suggested that

the concentration of most gut hormones (including the ones investigated in this study) are likely to be elevated in subjects who have undergone a colectomy procedure which connects the ileum to the anus (M'Koma *et al.* 2007). It is therefore possible that the hormone concentrations observed in this study are elevated compared to 'healthy' or 'normal' subjects, although this is not entirely clear.

This study not only adds to the existing literature that suggests that food structure and fibre play an important role in influencing the glycaemic response, but also offers new mechanistic insight into the structural and biochemical degradation of food during gastro-intestinal transit. One particular strength of the study design was the simplicity of the test meals: Previous studies of the effects of 'fibre' or food structure have used complex mixed meals that contained undetermined combinations of retrograded starch (which forms during storage), physically encapsulated starch, and β -glucans, and therefore provided limited insight (Holm and Bjorck 1992, Golay *et al.* 1986). Here, the test meals differed only in their structure and the proportion of starch that was physically encapsulated within plant cell walls. These particles were also swallowed without mastication, which allowed the specific effects of gastric and small intestine to be studied.

Analysis of ileal effluent revealed that the structural integrity of the coarse particles (from coarse porridge) was largely retained during gastro-ileal transit. By the time the test meals reached the terminal ileum, the extent of digestion appeared to be similar i.e., both meals contained the same amount of resistant starch, and most starch in the coarse (1.85 mm) endosperm particles had been digested from seemingly intact cells. This was consistent with results reported in *Chapters 4 and 5*, and supports the view that the durum wheat endosperm cell walls (unlike chickpea cell walls) are permeable to α -amylase; hence cell wall encapsulated starch was digested, albeit at a reduced rate.

One confounding variable worth considering, is that larger particles of food can be retained in the stomach for longer than finer particles ('gastric sieving'), and thereby influence the rate at which available substrate is delivered into the duodenum (Malagelada *et al.* 1984, Hellström *et al.* 2006, Kong and Singh 2008). It is possible that the coarse and smooth porridge test meals used in this study may have been emptied from the stomach at different rates, giving rise to different rates of glucose absorption (Ranawana *et al.* 2011). However, the time for plasma glucose concentrations to reach peak values was similar for the two test meals, and implies that initial absorption rates (i.e., of nutrients released from readily available starch that was present in both meals) were similar. Furthermore, if the gastric emptying rates were different between the two test meals, a slightly different ileal excretion profile or meal transit time might have been expected. Here, the ileal excretion profiles of the two meals were similar, and on the basis of biochemical analysis and observational notes, there is no reason to suspect different rates of test meal transit.

Considering the results of the present study together with results from the range of experiments conducted *in vitro* (Chapters 3 - 5), it certainly seems likely that the rate of amylase ingress is the predominant factor that influences the glycaemic response to these materials. Interestingly, the 33% difference in starch hydrolysis index (0 - 90 min) determined from *in vitro* and *in silico* work (Chapter 5 Table 5.3 page 169) was consistent with the observed 33% difference in the iAUC (120 min) of glucose curves. On a very basic level, this could be taken to imply that the food spent on average 30 min in the stomach, after which starch digestion followed a similar profile to the *in vitro* and *in silico* predictions. However, the digestion and gastro-intestinal transit of food is highly dynamic and far more complex than this, and further studies would be required before *in vitro* data can be used to predict *in vivo* glycaemia. Nevertheless, the observed compatibility between *in vitro*, *in silico*, and *in vivo* results is promising for the further development and future validations of these models.

One discrepancy between the *in vitro* and *in vivo* data was that the amount of resistant starch measured at the terminal ileum was lower than expected after both meals. Only ~6% of the starch from the original test meal was recovered in ileal effluent, which implies that 94% of the starch contained in these meals was digested. This is at least 10% higher than what is normally reported for *in vitro* amylolysis of gelatinised, purified starches, which should be more digestible than the starch in these meals (Goñi *et al.* 1997, Slaughter *et al.* 2001), although studies using other *in vitro* digestion methodologies have reported higher values. This discrepancy could reflect a limitation of the *in vitro* digestion methodology used in *Chapters 4* and *5*, which would underestimate starch digestion. However, based on the large inter-individual variation in starch and sugar excretion, it is also likely that, although steps were taken to minimise sample degradation, some microbial bacterial degradation of the starch, or indeed other resistant non-starch polysaccharides including cell wall polysaccharides and fructooligosaccharides, occurred (Englyst and Cummings 1985). Considering the 2 h sampling frequency, which was needed to ensure sufficient amounts of sample was collected for analysis, this was somewhat inevitable. The amount of resistant starch recovered is similar to what has been reported for other cereals (Livesey *et al.* 1995, Englyst and Cummings 1985), and also these authors suggested that microbial degradation probably led to an underestimation of resistant starch. This is currently a limitation of the ileostomy model that is not easy to overcome.

Nevertheless, in the light of the *in vitro* digestibility data presented in *Chapter 5*, and the microscopy analysis in the current study, an encapsulation barrier mechanism is a persuasive explanation for the substantial reductions in the postprandial blood concentrations of glucose, insulin and C-peptide. Thus, the slower ingress of amylase into coarse particles seems to be a primary factor in reducing the rate of amylolysis of starch.

Although chickpeas were not included in this *in vivo* study, it was especially interesting to find intact, starch-containing pea cells (originating from a pea-containing meal taken the previous day) at the terminal ileum. This suggests that starch encapsulated by pea cell walls is protected from digestion during transit to the terminal ileum. Assuming that leguminous cell walls have similar properties, this observation is compatible with data on chickpeas, in which the *in vitro* digestibility assays (*Chapters 4*) and the multi-compartmental digestion model (*Chapter 6*) both indicated a remarkably low starch bioaccessibility in isolated chickpea cells. This result is also consistent with the literature (Noah *et al.* 1998, Golay *et al.* 1986). Overall, the microstructural observations highlight the resistance of plant cell walls to digestion, with potential implications for not only starch bioaccessibility, but also the bioaccessibility of other nutrients (e.g. β -carotene, protein, lipid, iron).

7.5 CONCLUSIONS

Overall, cell wall encapsulation in durum wheat limits the rate of release of starch hydrolysis products, but not the extent. This has implications for the glycaemic and insulinaemic response, but not the amount of resistant starch reaching the colon. The novel findings of this study are consistent with the suggestion that durum wheat cell walls, which encapsulate starch during digestive transit to the terminal ileum, are permeable to digestive enzymes (see *previous chapters*), but have the potential to attenuate glycaemia by delaying the enzyme access and thereby glucose absorption.

CHAPTER 8

GENERAL CONCLUSIONS

The project presented in this thesis was designed to investigate the role of plant cell walls in regulating the bioaccessibility of starch in edible plant materials, and in turn, how this influences digestion kinetics and post-prandial metabolism. The approach was to use a combination of *in vitro*, *in silico* and *in vivo* studies to compare starch bioaccessibility in chickpeas and durum wheat. These edible plant tissues were selected because of their contrasting cell wall types and glycaemic potential.

Unlike many previous studies of dietary fibre, this work focused on the role of structurally-intact plant cell walls (a major component of dietary fibre) in *physically encapsulating* intracellular starch. Intact cells are present in a range of natural foods, and it was hypothesised that the physical encapsulation of the starch by plant cell walls protects it from digestion. *In vivo*, it was anticipated that the bioaccessibility of cell wall encapsulated starch in the small intestine would be reduced, leading to a decrease in the rate and/or extent of starch digestion and postprandial glycaemia.

Overall, the results from these studies have provided strong evidence that the physical encapsulation of starch by plant cell walls limits starch bioaccessibility and digestion, and consequentially the post-prandial rise in plasma glucose and insulin concentrations. The comparison between chickpeas and durum wheat provided additional insight into the underlying mechanisms involved, and into the contrasting properties of different plant species. The main findings are discussed further in the sections below.

8.1 EFFECT OF CELL WALL ENCAPSULATION ON STARCH DIGESTION

KINETICS

In order to explore the effects of cell wall encapsulation on starch digestion kinetics, a range of milled materials containing varying proportions of intact, starch-filled cells were prepared from de-branned durum wheat and de-hulled chickpeas. The finest flour (<0.21 mm) consisted almost entirely of ruptured cells, whereas the most coarsely

milled (~2.58 mm) fractions were estimated to consist of ~73 - 83% intact cells. The cellular integrity of these tissues was largely retained following hydrothermal processing, and incubating these materials with α -amylase enabled the mechanisms of starch digestion in relevant edible plant materials to be studied. The starch content was standardised across all materials examined, such that the observed differences in starch bioaccessibility were likely to arise from structural differences. Experiments were designed with the intention of improving on existing methodologies in which destructive treatments were employed to release cell wall encapsulated starch (e.g., (Englyst *et al.* 1992)) or where complex plant materials have been digested without supporting information about their structural characteristics (e.g., (Goñi *et al.* 1997)).

One problem with the milled materials, however, was that it was difficult to demonstrate that the observed effects on digestion kinetics were attributable to the integrity of the cell walls and not simply because of the change in surface area available for diffusion, which is inevitably a consequence of particle size manipulation. Therefore, experiments on isolated cells, which consisted of cell wall encapsulated starch, but without the large particle size seen in the milled macro-particles, were very valuable. However, these cells could only be obtained from chickpeas, and not from durum wheat. Nevertheless, the materials that were produced by milling to reflected the particle size range likely to exist in processed foods that are ingested (Hoebler *et al.* 1998). Hydrothermally processed chickpeas have a natural tendency to cell separate, and so isolated cells provide a good representation of post-masticated chickpea, or products such as hummus or soup. In the case of durum wheat, this seed tissue tends to fracture and so the results obtained with milled durum wheat macro-particles are actually more representative of cereal-based food products (Hoebler *et al.* 1998).

The importance of cell wall encapsulation on starch bioaccessibility became evident in the first *in vitro* digestibility experiments (*Figure 4.2, page 135*). The digestibility curves obtained for hydrothermally processed chickpea and durum wheat starches (i.e. no cell

wall material was present) and for flours (i.e. containing cell wall fragments, but no encapsulated starch), were all very similar, indicating little or no inherent differences in the starch reactivity or of interference from endogenous compounds (e.g. inhibitors) in these fractions. For the more coarsely milled materials, particle size manipulation gave rise to contrasting effects on the shape of the digestibility curves obtained for durum wheat and chickpeas. Interestingly, in durum wheat, increasing the particle size (and thereby the degree of cell wall encapsulation) reduced the *rate* of starch digestion, whereas in chickpeas, both the *rate* and the *total extent* of digestion were limited. Furthermore, in experiments on isolated chickpea cells, the extent of starch digestion was severely limited, confirming that, in chickpeas, it was the starch encapsulation that was responsible for the limited extent of starch digestion. This was an important finding which reflected the different characteristics (e.g., cell wall permeability or degree of starch gelatinisation) of these botanically different plant tissues.

The *in vitro* digestibility data was also used to develop an *in silico* model of starch digestion (see *Chapter 5*), which was one of the objectives of this PhD project. This involved applying Logarithm of Slope (LOS) plots to data obtained from the early stages of *in vitro* digestion to obtain parameters (C_{∞} and k) of the first-order equation describing the digestibility reaction. Although it was already known that starch amyolysis occurs by a first-order process, the digestion of starch in a heterogeneous food matrix was actually found to occur by two consecutive first-order reactions, reflecting the variations in the bioaccessibility of starch in these complex materials. For instance, in the milled materials, the first (rapid) phase seemed to represent digestion of more available starch on the fractured surfaces, whereas the subsequent slower phase represented digestion of encapsulated starch. This was a novel finding that demonstrates the usefulness of application of LOS analysis to a broad range of starch-rich food products. Moreover, unlike the popular, but flawed, Englyst starch classification system, which describes starch as rapidly and slowly digested fractions based on arbitrary time points, this model was based on the well-established principles

of first-order digestion kinetics. The values of parameters estimated from LOS plots (e.g., C_{∞} , k) provided excellent descriptions of the experimental data. Furthermore, the results obtained with this novel *in silico* model were consistent with the findings from the various *in vitro* and *in vivo* studies presented in this thesis. Hence, the work described in *Chapter 5* has introduced a new and valuable experimental tool for studying and comparing starch digestion mechanisms and for predicting the rate and extent of starch digestion in complex food matrices.

Overall these digestibility assays demonstrated that the physical encapsulation of starch by cell walls significantly impedes starch bioaccessibility. Furthermore, the fact that such large differences in *in vitro* starch digestion rate and/or extent could be achieved simply by manipulating particle size, provided encouragement that these effects would translate to physiologically relevant differences *in vivo*. It was of interest, therefore, to gain a deeper understanding of how, exactly, the physical encapsulation of cell walls limits starch bioaccessibility. Two main mechanisms were investigated: *i) the role of cell walls as physical barriers* and *ii) their effects on intracellular starch gelatinisation*. This proved to be a challenging research question, particularly because these mechanism were not mutually exclusive, and both may contribute significantly to the observed effects on starch bioaccessibility. Nevertheless, the results from this exploratory work provide a useful foundation for further studies. Evidence supporting each mechanism is reviewed in the two sections below.

8.1.1 CELL WALLS AS BARRIERS

Although the description of cell wall encapsulated starch as 'physically inaccessible' is common throughout the literature (Englyst *et al.* 1992), the underlying evidence for the existence of the so-called cell wall 'barrier mechanism' is very limited. The assumption seems to be based largely on microstructural observations of undigested starch contained within plant cells following *in vitro* or *in vivo* digestion (Würsch *et al.* 1986, Noah *et al.* 1998, Livesey *et al.* 1995), but this phenomenon can also be explained by

alternative mechanisms, including the restricted swelling and gelatinisation of intracellular starch (Fujimura and Kugimiya 1994, Marshall 1992), as discussed in *Section 4.4, page 144*. Few workers have attempted to measure the permeability of this supposed cell wall barrier to larger molecules such as digestive enzymes. The porosity studies presented in *Chapters 3 and 4* provided novel insights into the ability of amylase to penetrate the cell walls of hydrothermally processed chickpeas and durum wheat and thereby access the intracellular starch.

On the basis of the observed diffusion of various FITC-dextran, the pore radius of chickpeas cell walls lies between 1.4 - 2.3 nm, and the pore radius of durum wheat cell walls lies in the range of 2.3 - 4.5 nm. These values are similar to literature values (see *Table 1.3*) reported for other plant tissues) (Carpita 1982, Carpita *et al.* 1979, Tepfer and Taylor 1981, Baron-Epel *et al.* 1988, Chesson *et al.* 1997). Considering that the radius of gyration of the amylase molecule is 2.69 nm (Simon *et al.* 1974), these estimates of pore-size suggest that amylase may be able to diffuse across durum wheat cell walls, but would be too large to diffuse through chickpea cell walls, as was indeed observed with FITC-amylase (*Figure 4.4, page 137*). These results support the view that chickpea plant cell walls limit starch bioaccessibility by blocking enzyme penetration.

The results from porosity studies on durum wheat, were less clear-cut than for chickpeas, because the integrity of the cell walls (which are thinner than in chickpea, and not clearly defined on the fluorescence micrographs) could not be assured, making it difficult to ascertain if the FITC-dextran/amylase complex actually crossed the cell wall barrier. The most convincing evidence for the permeability of durum wheat cell walls to amylase was actually accumulated from other studies. For instance, the digestibility curves in *Figure 4.1, page 135* showed that a similar amount of starch was digested, regardless of particle size. Because a large proportion of the starch in larger particles was encapsulated by plant cell walls (see *Table 4.1*), it can be deduced that

the enzyme must be accessing the encapsulated starch as well as the more available starch on exposed fractured surfaces. This conclusion was supported by microscopy of sectioned wheat macro-particles recovered from ileal effluent (*Figure 7.14, page 229*), in which the starch in the seemingly intact cell layers appeared to have been digested. Although milling can generate cracks and sub-micron fissures that allow some enzyme ingress, it was unlikely that the enzyme gained access to the intracellular starch through random cracks or fissures, because the microscopy showed a uniform, radial pattern of starch digestion. Taken together, the micrographs and digestibility data obtained for wheat endosperm support the view that the durum wheat cell walls are permeable to amylase.

Overall, there is evidence to support the theory that cell walls may prevent and/or delay enzyme access, thereby limiting the rate and extent of release of starch hydrolysis products. The effects observed depend on the permeability and integrity of the cell wall barrier, giving rise to contrasting effects in different plant materials. **Certainly, the cell walls of durum wheat appear to be permeable to amylase, whereas in chickpea cells, the physical barrier effect is more pronounced.**

8.1.2 CELL WALLS RESTRICT STARCH GELATINISATION

The role of cell walls in restricting starch gelatinisation was explored using a combination of DSC (quantitative) and microstructural (qualitative) techniques.

Although chickpea starch gelatinises at a higher temperature ($T_p = 71.7\text{ °C}$) than durum wheat ($T_p = 57.0\text{ °C}$), similar gelatinisation enthalpies were observed for purified starches and flours ($\sim 9.6\text{ J/g starch}$). Hence, the presence of cell wall fragments in the chickpea and durum wheat flour fractions did not affect the extent of starch gelatinisation. When the plant cell walls physically encapsulated the starch, however, differences in the extent of starch gelatinisation were observed between these botanical sources. In chickpeas, the extent of starch gelatinisation was reduced with increasing particle size (a reflection of a higher proportion of encapsulated starch), and

birefringent starch was still observed post-processing (*Figure 4.10, page 144*). Also in the heated stage microscopy experiments on freshly prepared, isolated chickpea cells, the intracellular starch retained birefringent properties after heating, indicating a retention of molecular order, a characteristic of ungelatinised starch. This suggested that the cell wall barrier was responsible for imposing restrictions on the gelatinisation of intracellular starch.

In durum wheat particles, with the exception of the largest size fraction, the cell wall encapsulation of starch did not appear to decrease the extent of starch gelatinisation during the DSC runs, and no birefringent starch was observed in wheat endosperm recovered from the DSC instrument after these runs. Microstructural observations of processed durum wheat samples collected during other experiments, however, did show granules with a distorted shape thought to be indicative of limited swelling of pre-gelatinised starch. Also, it is worth noting that the processing conditions used in the DSC runs were set and standardised for the purpose of comparing the two different plant tissue samples. The different cooking procedures used throughout this thesis and elsewhere, may, of course, give rise to different effects on starch gelatinisation, tissue integrity and nutrient release properties. Future experiments could involve studying starch gelatinisation under a greater range of hydrothermal processing conditions.

As to how the chickpea cell walls limited starch gelatinisation, several potential mechanisms were discussed, but the two most likely explanations were that the cell walls of chickpea limited water ingress, and/or that they imposed spatial restrictions and thereby prevented swelling of intracellular starch, which is important to allow sufficient water ingress for complete starch gelatinisation (Wang and Copeland 2013). Accordingly, the water-binding capacity of cell walls and their resilience against intracellular pressure from expanding starch granules may be important factors that influence the behaviour of cell wall encapsulated starch during hydrothermal

processing. Experiments on water ingress into cells and tissues and the effects on starch gelatinisation could provide further insights.

Irrespective of mechanism, considering the magnitude of differences in digestibility between native and gelatinised starch (Slaughter *et al.* 2001), any restrictions on starch swelling and gelatinisation would be expected to have major consequences for the susceptibility of starch to amylolysis.

Overall, encapsulating cell walls restricted the gelatinisation of intracellular starch in chickpeas and in larger particles of durum wheat, with likely implications for starch digestion kinetics.

8.2 EFFECTS OF CELL WALL ENCAPSULATION ON POSTPRANDIAL METABOLISM

The dietary intervention study (*Chapter 7*) was designed to examine how the differences in starch bioaccessibility observed *in vitro* would impact on the glycaemic response. Although the *in vitro* studies presented in this thesis have largely dealt with mechanisms of digestion and bioaccessibility, the glycaemic response represents the amount of starch-hydrolysis products that have actually been absorbed (*i.e. that are 'bioavailable'*). Performing this *in vivo* study in subjects with an end-ileostomy enabled direct measures of bioaccessibility by analysis of the amount of undigested (resistant) starch remaining at the end of the small intestine. Thus, taken together, blood and ileal effluent analyses provided information about starch bioaccessibility ('release') and bioavailability ('absorption'), and also provided much needed insight into the structural degradation of food during digestive transit.

One benefit of the study described in *Chapter 7* is that, compared to previous post-prandial studies (Kristensen *et al.* 2010, Holm and Bjorck 1992, Golay *et al.* 1986), the test meals were kept relatively simple, and were prepared from milled material that had already been thoroughly examined *in vitro*. Using the results obtained from *in vitro*

starch hydrolysis as a guide, two durum wheat test meals (i.e., smooth and coarse porridges containing endosperms particles of average sizes <0.21 mm and ~1.85 mm, respectively) were formulated to give rise to different rates of release of starch hydrolysis products during luminal amylolysis. Another advantage of these porridge meals was that the wheat endosperm could be easily swallowed whole, and thereby minimise the problem of particle size reduction that occurs during mastication.

The differences in glycaemic responses between the two test meals were consistent with the differences *in vitro* starch hydrolysis rates (33% difference in HI₉₀ and glucose iAUC 0-120). The glycaemic and insulinaemic responses were significantly attenuated (≥30% reduction) following consumption of the porridge made of coarse particles (i.e., 62% encapsulated starch) compared with flour porridge (i.e., no encapsulated starch). To this author's knowledge, this is the first human study to demonstrate that the structural integrity of *de-branned* wheat endosperm significantly alters the post-prandial glycaemic and insulinaemic responses. In the light of results from *in vitro* studies of the milled wheat, the most likely mechanism by which the coarse macro-particles attenuate glycaemia is that the starch-encapsulating endosperm cell walls delay the release of starch-hydrolysis products from amylolysis in the upper gastrointestinal tract.

Despite structural differences, the ileal excretion of resistant starch and total dry matter did not differ between the two meals, and only ~6% of the starch in the test meals remained undigested at the terminal ileum. Hence, the same amount of starch was eventually released/bioaccessible in both test meals, but the rate of release differed, giving rise to differences in the post-prandial responses.

Indeed, microstructural examination of ileal effluent revealed that these coarse particles retained structural integrity during digestive passage to the terminal ileum, and the cells which constitute the tissue appeared intact, with well-defined cell walls. This verifies that the plant tissues used in the *in vitro* digestibility assays are representative of some of the structures that the enzymes are likely to encounter *in vivo*. Interestingly, the

micrographs of the recovered wheat particles revealed that a significant proportion of the intracellular starch had been digested from seemingly intact cells, with only some undigested starch remaining at the particle core. This supports the view that amylase is able to penetrate the cell walls of durum wheat, as discussed in *Section 8.1.1*.

Predictions from the *in silico* model of the resistant starch content of wheat samples digested *in vitro* were higher than those found in the ileostomy effluent. However, the amount of resistant starch recovered *in vivo* was consistent with values reported for cereals in other ileostomy studies (Livesey *et al.* 1995, Englyst and Cummings 1985). As discussed in *Chapter 7*, this discrepancy probably arises because microbial fermentation of excreted resistant starch occurs in the ileostomy bags between sample collections (i.e. every 2 h). One way to explore this further could be to include SCFA measurements in ileal effluents, although interpretation may prove difficult due to large fluctuations/variations in microflora. Another possibility is that other biochemical factors or enzymes that are present in the *in vivo* digestive environment, but were omitted in the *in vitro* study, increase starch bioaccessibility. This is currently being investigated by researchers at the Institute of Food Research, who are studying the digestion of these durum wheat porridge meals in the multi-compartment model (*Chapter 6*) which simulates the biochemical and mechanical conditions of the oral, gastric and duodenal stages of digestion (Wickham *et al.* 2012).

It was not possible to carry out a parallel ileostomy study with chickpea materials for this project, but on the basis of the limited starch digestion of chickpea cells in the *in vitro* multi-compartmental digestion model (reported in *Chapter 6*), encapsulated starch would be expected to be protected from digestion in the upper gastro-intestinal tract *in vivo*. Indeed, starch-filled cells of other pulses were observed in the ileal effluent of one subject (depicted in *Chapter 7*), and also in a previous human study where ileal effluent was recovered through nasal intubation (Noah *et al.* 1998). Chickpeas, and other pulses have a low glycaemic index (Foster-Powell *et al.* 2002), and this is likely

attributable to the cell wall encapsulation of starch. In future experiments, it would be valuable to quantify the proportion of ruptured cells in the cell preparations, and investigate glycaemic response and the excretion of resistant starch *in vivo*, which, according to the *in vitro* data, could account for 90% of the starch in the chickpea porridge.

Overall, this post-prandial ileostomy study demonstrated that **the limited starch bioaccessibility of cell wall encapsulated starch attenuates the glycaemic and insulinaemic responses**. The physical encapsulation of starch by cell walls was not greatly compromised by digestive transit, demonstrating the relevance of examining the cell wall barrier, which is clearly present also at the terminal ileum *in vivo*. The strong correlation between *in vitro* and *in vivo* data suggests that the *in vitro* observations are good predictors of the *in vivo* response, and provides encouragement for using *in silico* model for predicting the *in vivo* responses in a much broader range of edible plants.

8.3 NUTRITIONAL SIGNIFICANCE

Current nutrition-labelling, which is based on composition data and Atwater correction factors, does not provide adequate information about the nutritional value of food, because it fails to account for the differences in nutrient bioaccessibility (Livesey 1990). In the study described here, for instance, test meals that would not be distinguished on the basis of nutritional composition were found to vary greatly in terms of the rate and extent of nutrient release, with widely different effects on post-prandial metabolism. Food structure is considered to be a major factor in influencing nutrient bioaccessibility, but there are also a range of other factors that can influence nutrient release and absorption, as discussed in *Section 1.2.3*.

Cell-wall encapsulation could also play a major role in limiting the bioaccessibility of other intracellular nutrients, including lipids, iron, protein and β -carotene, as suggested by the micrographs of structurally intact plant tissues presented in *Chapter 7*, and also

the results of other published studies (Tydeman *et al.* 2010, Berry *et al.* 2008, Parada and Aguilera 2007, Melito and Tovar 1995). It is of particular importance to note that the results described in this thesis have highlighted the benefits of *limiting* starch bioaccessibility, for example, in terms of reducing risk factors associated with type 2 diabetes and cardiovascular disease, which are an increasing major health problem in the UK. Moreover, manipulating starch bioaccessibility has potential use in the management of disease, notably type 2 diabetes (*see next section*). It is, however, important to consider that there are likely to be occasions where it is desirable to *increase* the bioaccessibility of starch or other nutrients, for instance to maximise energy value of feedstuff in farm animals (Dandanell Daveby *et al.* 1998).

8.4 APPLICATIONS

With the rapidly increasing prevalence of diet and lifestyle related conditions such as diabetes and obesity, there is an emerging market for food products that can be used in the prevention and/or management of these diseases (Jenkins *et al.* 2002, McCormick *et al.* 2007, Würsch 1994). It is therefore of interest to develop novel ingredients, with 'slow-release' digestion behaviour, that are likely to elicit a low glycaemic response in targeted groups (e.g., people with or at risk of developing type 2 diabetes).

Other workers have tried to limit starch bioaccessibility by encapsulating starch in alginate or other hydrocolloids (Norton *et al.* 2007). The results presented in this thesis, however, indicate that similar, if not better, effects may be achieved by simply manipulating existing food ingredients to exploit the natural encapsulation of starch within plant cells. The human study (*Chapter 7*) demonstrated that manipulating the particle size of durum wheat endosperm had significant beneficial effects on glycaemia and insulinaemia, and it may be that these milled macro-particles may be suitable for incorporation into other food products to achieve similar effects. The most striking results, however, were observed with the chickpea cell preparations, in which ~90% of

the starch was resistant to *in vitro* digestion. These chickpea cells were also found to be remarkably resistant to thermal, mechanical and biochemical treatments, and show great potential as a novel low-glycaemic, high resistant starch ingredient.

8.5 RECOMMENDATIONS

A wide range of factors influence nutrient bioaccessibility and absorption, hence, predicting nutritional properties from food composition data is of limited value. Rather, it may be more insightful to assess these foods based on what they actually deliver, i.e. in terms of their nutrient release profile. For that purpose, *in vitro* and *in silico* methods, which have the capacity to reliably predict *in vivo* responses, are likely to become valuable and cost-effective. At the moment, the literature is contradictory and confusing, because foods are often poorly characterised, and the digestion methodologies used differ greatly. Therefore, it is recommended that digestion methodologies are standardised to enable direct comparison of different studies, and should also include a requirement for material characterisation, because this clearly has a major impact on the nutrient release profile. In the past, characterisation of foods has largely focused on identifying specific functional components in a food, yet the results presented in this thesis demonstrate that the structure and properties of the food matrix *per se* are also important. However, the disassembly of foods in the gastrointestinal tract is still poorly understood, and further work is needed to elucidate how food structure and cellular integrity changes during the various phases of digestive transit.

In the present work, large differences were observed between the behaviour and nutritional properties of chickpeas and durum wheat, but it remains unclear how these selected botanical species compare to other edible plant materials. Gaining further insight into the role of plant cell walls from different botanical species during processing and digestion may help to optimise the utilisation of edible plants in food products for optimised nutritional properties. For instance, are the cell walls of other pulses as

resilient and impermeable as chickpeas? How does durum wheat compare with soft wheat and indeed other cereals? These are interesting questions that warrant further exploration.

The broad range of methodologies applied in this project provides a strong foundation for further studies. In particular, the LOS analysis method presented in the current project shows great potential, and its ability to predict the *in vivo* response should be explored further. The *in vivo* validation of the LOS model as a predictor of glycaemia would require more extensive studies, and was beyond the scope of this study. However, this will be a very interesting area for further investigations, as a good *in vivo* predictor would be valuable, given that current *in vitro* and *in silico* models are somewhat limited.

8.6 CONCLUSIONS

The physical encapsulation of starch by plant cell walls was found to delay the rate and extent of starch digestion, and consequently attenuate post-prandial blood glucose and insulin concentrations. This effect was attributed predominantly to the role of plant cell walls as physical barriers to digestive enzymes (amylase), but may also be due to the role of cell walls in restricting starch gelatinisation and therefore its susceptibility to amylolysis after hydrothermal processing. The effects on starch bioaccessibility differed between chickpeas and durum wheat, reflecting the different plant cell wall properties (permeability and tendency to separate or fracture) of these edible-plant materials. **Overall, encapsulation by plant cell walls plays a major role in influencing starch bioaccessibility, with consequential effects on post-prandial metabolism.**

REFERENCES

- Al-Rabadi, G. J., Torley, P. J., Williams, B. A., Bryden, W. L. and Gidley, M. J. (2012). 'Particle size heterogeneity in milled barley and sorghum grains: Effects on physico-chemical properties and starch digestibility'. *Journal of Cereal Science*, **56**(2): 396-403.
- Al-Rabadi, G. J. S., Gilbert, R. G. and Gidley, M. J. (2009). 'Effect of particle size on kinetics of starch digestion in milled barley and sorghum grains by porcine alpha-amylase'. *Journal of Cereal Science*, **50**(2): 198-204.
- Åman, P., Pettersson, D., Zhang, J.-X., Tidehag, P. and Hallmans, G. (1995). 'Starch and dietary fiber components are excreted and degraded to variable extents in ileostomy subjects consuming mixed diets with wheat- or oat-bran bread'. *The Journal of Nutrition*, **125**(9): 2341-2347.
- Anderson, C. and Salmon, S., eds. (1999) *Manual of Methods for Wheat and Flour Testing, Guideline No. 3*, 2nd ed., Camden and Chorleywood Food Research Association.
- Anderson, J. W., Baird, P., Davis Jr, R. H., Ferreri, S., Knudtson, M., Koraym, A., Waters, V. and Williams, C. L. (2009). 'Health benefits of dietary fiber'. *Nutrition Reviews*, **67**(4): 188-205.
- Andersson, H. B. (1992). 'The ileostomy model for the study of carbohydrate digestion and carbohydrate effects on sterol excretion in man'. *European Journal of Clinical Nutrition*, **46**: S69-S76.
- Anguita, M., Gasa, J., Martín-Orúe, S. M. and Pérez, J. F. (2006). 'Study of the effect of technological processes on starch hydrolysis, non-starch polysaccharides solubilization and physicochemical properties of different ingredients using a two-step in vitro system'. *Animal Feed Science and Technology*, **129**(1-2): 99-115.
- Asp, N.-G., van Amelsvoort, J. M. M. and Hautvast, J. G. A. J. (1996). 'Nutritional implications of resistant starch'. *Nutrition Research Reviews*, **9**(01): 1-31.
- Aziz, A., Dumais, L. and Barber, J. (2013). 'Health Canada's evaluation of the use of glycemic index claims on food labels'. *The American Journal of Clinical Nutrition*.
- Bailey, J. M. and Whelan, W. J. (1961). 'Physical properties of starch: Relationship between iodine stain and chain length'. *The Journal of Biochemistry*, **236**(4): 969-973.
- Baldwin, P. M. (2001). 'Starch granule-associated proteins and polypeptides: A review'. *Starch - Stärke*, **53**(10): 475-503.

- Ballance, S., Sahlstrøm, S., Lea, P., Nagy, N., Andersen, P., Dessev, T., Hull, S., Vardakou, M. and Faulks, R. (2013). 'Evaluation of gastric processing and duodenal digestion of starch in six cereal meals on the associated glycaemic response using an adult fasted dynamic gastric model'. *European Journal of Nutrition*, **52**(2): 799-812.
- Baron-Epel, O., Gharyal, P. K. and Schindler, M. (1988). 'Pectins as mediators of wall porosity in soybean cells'. *Planta*, **175**(3): 389-395.
- Barron, C., Surget, A. and Rouau, X. (2007). 'Relative amounts of tissues in mature wheat (*Triticum aestivum* L.) grain and their carbohydrate and phenolic acid composition'. *Journal of Cereal Science*, **45**(1): 88-96.
- Berry, S. E., Tydeman, E. A., Lewis, H. B., Phalora, R., Rosborough, J., Picout, D. R. and Ellis, P. R. (2008). 'Manipulation of lipid bioaccessibility of almond seeds influences postprandial lipemia in healthy human subjects'. *The American Journal of Clinical Nutrition*, **88**: 922-929.
- Bjorck, I., Granfeldt, Y., Liljeberg, H., Tovar, J. and Asp, N. (1994). 'Food properties affecting the digestion and absorption of carbohydrates'. *The American Journal of Clinical Nutrition*, **59**(3): 699S-705S.
- Blazek, J., Salman, H., Rubio, A. L., Gilbert, E., Hanley, T. and Copeland, L. (2009). 'Structural characterization of wheat starch granules differing in amylose content and functional characteristics'. *Carbohydrate Polymers*, **75**(4): 705-711.
- Bogracheva, T. Y., Morris, V. J., Ring, S. G. and Hedley, C. L. (1998). 'The granular structure of C-type pea starch and its role in gelatinization'. *Biopolymers*, **45**(4): 323-332.
- Bogracheva, T. Y., Wang, Y. L., Wang, T. L. and Hedley, C. L. (2002). 'Structural studies of starches with different water contents'. *Biopolymers*, **64**(5): 268-281.
- Borgstrom, B., Dahlqvist, A., Lundh, G. and Sjoval, J. (1957). 'Studies of intestinal digestion and absorption in the human'. *Journal of Clinical Investigation*, **36**(10): 1521-1536.
- Bornhorst, G. M. and Singh, R. P. (2012). 'Bolus formation and disintegration during digestion of food carbohydrates'. *Comprehensive Reviews in Food Science and Food Safety*, **11**(2): 101-118.
- Brand-Miller, J. (1995). 'International tables of glycemic index'. *The American Journal of Clinical Nutrition*, **62**(4): 869S-.
- Brand, J. C., Colagiuri, S., Crossman, S., Allen, A., Roberts, D. C. and Truswell, A. S. (1991). 'Low-Glycemic Index foods improve long-term glycemic control in NIDDM'. *Diabetes Care*, **14**(2): 95-101.

- Brayer, G. D., Luo, Y. and Withers, S. G. (1995). 'The structure of human pancreatic alpha-amylase at 1.8 Å resolution and comparisons with related enzymes'. *Protein Science*, **4**: 1730-1742.
- Brett, C. and Waldron, K., eds. (1996) *Physiology and biochemistry of plant cell walls*, 2nd ed., London: Chapman & Hall.
- Brownlee, I. A. (2011). 'The physiological roles of dietary fibre'. *Food Hydrocolloids*, **25**(2): 238-250.
- Buchanon, B., Grisseem, W. and Jones, R., eds. (2000) *Biochemistry and molecular biology of plants*, USA: Wiley-Blackwell.
- Buléon, A., Colonna, P., Planchot, V. and Ball, S. (1998). 'Starch granules: structure and biosynthesis'. *International Journal of Biological Macromolecules*, **23**(2): 85-112.
- Buonocore, V., Petrucci, T. and Silano, V. (1977). 'Wheat protein inhibitors of alpha-amylase'. *Phytochemistry*, **16**(7): 811-820.
- Burton, R. A., Gidley, M. J. and Fincher, G. B. (2010). 'Heterogeneity in the chemistry, structure and function of plant cell walls'. *Nature Chemical Biology*, **6**: 724-732.
- Butterworth, P. J., Warren, F. J. and Ellis, P. R. (2011). 'Human α -amylase and starch digestion: An interesting marriage'. *Starch - Stärke*, **63**(7): 395-405.
- Butterworth, P. J., Warren, F. J., Grassby, T., Patel, H. and Ellis, P. R. (2012). 'Analysis of starch amylolysis using plots for first-order kinetics'. *Carbohydrate Polymers*, **87**(3): 2189-2197.
- Campbell, G. M. (2007). 'Chapter 7 Roller Milling of Wheat' in Agba D. Salman, M. G. and Michael, J. H., eds., *Handbook of Powder Technology*, Elsevier Science B.V., 383-419.
- Carpita, N. (1982). 'Limiting diameters of pores and the surface structure of plant cell walls'. *Science*, **218**(4574): 813-814.
- Carpita, N., Sabulase, D., Montezinos, D. and Delmer, D. P. (1979). 'Determination of the pore size of cell walls of living plant cells'. *Science*, **205**(4411): 1144-1147.
- Champagne, E. T., Marshall, W. E. and Goynes, W. R. (1990). 'Effects of degree of milling and lipid removal on starch gelatinization in the brown rice kernel'. *Cereal Chemistry*, **67**: 570-574.
- Chanvrier, H., Uthayakumar, S., Appelqvist, I. A. M., Gidley, M. J., Gilbert, E. P. and López-Rubio, A. (2007). 'Influence of storage conditions on the structure, thermal behavior, and formation of enzyme-resistant starch in extruded starches'. *Journal of Agricultural and Food Chemistry*, **55**(24): 9883-9890.

- Chen, J. (2009). 'Food oral processing—A review'. *Food Hydrocolloids*, **23**(1): 1-25.
- Chesson, A., Gardner, P. T. and Wood, T. J. (1997). 'Cell wall porosity and available surface area of wheat straw and wheat grain fractions'. *Journal of the Science of Food and Agriculture*, **75**(3): 289-295.
- Choi, H.-K., Mun, J.-H., Kim, D.-J., Zhu, H., Baek, J.-M., Mudge, J., Roe, B., Ellis, N., Doyle, J., Kiss, G. B., Young, N. D. and Cook, D. R. (2004). 'Estimating genome conservation between crop and model legume species'. *Proceedings of the National Academy of Sciences of the United States of America*, **101**(43): 15289-15294.
- Clemente, A., Sánchez-Vioque, R., Vioque, J., Bautista, J. and Millán, F. (1998). 'Effect of processing on water absorption and softening kinetics in chickpea (*Cicer arietinum*L) seeds'. *Journal of the Science of Food and Agriculture*, **78**(2): 169-174.
- Cosgrove, D. J. (2005). 'Growth of the plant cell wall'. *Nature Reviews Molecular Cell Biology*, **6**(11): 850-861.
- Cui, S. and Wang, Q. (2009). 'Cell wall polysaccharides in cereals: chemical structures and functional properties'. *Structural Chemistry*, **20**(2): 291-297.
- Cummings, J. H. (1983). 'Fermentation in the human large intestine: evidence and implications for health'. *The Lancet*, **321**(8335): 1206-1209.
- Cummings, J. H. and Macfarlane, G. T. (1968). 'The control and consequences of bacterial fermentation in the human colon'. *Journal of Applied Microbiology*, **31**(4): xi-xii.
- Cummings, J. H. and Macfarlane, G. T. (1991). 'The control and consequences of bacterial fermentation in the human colon'. *Journal of Applied Microbiology*, **70**(6): 443-459.
- Cummings, J. H. and Macfarlane, G. T. (1997). 'Role of intestinal bacteria in nutrient metabolism'. *Clinical Nutrition*, **16**: 3-11.
- D'Amico, S., Sohler, J. S. and Feller, G. (2006). 'Kinetics and energetics of ligand binding determined by microcalorimetry: Insights into active site mobility in a psychrophilic α -amylase'. *Journal of Molecular Biology*, **358**(5): 1296-1304.
- Dahlqvist, A. and Borgstrom, B. (1961). 'Digestion and absorption in man'. *Biochemical Journal*, **81**: 411-418.
- Dandanell Daveby, Y., Razdan, A. and Åman, P. (1998). 'Effect of particle size and enzyme supplementation of diets based on dehulled peas on the nutritive value for broiler chickens'. *Animal Feed Science and Technology*, **74**(3): 229-239.

- Daramola, B. and Osanyinlusi, S. A. (2006). 'Investigation on modification of cassava starch using active components of ginger roots (*Zingiber officinale* Roscoe)'. *African Journal of Biotechnology*, **5**(10): 917-920.
- Debet, M. R. and Gidley, M. J. (2006). 'Three classes of starch granule swelling: Influence of surface proteins and lipids'. *Carbohydrate Polymers*, **64**(3): 452-465.
- Debet, M. R. and Gidley, M. J. (2007). 'Why do gelatinized starch granules not dissolve completely? Roles for amylose, protein, and lipid in granule "ghost" integrity'. *Journal of Agricultural and Food Chemistry*, **55**(12): 4752-4760.
- Deng, S. P. and Tabatabai, M. A. (1994). 'Colorimetric determination of reducing sugars in soils'. *Soil Biology and Biochemistry*, **26**(4): 473-477.
- 'Diabetes UK', *Diabetes in the UK 2012: Key statistics on diabetes* [online], available: http://www.diabetes.org.uk/About_us/What-we-say/Statistics/Diabetes-in-the-UK-2012/ [accessed 2 April 2014].
- Dona, A. C., Pages, G., Gilbert, R. G. and Kuchel, P. W. (2010). 'Digestion of starch: In vivo and in vitro kinetic models used to characterise oligosaccharide or glucose release'. *Carbohydrate Polymers*, **80**(3): 599-617.
- Donovan, J. W. (1979). 'Phase transitions of the starch–water system'. *Biopolymers*, **18**(2): 263-275.
- Edwards, C. H., Grundy, M. and Grassby, T. (2013) 'Ileostomy volunteers needed for important nutritional research', *Hand-in Hand magazine*, 9.
- EFSA Panel on Dietetic Products Nutrition and Allergies (NDA) (2010a). 'Scientific Opinion on Dietary Reference Values for carbohydrates and dietary fibre'. *EFSA Journal*, **8**(3): 1462-1539.
- EFSA Panel on Dietetic Products Nutrition and Allergies (NDA). (2010b). 'Scientific Opinion on the substantiation of health claims related to dietary fibre (ID 744, 745, 746, 748, 749, 753, 803, 810, 855, 1415, 1416, 4308, 4330) pursuant to Article 13(1) of Regulation (EC) No 1924/2006'. *EFSA Journal*, **8**(10): 1735-1758.
- Ellis, P. R. (1999). 'The effects of fibre on diabetes' in Hill, M., ed. *The right fibre for the right disease*, London: Royal Society of Medicine Press Ltd., 33-41.
- Ellis, P. R., Kendall, C. W. C., Ren, Y., Parker, C., Pacy, J. F., Waldron, K. W. and Jenkins, D. J. A. (2004). 'Role of cell walls in bioaccessibility of lipids in almond seeds'. *The American Journal of Clinical Nutrition*, **80**: 604-613.

- Ellis, P. R., Picout, D. R., Wickham, M. S. J., Mandalari, G., Rich, G. T., Faulks, R. M. and Lapsley, K. (2007). 'Mathematical modelling of lipid bioaccessibility in almond seeds'. *The Journal of the Federation of American Societies for Experimental Biology*, **21**: A119.
- Ellis, P. R., Roberts, F. G., Low, A. G. and Morgan, L. M. (1995). 'The effect of high-molecular-weight guar gum on net apparent glucose absorption and net apparent insulin and gastric inhibitory polypeptide production in the growing pig: relationship to rheological changes in jejunal digesta'. *British Journal of Nutrition*, **74**(04): 539-556.
- Ells, L. J., Seal, C. J., Kettlitz, B., Bal, W. and Mathers, J. C. (2005). 'Postprandial glycaemic, lipaemic and haemostatic responses to ingestion of rapidly and slowly digested starches in healthy young women'. *British Journal of Nutrition*, **94**: 948-955.
- Englyst, H. N. and Cummings, J. H. (1985). 'Digestion of the polysaccharides of some cereal foods in the human small intestine'. *The American Journal of Clinical Nutrition*, **42**(5): 778-87.
- Englyst, H. N. and Cummings, J. H. (1986). 'Digestion of the carbohydrates of banana (*Musa paradisiaca sapientum*) in the human small intestine'. *The American Journal of Clinical Nutrition*, **44**: 42-50.
- Englyst, H. N. and Cummings, J. H. (1987). 'Digestion of polysaccharides of potato in the small intestine of man'. *The American Journal of Clinical Nutrition*, **45**: 423-431.
- Englyst, H. N. and Hudson, G. J. (1996). 'The classification and measurement of dietary carbohydrates'. *Food Chemistry*, **57**(1): 15-21.
- Englyst, H. N., Kingman, S. M. and Cummings, J. H. (1992). 'Classification and measurement of nutritionally important starch fractions'. *European Journal of Clinical Nutrition*, **46**: S33-S50.
- Englyst, K. N., Englyst, H. N., Hudson, G. J., Cole, T. J. and Cummings, J. H. (1999). 'Rapidly available glucose in foods: an in vitro measurement that reflects the glycemic response'. *The American Journal of Clinical Nutrition*, **69**(3): 448-454.
- European Commission directive 2008/100/EC of 28 October 2008 amending Council Directive 90/496/EEC on nutrition labelling for foodstuffs as regards recommended daily allowances, energy conversion factors and definitions.*
- European Commission directive 79/1067/EEC of 13 November 1979 laying down Community methods of analysis for testing certain partly or wholly dehydrated preserved milk for human consumption*

- Evans, I. D., Elson, D. R. H. E. L., Pasternak, C. and McConnaughey, W. B. (1986). 'The effect of salivary amylase on the viscosity behaviour of gelatinised starch suspensions and the mechanical properties of gelatinised starches'. *Journal of the Science of Food and Agriculture*, **37**: 573-590.
- Fang, C. and Campbell, G. M. (2002). 'Effect of roll fluting disposition and roll gap on breakage of wheat kernels during first-break roller milling'. *Cereal Chemistry Journal*, **79**(4): 518-522.
- Fang, C. and Campbell, G. M. (2003). 'On predicting roller milling performance IV: Effect of roll disposition on the particle size distribution from first break milling of wheat'. *Journal of Cereal Science*, **37**(1): 21-29.
- Fardet, A., Hoebler, C., Baldwin, P. M., Bouchet, B., Gallant, D. J. and Barry, J. L. (1998). 'Involvement of the protein network in the in vitro degradation of starch from spaghetti and lasagne: A microscopic and enzymic Study'. *Journal of Cereal Science*, **27**(2): 133-145.
- Finegold, S. M., Sutter, V. L., Boyle, J. D. and Shimada, K. (1970). 'The normal flora of ileostomy and transverse colostomy effluents'. *Journal of Infectious Diseases*, **122**(5): 376-381.
- Flint, O. (1994). *Food Microscopy: A manual of practical methods, using optical microscopy*, Oxford: Bios Scientific Publishers.
- Foster-Powell, K., Holt, S. H. and Brand-Miller, J. C. (2002). 'International table of glycemic index and glycemic load values: 2002'. *The American Journal of Clinical Nutrition*, **76**(1): 5-56.
- Frayn, K. N. (2010). *Metabolic Regulation: A Human Perspective*, 3rd ed., Chichester, UK: John Wiley & Sons Ltd.
- Frias, J., Vidal-Valverde, C., Sotomayor, C., Diaz-Pollan, C. and Urbano, G. (2000). 'Influence of processing on available carbohydrate content and antinutritional factors of chickpeas'. *European Food Research and Technology*, **210**(5): 340-345.
- Fried, M., Abramson, S. and Meyer, J. H. (1987). 'Passage of salivary amylase through the stomach in humans'. *Digestive Diseases and Sciences*, **32**(10): 1097-1103.
- Fry, S. C. (1988). *The growing plant cell wall: chemical and metabolic analysis*, Harlow: Longman Scientific & Technical, 149.
- Fujimura, T. and Kugimiya, M. (1994). 'Gelatinization of starches inside cotyledon cells of kidney beans'. *Starch - Stärke*, **46**(10): 374-378.

- Fukuoka, M., Ohta, K.-i. and Watanabe, H. (2002). 'Determination of the terminal extent of starch gelatinization in a limited water system by DSC'. *Journal of Food Engineering*, **53**(1): 39-42.
- Gallant, D. J., Bouchet, B., Bulion, A. and Perez, S. (1992). 'Physical characteristics of starch granules and susceptibility to enzymatic degradation'. *European Journal of Clinical Nutrition*, **46**: S3-S16.
- Gill, P., Moghadam, T. T. and Ranjbar, B. (2010). 'Differential scanning calorimetry techniques: Applications in biology and nanoscience'. *Journal of Biomolecular Techniques*, **21**(4): 167-193.
- Ginsberg, H. N., Zhang, Y.-L. and Hernandez-Ono, A. (2005). 'Regulation of plasma triglycerides in insulin resistance and diabetes'. *Archives of medical research*, **36**(3): 232-240.
- Golay, A., Coulston, A. M., Hollenbeck, C. B., Kaiser, L. L., Würsch, P. and Reaven, G. M. (1986). 'Comparison of metabolic effects of white beans processed into two different physical forms'. *Diabetes Care*, **9**(3): 260-266.
- Goñi, I., Garcia-Alonso, A. and Saura-Calixto, F. (1997). 'A starch hydrolysis procedure to estimate glycemic index'. *Nutrition Research*, **17**(3): 427-437.
- Granfeldt, Y. and Björck, I. (1991). 'Glycemic response to starch in pasta: a study of mechanisms of limited enzyme availability'. *Journal of Cereal Science*, **14**(1): 47-61.
- Granfeldt, Y., Björck, I., Drews, A. and Tovar, J. (1992). 'An in vitro procedure based on chewing to predict metabolic response to starch in cereal and legume products'. *European Journal of Clinical Nutrition*, **46**: 649-660.
- Grassby, T., Edwards, C. H., Grundy, M. and Ellis, P. R. (2013). 'Functional components and mechanisms of action of 'dietary fibre' in the upper gastrointestinal tract: Implications for health' in Harding, S. E., ed. *Stability of Complex Carbohydrate Structures: Biofuels, Foods, Vaccines and Shipwrecks*, Royal Society of Chemistry.
- Güzel, D. and Sayar, S. (2010). 'Digestion profiles and some physicochemical properties of native and modified borlotti bean, chickpea and white kidney bean starches'. *Food Research International*, **43**(8): 2132-2137.
- Haralampu, S. G. (2000). 'Resistant starch—a review of the physical properties and biological impact of RS3'. *Carbohydrate Polymers*, **41**(3): 285-292.
- Hellström, P. M., Grybäck, P. and Jacobsson, H. (2006). 'The physiology of gastric emptying'. *Best Practice & Research Clinical Anaesthesiology*, **20**(3): 397-407.

- HGCA, Federation of Bakers Flour Advisery Bureau (2014). 'Grain Chain', [online], available: http://www.grainchain.com/Resources/11-14/ip_looking-at-wheat-seeds [accessed 13th March 2014].
- Hoebler, C., Devaux, M. F., Karinthi, A., Belleville, C. and Barry, J. L. (2000). 'Particle size of solid food after human mastication and in vitro simulation of oral breakdown'. *International Journal of Food Sciences and Nutrition*, **51**: 353-366.
- Hoebler, C., Karinthi, A., Devaux, M.-F., Guillon, F., Gallant, D. J. G., Bouchet, B., Melegari, C. and Barry, J.-L. (1998). 'Physical and chemical transformations of cereal food during oral digestion in human subjects'. *British Journal of Nutrition*, **80**(05): 429-436.
- Holm, J. and Bjorck, I. (1992). 'Bioavailability of starch in various wheat-based bread products: evaluation of metabolic responses in healthy subjects and rate and extent of in vitro starch digestion'. *The American Journal of Clinical Nutrition*, **55**: 420-429.
- Hoover, R., Hughes, T., Chung, H. J. and Liu, Q. (2010). 'Composition, molecular structure, properties, and modification of pulse starches: A review'. *Food Research International*, **43**(2): 399-413.
- Horwitz, D. L., Starr, J. I., Mako, M. E., Blackard, W. G. and Rubenstein, A. H. (1975). 'Proinsulin, insulin, and C-peptide concentrations in human portal and peripheral blood'. *The Journal of Clinical Investigation*, **55**(6): 1278-1283.
- Hughes, T., Hoover, R., Liu, Q., Donner, E., Chibbar, R. and Jaiswal, S. (2009). 'Composition, morphology, molecular structure, and physicochemical properties of starches from newly released chickpea (*Cicer arietinum* L.) cultivars grown in Canada'. *Food Research International*, **42**(5-6): 627-635.
- Jarvi, A., Karlstrom, B., Granfeldt, Y., Bjorck, I., Vessby, B. and Asp, N. (1995). 'The influence of food structure on postprandial metabolism in patients with non-insulin-dependent diabetes mellitus'. *The American Journal of Clinical Nutrition*, **61**(4): 837-842.
- Jarvis, M. C. (2011). 'Plant cell walls: Supramolecular assemblies'. *Food Hydrocolloids*, **25**(2): 257-262.
- Jarvis, M. C., Briggs, S. P. H. and Knox, J. P. (2003). 'Intercellular adhesion and cell separation in plants'. *Plant, Cell & Environment*, **26**(7): 977-989.
- Jenkins, D. J. A., Ghafari, H., Wolever, T. M. S., Taylor, R. H., Jenkins, A. L., Barker, H. M., Fielden, H. and Bowling, A. C. (1982). 'Relationship between rate of digestion of foods and post-prandial glycaemia'. *Diabetologia*, **22**(6): 450-455.
- Jenkins, D. J. A., Jenkins, A. L., Wolever, T. M. S., Josse, R. G. and Wong, G. S. (1984). 'The glycaemic response to carbohydrate foods'. *The Lancet*, **324**(8399): 388-391.

- Jenkins, D. J. A., Kendall, C. W. C., Augustin, L. S. A., Franceschi, S., Hamidi, M., Marchie, A., Jenkins, A. L. and Axelsen, M. (2002). 'Glycemic index: overview of implications in health and disease'. *The American Journal of Clinical Nutrition*, **76**: 266S-273S.
- Jenkins, D. J. A., Thorne, M. J., Wolever, T. M. S., Jenkins, A. L., Rao, A. V. and Thompson, L. U. (1987). 'The effect of starch-protein interaction in wheat on the glycemic response and rate of in vitro digestion'. *The American Journal of Clinical Nutrition*, **45**(5): 946-51.
- Jenkins, D. J. A., Wolever, T. M. S., Taylor, R. H., Barker, H., Fielden, H., Baldwin, J. M., Bowling, A. C., Newman, H. C., Jenkins, A. L. and Goff, D. V. (1981). 'Glycemic index of foods: a physiological basis for carbohydrate exchange'. *The American Journal of Clinical Nutrition*, **34**(3): 362-6.
- Jobling, S. (2004). 'Improving starch for food and industrial applications'. *Current Opinion in Plant Biology*, **7**(2): 210-218.
- Jones, A. D., Burns, I. W., Sellings, S. G. and Cox, J. A. (1977). 'Preparation, optimisation and slurry packing of an amino bonded phase for the analysis of sugars in food by high-performance liquid chromatography'. *Journal of Chromatography A*, **144**(2): 169-180.
- Judd, P. A. and Ellis, P. R. (2005). 'Plant Polysaccharides in the Prevention and Treatment of Diabetes Mellitus' in Soumyanath, A., ed. *Traditional Medicines for Modern Times: Antidiabetic Plants*, Florida: Taylor & Francis Group LLC, 257-272.
- Kellett, G. L. and Brot-Laroche, E. (2005). 'Apical GLUT2: A major pathway of intestinal sugar absorption'. *Diabetes*, **54**(10): 3056-3062.
- Kendall, C. W. C., Esfahani, A. and Jenkins, D. J. A. (2010). 'The link between dietary fibre and human health'. *Food Hydrocolloids*, **24**(1): 42-48.
- Kent, N. and Evers, A. D. (1994). *Kent's Technology of Cereals*, 4th ed., Oxford: Elsevier Science Ltd.
- Kirk, R. S. and Sawyer, R., eds. (1991) *Pearson's Composition and Analysis of Foods*, 9th ed., Essex: Addison Wesley Longman Ltd.
- Knutson, C. A. (1986). 'A simplified colorimetric procedure for determination of amylose in maize starches'. *Cereal Chemistry*, **63**(2): 89-92.
- Knutson, C. A. (2000). 'Evaluation of variations in amylose-iodine absorbance spectra'. *Carbohydrate Polymers*, **42**(1): 65-72.
- Kong, F. and Singh, R. P. (2008). 'Disintegration of solid foods in the human stomach'. *Journal of Food Science*, **73**(5): R67-R80.

- Kristensen, M., Jensen, M. G., Riboldi, G., Petronio, M., Bügel, S., Toubro, S., Tetens, I. and Astrup, A. (2010). 'Wholegrain vs. refined wheat bread and pasta. Effect on postprandial glycemia, appetite, and subsequent ad libitum energy intake in young healthy adults'. *Appetite*, **54**(1): 163-169.
- Layer, P., Go, V. L. and DiMagno, E. P. (1986). 'Fate of pancreatic enzymes during small intestinal aboral transit in humans'. *American Journal of Physiology - Gastrointestinal and Liver Physiology*, **251**(4): G475-G480.
- Lentner, C., ed. (1981) *Geigy scientific tables: Volume 1: Units of measurement, body fluids, composition of the body, nutrition*, 8th ed., West Caldwell, NJ: CIBA-Geigy Corporation.
- Liljeberg H, G. Y., Björck I. (1992). 'Metabolic responses to starch in bread containing intact kernels versus milled flour'. *European Journal of Clinical Nutrition*, **46**(8): 561-575.
- Livesey, G. (1990). 'Energy values of unavailable carbohydrate and diets: an inquiry and analysis'. *The American Journal of Clinical Nutrition*, **51**(4): 617-637.
- Livesey, G., Buss, D., Coussement, P., Edwards, D. G., Howlett, J., Jonas, D. A., Kleiner, J. E., Müller, D. and Sentko, A. (2000). 'Suitability of traditional energy values for novel foods and food ingredients'. *Food Control*, **11**(4): 249-289.
- Livesey, G., Wilkinson, J. A., Roe, M., Faulks, R., Clark, S., Brown, J. C., Kennedy, H. and Elia, M. (1995). 'Influence of the physical form of barley grain on the digestion of its starch in the human small intestine and implications for health'. *The American Journal of Clinical Nutrition*, **61**: 75-81.
- Lucas, W. J. and Lee, J.-Y. (2004). 'Plasmodesmata as a supracellular control network in plants'. *Nature Reviews Molecular Cell Biology*, **5**(9): 712-726.
- M'Koma, A., Wise, P., Muldoon, R., Schwartz, D., Washington, M. and Herline, A. (2007). 'Evolution of the restorative proctocolectomy and its effects on gastrointestinal hormones'. *International Journal of Colorectal Disease*, **22**(10): 1143-1163.
- MacGregor, E. A., Janeček, Š. and Svensson, B. (2001). 'Relationship of sequence and structure to specificity in the α -amylase family of enzymes'. *Biochimica et Biophysica Acta (BBA) - Protein Structure and Molecular Enzymology*, **1546**(1): 1-20.
- Mahasukhonthachat, K., Sopade, P. A. and Gidley, M. J. (2010). 'Kinetics of starch digestion in sorghum as affected by particle size'. *Journal of Food Engineering*, **96**(1): 18-28.
- Mainville, I., Arcand, Y. and Farnworth, E. R. (2005). 'A dynamic model that simulates the human upper gastrointestinal tract for the study of probiotics'. *International Journal of Food Microbiology*, **99**(3): 287-296.

- Malagelada, J.-R., Robertson, J. S., Brown, M. L., Remington, M., Duenes, J. A., Thomforde, G. M. and Carryer, P. W. (1984). 'Intestinal transit of solid and liquid components of a meal in health'. *Gastroenterology*, **87**(6): 1255-1263.
- Malagelada, J. R., Longstreth, G. F., Summerskill, W. H. and Go, V. L. (1976). 'Measurement of gastric functions during digestion of ordinary solid meals in man'. *Gastroenterology*, **70**(2): 203-210.
- Mandalari, G., Faulks, R. M., Rich, G. T., Turco, V. L., Picout, D. R., Lo curto, R. P., Bisignano, G., Dugo, P., Dugo, G., Waldron, K. W., Ellis, P. R. and Wickham, M. S. J. (2008). 'Release of Protein, Lipid, and Vitamin E from Almond Seeds during Digestion'. *Journal of Agriculture and Food Chemistry*, **56**(9): 3409-3416.
- Mann, J. I. and Cummings, J. H. (2009). 'Possible implications for health of the different definitions of dietary fibre'. *Nutrition, Metabolism and Cardiovascular Diseases*, **19**(3): 226-229.
- Marshall, W. E. (1992). 'Effect of degree of milling of brown rice and particle size of milled rice on starch gelatinisation'. *Cereal Chemistry*, **69**(6): 632-636.
- Marze, S. (2012). 'Bioaccessibility of Nutrients and Micronutrients from Dispersed Food Systems: Impact of the Multiscale Bulk and Interfacial Structures'. *Critical Reviews in Food Science and Nutrition*, **53**(1): 76-108.
- McCance, R. and Widdowson, E. (2002). *McCance and Widdowson's The composition of foods*, 6th ed., Cambridge: Royal Society of Chemistry.
- McCleary, B. V., Solah, V. and Gibson, T. S. (1994). 'Quantitative measurement of total starch in cereal flours and products'. *Journal of Cereal Science*, **20**(1): 51-58.
- McCormick, B., Stone, I. and Corporate Analytical, T. (2007). 'Economic costs of obesity and the case for government intervention'. *Obesity Reviews*, **8**: 161-164.
- Meier, J. J. and Nauck, M. A. (2004). 'Glucose-dependent insulinotropic polypeptide/gastric inhibitory polypeptide'. *Best Practice & Research Clinical Endocrinology & Metabolism*, **18**(4): 587-606.
- Melito, C. and Tovar, J. (1995). 'Cell walls limit in vitro protein digestibility in processed legume seeds'. *Food Chemistry*, **53**(3): 305-307.
- Mercuri, A., Passalacqua, A., Wickham, M. S. J., Faulks, R. M., Craig, D. Q. M. and Barker, S. A. (2011). 'The effect of composition and gastric conditions on the self-emulsification process of ibuprofen-loaded self-emulsifying drug delivery systems: A microscopic and dynamic gastric model study'. *Pharmaceutical Research*, **28**: 1540-1551.

- Miller, G. L. (1959). 'Use of dinitrosalicylic acid reagent for determination of reducing sugar'. *Analytical Chemistry*, **31**(3): 426-428.
- Moller, I., Sørensen, I., Bernal, A. J., Blaukopf, C., Lee, K., Øbro, J., Pettolino, F., Roberts, A., Mikkelsen, J. D., Knox, J. P., Bacic, A. and Willats, W. G. T. (2007). 'High-throughput mapping of cell-wall polymers within and between plants using novel microarrays'. *The Plant Journal*, **50**: 1118-1125.
- 'Monocotyledon: internal structures of a corn seed with stages of germination', (2006) *Encyclopædia Britannica* [online], available: <http://www.britannica.com> [accessed 1 April 2014].
- Monro, J., Mishra, S. and Hardacre, A. (2011). 'Glycaemic impact regulation based on progressive geometric changes in solid starch-based food particles during digestion'. *Food Digestion*, **2**(1): 1-12.
- Morgan, J. E. and Williams, P. C. (1995). 'Starch damage in wheat flours: A comparison of enzymatic, iodometric, and near-infrared reflectance techniques'. *Cereal Chemistry*, **72**(2): 209-212.
- Morgan, L. M., Tredger, J. A., Wright, J. and Marks, V. (1990). 'The effect of soluble- and insoluble-fibre supplementation on post-prandial glucose tolerance, insulin and gastric inhibitory polypeptide secretion in healthy subjects'. *British Journal of Nutrition*, **64**(01): 103-110.
- Muir, J. and O'Dea, K. (1993). 'Validation of an in vitro assay for predicting the amount of starch that escapes digestion in the small intestine of humans'. *The American Journal of Clinical Nutrition*, **57**(4): 540-546.
- Murphy, K. G. and Bloom, S. R. (2006). 'Gut hormones and the regulation of energy homeostasis'. *Nature*, **44**: 854-859.
- Noah, L., Guillon, F., Bouchet, B., Buleon, A., Molis, C., Gratas, M. and Champ, M. (1998). 'Digestion of carbohydrate from white beans (*Phaseolus vulgaris* L.) in healthy humans'. *The Journal of Nutrition*, **128**: 977-985.
- Noda, T., Kottarachchi, N. S., Tsuda, S., Mori, M., Takigawa, S., Matsuura-Endo, C., Kim, S.-J., Hashimoto, N. and Yamauchi, H. (2007). 'Starch phosphorus content in potato (*Solanum tuberosum* L.) cultivars and its effect on other starch properties'. *Carbohydrate Polymers*, **68**(4): 793-796.
- Norton, I., Moore, S. and Fryer, P. (2007). 'Understanding food structuring and breakdown: engineering approaches to obesity'. *Obesity Reviews*, **8**(s1): 83-88.

- O'Dea, K., Snow, P. and Nestel, P. (1981). 'Rate of starch hydrolysis in vitro as a predictor of metabolic responses to complex carbohydrate in vivo'. *The American Journal of Clinical Nutrition*, **34**(10): 1991-1993.
- Oyman, S. (2007) *Cellular integrity: its effect on in vitro starch digestion*, unpublished thesis (PhD), University of Nottingham.
- Parada, J. and Aguilera, J. M. (2007). 'Food microstructure affects the bioavailability of several nutrients'. *Journal of Food Science*, **72**(2): R21-R32.
- Parada, J. and Aguilera, J. M. (2011). 'Review: Starch matrices and the glycemic response'. *Food Science and Technology International*, **17**(3): 187-204.
- Park, J. T. and Johnson, M. J. (1949). 'A submicro determination of glucose'. *Journal of Biological Chemistry*, **181**: 149-151.
- Parks, E. J. (2001). 'Effect of dietary carbohydrate on triglyceride metabolism in humans'. *The Journal of Nutrition*, **131**(10): 2772S-2774S.
- Payan, F., Haser, R., Pierrot, M., Frey, M., Astier, J. P., Abadie, B., Duee, E. and Buisson, G. (1980). 'The three-dimensional structure of alpha-amylase from porcine pancreas at 5 Å resolution - The active site location'. *Acta Crystallographica Section B Structural Crystallography and Crystal Chemistry*, **36B**: 416-421.
- Pedersen, H. L., Fangel, J. U., McCleary, B., Ruzanski, C., Rydahl, M. G., Ralet, M.-C., Farkas, V., von Schantz, L., Marcus, S. E., Andersen, M. C. F., Field, R., Ohlin, M., Knox, J. P., Clausen, M. H. and Willats, W. G. T. (2012). 'Versatile high resolution oligosaccharide microarrays for plant glycobiology and cell wall research'. *Journal of Biological Chemistry*, **287**(47): 39429-39438.
- Pereira, M. A. (2006). 'The possible role of sugar-sweetened beverages in obesity etiology: a review of the evidence'. *International Journal of Obesity*, **30**: S28-S36.
- Perera, A., Meda, V. and Tyler, R. T. (2010). 'Resistant starch: A review of analytical protocols for determining resistant starch and of factors affecting the resistant starch content of foods'. *Food Research International*, **43**(8): 1959-1974.
- Pérez, S. and Bertoft, E. (2010). 'The molecular structures of starch components and their contribution to the architecture of starch granules: A comprehensive review'. *Starch - Stärke*, **62**(8): 389-420.
- Perry, P. A. and Donald, A. M. (2002). 'The effect of sugars on the gelatinisation of starch'. *Carbohydrate Polymers*, **49**(2): 155-165.
- Petersen, O. H. and Dimaline, R. (2007). 'Digestive System' in Petersen, O. H., ed. *Lecture Notes in Human Physiology*, 5th ed., Oxford: Blackwell Publishing, 521-525.

- Pitino, I., Randazzo, C. L., Mandalari, G., Lo Curto, A., Faulks, R. M., Le Marc, Y., Bisignano, C., Caggia, C. and Wickham, M. S. J. (2010). 'Survival of *Lactobacillus rhamnosus* strains in the upper gastrointestinal tract'. *Food Microbiology*, **27**(8): 1121-1127.
- Poulsen, B., Ruitter, G., Visser, J. and Lønsmann Iversen, J. (2003). 'Determination of first order rate constants by natural logarithm of the slope plot exemplified by analysis of *Aspergillus niger* in batch culture'. *Biotechnology Letters*, **25**(7): 565-571.
- Ranawana, V., Clegg, M. E., Shafat, A. and Henry, C. J. (2011). 'Postmastication digestion factors influence glycemic variability in humans'. *Nutrition Research*, **31**(6): 452-459.
- Read, N. W., Welch, I. M., Austen, C. J., Barnish, C., Bartlett, C. E., Baxter, A. J., Brown, G., Compton, M. E., Hume, K. E., Storie, I. and Worlding, J. (1986). 'Swallowing food without chewing; a simple way to reduce postprandial glycaemia'. *British Journal of Nutrition*, **55**(01): 43-47.
- Rehman, Z.-u. and Shah, W. H. (2005). 'Thermal heat processing effects on antinutrients, protein and starch digestibility of food legumes'. *Food Chemistry*, **91**(2): 327-331.
- Robinson, D. S. (1973). 'Plasma triglyceride metabolism'. *Journal of Clinical Pathology*, **s1-5**(1): 5-10.
- Roby, J. F. and French, D. (1970). 'The action pattern of porcine pancreatic α -amylase in relationship to the substrate binding site of the enzyme'. *Journal of Biological Chemistry*, **245**(15): 3917-3927.
- Roder, N., Gerard, C., Verel, A., Bogracheva, T. Y., Hedley, C. L., Ellis, P. R. and Butterworth, P. J. (2009). 'Factors affecting the action of alpha-amylase on wheat starch: Effects of water availability. An enzymic and structural study'. *Food Chemistry*, **113**: 471-478.
- Rosenblum, J. L., Irwin, C. L. and Alpers, D. H. (1988). 'Starch and glucose oligosaccharides protect salivary-type amylase activity at acid pH'. *American Journal of Physiology - Gastrointestinal and Liver Physiology*, **254**(5): G775-G780.
- Rumney, C. J. and Rowland, I. R. (1992). 'In vivo and in vitro models of the human colonic flora'. *Critical Reviews in Food Science and Nutrition*, **31**(4): 299-331.
- Ruseler-van-Emden, J. G. H., Kool, J., Lieshout, L. M. C. V. and Hazenberg, M. P. (1991). 'Enzymic activity in ileostomy effluent with reference to the characteristic flora'. *Microbial Ecology in Health and Disease*, **4**: 215-222.
- Saltiel, A. R. and Kahn, C. R. (2001). 'Insulin signalling and the regulation of glucose and lipid metabolism'. *Nature*, **414**(6865): 799-806.

- Sayar, S., Turhan, M. and Gunasekaran, S. (2001). 'Analysis of chickpea soaking by simultaneous water transfer and water–starch reaction'. *Journal of Food Engineering*, **50**(2): 91-98.
- Seal, C. J., Daly, M. E., Thomas, L. C., Bal, W., Birkett, A. M., Jeffcoat, R. and Mathers, J. C. (2003). 'Postprandial carbohydrate metabolism in healthy subjects and those with type 2 diabetes fed starches with slow and rapid hydrolysis rates determined in vitro'. *British Journal of Nutrition*, **90**: 853-864.
- Selvendran, R. R. (1987). 'Chemistry of plant cell walls and dietary fibre'. *Scandinavian Journal of Gastroenterology*, **22**(s129): 33-41.
- Shomer, I. (1995). 'Swelling behaviour of cell wall and starch in potato (*Solanum tuberosum* L.) tuber cells -- I. Starch leakage and structure of single cells'. *Carbohydrate Polymers*, **26**(1): 47-54.
- Silvester, K. R., Englyst, H. N. and Cummings, J. H. (1995). 'Ileal recovery of starch from whole diets containing resistant starch measured in vitro and fermentation of ileal effluent'. *The American Journal of Clinical Nutrition*, **62**(2): 403-11.
- Sim, L., Quezada-Calvillo, R., Sterchi, E. E., Nichols, B. L. and Rose, D. R. (2008). 'Human intestinal maltase–glucoamylase: Crystal structure of the N-terminal catalytic subunit and basis of inhibition and substrate specificity'. *Journal of Molecular Biology*, **375**(3): 782-792.
- Simon, I., Móra, S. and Elödi, P. (1974). 'Studies on the active center of pancreatic amylase'. *Molecular and Cellular Biochemistry*, **4**(3): 211-216.
- Singh, F. and Diwakar, B. (1995) *Chickpea botany and production practices*, 16, Andhra Pradesh, India: International Crops Research Institute for the Semi-Arid Tropics.
- Singh, J., Dartois, A. and Kaur, L. (2010). 'Starch digestibility in food matrix: a review'. *Trends in Food Science & Technology*, **21**: 168-180.
- Singh, N., Singh, J., Kaur, L., Singh Sodhi, N. and Singh Gill, B. (2003). 'Morphological, thermal and rheological properties of starches from different botanical sources'. *Food Chemistry*, **81**(2): 219-231.
- Singh, U., Kherdekar, M. S. and Jambunathan, R. (1982). 'Studies on desi and kabuli chickpea (*Cicer arietinum* L.) cultivars. The levels of amylase inhibitors, levels of oligosaccharides and in vitro starch digestibility'. *Journal of Food Science*, **47**(2): 510-512.
- Slaughter, S. L. (2000) *The catalytic action of porcine pancreatic alpha-amylase on starch: the relationship between starch digestion kinetics and the physico-chemical characteristics of the substrate* unpublished thesis (PhD), King's College London, University of London.

- Slaughter, S. L., Ellis, P. R. and Butterworth, P. J. (2001). 'An investigation of the action of porcine pancreatic [alpha]-amylase on native and gelatinised starches'. *Biochimica et Biophysica Acta (BBA) - General Subjects*, **1525**(1-2): 29-36.
- Slaughter, S. L., Ellis, P. R., Jackson, E. C. and Butterworth, P. J. (2002). 'The effect of guar galactomannan and water availability during hydrothermal processing on the hydrolysis of starch catalysed by pancreatic [alpha]-amylase'. *Biochimica et Biophysica Acta (BBA) - General Subjects*, **1571**(1): 55-63.
- Smith, A. M. (2001). 'The biosynthesis of starch granules'. *Biomacromolecules*, **2**(2): 335-341.
- Smith, P., Krohn, R. I., Hermanson, G., Mallia, A., Gartner, F., Provenzano, M., Fujimoto, E., Goeke, N., Olson, B. and Klenk, D. (1985). 'Measurement of protein using bicinchoninic acid'. *Analytical Biochemistry*, **150**(1): 76-85.
- Snow, P. and O'Dea, K. (1981). 'Factors affecting the rate of hydrolysis of starch in food'. *The American Journal of Clinical Nutrition*, **34**(12): 2721-2727.
- Somerville, C., Bauer, S., Brininstool, G., Facette, M., Hamann, T., Milne, J., Osborne, E., Paredez, A., Persson, S., Raab, T., Vorwerk, S. and Youngs, H. (2004). 'Toward a systems approach to understanding plant cell walls'. *Science*, **306**(5705): 2206-2211.
- Soper, N. J., Chapman, N. J., Kelly, K. A., Brown, M. L., Phillips, S. F. and Go, V. L. W. (1990). 'The 'ileal brake' after ileal pouch-anal anastomosis'. *Gastroenterology*, **98**(1): 111-116.
- Sreerama, Y. N., Sashikala, V. B. and Pratapa, V. M. (2009). 'Expansion properties and ultrastructure of legumes: Effect of chemical and enzyme pre-treatments'. *LWT - Food Science and Technology*, **42**(1): 44-49.
- Stapley, A. G. F., Hyde, T. M., Gladden, L. F. and Fryer, P. J. (1997). 'NMR imaging of the wheat grain cooking process'. *International Journal of Food Science & Technology*, **32**(5): 355-375.
- Stein, E. A., Hsiu, J. and Fischer, E. H. (1964). 'Alpha-amylases as calcium-metalloenzymes. I. Preparation of calcium-free apoamylases by chelation and electro dialysis'. *Biochemistry*, **3**(1): 56-61.
- Steinmann, W., Walter, S., Beckers, M., Seide, G. and Gries, T. (2013). 'Thermal Analysis of Phase Transitions and Crystallization in Polymeric Fibers' in Elkordy, A. A., ed. *Applications of Calorimetry in a Wide Context - Differential Scanning Calorimetry, Isothermal Titration Calorimetry and Microcalorimetry*, InTech.
- Sumner, J. B. and Graham, V. A. (1921). 'Dinitrosalicylic acid: A reagent for the estimation of sugar in normal and diabetic urine'. *Journal of Biological Chemistry*, **47**(1): 5-9.

- Svihus, B., Uhlen, A. K. and Harstad, O. M. (2005). 'Effect of starch granule structure, associated components and processing on nutritive value of cereal starch: A review'. *Animal Feed Science and Technology*, **122**(3-4): 303-320.
- Tahir, R. (2008) *Amylolysis of native and hydrothermally treated starches. A comparative study using enzyme kinetics as an approach to understanding starch digestibility*, unpublished thesis (PhD), King's College London, University of London.
- Tahir, R., Ellis, P. R. and Butterworth, P. J. (2010). 'The relation of physical properties of native starch granules to the kinetics of amylolysis catalysed by porcine pancreatic α -amylase'. *Carbohydrate Polymers*, **81**(1): 57-62.
- Tappy, L. (2012). 'Q&A: 'Toxic' effects of sugar: Should we be afraid of fructose?'. *Bio Med Central Biology*, **10**(42): 1-7.
- Tepfer, M. and Taylor, I. E. P. (1981). 'The permeability of plant cell walls as measured by gel filtration chromatography'. *Science*, **213**: 761-763.
- Tester, R. F., Karkalas, J. and Qi, X. (2004). 'Starch—composition, fine structure and architecture'. *Journal of Cereal Science*, **39**(2): 151-165.
- Tester, R. F. and Morrison, W. R. (1990). 'Swelling and gelatinization of cereal starches. I. Effects of amylopectin, amylose, and lipids'. *Cereal Chemistry*, **67**(6): 551-557.
- Tovar, J., Bjorck, I. M. and Asp, N.-G. (1992). 'Incomplete digestion of legume starches in rats: A study of precooked flours containing retrograded and physically inaccessible starch fractions'. *The Journal of Nutrition*, **122**: 1500-1507.
- Tydeman, E. A., Parker, M. I., Faulks, R. M., Cross, K. I., Fillery-Travis, A., Gidley, M. J., Rich, G. T. and Waldron, K. W. (2010). 'Effect of carrot (*Daucus carota*) microstructure on carotene bioaccessibility in the upper gastrointestinal tract. 2. In vivo digestions'. *Journal of Agricultural and Food Chemistry*, **58**: 9855-9860.
- 'UK National Statistics', (2013) *Statistics on obesity, physical activity and diet* [online], available: <http://www.statistics.gov.uk> [accessed 2 April 2014].
- van Dam, R. M. and Seidell, J. C. (2007). 'Carbohydrate intake and obesity'. *European Journal of Clinical Nutrition*, **61**(S1): S75-S99.
- Van Kempen, T. A. T. G., Regmi, P. R., Matte, J. J. and Zijlstra, R. T. (2010). 'In vitro starch digestion kinetics, corrected for estimated gastric emptying, predict portal glucose appearance in pigs'. *The Journal of Nutrition*, **140**: 1227-1223.
- Vansteelandt, J. and Delcour, J. A. (1999). 'Characterisation of starch from durum wheat (*Triticum durum*)'. *Starch - Stärke*, **51**(2-3): 73-80.

- Vardakou, M., Mercuri, A., Barker, S. A., Craig, D. Q. M., Faulks, R. M. and Wickham, M. S. J. (2011). 'Achieving antral grinding forces in biorelevant in vitro models: Comparing the USP dissolution apparatus II and the dynamic gastric model with human in vivo data'. *AAPS PharmSciTech*, **12**(2): 620-626.
- Waldron, K. W., Smith, A. C., Parr, A. J., Ng, A. and Parker, M. L. (1997). 'New approaches to understanding and controlling cell separation in relation to fruit and vegetable texture'. *Trends in Food Science & Technology*, **8**(7): 213-221.
- Wang, S. and Copeland, L. (2013). 'Molecular disassembly of starch granules during gelatinization and its effect on starch digestibility: A review'. *Food & Function*, **4**: 1564-1580.
- Wang, T. L., Bogracheva, T. Y. and Hedley, C. L. (1998). 'Starch: as simple as A, B, C?'. *Journal of Experimental Botany*, **49**(320): 481-502.
- Warren, F. J. (2011) *The interactions of alpha-amylase with the surface of starch granules: The influence of particle size and supramolecular structure*, unpublished thesis (PhD), King's College London.
- Weurding, R. E., Veldman, A., Veen, W. A. G., van der Aar, P. J. and Versteegen, M. W. A. (2001). 'In vitro starch digestion correlates well with rate and extent of starch digestion in broiler chickens'. *The Journal of Nutrition*, **131**(9): 2336-2342.
- Wickham, M. J. S., Faulks, R. M., Mann, J. and Mandalari, G. (2012). 'The design, operation, and application of a dynamic gastric model'. *Dissolution Technologies*, **19**(3): 15-22.
- Wolever, T. M. S. (2000). 'Dietary carbohydrates and insulin action in humans'. *British Journal of Nutrition*, **83**(S1): S97-S102.
- Wolever, T. M. S., Jenkins, D. J. A., Collier, G. R., Lee, R., Wong, G. S. and Josse, R. G. (1988). 'Metabolic response to test meals containing different carbohydrate foods: 1. Relationship between rate of digestion and plasma insulin response'. *Nutrition Research*, **8**(6): 573-581.
- Wolever, T. M. S., Jenkins, D. J. A., Vuksan, V., Jenkins, A. L., Buckley, G. C., Wong, G. S. and Josse, R. G. (1992). 'Beneficial effect of a low glycaemic index diet in type 2 diabetes'. *Diabetic Medicine*, **9**(5): 451-458.
- Woolnough, J. W., Bird, A. R., Monro, J. A. and Brennan, C. S. (2010). 'The effect of a brief salivary α -amylase exposure during chewing on subsequent in vitro starch digestion curve profiles'. *International Journal of Molecular Sciences*, **11**: 2780-2790.

- Woolnough, J. W., Monro, J. A., Brennan, C. S. and Bird, A. R. (2008). 'Simulating human carbohydrate digestion in vitro: a review of methods and the need for standardisation'. *International Journal of Food Science & Technology*, **43**(12): 2245-2256.
- Wu, T., Rayner, C. K., Young, R. L. and Horowitz, M. (2013). 'Gut motility and enteroendocrine secretion'. *Current Opinion in Pharmacology*, **13**(6): 928-934.
- Würsch, P. (1994). 'Carbohydrate foods with specific nutritional properties--a challenge to the food industry'. *The American Journal of Clinical Nutrition*, **59**(3): 758S-762.
- Würsch, P., Del Vedovo, S. and Koellreutter, B. (1986). 'Cell structure and starch nature as key determinants of the digestion rate of starch in legume'. *The American Journal of Clinical Nutrition*, **43**: 25-29.
- Würsch, P. and Pi-Sunyer, F. X. (1997). 'The role of viscous soluble fiber in the metabolic control of diabetes: A review with special emphasis on cereals rich in β -glucan'. *Diabetes Care*, **20**(11): 1774-1780.
- Zhang, J., Cui, J.-H., Yin, T., Sun, L. and Li, G. (2013). 'Activated effect of lignin on α -amylase'. *Food Chemistry*, **141**(3): 2229-2237.

APPENDICES

All appendices relate to work presented in Chapter 7.

APPENDIX A: PARTICIPANT INFORMATION SHEET

“IMPORTANT INFORMATION

We would like to invite you to take part in our research study. Before you decide, we would like you to understand why the research is being done and what it would involve for you. We will be happy to answer any questions you may have before you decide to take part. You may also discuss the study with friends and family. Participation is entirely voluntary and you may withdraw from the study at any time without giving any reason.

What is the study for?

Accumulating evidence shows that the structure and properties of plant foods, particularly of the cell wall component ('dietary fibre'), play an important role in regulating the release (bioaccessibility) of nutrients from plant foods during chewing and digestion. Cell walls may act as a physical barrier to the digestion of carbohydrate and/or fat thus attenuating the blood glucose or lipid response induced. In a meal, fat and/or starch availability can therefore be controlled by modifying the amount of the nutrients encapsulated by cell walls.

Because glucose and lipid responses following the consumption of a meal are associated with reduced risk factors for type 2 diabetes mellitus and cardiovascular disease, this work has implications for the prevention and management of these diseases.

Therefore, we want to understand how much lipid or starch are lost at the terminal ileum after consumption of plant foods, either almonds for lipids or wheat for starch, and relate this to the blood glucose and lipid response generated.

Am I eligible to take part?

We are looking for ileostomy patients, who are not allergic to almonds or any other ingredients incorporated in any of the test meals to participate in this study.

To be eligible, you must:

- Be a male or female aged 20-75 years, who previously had proctocolectomy for ulcerative colitis, colon cancer or Crohn's disease (pure colonic form).
- Be stable at least 12 months post-operative
- Have eaten almonds with no adverse effects.

You must not:

- Be allergic to nuts of any kind or gluten
- Have previous case of obstruction of the stoma.

These eligibility criteria have been selected to ensure the safety of the study volunteers and researchers involved, and also to produce consistent samples between individuals. We will also record your age, BMI and sex.

What does the study involve?

Once we have checked your eligibility and you have given consent, we will ask you to attend a screening session and five study visits at the Clinical Research Facility of St Thomas' Hospital, Westminster Bridge Road, London SE1 7EH. **Note that the study will take place on Tuesdays and Thursdays ONLY. Furthermore, each visit session will last approximately 11 hours starting at either 8 or 8.30 am and finishing around 9 pm. Therefore, before agreeing to take part, make sure that you can attend these days at these times.**

The study visits are divided into two studies: **Study 1** looking at **fat** release and **Study 2** looking at **starch** release.

During the session (between 10 and 11 hours) you will be given for breakfast either:

Study 1: Fat availability (2 visits)

- a muffin containing almond flour and almond oil with some custard
- a muffin containing 2 mm almond pieces and some custard

Study 2: Starch availability (2 visits)

- porridge containing durum wheat flour (77g dry) and 300 mL water
- porridge containing 2 mm durum wheat large semolina (77g dry) and 300 mL water.

You will attend Study 2 first and if you wish you could carry on with Study 1.

Screening visit (lasting about 1h½):

- (1) You should avoid eating or drinking anything, except water, from 10 pm the previous night.
- (2) You will arrive at the Clinical Research Facility of St Thomas' Hospital at between 8 and 9.30 am.
- (3) We will give you a copy of this information sheet, explain to you all the details of the study and answer any questions you have. If you are still happy to take part in the study, you will be asked to sign a consent form.
- (4) We shall ask you questions about your medical history, your food habits and measure your weight, height, blood pressure and waist and hip circumference.
- (5) We will need to take a blood sample (approximately 15 mL = 3 x teaspoons)
- (6) You will try a smaller portion of the almond meals: muffin containing 2 mm almond particles
- (7) Finally, you will be given a 3 day diet diary to fill up as well as instructions for the day before the study visits.

Study visit:Day before your visit:

- (1) You will have eaten for dinner the meal provided.
- (2) You should avoid eating or drinking anything, except water, from 10 pm the previous night.

Visit day:

- (3) You will arrive at the Clinical Research Facility of St Thomas' Hospital at 8.00 or 8.30 am.
- (4) A venous cannula (fixed needle) will be inserted into your arm by an experienced nurse and a fasting blood sample collected.
- (5) You will eat the test meal.
- ~~(6) You will be given a marker, a food colorant dissolved in water (not a licenced medication).~~
- (7) Effluent will be collected once every 2h up to 10h and at your convenience in the evening and overnight.
- (8) For Study 2, blood will be collected (about 200 mL) after the meals at different time intervals up to 4 h.
- (9) We will provide you with a meal 4 h and 10 h after breakfast.

You will be paid £100 per session completed included screening (£600 in total), which will be paid by cheque or bank transfer after completion of the appropriate form.

What do I have to do?

We would like you to visit the Clinical Research Facility at St Thomas before agreeing to participate so you can see the area where you would stay and meet some of the staff, so we can describe the research in more detail, and so we can answer any questions. On that day we will also process to the screening as described above. A light breakfast will also be provided before you leave the screening session.

On the day preceding each of the 5 visits, you will be given a ready meal (low in fat or residue) to have for your dinner and asked to drink enough water to avoid dehydration. We will also ask you to fast overnight and avoid eating or drinking anything, except water, after 10 pm. We would then like you to come to the Clinical Research Facility for five study visits on the days and at the time we agree. We would like you to eat the lunch and evening meals that we provide (we would discuss your food preferences before you come, and would try to accommodate them). We would provide drinks when you wish, but these would be free from caffeine. Before you start eating your breakfast and lunch, we will ask you to ingest a marker (a capsule containing small pieces of different shape) to estimate transit time. We would like to collect effluents during your time spent at the Clinical Research Facility as well as overnight at home. We will give you a kit with some explanation on how to store the samples. Overnight effluent may be brought to King's

College London (Franklin Wilkins Building, Waterloo Campus, London) the next day or may be collected by a courier (your choice).

Each visit of Study 2 will also include blood collection (about 200 mL which corresponds to less than 1/2 pint) as described above. During your visit we would like you to remain within the Clinical Research Facility until around 13 hours after your arrival. For the duration of your visit there will be a room for you to sit and study/work/read in, with a DVD player and a selection of films for your entertainment.

What will happen to my samples?

Your samples will be marked with your participant number, the date, sample type and sample code only, so you will not be identifiable to the researchers studying your samples. The effluent samples produced will be used for nutrient analysis (lipid or starch), microscopy and particle sizing. Glucose and lipid levels will be measured in the collected blood samples. They will either be analysed immediately or be stored in a freezer in a locked laboratory on a corridor not accessible to the public until October 2014. Also, some of the blood that we will be collecting may be analysed for gut hormones (peptide YY (PYY), cholecystokinin (CCK), glucagon-like peptide-1 (GLP-1) and gastric inhibitory polypeptide (GIP) and may be stored for use in a later study.

No genetic tests will be done.

What are the advantages/disadvantages in taking part?

We do not anticipate any direct benefits to volunteers from taking part, but it will help us understand the digestion and absorption of fat and starch from plant foods (almond and wheat).

We believe the risks to participants are minimal as the study involves everyday activities. Our main concern is for individuals who are allergic to nuts, gluten and/or have previously experienced obstruction of the stomach, and we therefore specify that individuals who fall into this category should not take part. There is also a small risk of bruising from blood collection.

What will happen if I wish to withdraw from the study?

You are free to withdraw from the study at any time without giving a reason. However when we ask for your consent at the start of the study, we will also ask you for permission to continue to use any samples you have already provided.

Will my taking part in this study be kept confidential?

We will request your contact details in order to organise sessions. They will be stored on an encrypted pen drive that will be kept in a locked filing cabinet in the private office of the researchers. Only the researchers organising sessions will be authorised to access your details.

Should you wish to find out the results of this study you are welcome to contact either Myriam Grundy or Cathrina Edwards (details below) for a copy of the final report once the study is finished.

Who is organising and funding the study?

The project is organised by researchers from Kings College London and funded by the Biotechnology and Biological Sciences Research Council (BBSRC) under reference BB/H004866/1. The study has also been reviewed and given a favourable opinion by the Research Ethics Committee of South East Coast – Kent (reference no. 12/LO/1016), an independent group who protect the interests of research participants.

What if I have questions/want to make a complaint?

If you have any questions/concerns about any aspect of this study, you should ask to speak to the researchers (020 7848 4345, myriam.grundy@kcl.ac.uk or cathrina.edwards@kcl.ac.uk), who will do their best to answer your questions.

Address:

King's College London
Diabetes and Nutritional Sciences Division
4.131 Franklin-Wilkins Building
150 Stamford Street
London
SE1 9NH

If this study has harmed you in any way you can contact KCL using the details below for further advice and information: Dr Peter Ellis, p.ellis@kcl.ac.uk (telephone 020 7848 4238), Nutritional Sciences Division, King's College London, Franklin Wilkins Building, 150 Stamford Street, London SE1 9NH. In the event that something does go wrong and you are harmed during the research, and this is due to someone's negligence then you may have grounds for a legal action for compensation against King's College London, but you may have to pay your legal costs.

Thank you for your interest.

For further information, please contact:

Myriam Grundy or Cathrina Edwards

Diabetes and Nutritional Sciences Division

Tel.: 020 7848 4345

email: biogut@kcl.ac.uk “

APPENDIX B: SUBJECT SCREENING PROCESS

Prior to screening, volunteers were asked to complete pre-screening questionnaires with general questions about their health (e.g., regarding medical conditions, medicines, allergies, smoking and dietary habits). The completed questionnaires were used to assess the volunteers suitability for Study 1 and Study 2. If the volunteers were likely to be eligible for either one of these studies, they were invited to attend a screening visit at the CRF. Invited volunteers were provided with further information about the study, and instructed not to eat any food or drink (except water) for 12 h prior to their screening appointment.

At screening, the study was explained again, and the volunteers had several opportunities to ask questions about the study before written consent was taken.

Once consent was obtained, a fasted blood sample (~15 mL) was collected by venupuncture by the nurse appointed to the study, and dispensed into BD 4 mL vacutainers. These were sent to GSTS pathology for biochemical analysis: Fasted glucose concentration was determined by glucose-oxidase assay using the Bayer-Advia method, Full blood count and Full Lipid Profile (TAG, total-, HDL- and LDL-cholesterol) were measured on Siemens Advia 2120, and Liver Function Test was performed on the Siemens Advia 1650. Blood test results were confirmed to be within normal range before subjects were enrolled on the study.

Seated blood pressure was measured in triplicate according to British hypertension guidelines (O'Brien *et al.*, 2005) using an OMRON 705 CPII auto upper arm blood pressure monitor. Weight was measured in minimum indoor clothing using a beam balance and height was measured, without shoes, using a stadiometer. These measurements were used to calculate body mass index (BMI). Waist circumference was measured over light clothing at the mid-point between the lower costal margin and

the level of the superior iliac crests, and hip circumference was measured at the level of the greater trochanter of the femur.

A brief medical examination of the subjects was performed by the consultant gastroenterologist appointed to the study to screen for gastro-intestinal problems or stoma-related issues. Finally, subjects were given a 3-day food diary with instructions on how to complete it.

Subjects found not to meet the entry criteria for the study were excluded at this stage.



REFERENCES: O'Brien, E., Asmar, R., Beilin, L., Imai, Y., Mancia, G., Mengden, T., Myers, M., Padfield, P., Palatini, P., Parati, G., Pickering, T., Redon, J., Staessen, J., Stergiou, G., Verdecchia, P. (2005). 'Practice guidelines of the European Society of Hypertension for clinic, ambulatory and self-blood pressure measurement'. *Journal of Hypertension*, **23**(4): 697-701.

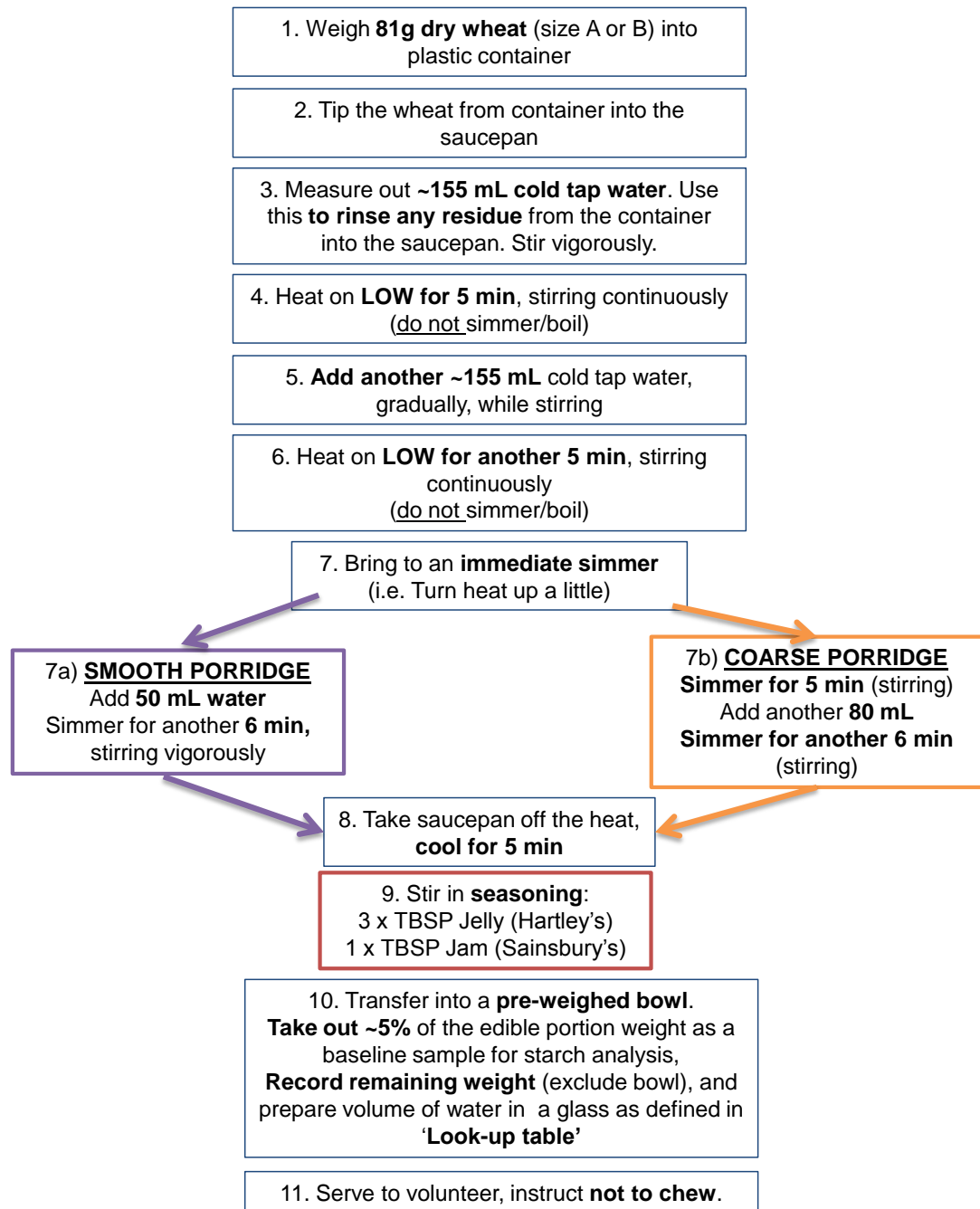
APPENDIX C: PREPARATION OF TEST MEALS

The test meals were prepared and served by a trained researcher independent to the study. For blinding purposes, the meals were coded as meals A or B, and only the researcher independent to the study who prepared and served the meals new the code. The following description makes enough for one portion and a sub-sample, which was taken out prior to serving the meal to subjects.

Porridge meals were prepared from 81 g small ~0.11 mm ('Smooth Porridge') or large ~1.85 mm particles ('Coarse Porridge'), of durum wheat endosperm cooked in water and flavoured with 1 tablespoon low sugar blackcurrant jam (Sainsbury's Reduced Sugar Blackcurrant Jam; Sainsbury's Supermarket Ltd., London, UK) and 3 table spoons jelly (Hartley's Ready To Eat Blueberry and Blackcurrant Jelly, Hartley's, London, UK). Flavouring details are shown in **Table C.1**.

TABLE C.1: DETAILS OF FLAVOURING USED IN PREPARATION OF TEST MEALS

Sainsbury's Reduced Sugar Blackcurrant Jam	Hartley's Ready To Eat Blueberry and Blackcurrant Jelly																																								
<p>Ingredients: Sugar, Blackcurrants, Water, Gelling Agent: Pectin, Citric Acid, Preservative: Potassium Sorbate, Acidity Regulator: Sodium Citrate. Prepared from 40 g fruit per 100g.</p> <p>Nutrition (g/100g):</p> <table> <tr><td>Energy</td><td>175 kCal</td></tr> <tr><td>Energy</td><td>740 kJ</td></tr> <tr><td>Protein</td><td>0.5 g</td></tr> <tr><td>Carbohydrate</td><td>40.0 g</td></tr> <tr><td>of which sugars</td><td>30.0 g</td></tr> <tr><td>Fat</td><td>0.6 g</td></tr> <tr><td>of which saturates</td><td>0.5 g</td></tr> <tr><td>Fibre</td><td>2.7 g</td></tr> <tr><td>Sodium</td><td>N/A</td></tr> <tr><td>Salt</td><td>0.2 g</td></tr> </table>	Energy	175 kCal	Energy	740 kJ	Protein	0.5 g	Carbohydrate	40.0 g	of which sugars	30.0 g	Fat	0.6 g	of which saturates	0.5 g	Fibre	2.7 g	Sodium	N/A	Salt	0.2 g	<p>Ingredients: Water, Gelling Agents (Potassium Citrates, Locust Bean Gum, Xanthan Gum, Gellan Gum), Citric Acid, Blueberry Flavouring (0.08%), Sweeteners (Aspartame, Acesulphame K), Colours (Carmoisine, Green S).</p> <p>Nutrition (g/100g):</p> <table> <tr><td>Energy</td><td>5 kCal</td></tr> <tr><td>Energy</td><td>19 kJ</td></tr> <tr><td>Protein</td><td>Nil</td></tr> <tr><td>Carbohydrate</td><td>1.0 g</td></tr> <tr><td>of which sugars</td><td>1.0 g</td></tr> <tr><td>Fat</td><td>Nil</td></tr> <tr><td>of which saturates</td><td>Nil</td></tr> <tr><td>Fibre</td><td>N/A</td></tr> <tr><td>Sodium</td><td>N/A</td></tr> <tr><td>Salt</td><td>0.2 g</td></tr> </table>	Energy	5 kCal	Energy	19 kJ	Protein	Nil	Carbohydrate	1.0 g	of which sugars	1.0 g	Fat	Nil	of which saturates	Nil	Fibre	N/A	Sodium	N/A	Salt	0.2 g
Energy	175 kCal																																								
Energy	740 kJ																																								
Protein	0.5 g																																								
Carbohydrate	40.0 g																																								
of which sugars	30.0 g																																								
Fat	0.6 g																																								
of which saturates	0.5 g																																								
Fibre	2.7 g																																								
Sodium	N/A																																								
Salt	0.2 g																																								
Energy	5 kCal																																								
Energy	19 kJ																																								
Protein	Nil																																								
Carbohydrate	1.0 g																																								
of which sugars	1.0 g																																								
Fat	Nil																																								
of which saturates	Nil																																								
Fibre	N/A																																								
Sodium	N/A																																								
Salt	0.2 g																																								
																																									



TOTAL prep-time: ~35 min

FIGURE C.1: PREPARATION OF TEST MEALS. Porridge was prepared from flour (particles <0.21mm) for smooth porridge or from 1.85 mm particles for coarse porridge. The meals were coded a or b until the study was un-blinded.

Evaporative losses were accounted for using a 'look-up' table, which specified the amount of water required to make up the total weight of the meal for a likely range of cooked porridge weights.

APPENDIX D: BLOOD SAMPLE COLLECTION, PROCESSING AND ANALYSIS

A venous cannula (BD Nexiva 20 GA) was inserted into a vein on the forearm by the nurse appointed to this study. Two fasted blood samples were collected from the cannula with a syringe 15 min apart. Immediately after the second fasted blood sample was taken, participants were served the test meal (time = 0) and accompanying drink of water. Bloods were then collected at 15, 30, 45, 60, 90, 120, 150, 180, 240 min. Apart from the -15 min sample, which was needed to obtain a reliable estimate of fasted plasma glucose concentration, five 4 mL BD vacutainer® collection tubes were filled at each time point (**Table D.1**) These were centrifuged, and duplicate aliquots of serum were taken and stored in freezers at -40 °C or -70 °C.

TABLE D.1: BLOOD COLLECTION TUBES OVERVIEW¹.

TUBE	ADDITIVE	ICE	SPIN	ANALYTE	ANALYSIS ¹
GREY	Sodium fluoride (antiglycolytic agent) and Potassium Oxalate (anti-coagulant)	YES	10 min 1300xG 4 °C	GLUCOSE	IL Test™ Glucose (Oxidase)
GOLD	Clotting accelerator and separation gel	NO	10 min 1300xG 4 °C	TAG	IL Test™ Triglycerides
				NEFA	Randox NEFA
GOLD	Clotting accelerator and separation gel	NO	10 min 1300xG 4 °C	INSULIN	Immulite® Insulin Test (Siemens)
				C- PEPTIDE	Immulite® C-peptide Test (Siemens)
LAVENDER	Spray-coated K ₂ EDTA (anti-coagulant) added DPPIV- inhibitor* (Merck Millipore)	YES	10 min 1300xG 4 °C	GLP-1	GLP-1 ELISA kit Merck Millipore
				GIP	GIP ELISA kit Merck Millipore
LAVENDER	Spray-coated K ₂ EDTA (anti-coagulant) added Aprotinin (10,000 KIU/mL, Nordic Pharma)*	YES	10 min 1300xG 4 °C	PYY	PYY (total) RIA kit Millipore
				CCK	CCK ELISA kit USCN Life Science Inc.

Abbreviations: TAG; triacylglycerides, NEFA; non-esterified fatty acid, (PYY) Polypeptide YY, CCKI; Cholecystokinin, GLP-1; Glucagon-Like Peptide-1, GIP; Glucose-Dependent Insulinotropic Peptide (GIP)

* additives marked with an asterisk, were added to the vacutainer tubes one day before use.

Further details of blood sample analysis methodology is provided in the next section.

Glucose, TAG and NEFA were determined at King's College London, UK. Insulin and C-peptide were analysed by GSTS pathology, St Thomas Hospital, London, UK, and gut hormones (PYY, CCK, GLP-1 and GIP) were analysed by GSTS pathology at Denmark Hill, King's College Hospital, UK.

Plasma glucose, TAG and NEFA analysis was performed on an iLab 650 auto-analyzer (Instrumentation Laboratories). Calibrations were carried out before each set of analysis, and quality control standards (i.e. upper and lower end of working range) were run between each sample tray. ReferrIL G (Instrumentation Laboratories) was used as the calibrant for IL Test™ kits, whereas the internal Randox calibrant (Randox Laboratories) was used for NEFA calibrations.

Glucose was determined using a glucose oxidase assay kit (IL Test™), which is based on a two-step reaction in which glucose is first converted to gluconic acid and hydrogen peroxide by glucose oxidase. The hydrogen peroxide then reacts, in the presence of peroxidase, 4-aminophenazone and phenol to produce a red quinoneimine dye. The increase in absorbance as generated by the red dye is proportional to the glucose concentration in the sample. Primary absorbance measurements are taken at 510 nm, and a blank reading is taken at 600 nm on the iLab 650. This assay has a linear working range for serum glucose levels between 0.1 and 28.2 mmol.L⁻¹.

TAG were determined with an IL Test™ Triglycerides assay kit, which is based on an end-point colorimetric assay. In this assay, TAG are first broken down into glycerol and fatty acids by lipoprotein lipase. The glycerol is then phosphorylated by glycerol kinase, forming glycerol-3-phosphate (G3P), which, in turn is oxidized in a reaction catalysed by glycerolphosphate oxidase to form dihydroxyacetone phosphate and peroxide. The peroxide then reacts, in the presence of aminoantipyrine and 4-chlorophenol to form a red quinoneimine dye. Thus, the increase in absorbance generated by the red dye is proportional to the TAG concentration of the sample. Absorbance measurements are

taken at 510 nm. The assay has a linear working range for serum or plasma TAG between 0.02 and 11.4 mmol.L⁻¹.

NEFA were determined with a Randox NEFA Kit (Randox Laboratories, County Antrim, UK), which is based on a colorimetric end-point reaction in which NEFA is first converted to Acyl Co A by Acyl Co A Synthetase, which is then converted to 2,3,-trans-Enoyl-CoA and peroxide by Acyl CoA Oxidase. Peroxide, in the presence of 4-aminoantipyrine and toluidine, reacts with peroxidase to form a purple adduct. The increase in absorbance as generated by the purple complex is proportional to the NEFA concentration of the sample. Absorbance measurements are taken at 546 nm. This assay has a linear working range for serum or plasma NEFA levels up 0.072 to 2.24 mmol.L⁻¹

Insulin and C-peptide concentrations were determined by Immulite® (electro-) chemiluminescence assays with an Immulite 2000 analyser, according to manufacturer specifications (Siemens Medical Solutions, Diagnostics Europe Ltd.). In brief, these assays are both based on a two-site sandwich assay in which C-peptide or Insulin is sandwiched between two antibodies. One antibody is covalently linked to paramagnetic particles, whereas the second antibody is labelled with either acridinium ester (for insulin detection) or with ruthenium (C-peptide). Insulin is detected by the light emitted upon reaction of the complex with horseradish peroxidase (HRP), whereas C-peptide is detected under voltage, which causes emission from ruthenium. Thus, the light intensity measured in a luminometer was proportional to the insulin or C-peptide concentration.

GLP-1 and GIP concentrations were determined by sandwich-ELISA using human GIP and GLP-1 (active) ELISA kits from Merck Millipore Corp. In brief, GLP-1 or GIP are immobilised on a microwell plate, washed to remove unbound materials, and then bound to a biotinylated anti-GLP-1 or anti-GIP monoclonal antibody. Unbound conjugate is then washed off, and HRP-labelled Streptavidin, which binds to the

biotinylated antibodies, is added. Free enzyme conjugates are washed off, and the chromogenic substrate 3,3',5,5'-tetramethylbenzidine (TMB) is added. HRP catalyses the oxidation of this substrate in the presence of hydrogen peroxides. The resulting diimine can be quantified spectrophotometrically. The increase in absorbance at 450 nm is directly proportionate to the amount of GLP-1 or GIP in the sample.

CCK was determined using an ELISA kit obtained from USCN Life Science Inc. This kit is based on a competitive inhibition enzyme immunoassay technique. In brief, the microplate is coated with a monoclonal antibody specific to CCK. Biotin-labelled CCK and the sample (contains CCK) are then added to the plate and will competitively bind to the coating. Next, the plate is washed to remove any unbound conjugate. Avidin (a biotin binding protein) conjugated to HRP is then added to each well. This binds to the biotin labelled CCK, and is visualised, after a period of incubation, by the addition of a chromogenic substrate (TMB, as above). Thus, the amount of colour intensity developed on addition of the visualisation substrate (as described above) is reversely proportional to the concentration of CCK in the sample.

PYY was determined using a Human PYY (total) radioimmunoassay kit (Merck Millipore Corp.), which measures both the 1-36 and 3-36 forms of this peptide. This assay kit uses ¹²⁵I-labeled PYY and a PYY antiserum to determine the concentration of total PYY in serum samples. The ¹²⁵I-labeled PYY and the sample containing PYY are incubated with PYY antiserum and competitively bind to binding sites on the PYY antibody. Any unbound material is then removed and the amount of radiolabelled antigen is quantified (bound or unbound) using an instrument to count radioactivity.

APPENDIX E: ILEAL EFFLUENT SAMPLE COLLECTION, PROCESSING AND ANALYSIS

Immediately prior to receiving the test meals, subjects were instructed to either completely empty their ileostomy pouch or to attach a new pouch. Ileal effluent was collected into Whirl-pak[®] (Nasco Ltd., Middlesex, UK) specimen bags by the subjects every 2 h, and sub-sampled by the researchers in the sluice room. Each sample was weighed, and, volume-permitting, blended (HR1363 Hand Blender, Philips Ltd., Guildford, UK), before sub-sampling. A visual inspection of the sample was also performed. For micro-structural analysis, a small sub-sample was collected into a glass vial loaded with fixative (approximately one part sample per 20 parts fixative) before blending. For starch analysis, ~2 g of ileal effluent was added to 4 x 15 mL falcon tubes pre-loaded with 95% (v/v) ethanol. The exact weight of sample added to each tube was recorded. The tubes were shaken vigorously to disperse the sample in the ethanol, and thereby inactivate residual enzyme activity. For moisture analysis, 3 x 2.1 mL cryovials were loaded with a sub-sample of the effluent and immediately placed in the -70 °C freezer. Any remaining sample was transferred to a smaller Whirl-pak[®] bag and stored at -70 °C.

For the overnight collections, participants were provided with an overnight collection pack consisting of eutectic freezer blocks (PlusIce PCM, E-78, Phase Change Material Products Ltd., Yaxley, Cambridgeshire), protective gloves, 5 numbered Whirl-pak[®] bags, a larger minigrip bag, and absorbent padding contained within a polystyrene box and carrying case. Subjects were instructed to wake up as they would normally during the night, making a note of the time on the overnight log. They then emptied their ileostomy bag into a specimen bag, wrapped it in absorbent padding and placed it flat between the ice blocks in the polystyrene box. This froze the sample and kept it frozen until the following morning. The overnight pack was delivered to King's College the following morning. Samples defrosted at room temperature (~4 h), before weighing, blending and sub-sampling as described above.

The total starch content of ileal effluent was determined using the high-throughput method described in *Section 2.3.3*. For this analysis, the two pairs of sub-sample collected at each time point were combined into two 50 mL falcon tubes, and rapidly mixed using an Ultra-Turrax[®] (IKA T25 digital) to achieve a homogeneous mass. Eight aliquots were taken from each tube, such that a total of 16 replicates were analysed per time point. This contributed to overcome difficulties with representative sub-sampling and subsequent pipetting. These aliquots were diluted in 95% (v/v) ethanol, centrifuged and the pellet analysed as described previously. Aliquots of the homogenised ileal effluent were also taken for sugar analysis, where the concentration of reducing sugar in the supernatant was determined using the DNS method (see *Section 2.3.4.1*). Sub-samples taken for moisture analysis were defrosted and used to determine the moisture content of ileal effluent using the oven-drying method described in *Section 2.3.2*. Micro-structural analysis was performed as described in *Section 2.4.1*.

APPENDIX F: MEALS OPTIONS FOR STUDY VISIT MENU

Each subject was able to choose from the following meal components to create a 'menu', but were required to eat exactly the same menu on the subsequent visit. The meal components were similar in nutrient content, as shown in *Tables F.1* and *F.2*.

TABLE F.1: MEAL OPTIONS FOR LUNCH

	LUNCH												
	<i>1. choose a cheese</i>		<i>2. choose a drink</i>		<i>(fixed)</i>	<i>3. Choose from the following toppings</i>				<i>4. Choose a yoghurt</i>			
	<i>(cheese)</i>		<i>(juice concentrate)</i>		<i>(Salad)</i>	<i>(beef)</i>	<i>(chicken)</i>	<i>(tuna)</i>	<i>(tofu)</i>	<i>(yoghurt flavours)</i>			
LUNCH Options:	Mini babybell	Greek Feta	Orange juice	Apple juice	Classic salad	Peppered beef	Chicken breast	Canned Tuna	Marinated tofu	Rasp-berry	Mango	Rhubarb	Straw-berry
<i>Brand:</i>	<i>Babybell</i>	<i>SBsBG</i>	<i>SBs</i>		<i>SBs</i>	<i>SBs</i>	<i>SBs</i>	<i>JW</i>	<i>Couldron</i>	<i>SBsTD</i>	<i>SBsTD</i>	<i>SBsTD</i>	<i>SBsTD</i>
<i>Portion:</i>	20g	30g	200mL pk	200mL pk	80g (1/2 pk)	170g (6 slices)	125g (1xpk)	130g (can)	80g (1/2 pk)	150g pot	150g pot	150g pot	150g pot
Calories (kcal)	60	52	94	94	87	204	203	212	182	192	195	181.5	193
Protein (g)	4	5	1	0.2	2.6	40.8	36.1	34.4	14	4.1	3.9	3.9	4.5
Carbohydrate (g)	0	0.2	20.8	22.6	4.1	1.8	0.5	0	0.8	19.8	22.2	18.9	19.8
Sugars (g)	0	0	20.8	22.6	2.7	0	0.3	0	0.8	17.6	20.9	18.6	19.8
Fat (g)	5	3.5	0.2	0	6.4	4.2	6.1	8.2	13.6	10.5	9.9	9.9	10.4
Saturated fat (g)	3.5	3.1	0	0	2	1.8	1.6	1.2	2	6.5	6.2	6.15	6.4
Fibre (g)	0	0	0	0	1.2	0	0.6	0	2.2	0.8	0.8	0.6	1.2
Salt (g)	0	0.5	0	0	0.87	1.68	0.89	1.3	1.2	0.15	0.15	0.15	0.15

Abbreviations: SBs; Sainsbury's, BG; Be Good to Yourself (product range in SBs), pk; pack, TD; Taste the Difference (product range in SBs), JW, John West. Tuna was in sunflower oil, juices were from concentrate. All meal components were served together, straight from the refrigerator, without pre-heating.

TABLE F.2: MEAL OPTIONS FOR DINNER

DINNER Options:	DINNER										
	1. Choose a main				(fixed)	2. Choose a dessert		3. Choose a drink			
	(beef)	(lamb)	(chicken)	(fish)	(side dish)	(chocolate)	(lemon)	(fizzy)	(juice from concentrate)	(fizzy)	
	Cottage Pie	Shepherd's Pie	Chicken w/ mash	Fish Pie	Baby carrots	Chocolate melt pud	Lemon cheesecake	Coke	Orange juice	Apple juice	Lemonade
Brand:	SBsTD	SBsTD	SBsTD	SBsTD	SBs	Gü Brand	Gü Brand	Coca Cola	SBs	SBs	Schweppes
Portion:	400g	400g	450g	400g	80g	100g (1 pot)	90g pot	330mL can	200mL pk	200mL pk	330mL can
Calories (kcal)	581	476	522	381	18	421	358	139	94	94	60
Protein (g)	36.6	20.8	37.4	26.4	0.3	6.2	4.2	0	1	0.2	0
Carbohydrate (g)	46.3	48.3	45.1	38.4	3.5	37.6	34.3	35	20.8	22.6	13.9
Sugars (g)	3.9	9.6	7.8	2.6	2.5	31.4	20.8	35	20.8	22.6	13.9
Fat (g)	27.7	20.1	18.1	12.2	0.2	27.4	23	0	0.2	0	0
Saturated fat (g)	16.2	10.5	10.4	6.6	0	16.3	12.9	0	0	0	0
Fibre (g)	9.7	9.2	14.4	5.9	1.8	2.7	1.7	0	0	0	0
Salt (g)	2.5	1.78	2.41	1.92	0	0	0.2	0	0	0	0.01

Abbreviations: SBs; Sainsbury's, pk; pack, TD; Taste the Difference (product range in SBs). Main courses (ready meals) were oven-cooked as per manufacturer specifications. Baby carrots were microwaved from frozen. Chocolate melt-in-the-middle pud was oven cooked as specified on food packaging. Lemon cheesecake was served cold straight from the refrigerator. All meal components were served together.

